universität wien

DISSERTATION

Titel der Dissertation

The Role of the AP-1 Member Fra-1 in Epithelial-Mesenchymal Transition and Carcinogenesis

angestrebter akademischer Grad

Doktorin der Naturwissenschaften (Dr. rer.nat.)

Verfasserin / Verfasser:	Ivana Ćustić
Matrikel-Nummer:	9812742
Dissertationsgebiet (lt. Studienblatt):	Molekulare Biologie
Betreuerin / Betreuer:	Dr Hartmut. Beug und Dr. Erwin Wagner

Wien, im Oktober 2009

In loving memory of my parents

Acknowledgements

First and foremost, I would like to thank my supervisors, Drs. Hartmut Beug and Erwin Wagner for setting up the collaboration and giving me the opportunity to work in their labs on this exciting project. I am very grateful for their continuous support and guidance. I am particularly grateful to Erwin for his help, understanding and support during personally and scientifically difficult times through out my PhD studies. It was a great pleasure to work with and learn from Erwin and Hartmut.

I am very grateful to my PhD committee members Drs. Roland Foisner and Josef Penninger for the help and scientific feedback they provided during my PhD committee meetings. I would also like to thank Dr. Roland Foisner for agreeing to participate in my PhD defence as examiner.

I am very thankful to Drs. Dany Chalbos and Robert Eferl for agreeing to review my thesis.

I would like to thank all the Wagner lab members for giving me the opportunity to learn from them, for creating a stimulating working atmosphere in the lab, helpful discussions, suggestions and constant encouragements as well as for having great fun outside the lab. I have missed you all greatly in the last year.

My special thanks goes to Latifa for her everlasting scientific enthusiasm, interest and involvement in this project and invaluable help with designing experiments. Thank you for sharing your knowledge and saying all the right words when needed.

I am also thankful to all Beug lab members who welcomed me in the lab, and I am particularly thankful to Agnes, Boris and Memo for their helpful suggestions and help with experiments. I would also like to thank Gabi for outstanding technical support in the lab.

Last but not least, I would like to thank my family and friends for their trust and support during my PhD studies. Thank you for being there when I needed you the most.

Table of contents

Summary.....9
Zusammenfassung.....11

1. INTRODUCTION.....13

1.1 Epithelial to mesenchymal transition.....13
1.1.1 EMT in development.....15
1.1.2 EMT in disease.....16
1.1.2.1 EMT in Fibrosis.....16
1.1.2.2 EMT in cancer progression and metastasis.....17
1.1.3 Molecular hallmarks of EMT.....19
1.1.4 Signalling pathways in EMT.....22
1.1.5 Studying EMT *in vivo*.....24
1.1.5.1 The EpH4/EpRas *in vitro/in vivo* cell model.....26
1.2 The AP-1 transcription factor complex.....27
1.2.1 Fos and Jun proteins.....28
1.2.2 The AP-1 structure and dimer formation.....29
1.2.3 Dimerizing partners.....31
1.2.4 Biological functions of AP-1.....32
1.2.4.1 Functions of Jun proteins.....32
1.2.4.2 Functions of Fos proteins.....36
1.2.4.2.1 Fra-1 structure and regulation.....39
1.2.4.2.2 Biological function of Fra-1.....40
1.2.4.2.3 Fra-1 in cancer development.....41

2. AIM OF THE THESIS.....43

3. RESULTS.....44

PART I. Investigating the role of Fra-1 in EMT: generation and characterization of EpH4-*fra1* and EpRas-*fra1* cells.....44
3.1 Fra-1 expression level correlates with EMT in EpH4/EpRas cell system.....44

3.2 Exogenous overexpression of Fra-1 in EpH4 and EpRas cells 46
3.3 Ectopic Fra-1 expression increases cell proliferation and causes prominent morphological changes in EpH4 and EpRas cells 53
3.4 Fra-1 expressing cells show increased motility and invasiveness *in vitro* 56
3.5 Fra-1 triggers EMT in EpH4 and EpRas cells 58
3.6 Induction and maintenance of EMT by Fra-1 in EpH4/EpRas system is independent of TGF-β1 63
3.7 Fra-1 renders EpH4 cells tumorigenic/metastatic and increases the metastatic potential of EpRas cells 64
3.8 Summary and conclusions 73

PART II. Mechanism of Fra-1-induced EMT: identification of Fra-1/AP-1 targets 74
3.9 Fra-1 induces transcriptional downregulation of E-cadherin.....74
3.9.1 Transcriptional downregulation of E-cadherin in EpH4-*fra1* cells does not involve promoter hypermethylation or histone acetylation 75
3.10 Gene expression profiling in EpH4-*fra1* and EpRas-*fra1* cells: Fra-1 modulates RNA expression of genes implicated in EMT.....78
3.10.1 Transient silencing of ZEB1 and/or ZEB2 in EpH4-*fra1* and EpRas-*fra1* cells relieves transcriptional repression of E-cadherin 91
3.10.2 Fra-1 binds to the ZEB1 promoter *in vivo* 93
3.10.3 ZEB2 as a potential Fra-1/AP-1 target gene.....95
3.11 Summary and conclusions 96

PART II. Fra-1 expression is both necessary and sufficient for EMT: Fra-1 knock-down by RNAi in EpRas and EpRasXT cells.....103
3.12 Effect of Fra-1 silencing on TGF-β1-induced EMT 98
3.12.1 Silencing Fra-1 reverses morphological changes and restores the expression of epithelial marker proteins in EpH4-*fra1* cells 104
3.12.2 Fra-1 expression is needed for effective proliferation of EpRasXT cells.....106
3.13 Summary and conclusions 108

4. DISCUSSION.....109
4.1 Summary and future perspectives 117

5. MATERIALS AND METHODS 124

5.1 Abbreviations 124
5.2 Materials 126
5.2.1 Chemicals and reagents 126
5.2.2 Media 127
5.2.3 Antibodies used for Western Blotting and Immunohistochemistry 127
5.2.4 Antibodies used for Immunofluorescence 128
5.2.5 Antibodies used for Chromatin Immunoprecipitation (ChIP) 129
5.2.6 MISSION™ shRNA Library 129
5.2.7 siRNA oligonucleotides 130
5.3 Methods 131
5.3.1 Transformation of *E. coli* with plasmid DNA 131
5.3.2 Plasmid DNA preparation 131
5.3.3 RNA isolation 132
5.3.4 RNase Protection Assay (RPA) 132
5.3.5 cDNA synthesis 132
5.3.6 Quantitative Real-time RT-PCR 133
5.3.7 RNA preparation and microarray analysis 134
5.3.8 Chromatin Immunoprecipitation (ChIP) 135
5.3.9 Nuclear extract preparation 138
5.3.10 Total cell lysate preparation 138
5.3.11 Western blotting 139
5.3.12 Immunodetection of proteins 139
5.3.13 Immunofluorescence 140
5.3.14 Cells and cell culture 140
5.3.14.1 Culturing of cells 141
5.3.14.2 Retroviral production 141
5.3.14.3 Lentiviral production 142
5.3.14.4 Retroviral and Lentiviral infection 142
5.3.14.5 Cell doubling time 143
5.3.14.6 Cell proliferation assay 143
5.3.14.7 Cell migration assays 143
5.3.14.8 Cell Invasion assay 144
5.3.14.9 Inhibitor treatments 145

5.3.14.10 TGF-β1 ELISA 145
5.3.15 Animal experiments and histological analysis 146
5.3.15.1 *In vivo* Tumorigenicity Assay 146
5.3.15.2 Metastasis induction 146
5.3.15.3 Preparation of tissue samples for histological analysis 147
5.3.15.4 Immunohistochemical staining procedures 147
References 148
CURRICULUM VITAE 169

Summary

Epithelial-to-mesenchymal transition (EMT) is a multi-step process whereby polarized, adherent epithelial cells convert into non-polarized and migratory mesenchymal cells. An important step in cancer progression is the ability of primary tumor cells to disseminate and metastasize to distant organs. To date, a large amount of evidence indicates that EMT is central to these processes. Therefore, elucidating the molecular mechanisms that control EMT might unravel potential therapeutic targets. The dimeric transcription factor AP-1 (Fos/Jun) has been associated with oncogenic transformation and ectopic expression of c-Fos and to a lesser extent c-Jun have been reported to cause cellular depolarization reminiscent of EMT. More recently, the Fos protein Fra-1 has been shown to modulate the motility and invasiveness of human cancer cell lines. However, the molecular mechanisms and targets of AP-1 in EMT are still unknown.

In this study I have addressed the role of Fra-1/AP-1 in EMT using a cellular model *in vitro* as well as transplantations *in vivo*. Ectopic expression of *fra-1* in fully polarized, non-tumorigenic mouse mammary epithelial cells EpH4 and their HaRasV12-transformed, tumorigenic but still polarized derivatives resulted in dramatic changes in cell morphology and behaviour. The major epithelial marker E-cadherin was downregulated, while mesenchymal markers such as fibronectin were upregulated suggesting that Fra-1 triggers EMT. Further *in vitro* characterization revealed increased proliferative, migratory and invasive potential of the Fra-1-expressing cells. Transient knock-down experiments indicated that the observed changes were Fra-1-dependent. Most importantly, xenograft transplantation experiments revealed that the EpH4*fra-1 ce*lls are tumorigenic and metastatic *in vivo,* while Fra-1 overexpression increased the metastatic potential of EpRas cells. Gene expression profiling confirmed the loss of epithelial gene expression and the upregulation of several mesenchymal markers in the Fra-1-expressing cells. Furthermore, several genes previously associated with EMT, migration and invasiveness were found deregulated, among them AP-1 transcriptional targets such as matrix metalloproteases. Subsequent molecular analysis revealed that the transcription factors, E-cadherin repressors and EMT-associated ZEB1/2 proteins are novel direct Fra-1/AP-1 transcriptional targets. Finally, transient knock-down experiments indicated that up-

regulation of ZEB1 and/or ZEB2 is responsible for the induction of EMT in Fra-1-overexpressing cells. In summary, this study revealed a new function of Fra-1/AP-1 as an important inducer and regulator of EMT and unravelled a potential link between the AP-1 transcription factors and the E-cadherin transcriptional repressors ZEB1 and ZEB2.

Zusammenfassung

Die epithelial-mesenchymale Transition (EMT) ist ein mehrstufiger Prozess in welchem sich polarisierte, adhäsive, epitheliale Zellen zu nicht-polarisierten und wandernden mesenchymalen Zellen verändern. Ein wichtiger Schritt im Fortschreiten eines Tumors ist die Fähigkeit, in entfernte Organe zu metastasieren. In den letzten Jahren wurden eine große Zahl von Ergebnissen und Argumenten publiziert, dass EMT in diesen Prozessen eine zentrale Rolle spielt. Aus diesem Grund sollte die Erforschung der molekularen Mechanismen, welche die EMT kontrollieren, auch zu neuen Strategien für therapeutische Intervention führen. Der dimer-bildende Transkriptionfaktor AP-1 (Fos/Jun) ist mit onkogener Transformation assoziiert und viele Studien zeigten, dass die ektopische Expression von c-Fos, und zu einem geringerem Ausmaß auch von c-Jun, zelluläre Depolarisation und viele Eigenschaften von EMT hervorrufen. Vor kurzem konnte gezeigt werden, dass das Fos Protein Fra-1 die Motilität und die Invasivität von humanen Krebszell-Linien moduliert. Die molekularen Mechanismen hinsichtlich der Mitwirkung von AP-1 Proteinen bei EMT sind noch unbekannt.

In dieser Arbeit befasse ich mich mit der Rolle von Fra-1/AP-1 in der EMT unter Verwendung eines zellulären *in vitro* Systems und *in vivo* Transplantation dieser Zellen in Mäuse. Die ektopische Expression von *fra-1* in vollständig polarisierten, nicht-tumorigenen Maus-Brustepithelzellen (EpH4) und deren tumorigenen, aber noch polarisierten Derivat, den HaRasV12 Zellen (EpRas), hatte drastische Veränderungen von Morphologie und Verhalten der Zellen zur Folge. Der bekannte epitheliale Marker E-Cadherin wurde hinunter,- und mesenchymale Marker wie Fibronektin hinaufreguliert, was die Vermutung nahe legt, dass Fra-1 EMT auslösen kann. Weitere *in vitro* Charakterisierungen ergaben ein erhöhtes proliferatives, migratorisches und invasives Potential von Fra-1-exprimierenden Zellen. Transiente Knock-down Experimente wiesen darauf hin, dass die beobachteten Veränderungen von Fra-1 abhängig sind. Von besonderer Bedeutung ist, dass sich in Xenograft-Experimenten herausstellte, dass EpH4*fra-1* Zellen tumorigen und metastasierend sind, während eine Überexpression von Fra-1 das metastatische Potential der EpRas Zellen erhöhte. Das Genexpressionsprofil bestätigte den Verlust an Expression epithelialer Gene und die Hinaufregulierung

mehrerer mesenchymaler Marker in Fra-1-exprimierenden Zellen. Weiters konnten mehrere deregulierte Gene gefunden werden, die bereits mit EMT, Migration oder Invasivität assoziiert wurden unter ihnen AP-1 regulierte Gene wie Matrix-Metalloproteasen. Eine nachfolgende molekulare Analyse ergab, dass die Transkriptionsfaktoren, E-Cadherin Repressoren und EMT-assoziierten ZEB Proteine neue, direkt von Fra-1/AP-1 regulierte Gene sind. Schließendlich zeigten transiente Knock-down Experimente, dass eine Hinaufregulation von ZEB1 und/oder ZEB2 für die Induktion von EMT in Fra-1 überexprimierenden Zellen verantwortlich ist. Zusammenfassend zeigt diese Studie eine neue Funktion von Fra-1/AP-1 als wichtigen Auslöser und Regulator von EMT und eröffnet eine potentielle Verbindung zwischen AP-1 Transkriptionsfaktoren und den E-Cadherin Repressoren ZEB1 und ZEB2.

1. Introduction

1.1 Epithelial to mesenchymal transition

Epithelial to mesenchymal transition (EMT) is a process that was originally discovered during lens development and is considered by embryologists as a major embryological mechanism for tissue remodelling during gastrulation. If impaired, the process of embryogenesis can not proceed past the blastula state (Thiery and Sleeman, 2006). EMT is a multi-step process beginning with well polarized and adhesive epithelial cells that acquire fibroblast-like properties and show reduced intercellular adhesion and increased motility thereby producing non-polarized mesenchymal cells embedded in extracellular matrix (ECM) (Levayer and Lecuit, 2008) (**Figure 1**).

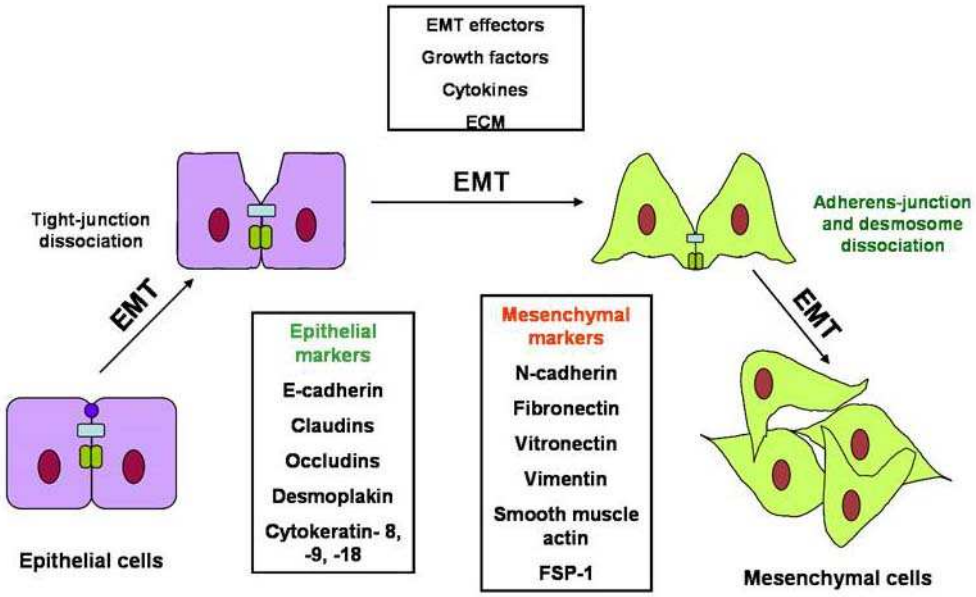

Figure 1. Schematic representation of events during EMT (adapted from Thiery and Sleeman, 2006)

Epithelial cells are characterized by a cuboidal or cobblestone morphology. They are organized as a sheet or layers of cells that are laterally tightly connected by specialized junction structures including tight junctions, adherens junctions, gap junctions and desmosomes (Yang and Weinberg, 2008). These tight connections

serve to ensure the mechanical integrity of the tissue. Epithelial cells have a well established apical-basal polarity with strong anchorage to the basement membrane (basal lamina) at their basal side. As a consequence of this anchorage they can only migrate laterally as a sheet of cells. On the other hand, mesenchymal cells display either ameboid or spindle-like morphology. They rarely form direct contacts with neighbouring cells and form only transient contacts with the ECM. These contacts are mediated by focal adhesion complexes which facilitate cell migration. Mesenchymal cells are also characterized by anterior-posterior rather than lateral polarity, which allows them to migrate as single cells in a directional fashion.

One important feature of EMT is that it is a strictly controlled process defined by several distinct steps that do not necessarily occur consecutively and are not all necessarily present in a given example of EMT (Levayer and Lecuit, 2008). The first step involves the disruption of cell-cell contacts. In order to successfully disseminate, epithelial cells first need to resolve intercellular contacts with neighbouring cells. This is accomplished by disassembly of tight junctions, adherens junctions, gap junctions and desmosomes (Zavadil and Böttinger, 2005; Baum et al., 2008; Levayer and Lecuit, 2008). In the second step, the released cells undergo concomitant change in cell shape and polarity establishing an anterior, leading end and the posterior, rear end. Loss of apico-basolateral polarity and dissociation of intercellular junctions is accompanied by fundamental remodeling of the actin cytoskeleton from cortical actin to actin stress fibers, a hallmark of migratory, mesenchymal cells (Miettinen et al., 1994; Piek et al., 1999; Bakin et al., 2000; Zavadil et al., 2001; Zavadil and Böttinger, 2005). The final step involves secretion of matrix-degrading proteases that degrade the ECM enabling the cells to successfully migrate and invade the basement membrane.

The process of EMT has so far been described in three major physiological and patho-physiological contexts. Besides being a fundamental process governing morphogenesis during development of the majority of multicellular organisms, it also plays an important role in tissue fibrosis and cancer progression and metastasis (Zavadil and Böttinger, 2005; Thiery, 2003).

1.1.1 EMT in development

EMT was for the first time identified and described in the developmental context by Elisabeth Hay over four decades ago but it wasn't till the early 1980s that it was recognized as a distinct process. During development, EMT plays a crucial role in formation of three germ layers (ectoderm, mesoderm and endoderm) in the process of gastrulation (Moustakas and Heldin, 2007). During early embryogenesis of most metazoans, mesenchymal cells arise from the primitive epithelium (primitive ectoderm) (Yang and Weinberg, 2008). In higher vertebrates (birds and mammals) EMT produces the primary mesenchyme that condenses to form definitive mesoderm and endoderm (Hay, 2005). During gastrulation the mesoderm is formed by ingression of cells from the medial region of epiblast (epithelial monolayer) called the primitive streak in higher vertebrates. Upon ingression these cells eventually fill out the space between epiblast and hypoblast giving rise to mesoderm and endoderm. This is regarded as the initial developmental EMT (Hugo et al., 2007).

At a later stage of embryogenesis, the second example of EMT is the development of the neural crest (a defining tissue of vertebrates) that is regarded as a second gastrulation event in vertebrates (Duband et al., 1995; Moustakas and Heldin, 2007; Yang and Weinberg, 2008). The neural crest develops at the boundary between the neural plate and the epidermal ectoderm where the epithelial cells from the neural tube in the dorsal side of the embryo undergo EMT and ingress to form a transient population of cells called neural crest cells (Thiery and Chopin, 1999; Yang and Weinberg, 2008). These cells have the capacity to migrate over long distances in the embryo where they form the peripheral nervous system and differentiate into several new mesenchymal cell types such as melanocytes, somites, bone and chondrocytes (Moustakas and Heldin, 2007; Hugo et al., 2007). Both, the mesoderm formation and neural crest development, are the key EMT programs that occur during early embryonic development. The resulting mesenchymal and neural crest cells maintain oliogopotentiality that enables them to further differentiate into various cell types (Yang and Weinberg, 2008).

However, EMT is not restricted only to the earliest developmental events, but also takes part in later stages of development. It is involved in the heart valve development, male Müllerian duct regression and the secondary palate formation resulting in the separation of nasal and oral cavities (Fitchett and Hay, 1989; Hugo et al., 2007; Thiery and Sleeman, 2006). In addition, a partial EMT has been implicated in the branching morphogenesis that occurs during the formation of several organs including the trachea (*Drosophila*), the kidneys, and the mammary glands (reviewed by Yang and Weinberg, 2008).

1.1.2 EMT in disease

EMT plays essential roles during embryogenesis and tissue homeostasis (Shook and Keller, 2003). However, if deregulated, EMT can lead to disturbance of normal epithelial homeostasis, therefore contributing to the development and progression of pathological conditions such as fibrosis and cancer cell metastasis (Baum et al., 2008).

1.1.2.1 EMT in Fibrosis

During tissue fibrosis the accumulation of fibroblasts and excessive deposition of collagen, and other extracellular matrix components, at sites of chronic inflammation leads to formation of scar tissue and progressive tissue injury (Lee et al., 2006). It is believed that these fibroblasts partially derive from the bone marrow, but also arise from EMT of epithelial cells at the site of injury (Kalluri and Neilson, 2003; Neilson, 2005). The occurrence of EMT during fibrosis has so far been reported for the lung, kidney, liver, heart and eye, but it is so far best characterized in kidneys, where it is estimated that one third of renal interstitial fibroblasts, the main mediator of renal interstitial fibrosis, are derived from tubular epithelial cells via EMT (reviewed by Iwano et al., 2002; Kisseleva and Brenner, 2008).

Inflammation normally precedes fibrosis since recruitment of inflammatory cells (neutrophils, macrophages) to sites of acute injury is part of normal wound healing

process. However, sustained injury and inflammation can lead to an imbalanced microenvironment and the onset of aberrant EMT due to the abundant production and secretion of growth factors and pro-inflammatory cytokines such as TGF-β1, PDGF, EGF, FGF-2 and IL1. These cytokines are produced by inflammatory cells, mainly macrophages, at the site of injury. This leads to activation of epithelial cells that undergo EMT generating activated fibroblasts - myofibroblasts. Myofibroblasts are characterized by expression of αSMA and are responsible for production and deposition of collagen and other extracellular matrix components. In addition, myofibroblasts secrete angiogenic and proinflammatory factors that stimulate the proliferation and invasion of epithelial cells (Radisky et al., 2007). The main mediator of EMT in fibrosis is the cytokine TGF-β1, which under normal conditions promotes wound healing and repair. However, under pathological conditions, it plays a key role in stimulating fibrosis. In normal conditions the injury repair process requires the degradation of provisional ECM and removal of myofibroblasts by apoptosis. However, sustained myofibroblast activation stimulates dysfunctional repair mechanisms, leading to accumulation of fibrotic ECM that is resistant to degradation and can stimulate epithelial cell proliferation (Thannickal et al., 2004; Radisky et al., 2007). This provides an environment that favours cancer formation and development. Therefore, the presence of fibrotic lesions significantly increases the risk of cancer in many tissues, including lung (Artinian and Kvale, 2004; Daniels and Jett, 2005), liver (Bissell, 2001; Bataller and Brenner, 2005), and breast (Boyd et al., 2002; Boyd et al., 2005; Radisky et al., 2007).

1.1.2.2 EMT in cancer progression and metastasis

Cancers of epithelial origin (carcinomas) are the most prevalent type of cancers in humans comprising over 90% of all malignancies (Baum et al., 2008). A fatal step in cancer progression is metastasis and the vast majority of patients actually die from metastasis rather than from primary tumors. In recent years there have been numerous reports that support the idea that EMT has a central role in cancer progression (reviewed by Thiery and Sleeman, 2006). There are several steps required for the progression from normal epithelium to invasive carcinoma and the subsequent establishment of metastasis to secondary organs (Tse and Kalluri,

2007). Schematic exemplification of tumor development and the role of EMT in metastatic progression of carcinoma is shown in **Figure 2**.

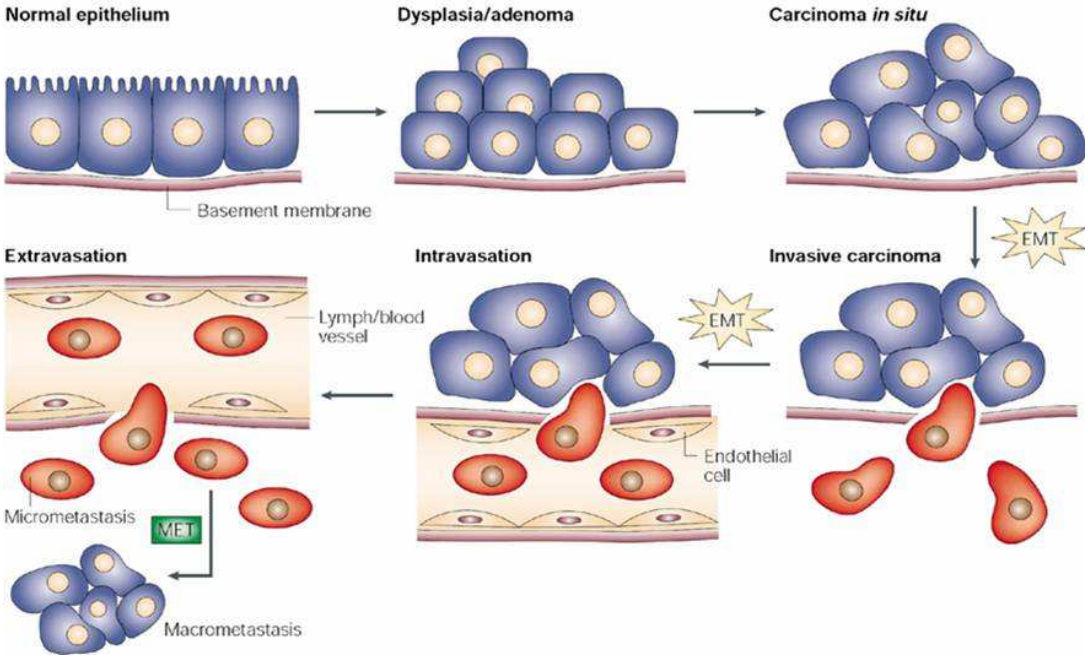

Figure 2. **Emergence and metastatic progression of carcinoma - the role of EMT** (adapted from Thiery, 2002)

Besides the initial step that involves uncontrolled local proliferation of normal epithelia that yields benign adenomas, additional genetic and epigenetic alternations are required for progression to carcinoma *in situ*. At this point the basement membrane that underlines the epithelium is still intact and the cells do not exhibit invasive behaviour. In order to become invasive, the carcinoma cells need to acquire motility and the ability to degrade or remodel the extracellular matrix (Moustakas and Heldin, 2007). It is believed that the migratory characteristics acquired by the transition to a mesenchymal-like state facilitate cell migration and enables the invasive capabilities of cancer cells (Tse and Kalluri, 2007). Cancer cell invasiveness is therefore thought to be directly linked to the process of EMT (Moustakas and Heldin, 2007).

In order to successfully establish the metastatic tumor, cells from the primary tumor need to access the circulatory system. This is aided by angiogenesis and remodelling of the basement membrane (Tse and Kalluri, 2007). Local dissemination enables the cells to intravasate into lymph or blood vessels allowing

their passive transport to distant organs. Upon reaching their metastatic sites, the cancer cells extravasate and either remain solitary forming micrometastasis or proliferate to form secondary tumors at the distant site, often undergoing the reverse process of mesenchymal-epithelial transition (MET) to regain an epitheloid phenotype and form organized tumorigenic nodules (Thiery, 2002; Moustakas and Heldin, 2007; Tse and Kalluri, 2007).

However, not only highly metastatic but also non-metastatic, non-invasive carcinoma cell lines, and even nonneoplastic carcinoma-associated stroma cells undergo EMT and promote tumor growth (Tester et al., 2001; Prindull, 2005). Therefore, the EMT program can also affect the cells in the tumor microenvironment, such as cancer-associated stromal fibroblasts or myofibroblasts, immune cells and microvessels resulting in synergistic interactions between the cancer cells and tumor environment that directs the progression of metastasis (Prindull, 2005).

1.1.3 Molecular hallmarks of EMT

EMT is characterized by loss of proteins associated with polarized epithelial phenotype and *de novo* synthesis of proteins associated with mesenchymal, migratory morphology of transitioning cells (Zavadil and Böttinger, 2005). On the other hand, the acquisition of the ability to migrate and invade ECM as single cells is considered as a functional hallmark of the EMT program (Yang and Weinberg, 2008). Epithelial cells are distinguished from mesenchymal cells by the expression of specific markers among which E-cadherin is regarded as the most important one (Berx et al., 2007) and functional loss of E-cadherin in epithelial cells is considered as the major hallmark of EMT (Yang and Weinberg, 2008).

E-cadherin is the prototypic type I cadherin that is regarded as a central organizer of the epithelial phenotype (Thiery, 2002). It is a 120 kDa transmembrane glycoprotein that is the main component of adherens junctions where it mediates calcium-dependent homophilic interactions with E-cadherin molecules on adjacent cells. The cytoplasmic domain of E-cadherin is highly conserved among all

members of the cadherin family and interacts with cytosolic catenins (Christiansen and Rajasekaran, 2006; Kuphal and Behrens, 2006). The E-cadherin-catenin complex is composed of α-catenin (102 kDa), β-catenin (92 kDa) and γ-catenin/plakoglobin (83 kDa) that bind to E-cadherin and each other in a specific manner (Kuphal and Behrens, 2006) providing a link with the actin cytoskeleton and hence strengthening adhesion (Cavallaro and Christofori, 2004; Connaci-Sorrell et al., 2002).

In vitro, there is a direct correlation between lack of E-cadherin and loss of the epithelial phenotype (Behrens at al., 1989). E-cadherin is frequently lost in carcinomas and correlates with susceptibility to EMT, acquisition of an invasive phenotype and generally poor prognosis (Thiery, 2002; Hugo et al., 2007; Yang and Weinberg, 2008). The loss of E-cadherin function during tumour progression can be caused by various genetic or epigenetic mechanisms. However, loss of E-cadherin due to genetic mutations resulting either in complete loss of expression or the expression of a non-functional protein are rarely found in sporadic cancers (Berx et al., 1998) and the majority of cancers downregulate E-cadherin by epigenetic mechanisms that include direct transcriptional repression, promoter hypermethylation and posttranslational modifications (Berx and Van Roy, 2001; Hajra and Fearon, 2002a; Thiery, 2002; Berx et al., 2007).

There are three transcription factors families that act as direct E-cadherin repressors by binding to E-box elements CAGGTG in the E-cadherin promoter (Peinado et al., 2004; Peinado et al., 2007). These include the zinc-finger protein members of Snail family Snail1, Snail2 (Slug), and Snail3 (Smuc) (Batlle et al., 2000; Cano et al., 2000; Bolos et al., 2002; Nieto, 2002), the ZEB family (ZEB1/δEF-1 and ZEB2/SIP1) (Comijn et al., 2001; Eger et al., 2005) and the members of the basic-helix-loop-helix (bHLH) family the class I proteins E47/E12 (alternative splicing products of the E2A gene (Perez-Moreno et al., 2001) and class II proteins Twists (Twist1 and Twist2) (Yang et al., 2004; Peinado et al., 2007). In addition, proteolytic degradation of E-cadherin by matrix metalloproteases (MMPs) yielding a soluble form of E-cadherin is another mechanism of E-cadherin downregulation. A soluble, 80 kDa, form of E-cadherin is frequently found in cultured tumor cell lines and in tumor biopsy samples where it promotes tumor cell

invasion by upregulating MMPs such as MMP2, MMP9 and MMP14 (Cavallaro and Christofori, 2004).

Besides E-cadherin down-regulation responsible for the loss of cell-cell adhesion, further molecular hallmarks of EMT include: up-regulation of matrixdegrading proteases and mesenchymal-related proteins such as vimentin, fibronectin, α-SMA, FSP-1 and N-cadherin; actin cytoskeleton reorganization mediated by Rho small GTPases that activate the motility machinery; up-regulation and/or nuclear translocation of transcription factors regulating a large number of genes specific for EMT (Huber et al., 2005; Thiery and Sleeman, 2006; Guarino, 2007).

De novo expression or upregulation of adhesion molecule N-cadherin, of the intermediate filament protein vimentin and other cytoskelatal proteins like α-SMA and FSP-1 correlates with E-cadherin downregulation and the epithelial cytokeratin switch promoting cell migration. The cytoskeletal protein vimentin and the adhesion molecule N-cadherin contribute to the metastatic potential of tumor cells by direct or indirect interactions with microfilaments and microtubules facilitating pseudopodia formation and cytoskeletal remodeling (Christiansen and Rajasekaran, 2006). FSP-1/S100A4 is an intracellular calcium-binding protein that is also involved in modifying cytoskeletal-membrane interactions by its ability to influence levels of intracellular calcium and actin disassembly (Okada et al., 1997; Kalluri and Neilson, 2003). These cytoskeletal rearrangements are aided by the activation of the small Rho GTPases Rho, Rac, and Cdc42. They are the key regulators of the cytoskeleton that regulate the formation of lamellipodial protrusions and filopodial extensions by activating the actin polymerization apparatus at these sites (Hall, 1998; Bar-Sagi and Hall, 2000; Bhowmick et al., 2001; Etienne-Manneville and Hall, 2002).

The production and deposition of ECM proteins such as fibronectin and collagens combined with upregulation of MMPs is involved in remodelling of the ECM that further enhances the motility and invasive capabilities of tumor cells undergoing EMT. Matrix metalloproteinases (MMPs) are zinc dependent endopeptidases that are upregulated in almost every type of cancer. They are capable of cleaving virtually every type of extracellular matrix components and molecules that mediate

cell-cell and cell-ECM interactions (Sternlicht and Werb, 2001). In addition, MMPs can cleave and activate growth factors and growth factor receptors thereby promoting invasion of the basement membrane, blood vessel penetration, angiogenesis and metastasis (McCawley and Matrisian, 2001; Radisky et al., 2007).

Despite our increasing understanding of molecular basis of the EMT program, it is currently only loosely defined by certain cell morphological changes, changes of differentiation markers from epithelial to mesenchymal patterns, and the functional changes required for cells to migrate and invade through ECM. However, loss of E-cadherin (N-cadherin in the neural crest) seems to be the major consistently reported molecular change occurring during the various EMTs involved in both development and tumor metastasis (Yang and Weinberg, 2008).

1.1.4 Signalling pathways in EMT

Although the molecular mechanism of EMT have at most been partially elucidated, a rapidly increasing number of interconnected signalling pathways and signalling molecules potentially involved in the EMT program were identified during the last 10 years. EMT is induced or regulated by various growth and differentiation factors and by multiple major signalling pathways involved in developmental EMT, the five major pathways being Wnt/β-catenin, TGFβ/BMP, Hedgehog, Notch and receptor tyrosine kinase (RTK) – Ras. These pathways are often deregulated in cancer where they cooperate with each other and frequently with oncogenic Ras to drive EMT (Hay, 2005; Huber et al., 2005; Thiery and Sleeman, 2006; Berx et al., 2007).

As already mentioned in the context of tissue fibrosis, TGFβ is a very potent and one of the best studied EMT inducers. TGFβ signals via two distinct receptor serine/threonine kinases in a classical signalling cascade involving the phosphorylation and subsequent activation of cytoplasmic Smad proteins that translocate to the nucleus and promote transcription of target genes controlling cell proliferation, differentiation, apoptosis and cell migration (Derynck et al., 1998; Xu et al., 2009). In addition, TGFβ can exert its EMT-inducing properties via Smad-

independent pathways through cooperation with oncogenic Ras and RTK signalling that results in activation of PI3K/Akt and MAPK (ERK, p38, JNK) signalling cascades, activation of small GTPases RhoA and Rac1, as well as through direct interaction with the polarity protein Par6 that leads to disassembly of tight junctions (Bakin et al., 2000; Bhowmick et al., 2001; Ozdamar et al., 2005; Huber et al., 2005; Moustakas and Heldin, 2007; Xu et al., 2009).

Wnt/β-catenin signalling pathway is another well characterized signalling pathway that is crucial for developmental EMT and often deregulated in cancer. The canonical Wnt signalling pathway is initialized by binding of Wnt proteins to their cognate receptor Frizzeld. This triggers a signalling cascade leading to the inhibition of glycerol synthase kinase 3β (GSK3β) - dependent phosphorylation of β-catenin that targets it for proteosomal degradation in the absence of Wnt. Stabilised, hypophosphorylated β-catenin translocates to the nucleus where it alters gene expression by interacting with the T cell factor/lymphocyte enhancer (TCF/LEF) complex (Willert and Nusse, 1998). In epithelial cells, β-catenin is a member of cadherin-catenin adherens junction complex where it is sequestered at the cell membrane by its interaction with E-cadhein. However, during EMT the downregulation of E-cadherin and disassembly of adherens junctions releases β-catenin to the cytoplasm where it is free to translocate to the nucleus and regulate the expression of downstream target genes in a Wnt-independent manner.

A role for Notch and Hedgehog-Patched-Gli signalling has been postulated both in developmental and neoplastic EMT. The activation of the trans-membrane receptor Notch by the Jagged ligand results in Notch nuclear translocation and activation of target genes including Hey1 that promotes E-cadherin down-regulation and EMT. TGFβ can also interact with the Notch pathway by inducing the expression of Hey1 and Jagged ligand. The binding of Hedgehog ligands to their receptor Patched initiates the signalling cascade leading to the expression of the transcription factor Gli-1 resulting in E-cadherin downregulation (Huber et al., 2005; Thiery and Sleeman, 2006; Guarino, 2007)

The receptor tyrosine kinase (RTK) signalling cascade is activated by numerous growth factors, such as EGF, FGF, HGF, IGF and PDGF that have been implicated

in induction and maintenance of EMT. They signal through their cognate receptor tyrosine kinases resulting in activation of downstream kinases such as Ras, Src, PI3K and MAPK. All of these RTK-induced signalling pathways converge at transcriptional and post-transcriptional induction of a number of EMT-linked transcription factors leading to E-cadherin down-regulation, expression of mesenchymal genes and/or to dynamic changes in the cytoskeleton (Huber et al., 2005; Thiery and Sleeman, 2006; Guarino, 2007) revealing a complex and interconnected signalling network that governs the EMT program both in development and cancer progression.

1.1.5 Studying EMT *in vivo*

Apart from developmental studies most of our knowledge on molecular mechanisms involved in EMT comes from studies in *in vitro* cell systems. Since EMT is a dynamic process, its transient nature renders it hard to study *in vivo*. While EMT seems relevant for cancer progression (Bhowmick et al., 2001; Janda et al., 2002; Tse and Kalluri, 2007) it has been difficult to establish an *in vivo* correlative of EMT induced metastasis. Standard histological analysis of tumors fails to reveal mesenchymal cells formed during EMT since they are indistinguishable from fibroblastoid tumor stroma cells. The major difficulty in demonstrating the role of EMT in pathological conditions such as fibrosis and cancer metastasis is in identifying the carcinoma cells that have passed through EMT in primary human tumor samples (Yang and Weinberg, 2008), as well as activated fibroblasts that arise due to EMT of epithelial cells at fibrotic sites. This is due to the lack of markers that are invariably specific of either the epithelial or mesenchymal phenotypes (Berx et al., 2007; Yang and Weinberg, 2008). It has been only recently that studies in transgenic mice provided an *in vivo* proof of principle that fibroblasts can form locally via EMT during renal and lung fibrosis as well as in cancer progression (see below).

In the first study, transgenic mice that express LacZ in cortical tubular epithelium were subjected to unilateral ureteral obstruction (UUO) that produces experimental renal fibrosis. The LacZ positive epithelial cells were distinguished from renal

fibroblasts by lack of expression of the fibroblast marker FSP-1/S100A4. The identification of fibroblasts double positive for FSP-1 and LacZ clearly proved that these fibroblasts arise from tubular epithelial cells that underwent EMT (Iwano et al., 2002). In the second study, a similar approach was employed using transgenic mice in which lung epithelial cells were permanently tagged for expression of β-galactosidase. The mice were subjected to induction of pulmonary fibrosis by TGFβ and revealed that the increases in myofibroblasts were largely due to transdifferentiation from epithelial cells (Kim et al., 2006; Radisky et al., 2007).

FSP-1/S100A4 has also been used as an EMT marker in cancer progression studies. Mice transgenic for the FSP1/S100A4 promoter coupled to thymidine kinase (TK) as a suicide gene have elegantly provided evidence that EMT is indeed required for metastasis. The FSP1/TK reporter mice were crossed with PyV-MT mice that develop metastatic breast cancer. Treatment of these transgenic mice with gancyclovir suppressed metastasis formation, suggesting that those cells that contribute to metastasis formation are FSP-1-positive. Furthermore, PyV-MT/FSP-1 deficient mice showed reduced metastasis formation as compared to PyV-MT mice, providing direct *in vivo* evidence that EMT is coupled to metastasis formation (Xue et al., 2003; Berx et al., 2007).

In addition, the recent development of intravital multiphoton microscopy combined with new approaches in the use of fluorescent cell markers has enabled the *in vivo* analysis of the initial steps of tumor dissemination. Using this approach, the single carcinoma cells that have lost their epithelial polarity can be seen to migrate out of primary tumours thereby providing the first direct *in vivo* evidence of EMT at the initial stages of metastasis (Wang et al., 2002; Condeelis and Segal, 2003; Nieto, 2008). The visualisation of these fluorescent cells disseminating from tumors has enabled their isolation, purification and subsequent molecular analysis (Nieto, 2008).

1.1.5.1 The EpH4/EpRas *in vitro/in vivo* cell model

The EpH4/EpRas cell system is one of the best characterized cellular models of EMT *in vitro* and *in vivo* (**Figure3**).

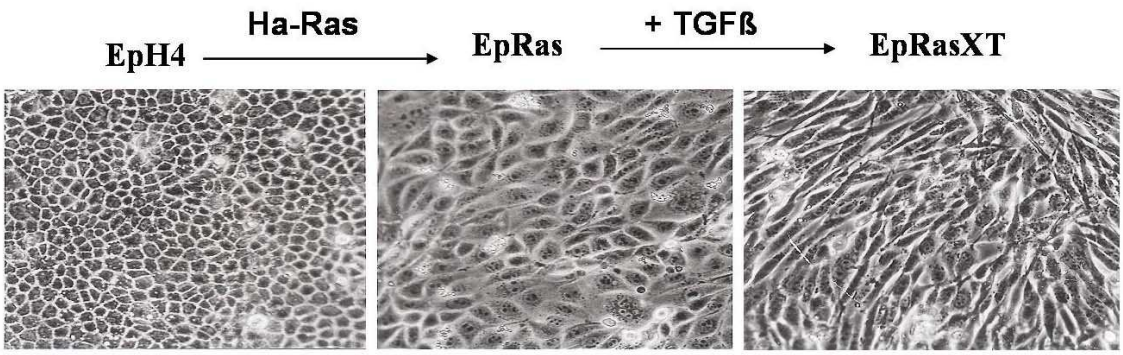

Figure 3. EpH4/EpRas model of Epithelial-Mesenchymal transition. The parental EpH4 cells show typical epithelial cobblestone morphology when grown on plastic. Their Ha-RasV12 transformed derivatives-EpRas cells retain epithelial morphology, but upon TGFβ treatment undergo EMT yielding fibroblastoid EpRasXT cells (Oft et al., 1996).

The parental EpH4 cells are spontaneously immortalized, non-tumorigenic and fully polarized murine mammary epithelial cells derived from the mammary glands of mid-pregnant BALB/c mice (Reichmann et al., 1989). They show a typical epithelial cobblestone morphology with tight cell-cell contacts and undergo cell cycle arrest and apoptosis, when treated with TGF-β1. EpRas cells were derived from EpH4 cells upon stable transformation with oncogenic Ha-RasV12, which renders them tumorigenic (Oft et al., 1996; Janda et al., 2002). These cells have hyperactivated MAPK- and PI3K pathways and show increased proliferation, when compared to EpH4 cells. Although EpRas cells retain their epithelial morphology, the cells are no longer sensitive to TGF-β1-induced apoptosis and undergo complete EMT giving rise to EpRasXT cells with a spindle-like, fibroblastoid phenotype. This phenotype is further sustained by the establishment of a TGF-β1 autocrine loop that maintains EMT in the absence of exogenous TGFβ.

1.2 The AP-1 transcription factor complex

Activator Protein 1 (AP-1) is a dimeric transcription factor complex composed of members of the Jun, Fos, ATF (activating transcription factor) and Maf (musculoaponeurotic fibrosarcoma) families of proteins (Chinenov and Kerppola, 2001; Shaulian and Karin, 2001). It was first identified in HeLa cell extracts as the protein complex that binds in the enhancer regions of simian virus 40 (SV40) and human methallothionein IIA (hMTIIA) gene (Lee et al., 1987a). The AP-1 binding site was identified shortly after as a TPA response element (TRE) since it was strongly induced by the tumour promoter 12-*O*-tetradecanoylphorbol-13-acetate (TPA) (Lee et al., 1987b; Angel et al., 1987; Abate et al., 1990). This heptanucleotide palindromic TGA(C/G)TCA element is found in the promoter and enhancer regions of many cellular and viral genes. The binding affinity for a given TRE is determined by the different AP-1 dimer combinations and the context of the surrounding sequence. In addition, the Fos and Jun proteins bind to the symmetric octanucleotide (TGACGTCA) CRE (cAMP response element) sequence (Nakabeppu et al., 1988; Rauscher et al., 1988). Different dimer complexes of Fos and Jun proteins exhibit different *in vitro* transactivation properties resulting in positive or negative transcriptional modulation (Cohen et al., 1989; Angel and Karin, 1991; Ryseck and Bravo, 1991; De Cesare et al., 1995). Furthermore, AP-1 is also capable of activating and repressing gene activity through protein-protein interactions with other transcription factors (Angel and Karin, 1991; Kerppola and Curran, 1991; Ransone and Verma, 1990; Bergers et al., 1995; Song et al., 2008).

Numerous signalling pathways converge in activation of AP-1, which in turn modifies the expression of genes involved in a variety of biological processes. AP-1 has been implicated in the control of many fundamental processes including cell proliferation, differentiation, apoptosis and oncogenic transformation. A vast number of extracellular stimuli, such as growth factors, cytokines, extracellular matrix components, and phorbol esters induce AP-1 activity at the end of signalling cascades. AP-1 activity is itself controlled at multiple levels and can be regulated by dimer composition, transcription, post-translational modification and interactions with other proteins (reviewed by Eferl and Wagner, 2003).

1.2.1 Fos and Jun proteins

The best characterized AP-1 proteins in mammals are the members of Jun and Fos families (Eferl and Wagner, 2003). The Jun family consist of three members: c-Jun, JunB and JunD, while the Fos family has four members: c-Fos, FosB, Fra-1 and Fra-2. In addition, a splice form of FosB, ΔFosB (FosB2), with C-terminal truncation can naturally occur (Mumberg et al., 1991; Nakabeppu, and Nathans, 1991). The prototypes of each family, c-*jun* (cellular jun) and c-*fos* (cellular fos) are nuclear phosphoproteins that were first identified as cellular homologues of viral oncogenes *v-jun* and *v-fos*. *Jun* was identified as a novel retroviral insert of cellular origin in the genome of Avian Sarcoma Virus 17 (AVS17) (Maki et al. 1987), while *fos* was identified as a retroviral oncogene accountable for the induction of osteogenic sarcomas by the Finkel-Biskis-Jinkins Murine Sarcoma Virus (FBJ-MSV) (Curran et al., 1982; Curran and Teich, 1982).

Screening of murine cDNA library for growth factor inducible immediate early genes using oligonucleotide probe derived from the C-terminal domain of *c-jun* resulted in identification of two additional *jun* family members: *junB* (Ryder et al., 1988) and *junD* (Hirai et al., 1989). The remaining three members of the *fos* family have also been identified and subsequently cloned due to sequence homology with *c-fos*. *FosB* was identified by screening a cDNA library with an oligonucleotide probe corresponding to DNA binding domain of the mouse *c-fos* gene (Zerial et al., 1989). *Fos*-related antigens *fra-1* (Cohen and Curran, 1988) and *fra-2* (Nishina et al., 1990; Foletta et al., 1994) have been identified due to antigenic similarity of the protein to the peptide used for raising anti-c-Fos antibodies.

Identification of c-Fos and c-Jun, the mammalian homologs of the retroviral oncoproteins *v-fos* and *v-jun* as well as the identification of other *fos* and *jun* family members as immediate early genes that are rapidly induced upon serum or growth factor stimulation immediately implicated the AP-1 in cell proliferation and growth control as well as in oncogenic transformation.

1.2.2 The AP-1 structure and dimer formation

The AP-1 proteins belong to the basic-leucine zipper (bZip) family of proteins. They have an alpha helical structure and are characterized by a leucine zipper domain that enables them to dimerize and form a functional transcription factor complex (Angel and Karin, 1991). This domain is characterized by a periodic repetition of leucine residues at every seventh position. The two leucine zippers form a two-stranded parallel coiled-coil where the two right handed α-helices are wrapped around one another with a slight left handed superhelical twist. Adjacent to the leucine zipper domain immediately to its N-terminal is the so-called basic region, formed by basic residues adjacent to leucines. The basic region is highly conserved among all Jun and Fos proteins and is necessary for DNA binding (Vogt and Bos, 1990; Angel and Karin, 1991; Chinenov and Kerppola, 2001; Eferl and Wagner, 2003). The structural organisation of Fos and Jun proteins is depicted in **Figure 4**.

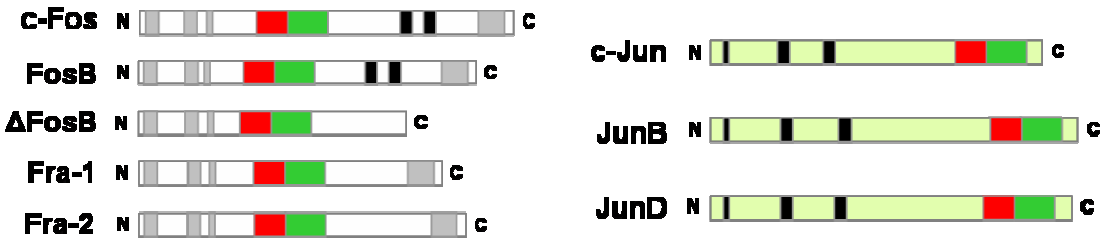

Figure 4. Structural organization of Fos and Jun proteins. Schematic representation of structural domains of Fos and Jun proteins. The basic DNA-binding domain is depicted in red box and the dimerization leucine zipper domain in green. The black boxes represent the transactivation domains located at the N-terminus in Jun protein and at the C-terminus in C-Fos and FosB. The grey boxes represent the regions of high sequence conservation among Fos proteins that influence transcriptional activation.

Different members within the Jun or Fos families of proteins share a high degree of sequence homology. All Fos proteins have highly conserved bZip domains centrally located, while Jun proteins have them at their C terminus. Unlike the Jun proteins, who have three highly conserved transactivation domains (composed of clusters of negatively charged amino acids at their N-terminal part, among Fos proteins only c-Fos and FosB harbour such domains at their C terminus (Angel and Karin, 1991; Chinenov and Kerppola, 2001). These domains are crucial for transcriptional

activation and transforming activity. In line with this, the remaining two members of the Fos family, Fra-1 (Fos-related antigen 1) and Fra-2 (Fos -related antigen 2) that do not have potent transactivation domains exhibit weaker transforming activity both *in vitro* and *in vivo* when compared to c-Fos and FosB (Widson and Verma, 1993).

Dimer formation is a prerequisite for effective DNA binding and occurs by a parallel interaction of the leucine-zipper domains. Leucine side chains protrude from one side of the α-helix and form a hydrophobic surface that mediates dimerization (Landschultz et al., 1988). This brings the adjacent basic regions in close proximity and enables DNA binding. The X-ray structure of Jun/Fos dimers bound to DNA revealed that the binding affinity of two juxtaposed α-helices depends on the charge of amino acids in the two interacting proteins (Glover and Harrison, 1995) (**Figure 5**).

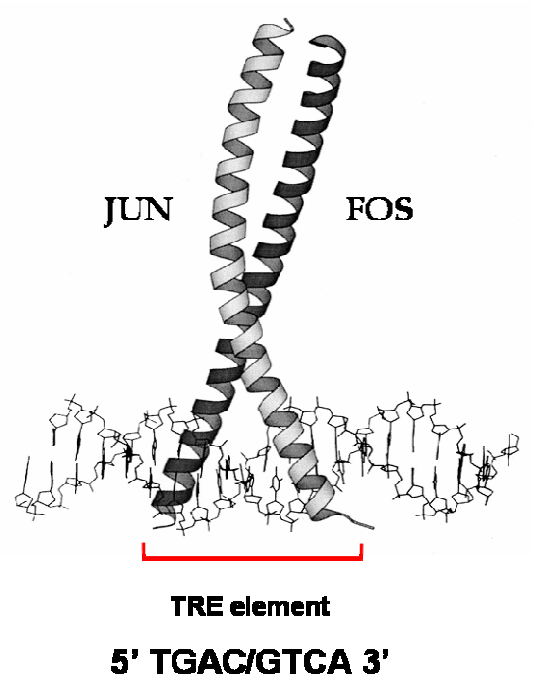

Figure 5. Schematic representation of a Jun/Fos heterodimer bound to its DNA palindromic recognition sequence. The structure of the bZIP domain of the Jun/Fos heterodimer bound to its DNA palindromic recognition sequence has been determined by X-ray crystallography (adapted from Glover and Harrison, 1995).

The binding of the dimer to the palindromic AP-1 site is described with the "scissors-grip" model where the two helices bifurcate beyond the leucine zipper region forming a Y-shaped structure that interacts with the DNA in the middle of the site (Vinson et al., 1989). The two arms of the "Y" interact with the two halves of the DNA recognition sequence in opposite directions along the major groove directly contacting the DNA (Abate et. al., 1990; Risse et al., 1989; Glover and Harrison, 1995) (**Figure 5**).

1.2.3 Dimerizing partners

All Jun proteins can form functional homodimers as well as heterodimers with Fos proteins while Fos proteins can not homodimerize (Angel and Karin, 1991). However, Fos proteins can associate with any of the Jun proteins to generate stable heterodimers with higher DNA-binding activity than the Jun homodimers. This increased DNA-binding activity of Jun-Fos heterodimer is in part due to the increased thermostability in comparison to Jun-Jun homodimer. In addition, in Fos-Jun homodimers only amino acids with opposite charge make contact while in the Jun-Jun homodimers, two residues with the same charge interact, making these dimers less stable. The inability of Fos proteins to form homodimers is due to the electrostatic repulsion between four residues of the same charge located in their leucine zipper region. Interestingly, these same negatively charged residues contribute to increased stability of Jun-Fos heterodimers by increasing the number of salt bridges between the two leucin zipper regions upon interaction with basic residues in the leucine zipper of Jun proteins (Angel and Karin, 1991; Glover and Harrison, 1995).

In addition to cross-family dimerization Fos and Jun proteins can modulate gene expression by protein-protein interactions with structurally unrelated proteins such as members of the NFAT (Nuclear Factor of Activated T Cells) or Ets family of proteins as well as with other transcription factors, coactivators and chromatin remodelling factors. Interactions with Fos/Jun proteins have so far been reported for more than 50 different proteins (reviewed by Chinenov and Kerppola, 2001; Eferl and Wagner, 2003). Formation of these multiprotein transcription regulatory

complexes greatly enhances transcriptional activity and together with the combinatorial diversity of AP-1 proteins influence how a specific cell type responds to a certain stimulus.

1.2.4 Biological functions of AP-1

Fos and Jun proteins were among the first identified mammalian transcription factors. Since they were originally discovered as cellular counterparts of viral oncogenes the first role attributed to AP-1 was involvement in oncogenic transformation (Hess et al., 2004). Since that time numerous studies, aimed at depicting the biological functions of AP-1, have implicated it in the regulation of a variety of cellular processes including cell proliferation and survival, differentiation, growth, apoptosis, cell migration, transformation and invasion (reviewed by Shaulin and Karin, 2001; Shaulin and Karin, 2002; Eferl and Wagner, 2003). Initial knowledge on the biological role of different AP-1 proteins was based on the *in vitro* studies done mainly in fibroblasts. However, more recent studies, utilizing genetically modified mice and primary cells derived from these mice have significantly increased our understanding of the function of AP-1 proteins in normal development and pathological conditions (Eferl and Wagner, 2003). These studies have also shown that the biological functions of Fos/Jun proteins depend on the specific cell type in which they are expressed.

1.2.4.1 Functions of Jun proteins

The Jun protein family has three members c-Jun, JunB and JunD. It is believed that all Jun proteins evolved from a common ancestor by gene duplications since they all share a similar genomic organization with no introns (Zhang et al., 1990). Nevertheless, they exhibit markedly different functions both *in vitro* and *in vivo*. In addition, the function of particular Jun protein depends on the specific cellular context. The prototype of the family, c-Jun was shown to be a positive regulator of cell proliferation while JunB and JunD negatively regulate cell cycle progression. This is mainly mediated by their dual effects on the expression of cyclin D1 (Bakiri

et al., 2000; Wisdom et al., 1999) and p16 and p21 cdk inhibitors (Passegue and Wagner, 2000). However, in the case of JunD, the effect appears to be cell context dependent and at least in part mediated by the p19/Arf tumor suppressor since primary mouse embryonic fibroblasts (MEFs) lacking *junD* show reduced proliferation and increased p53-dependent senescence (Weitzman et al., 2000). While *c-jun* is regarded as a highly transforming oncogene whose overexpression alone is sufficient for transformation of immortalized rodent fibroblasts and causes density and anchorage independent growth in these cells (Schutte et al., 1989; Vogt, 2001), no transforming activity has been reported neither for JunB or JunD. Furthermore, both JunB and JunD can exert anti-oncogenic effects. Expression of c-Jun is stimulated by Ras signalling and c-Jun is required for Ras-induced transformation since it has been shown that the inhibition of c-Jun reverts the transformed phenotype in fibroblasts (Johnson et al., 1996; Lloyd et al., 1991; Suzuki et al., 1994). Unlike c-Jun that cooperates with Ras in transformation of fibroblasts, JunB and JunD are regarded as negative regulators of Ras-mediated transformation. The level of JunD strongly decreases in Ras-transformed fibroblasts and its overexpression partially suppresses transformation by oncogenic Ha-ras (Pfarr et al., 1994). Similarly, overexpression of *junB* in mouse fibroblasts significantly reduced transformation by v-ras or v-src (Passegue and Wagner, 2000). Eleveted c-Jun levels are often found in tumors and many carcinoma cell lines and it has been shown that ectopic expression of c-Jun in human breast carcinoma cells MCF-7 enhances cell motility and invasion (Rinehart-Kim et al., 2000). In addition, expression of an inducible JunER fusion protein in non-transformed mouse mammary epithelial EpH4 cells, induced incomplete EMT characterized by the loss of cell polarity and a reversible change in cell morphology, but was not sufficient to promote *in vivo* invasiveness (Fialka et al., 1996).

Studies in genetically modified mice have further highlighted the role of Jun proteins in cell proliferation and transformation as well as their role in normal development. While c-Jun and JunB are essential for embryonic development, JunD is dispensable and only required postnatally (Thepot et al., 2000). Surprisingly, overexpression of both c-Jun and JunB in transgenic mice resulted in no overt phenotype (Grigoriadis et al., 1993). However, *c-jun* cooperates with *c-fos*

in the formation of osteosarcomas (Wang et al., 1995; Behrens et al., 2000) Mice lacking *c-jun* die between embryonic day E12.5 and E14.5 and show defects in heart morphogenesis and liver development (Hillberg et al., 1993; Eferl et al., 1999). It was shown that the functions of c-Jun in embryonic development do not depend on N-terminal phosphorylation by JNK (Jun-amino-terminal kinase), since the mice carrying JNK-targeted serine residues (Ser63 and Ser73), replaced by alanines ($Jun^{A/A}$ mice), are viable and develop normally (Behrens et al., 1999). Mouse embryonic fibroblasts (MEFs) lacking *c-jun* exhibit severe proliferation defect and enter premature senescence due to the increased levels of p53 and the cyclin-dependent kinase inhibitor (CKI) p21 (Schreiber et al., 1999). Conditional inactivation of *c-jun* in hepatocytes causes impaired liver regeneration following partial hepatectomy (Behrens et al., 2002). Additional deletion of *p53*, *p21* or *p38α* was able to restore hepatocyte proliferation showing that c-Jun controls liver regeneration by repressing p53/p21 and p38 MAPK activity (Stepniak et al., 2006). Inactivation of *c-Jun* in chondrocytes results in a severe scoliosis due to the impaired formation of intervertebral discs and vertebral arches (Behrens et al., 2003).

JunB deficient mice die at E9.5 due to impaired vasculogenesis and angiogenesis in the extra-embryonic tissues (Schorpp-Kistner et al., 1999). Conditional deletion of *junB* in the embryo proper but not in the placenta using a MORE-Cre allele, rescues the lethality, but such $junB^{\Delta/\Delta}$ mice develop severe osteopenia caused by cell-autonomous defects in osteoclasts and osteoblasts as well as a chronic myeloid leukemia (CML)-like disease (Kenner et al., 2004). On the other hand, *junB* transgenic mice that lack JunB expression specifically in the myeloid lineage also develop transplantable myeloproliferative disease that resembles human chronic myeloid leukemia (Passegue et al., 2001) supporting the anti-oncogenic role for JunB (Eferl and Wagner, 2003). Although $junB^{-/-}$ MEFs proliferate normally in culture, MEFs derived from *junB* transgenic mice show limited proliferation capacity that is directly linked to cyclin D1 repression and CKI p16 induction (Schorpp-Kistner et al., 1999; Passegue and Wagner, 2000).

Interestingly, using knock-in and transgene complementation approaches it was shown that JunB can substitute for c-Jun in mouse development and cell

proliferation in mice, where the entire *c-jun* coding region was removed and replaced by *junB* under the control of the endogenous *c-jun* promoter as well as in *junB* overexpressing mice in a *c-jun* null background (Passegue et al., 2002). Similarly, knock-in of JunD in the c-Jun locus was also able to rescue the lethality of *c-jun*$^{-/-}$ mice until birth (Eferl and Wagner, 2003), whereas double knock-out embryos lacking both c-Jun and JunD died earlier than *c-jun*$^{-/-}$ fetuses (Mechta-Grigoriou et al., 2001). This revealed overlapping functions between c-Jun, JunB and JunD during development despite the described antagonism in cell proliferation and cell transformation and suggested that in the absence of c-Jun, JunB may function as a positive growth regulator (reviewed by Shaulian and Karin, 2002; Eferl and Wagner, 2003). In contrast to c-Jun and JunB, JunD knock-out mice are viable, although slightly growth retarded when compared to control mice and display age-dependent male sterility due to impaired spermatogenesis with incomplete penetrance (Thepot et al., 2000).

Further studies have shown that Jun proteins are key regulators of skin and liver biology and tumorigenesis. Although overexpression of *c-jun* in transgenic mice does not result in an overt phenotype (Grigoriadis et al., 1993), conditional inactivation of *c-jun* in the epidermis interfered with tumor formation in tumor-prone K5-SOS-F transgenic mice in an epidermal growth factor receptor (EGFR) dependent manner (Zenz et al., 2003). Keratinocytes from *c-jun*$^{\Delta ep}$ mice showed severe proliferation defect due to reduced levels of EGFR and its ligand heparin-binding EGF (HB-EGF). In addition, transgenic mice expressing a c-Jun dominant-negative mutant TAM67 (Brown et al., 1993) that lacks the transactivation domain of c-Jun are resistant to DMBA/TPA chemically-induced skin tumorigenesis and human papiloma virus-induced hyperplasia further supporting the role of AP-1 in tumorigenesis (Young et al., 1999; Young et al., 2002a).

Conditional inactivation of *junB* using COL1A2-Cre transgenic mouse line results in delayed wound healing and epidermal hyperproliferation in these mice (Florin et al., 2006). It was recently shown that mice with conditional inactivation of *junB* in the epidermis (*JunB*$^{\Delta ep}$ mice) develop severe skin ulcerations in the face at 2-3 months of age with 100% penetrance. In addition, these mice exhibit osteopenia, myeloproliferative disease and become moribund by 6 months and die at 8-10

months of age (Meixner et al., 2008). Furthermore, it has been shown that the loss of JunB activity enhances MMP-3 expression in an EMT model of mouse skin tumors (Hulboy et al., 2001). On the other hand, inducible deletion of both c-Jun and JunB in the epidermis results in the development of a psoriasis-like disease and arthritis that requires TNFα signalling and both B and T cells, since the deletion in a TNFR-1$^{-/-}$ or a Rag2$^{-/-}$ background resulted in a milder phenotype (Zenz et al., 2005).

1.2.4.2 Functions of Fos proteins

The Fos family of proteins consists of four members; c-Fos, FosB, Fra-1 and Fra-2. In addition, a shorter form of FosB, i.e. ΔFosB (FosB2) can naturally occur due to alternative splicing (Mumberg et al., 1991; Nakabeppu and Nathans, 1991). Since all mammalian *fos* family genes share a similar organization with 4 exons it is believed that they also, like *jun* genes, originated from a common ancestor. Although all Fos proteins share the same affinity for the TRE sequence and dimerize with Jun proteins, they regulate different target genes and therefore have distinct biological functions in different mouse tissues and cell lines (reviewed by Tulchinsky 2000; Eferl and Wagner, 2003). Unlike the Jun proteins that exert specific roles in cell proliferation through regulation of the cell cycle progression, the absence of cell-autonomous proliferation defects in MEFs, lacking distinct Fos family members, suggests a possible functional redundancy between Fos proteins in normal cell-cycle control (Brown et al., 1998; Schreiber et al., 2000; Eferl et al., 2004). Numerous *in vitro* studies, complemented with the *in vivo* analysis of genetically modified mice and primary cells derived thereof, have shown that the Fos proteins are major regulators of tumorigenesis and bone biology (reviewed by Eferl and Wagner, 2003; Wagner and Eferl, 2005; Zenz et al., 2008).

Mice deficient in both c-Fos and FosB are viable and fertile showing that *c-fos* and *fosB* are dispensable for embryonic development. The *fosB*$^{-/-}$ mice do not show a major phenotype (Gruda et al., 1996), except for a behavioural phenotype observed only in one study (Brown et al., 1996). On the other hand, the *c-fos*$^{-/-}$ mice are growth retarded and display severe osteopetrosis due to a differentiation block in

bone resorbing cells, the osteoclasts (Wang et al., 1992; Johnson et al., 1992; Grigoriadis et al., 1994; Matsuo et al., 2000). Transgenic mice that ubiquitously express c-Fos develop bone tumors, osteosarcomas caused by transformed bone producing cells, the osteoblasts (Grigoriadis et al., 1993). In addition, *c-jun* was shown to cooperate with *c-fos* in induction of osteosarcomas, since double transgenic mice develop osteosarcomas at a higher frequency (Wang et al., 1995). The important role of c-Fos in malignant transformation was further supported in a skin carcinogenesis study using *c-fos* deficient mice in a transgenic model of oncogenic Ras. It was shown that these mice fail to undergo malignant progression of skin tumors characterized by the blocked progression of benign papillomas to malignant squamous cell carcinomas (Saez et al., 1995). Moreover, this role of *c-fos* was confirmed in another study using skin-specific conditional expression of *A-fos* transgene, a dominant-negative mutant of c-Fos that inhibits AP-1 DNA-binding. These mice failed to develop benign or malignant squamous cell lesions during chemically-induced skin carcinogenesis, but rather develop benign sebaceous adenomas with the mutation in *H-ras* oncogene (Gerdes et al., 2006). In addition, it was shown that conditional deletion of *c-fos* in the epidermal compartment reduces papilloma formation in tumor prone transgenic mice expressing a dominant form of Son of Sevenless (SOS-F) in basal keratinocytes (K5-SOS-F) (Durchdewald et al., 2008). Furthermore, ectopic expression of an inducible c-Fos protein fused to the hormone-binding domain of human ER - FosER was shown to induce a full EMT in non-transformed mouse mammary epithelial cells (Reichmann et al., 1992). Although c-Fos possesses high transforming potential its expression at the transcriptional level is often inhibited in malignant cells probably due to its capability of repressing its own transcription (Lee et al., 1998).

Interestingly, although described as a *bona-fide* oncogene, it was shown that c-Fos can also exert anti-oncogenic properties. Deletion of *c-fos* in a tumor suppressor *trp53*-deficient background resulted in the development of rhabdomyosarcomas (Fleischmann et al., 2003b). Reexpression of *c-fos* in *trp53/fos* mutant rhabdomyosarcoma cell lines increased the apoptosis of tumor cells proving the pro-apoptotic role and tumor-suppressive role of *c-fos* in this particular cellular context. In addition to its role as positive regulator of apoptosis indicated by *in vivo* studies with *fos-lacZ* reporter mice, where constitutive *c-fos* expression was found

in cell populations undergoing terminal differentiation and at sites of naturally occurring cell death (Smeyne et al., 1993a; Smeyne et al., 1993b), *c-fos* can also negatively regulate cell death, as it was shown that c-Fos-deficient fibroblasts are more susceptible to UV-induced cell death (Schreiber et al., 1995).

Besides its role in bone biology and tumorigenesis, c-Fos participates in the regulation of rather diverse biological processes such as learning. Mice that specifically lack c-Fos in the CNS (*c-fos*$^{\Delta CNS}$ mice) have impairments in behavioural learning as shown in the Morris watermaze task and Pavlovian fear conditioning indicating a role of c-Fos in molecular processes underlying spatial and contextual learning (Fleischmann et al., 2003b). Even though FosB transgenic mice do not show an overt phenotype (Grigoriadis et al., 1993), a significant correlation of *fosB* expression and well-differentiated, estrogen/progesterone receptor positive status was reported for human breast tumors (Bamberger et al., 1999). Furthermore, overexpression of FosB splice variant -ΔFosB in mice causes osteosclerosis and interferes with normal cell differentiation of osteoblasts and thymocytes (Carrozza et al., 1997; Sabatakos et al., 2000).

Unlike c-Fos and FosB that are dispensable for embryonic development and postnatal survival, Fra-2 is required for pups survival beyond day 5 (Eferl et al., 2007). These pups exhibit severe growth retardation, runted appearance and develop severe osteopenia characterized by giant osteoclasts as early as embryonic day E18.5 (Eferl et al., 2007; Bozec et al., 2008). In addition, the mutant pups exhibit heart, gut and cartilage defects (A. Bozec and R. Eferl pers.comm.; Karreth et al., 2004). Ectopic expression of Fra-2 in transgenic mice causes fibrosis in several organs, although it mainly affects the lung. Furthermore, these mice show increased bone mass and rare fibrosarcoma occurrence in head/neck region (Eferl et al., 2008).

Although Fra-2 lacks the C-terminal transactivating domain present in c-Fos and FosB and consequently fails to transactivate artificial AP-1-responsive promoters *in vitro* (Wisdom and Verma, 1993; Tulchinsky, 2000), leading to lower transforming activity compared with c-Fos, several recent reports indicate that it might play an important role *in vivo* in the progression of various human tumors (Milde-Langosch,

2004; Milde-Langosch, 2005). Fra-2 expression level was found increased in a variety of transformed and neoplastic cells (Mechta et al., 1997; Murakami et al., 1997) as well as in breast cancer cell lines and tumor tissues (Bamberger et al., 1999; Milde-Langosch et al., 2008) suggesting a role for Fra-2 in breast cancer progression.

1.2.4.2.1 Fra-1 structure and regulation

The cellular immediate early gene *fra-1* (Fos-related antigen 1; also termed *fos*-like 1, *fosl1*) encodes the AP-1 protein Fra-1 which belongs to the *fos* gene family. It was originally identified due to the antigenic similarity of the protein to the peptide used for raising anti-c-Fos antibodies (Cohen and Curran, 1988). It shares a high degree of homology with other Fos proteins and it is positively regulated by AP-1 activity itself via three AP-1-like binding sites in the first intron of the *fra-1* gene (Brüsselbach et al., 1995: Bergers et al., 1995). It has been shown that *fra-1* is a transcriptional target of *c-fos*, whose induction upon growth factor stimulation is delayed and prolonged compared to *c-fos* (Cohen and Curran, 1988; Bergers et al., 1995; Schreiber et al., 1997; Matsuo et al., 2000). In addition, *fra-1* can transactivate its own promoter and thereby influence its expression level by a positive autoregulatory mechanism in a RAS- and extracellular signal-regulated kinase (ERK)-dependent manner (Casalino et al., 2003). Although *fra-1* does not harbour a potent transactivation domain and was originally proposed to act as transcriptional repressor, recent studies have shown that it is also able to positively regulate transcription, a feature that is not directly linked to the transactivation ability (Andersen et al., 2002; and reviewed in Young and Colburn, 2006). Even though Fra-1 only marginally induced the activity of the synthetic AP-1-responsive reporter, it successfully induced the transcription of several genes including uPA and thrombospondin-1 in murine epithelioid adenocarcinoma (CMSL0) cells. This feature of Fra-1 was proposed to be dependent on the context of natural enhancers and recruitment of other transcription factors different from Jun (Andersen et al., 2002). In addition, the N-terminal domain of Fra-1 which is not conserved in the Fos proteins, and is more potent in Fra-1 than in the c-Fos protein (Matsuo et al., 2000), was proposed to be involved in such interactions.

Another study using neoplastic transformation resistant (ERK-deficient-P^-) and transformation sensitive (ERK-sufficient-P^+) JB6 mouse epidermal cell lines, has shown that the transactivation domain of Fra-1 can be activated. This Fra-1 activation is ERK-dependent and requires Thr-231(Young et al., 2002b; Chalmers et al., 2007). In addition, it has been shown that the increased ERK activity is required to prevent the proteasomal degradation of Fra-1 in human colon carcinoma cell lines expressing the K-RAS or B-RAF oncogenes (Hurd et al., 2002, Vial and Marshall, 2003). In a region highly homologous to c-Fos, Fra-1 contains a single C-terminal destabilizer that is targeted by ERK phosphorylation at two serine residues, Ser252 and Ser265. This phosphorylation increases the stability of Fra-1 and inhibits its proteasome-dependent degradation in response to MEK pathway activators. In addition to phosphorylation by ERK1/2, it is speculated that Fra-1 stability is controlled by other MAP kinases such as ERK5 (Young et al., 2002b; Terasawa et al., 2003). In addition, in a very recent study, it was shown that Fra-1 expression is stimulated by RSK kinase both at the transcriptional and posttranscriptional levels (Doehn, et al., 2009).

1.2.4.2.2 Biological function of Fra-1

Although the initial studies reported that Fra-1 lacks a functional transactivation domain and was originally proposed to function as a negative regulator of AP-1 activity (Suzuki et al., 1991; Wisdom and Verma, 1993; Yoshioka et al., 1995; Bergers et al., 1995), a number of *in vitro* and *in vivo* studies have shown that it is essential for embryonic development and involved in the regulation of cell proliferation, differentiation, apoptosis, cell motility and invasiveness (Schreiber et al., 2000; Jochum et al., 2000; Eferl et al., 2004; Kustikova et al., 1998; Belguise et al., 2005; Milde-Langosch, 2005). Conventional *fra-1* knockout mice die *in utero* between embryonic day E10 and E10.5 due to defects in the vascularisation of the placenta. In addition, mutant fetuses are severely growth retarded. Interestingly, this growth retardation does not seem to be due to a cell-autonomous defect, since primary MEFs and ES cells have a normal proliferation rate in culture (Schreiber et al., 2000). The lethality can be rescued either by injection of *fra1*$^{-/-}$ ES cells into tetraploid wild-type blastocyts (Schreiber et al., 2000) or by MORE-Cre-mediated

embryo-specific deletion of *fra-1* (Eferl et al., 2004). These *fra1*$^{\Delta/\Delta}$ mice are viable but develop osteopenia, a low bone mass disease that is characterized by decreased production of extracellular bone matrix components, mainly collagen1a2 and matrix Gla protein. Transgenic mice overexpressing *fra-1* in a broad range of organs develop osteosclerosis due to accelerated differentiation of osteoprogenitors into mature bone forming osteoblasts (Jochum et al., 2000) as well as lung fibrosis. Interestingly, Fra-1 is a transcriptional target of c-Fos during osteoclast differentiation (Matsuo et al., 2000) and can functionally substitute for c-Fos in bone development in a dosage-dependent manner (Fleischmann, et al., 2000). Moreover, Fra-1 was able to substitute for c-Fos in light-induced photoreceptor apoptosis, but in contrast failed to substitute for c-Fos in inducing target genes in fibroblasts. Interestingly, Fra-1 was only partially able to replace c-Fos functions in hippocampal synaptic plasticity and behavioural learning (Gass et al., 2004).

1.2.4.2.3 Fra-1 in cancer development

Although *fra-1* transgenic mice do not show a cancer phenotype, and its expression seems to be dispensable for tumor induction and tumor-cell proliferation in a mouse model of chemically-induced colitis-associated cancer (CAC) (Hasselblatt et al., 2008), recent reports have strongly implicated Fra-1 in cancer progression. The initial studies have shown that ectopic expression of Fra-1 in Rat-1 fibroblasts was sufficient for anchorage-independent growth *in vitro* and tumor formation in nude mice (Bergers et al., 1995). Furthermore, Fra-1 was found overexpressed and shown to be essential for the transformed phenotype in mouse fibroblasts and RAS-transformed thyroid cells (Mechta et al., 1997; Vallone et al., 1997). Screening for *ras* transformation targets identified *fra-1* as one of the highly transcriptionally upregulated genes, supporting previous results that showed Fra-1 to be the major Fos family member expressed upon Ras transformation in mouse fibroblasts (Mechta et al., 1997; Zuber et al., 2000). Another study using two mouse mammary adenocarcinoma cell lines with distinct metastatic capabilities showed that Fra-1 expression is elevated in highly metastatic line (CMSL 100), while almost absent in the non-metastatic (CSML0) cell line (Kustikova et al., 1998; Tkach et al., 2003). It

was shown that Fra-1 expression correlated with mesenchymal characteristics of the cells and that its ectopic expression in non-metastatic cell line caused morphological and molecular changes reminiscent to EMT accompanied by upregulation of several genes involved in cell migration, metastasis and angiogenesis (Kustikova et al., 1998). Several recent studies using highly metastatic and non-metastatic cancer cell lines combined with gene expression profiling have shown that Fra-1 regulates the expression of genes involved in cancer progression and correlates with the invasive potential of the cells (Ramos-Nino et al., 2003; Song et al., 2005; Belguise et al., 2005; Debinski and Gibo, 2005; Chiappetta et al., 2007).

In human, Fra-1 overexpression was found associated with a variety of epithelial tumors. These include thyroid, breast, lung, brain, nasopharyngeal, esophageal, endometrial, prostate, colon and head and neck squamous cell carcinomas, as well as glioblastomas and mesotheliomas (Milde-Langosch, 2005; Young and Colburn, 2006; Verde et al., 2007). Recently, the prognostic relevance of Fra-1 has been well documented for breast cancer, where it is regarded as a marker for the aggressive phenotype (Belguise et al., 2005; Giancotti 2006; Chiappetta et al., 2007). Gene expression profiling of 22 human mammary epithelial cell lines revealed consistent overexpression of Fra-1 in highly aggressive cell lines (Zajchowski et al., 2001). In that study, among 588 studied genes potentially important in human cancer, only Fra-1 and vimentin were found to be consistently associated with highly aggressive phenotype. Besides this prognostic value, Fra-1 also presents a potent anti-cancer therapeutic target as it was shown that an oral DNA vaccine encoding murine Fra-1 and coexpressing secretory murine interleukin 18 induced an effective cellular immune response capable of eradicating established breast cancer metastasis in mice and induced long-lived T-cell memory against tumor recurrence (Luo et al., 2003; Luo et al., 2005).

Taken together, there is a growing body of evidence that highlights the important role for Fra-1 in cancer progression, its role as a prognostic marker at least in some cancer types, as well as its role as a potential anti-cancer therapeutic target.

2. Aim of the thesis

The aim of my PhD project was to investigate the role of Fra-1/AP-1 in induction and regulation of epithelial-mesenchymal transition (EMT) and carcinogenesis.

Cancers of epithelial origin are the most prevalent type of cancer in humans. In recent years, it is becoming more evident that EMT plays a central role in late stage cancer progression and metastasis. Recent investigations have reported that there is a significant correlation between increased Fra-1 expression and the invasive behaviour of several cancer cell lines and human tumors. Since Fra-1 was implicated in the regulation of cell motility and invasiveness, I was interested to determine whether this might be directly linked to the induction of EMT. To address this, I employed the well characterized EpH4/EpRas cellular model of EMT, where it was previously shown that the prolonged activation of c-Fos, and to a lesser extend of c-Jun, is able to induce cellular depolarization with features of EMT. Based on the observation that Fra-1 expression correlates with EMT in this system, I have used *in vitro* gain-of-function and loss-of-function approaches combined with *in vivo* xenograft transplantation experiments to better define the specific aspects of Fra-1 function. Finally, I employed genome-wide gene expression profiling to identify potential direct transcriptional targets of Fra-1/AP-1.

3. Results

PART I.

Investigating the role of Fra-1 in EMT: generation and characterization of EpH4-*fra1* and EpRas-*fra1* cells

3.1 Fra-1 expression level correlates with EMT in EpH4/EpRas cell system

Initial analysis of the expression pattern of AP-1 members in EpH4/EpRas cell system revealed a significant increase in Fra-1 expression that correlates with EMT (**Figure 6 A-B**). Detectable Fra-1 expression is low both on RNA and protein level in epithelial and non-tumorigenic EpH4 cells.

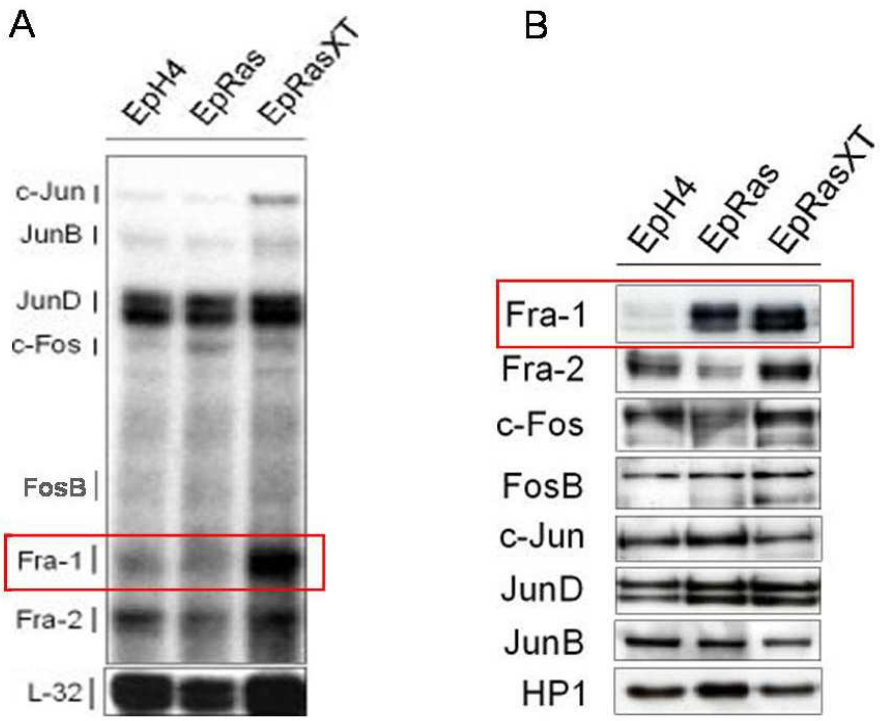

Figure 6. Expression of AP-1 members in EpH4/EpRas cell system. Expression of AP-1 members was analysed by RNase protection assay (RPA) (A) and Western blot (B). Bands corresponding to Fra-1 transcript (A) or protein (B) are highlighted by red square box.

Interestingly, it is increased in both tumorigenic EpRas cells and mesenchymal EpRasXT cells (see above, **Figure 6A-B**). EpRas cells were originally derived from EpH4 cells by stable overexpression of oncogenic Ha-RasV12 and-although still epithelial-undergo an EMT *in vitro* after treatment with TGF-β1 or *in vivo* upon orthotopic injections into immunocompromised mice (Oft et al., 1996). This observation is consistent with published studies that have reported increased Fra-1 expression upon activation of Ras signalling (Mechta et al., 1997; Zajchowski et al., 2001; Casalino et al., 2003). Further increase in Fra-1 transcript and protein levels was detected in the mesenchymal EpRasXT cells isolated from primary tumors formed by EpRas cells. These cells have undergone an EMT and show a mesenchymal phenotype sustained by a TGF-β1 autocrine loop and only partially reversible by TGF-RI kinase inhibitors (Oft et al., 1996). No other member of the AP-1 family showed such a striking correlation of their expression with EMT in this system. An increase in transcripts of all three Jun members was detected in EpRasXT cells although it was most prominent in the case of c-Jun (**Figure 6A**). However, when compared with the total protein levels the corresponding increase could only be confirmed for JunB and JunD (**Figure 6B**) suggesting that the expression of c-Jun in EpRasXT cells is most likely regulated at the posttranscriptional level. Although FosB transcript levels were unchanged, the protein level was slightly increased in EpRasXT cells (**Figure 6A-B**). This suggests that the detected increase of FosB protein in EpRasXT cells is most likely due to increased protein stability rather than transcriptional upregulation. The expression of c-Fos and Fra-2 was also increased both at the mRNA- and protein level in EpRasXT cells when compared to EpH4 cells. However, an increase in c-Fos mRNA in EpRas cells did not correspond to the protein level that was decreased. This is most likely due to decreased protein stability. Interestingly, in the case of Fra-2 that was highly expressed in EpH4 cells a significant decrease in both transcript and protein levels was detected in EpRas cells followed by strong upregulation in EpRasXT cells. Furthermore, in EpH4 and EpRas cells, Fra-1 and Fra-2 showed an inverse correlation in their expression pattern both on mRNA and protein levels that might possibly reflect different functional roles for Fra-1 and Fra-2 in normal and transformed cells. However, the expression of both genes was highly upregulated following EMT in EpRasXT cells, suggesting that they both might be involved in the maintenance of a mesenchymal phenotype. The observed,

overall increased expression of AP-1 members in mesenchymal EpRasXT cells clearly indicated that AP-1 plays a role in EMT. However, the strong correlation of Ras activation and EMT, and the matching increased expression detected only in the case of Fra-1 suggested that Fra-1 might be the major Fos family member involved in both induction and maintenance of EMT in this system.

3.2 Exogenous overexpression of Fra-1 in EpH4 and EpRas cells

To investigate whether Fra-1 is able to induce EMT I stably overexpressed Fra-1 in EpH4 and EpRas cells. For this, cells were infected with retroviral vector pBabe*fra-1*-PURO or the control vector pBabe-PURO (Matsuo et al., 2000). Pools of infected cells were selected in the presence of puromycin for 14 days and single-cell clones were subsequently derived. Based on their altered, less epithelial appearance, I have selected several clones from each cell type and analysed them for Fra-1 expression (data not shown). Following confirmation of increased Fra-1 expression, I have selected two highly expressing clones of each cell type for further characterization. The expression of Fra-1 was significantly increased in all selected clones both on mRNA and protein level (**Figure 7A-B**), while it remained unchanged in the control cells. The clone with lower ectopic Fra-1 expression was designated as clone 1, while the higher Fra-1 expressing clone is referred to as clone 2. In EpH4 cells that normally express significantly lower levels of Fra-1 than EpRas or EpRasXT cells, I was able to increase Fra-1 protein expression by 4.7 and 8.5 fold. However, in EpRas cells that already express an intermediate level of Fra-1, when compared to EpH4 and EpRasXT cells, I was able to further increase the expression of Fra-1 protein by 1.9 and 2.5 fold (**Figure 7B**). Interestingly, in EpRas-*fra1* and to a lesser extent in EpH4-*fra1* cells, an increase in slower migrating protein, most probably corresponding to previously published hyperphosphorylated form of Fra-1 (Gruda et al., 1994; Vial and Marshall, 2003) was detected by Western blot (**Figure 7B**).

Several studies have reported that increased Fra-1-phosphorylation, mediated mainly by MAPK-ERK, increases Fra-1 protein stability and protects it from protesomal degradation (Casalino et al., 2003; Vial and Marshall, 2003). Therefore,

I have checked the protein levels of total and active ERK1/2 in these cells to determine whether the observed increase in slower migrating Fra-1 protein might be due to increased ERK activity (**Figure 8**). Although total ERK protein levels remained unchanged in EpH4-*fra1* cells, I detected a marked increase in phospho-ERK1/2 levels (**Figure 8**, lane 1-3).

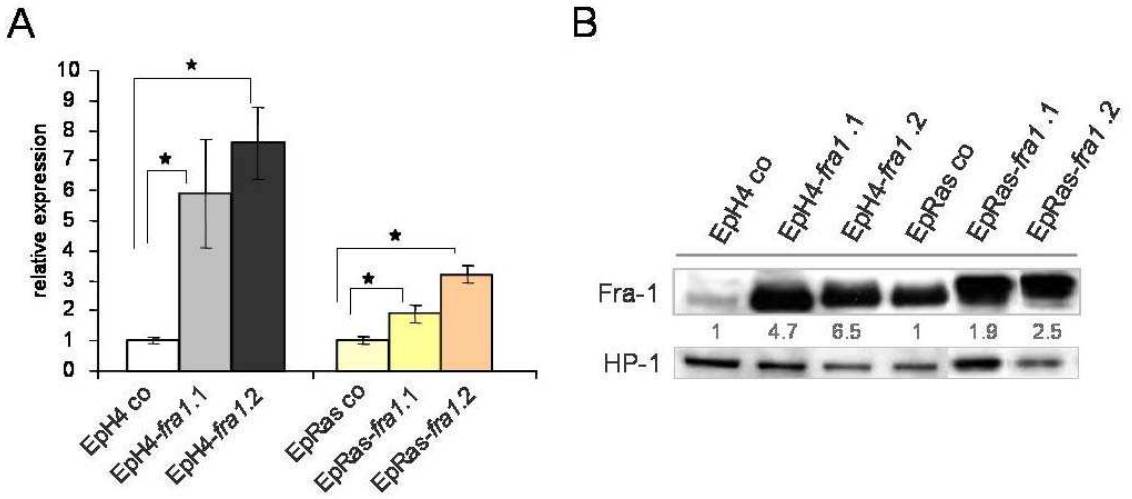

Figure 7. Fra-1 overexpression in EpH4 and EpRas cells. (A) Total RNA was isolated from cells and *fra-1* expression was analysed by quantitative real-time RT-PCR (qPCR). All selected clones show a significant increase in *fra-1* transcript when compared to respective control cells. **(B)** Fra-1 protein levels in nuclear extracts were determined by Western blot. HP-1 was used as the loading control. Quantification of bands after normalisation for loading is shown as fold change when compared to the respective control cells. Results are shown as mean values, error bars represent the standard deviation; *p-values* ≤ 0.05 were considered significant (*).

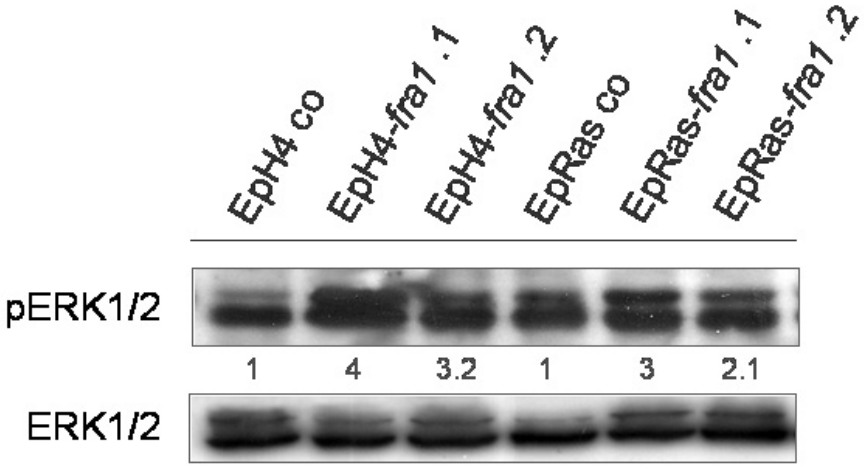

Figure 8. Increased ERK1/2 kinase activity upon Fra-1 overexpression. Total cell extracts were analysed by Western blot to detect the expression of total and phospho-ERK1/2. Expression levels of pERK1/2 were normalised to total ERK1/2 level.

Phosphorylation of ERK is necessary for its activation and translocation to the nucleus (Hill and Treisman, 1995; Lewis et al., 1998). Once in the nucleus, ERK1/2 can phosphorylate and thereby activate a number of transcription factors, including Fra-1(Hurd et al., 2002; Young et al., 2002b; Yang et al., 2003). Interestingly, in EpRas-*fra1* cells I have observed an increase in both total and active ERK1/2 levels when compared to the control cells (**Figure 8**, lane 4-6). The observed overall increase in active ERK1/2 is consistent with previously published results that have reported a positive correlation in Fra-1 expression and MAPK-ERK activity (Young et al., 2002b; Casalino et al., 2003; Vial and Marshall, 2003). Therefore, it is likely that the detected accumulation of slower migrating Fra-1 protein might be due to its hyperphosphorylation mediated by ERK kinases. However, the exact link between increased activities of ERK kinases as a consequence of ectopic Fra-1 expression remains to be determined.

Next, I have analysed the effect of ectopic Fra-1 expression on the expression of other AP-1 members by RNase protection assay (RPA) (**Figure 9A-B**), quantitative real-time RT-PCR (qPCR) (**Figure 9C**) and Western blot (**Figure 10**). RPA analysis did not reveal a strong effect of Fra-1 overexpression on the transcription of other AP-1 members. Even though I could observe a slight decrease in Fra-2 transcript levels in both EpH4-*fra1* and EpRas-*fra1* cells, the expression of c-Fos was not strongly affected and FosB transcript was not detectable by RPA in none of the cells. However, I could detect an increase in c-Jun and JunB transcript levels in all Fra-1 expressing cells by the same method. Interestingly, in contrast to the results obtained by the RPA, qPCR analysis revealed upregulaton of c-Fos, and to a lesser extent FosB mRNA in EpH4-*fra1* cells. Similarly, in EpRas-*fra1* cells, I detected transcriptional downregulation of c-Fos, FosB and Fra-2 by qPCR. In accordance with the results obtained by the RPA, qPCR analysis revealed upregulation of c-Jun and JunB mRNA in EpH4-*fra1* cells (**Figure 9C**). However, in contrast to the results obtained by the RPA, in EpRas-*fra1* cells, no significant change in JunB mRNA (data not shown) and downregulation of c-Jun mRNA was detected by qPCR. These discrepancies, between the results obtained by these two methods, are most probably due to higher sensitivity of the qPCR method. In addition, the inability to detect FosB transcripts by the RPA in none of the cells, even though qPCR

analysis revealed its transcriptional regulation, might be due to low quality or specificity of the provided FosB probe used for the RPA analysis.

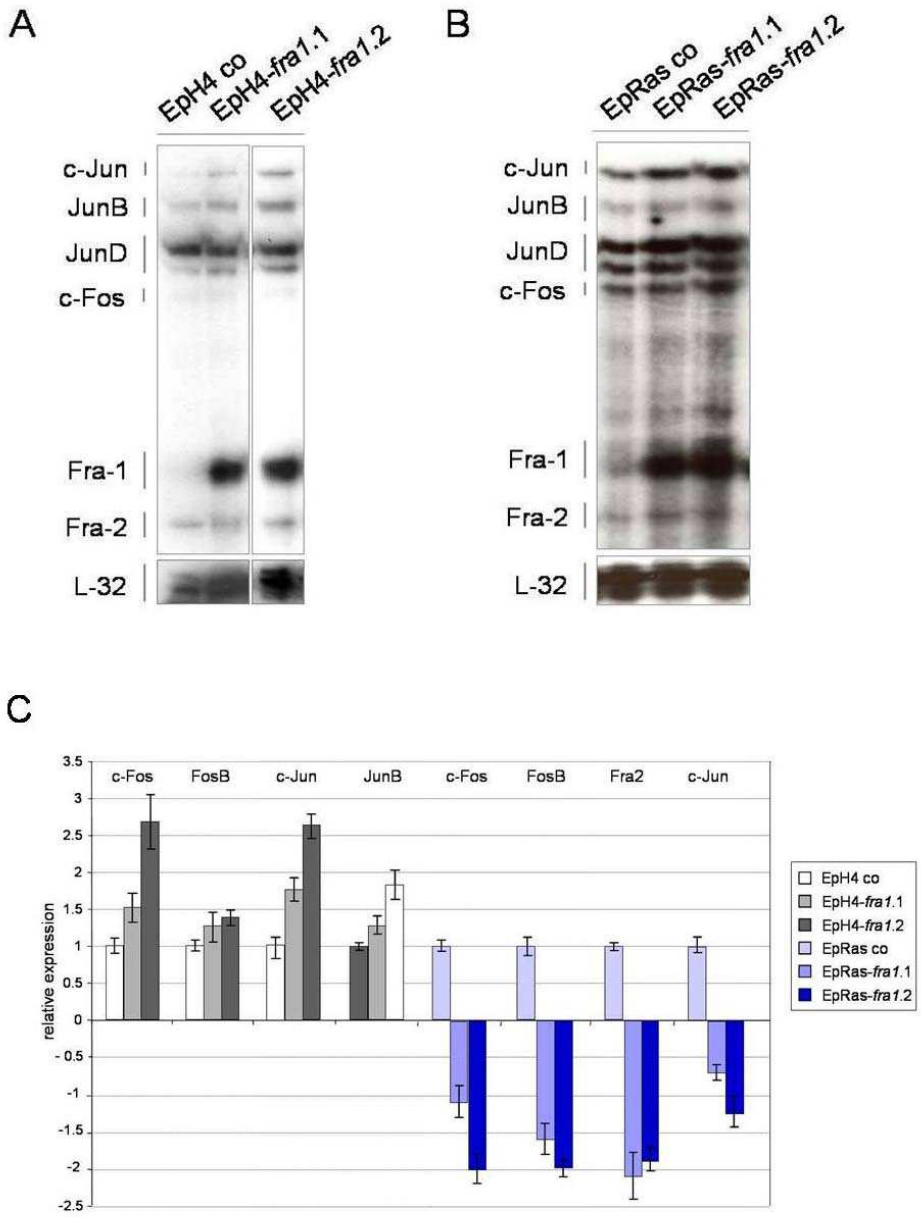

Figure 9. Transcriptional regulation of AP-1 members in EpH4-*fra1* and EpRas-*fra1* cells. The effect of Fra-1 overexpression on the expression of other AP-1 members was analysed by RNase protection assay (RPA) **(A and B)** and qPCR **(C)**. Data are presented as mean and error bars are indicated.

Interestingly, when I compared the mRNA levels of AP-1 members with the corresponding protein levels, I have observed a stronger effect of Fra-1 expression

on the expression of other AP-1 members (**Figure 10**). Both Fra-2 and c-Fos protein levels were downregulated in all Fra-1 expressing cells. The downregulation of Fra-2 protein was most probably transcriptional in nature, since a similar decrease in its transcript levels was detected both by RPA and qPCR. However, unlike in the EpRas-*fra1* cells, in which the decreased levels of c-Fos protein corresponded to the detected downregulation of c-Fos mRNA, the downregulation of c-Fos protein in EpH4-*fra1* cells did not match with the level of transcript detected by qPCR. This result suggested that c-Fos expression was most likely modulated at the posttranscriptional level in these cells.

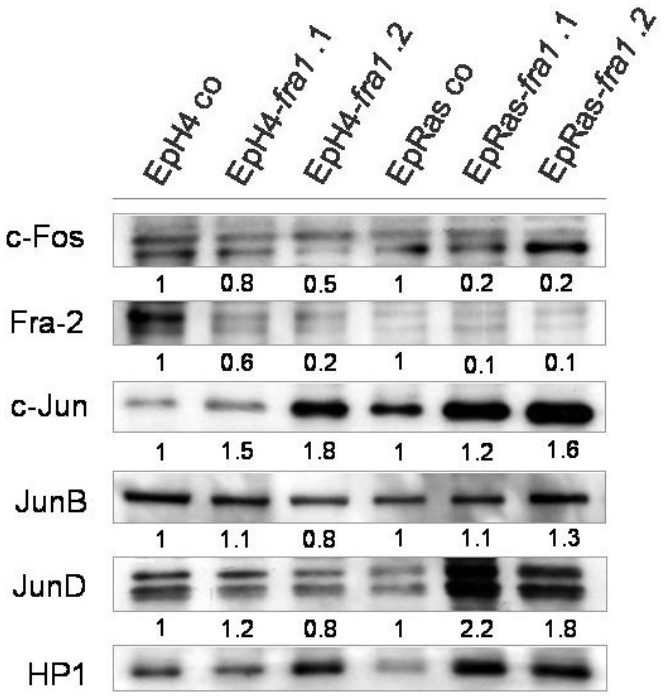

Figure 10. Expression of AP-1 proteins in EpH4-*fra1* and EpRas-*fra1* cells. Differential expression of AP-1 proteins following Fra-1 overexpression was determined by Western blot. Quantification of protein bands after normalisation for loading is shown as fold change when compared to the respective control cells.

Furthermore, protein levels of all three Jun members were increased in all Fra-1 expressing cells. Only in case of the EpH4-*fra1*.2 clone, a slight decrease in JunB and JunD levels was observed. There was a good correlation in increased levels of c-Jun and JunB mRNA and protein levels in EpH4-*fra1* cells, suggesting their transcriptional regulation. However, even though JunD protein levels were increased in all Fra-1 expressing cells, no significant difference in mRNA levels

could be detected. This suggested that JunD expression is most likely regulated at the posttranscriptional level. The same was true for the expression of JunB in EpRas-*fra1* cells (**Figure 10**). Similarly, even though I detected a slight downregulation of c-Jun mRNA by qPCR in EpRas-*fra1* cells, its protein levels were increased, suggesting that c-Jun is also regulated at posttranscriptional level in EpRas-*fra1* cells.

To examine the effect of ectopic Fra-1 expression on the composition of AP-1 complexes, I performed qualitative and quantitative analysis using colorimetric ELISA-based assay (**Figure 11**). Nuclear extracts were incubated in 96-well plates with immobilized synthetic oligonucleotides containing the TRE element. AP-1 complexes bound to these oligonucleotides were detected by addition of antibodies specific for the different AP-1 protein, followed by incubation with horseradish-peroxidase conjugated secondary antibody and colorimetric evaluation by spectrophotometry.

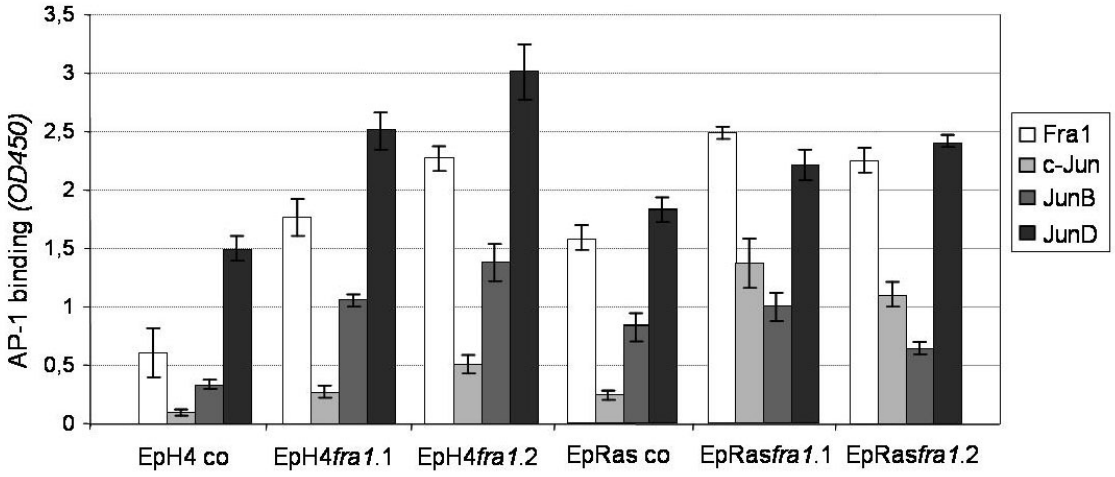

Figure 11. Qualitative and quantitative analyses of the TRE-bound AP-1 complexes. Nuclear extracts from EpH4-*fra1* **and** EpRas-*fra1* cells were assayed using TransAm AP-1 Family transcription assay ELISA-based kit.

In all Fra-1 expressing cells, an overall increase in AP-1 binding to the synthetic TRE-containing oligonucleotides was detected. However, qualitative and quantitative composition of TRE-bound AP-1 complexes did not significantly differ

between EpH4-*fra1* and EpRas-*fra1* cells. In EpH4 control cells, Fra-1, JunB and JunD were identified as major components of AP-1 complexes. Interestingly, upon ectopic Fra-1 expression, in addition to 2-3 fold increase in Fra-1 binding, 3-fold and 5-fold increase in c-Jun binding was detected. Similarly, roughly 3-fold and 5-fold increase in JunB, and 1.5-fold and 2-fold increase in JunD binding was detected. However, no overall change in Fos proteins other than Fra-1 was detected. This indicated that the TRE-bound AP-1 complexes upon Fra-1 overexpression are mainly composed of Fra-1, JunB, JunD and c-Jun (**Figure 11**). Similarly, in EpRas control cells, the major identified components of TRE-bound AP-1 complexes were again Fra-1, JunB and JunD. However, upon Fra-1 overexpression, only c-Jun binding was significantly increased. No significant change in JunD and JunB binding as well as binding of other Fos members other than Fra-1, could be observed (**Figure 11**). This indicated that in EpRas-*fra1* cells, just like in EpH4-*fra1* cells, TRE-bound AP-1 complexes are mainly composed of c-Jun, JunB, JunD and Fra-1.

An unexpected finding was that in EpH4 control cells, Fra-1 seemed to be the predominant Fos member of the TRE-bound AP-1 complexes, even though EpH4 control cells express very low detectable levels of Fra-1 protein. Furthermore, the involvement of Fra-2 in the formation of an AP-1 complex was rather low, even though much higher levels of Fra-2 protein were detected by Western blot using the same nuclear extracts. The most likely explanation for this discrepancy could be the low specificity and cross-reactivity of Fra-1 antibody which was provided with the kit. It is likely that, due to cross-reactivity of Fra-1 antibody with Fra-2 protein, a false readout was obtained. Other possible explanations could be that even though detectable Fra-1 protein levels are low in EpH4 cells, it actively participates in the formation of AP-1 complexes. Nevertheless, a good correlation between the levels of Jun proteins detected by Western blot and this assay was observed. This suggests that most likely the problem of the assay is low specificity of Fra antibodies provided with the kit. Taken together, I conclude that an increase in Fra-1, c-Jun, JunB and JunD binding to synthetic TRE-containing oligonucleotides correlates with increased protein levels detected by Western blot.

3.3 Ectopic Fra-1 expression increases cell proliferation and causes prominent morphological changes in EpH4 and EpRas cells

As a next step, I examined the cells for their proliferation capacity and morphology. All Fra-1 expressing cells showed a significant increase in proliferation rate when compared to the respective control cells (**Figure 12A-B**).

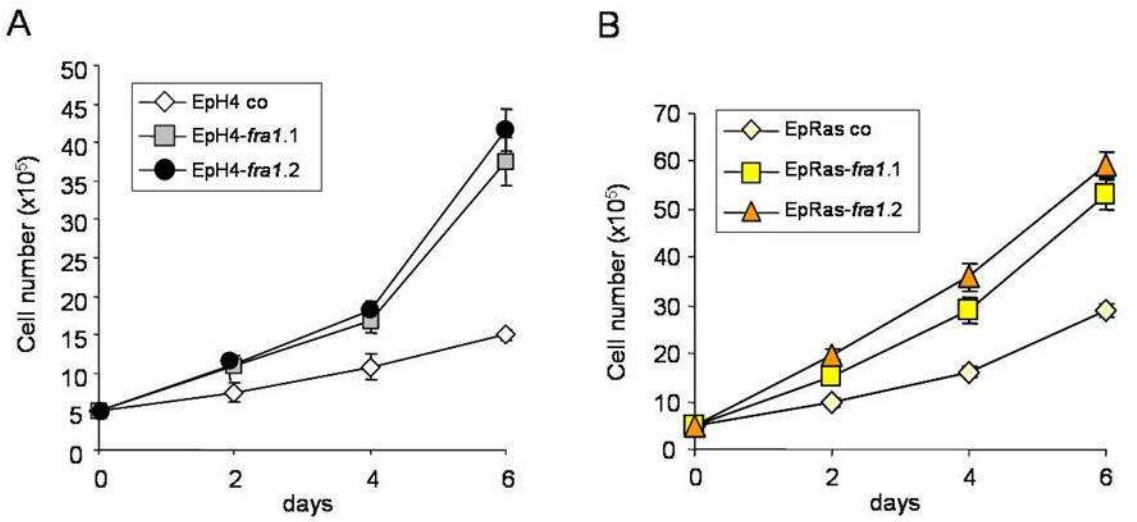

Figure 12. Stable Fra-1 expression in EpH4 and EpRas cells increases cell proliferation rate. Growth curves of EpH4-*fra1* **(A)** and EpRas-*fra1* **(B)** cells show increased proliferation when compared to respective control cells. The cells were grown in standard growth medium and counted in 48h intervals. Mean cumulative cell number values determined in triplicate cultures are shown, plotted against time.

This observation is consistent with recent reports that have identified Fra-1 as a positive regulator of cell proliferation (Belguise et al., 2005; Casalino et al., 2007; Song et al., 2007). In addition to increased proliferation rate, both EpH4-*fra1* and EpRas-*fra1* cells showed dramatic changes in cell shape (**Figure 13A-B**, upper panel). While the control cells retained a fully polarized epithelial morphology, Fra-1 expressing cells acquired a fibroblastoid morphology. The cells became elongated and spindle-shaped forming long cellular protrusions. Furthermore, when grown at low densities, these cells no longer formed epithelial cell clusters but displayed a strong scattering phenotype. In addition, Fra-1 expressing cells have lost cell-contact mediated growth inhibition and were able to grow in a multilayered fashion upon reaching confluence (data not shown).

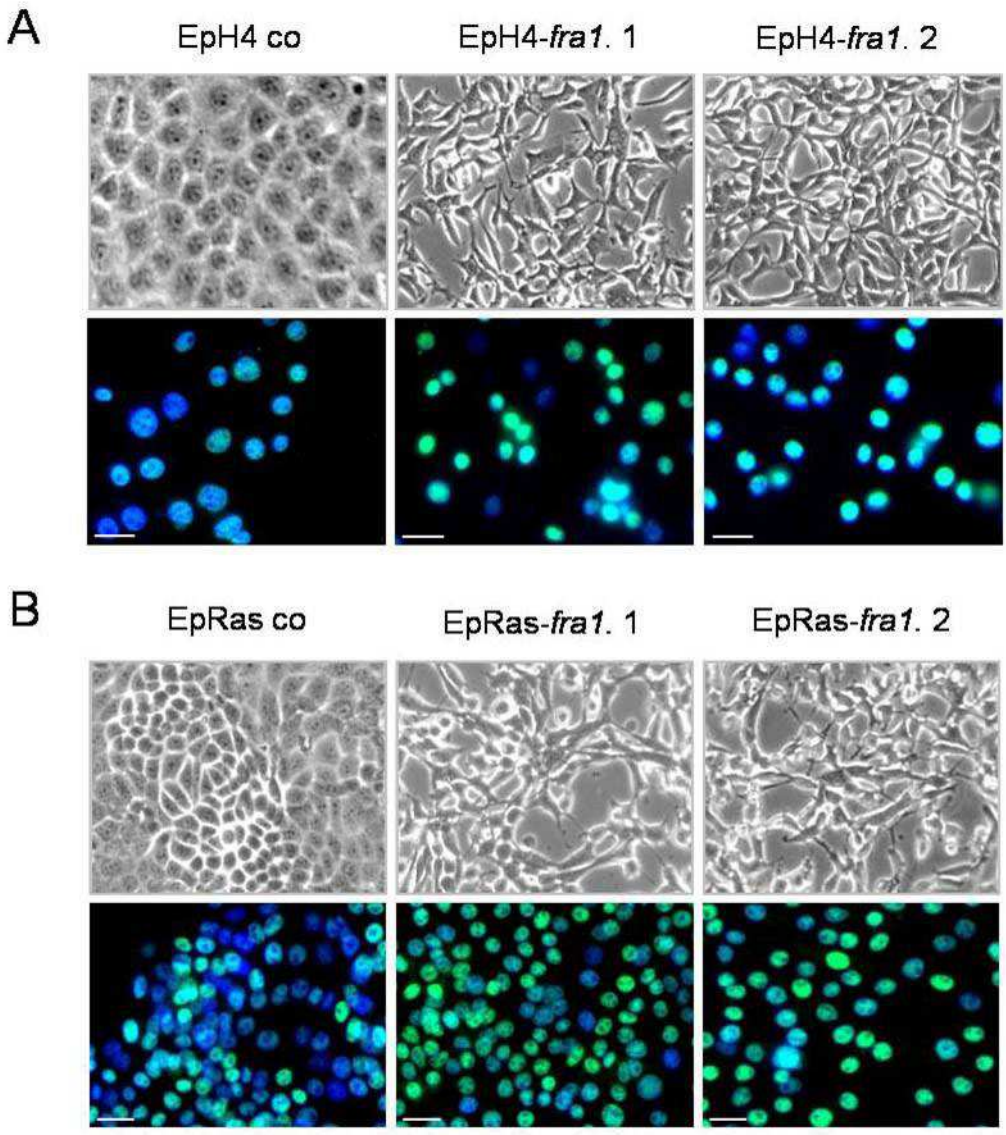

Figure 13. Ectopic Fra-1 expression in epithelial EpH4 and EpRas cells causes a conversion to fibroblastoid morphology. Phase contrast images of EpH4-*fra1* **(A)** and EpRas-*fra1* **(B)** cells and their respective control cells are shown in the upper panels. Fra-1 protein expression and subcellular localisation was determined by immunofluorescence and is shown in the lower panels. Nuclei were counterstained with DAPI (blue). Scale bar, 20µM.

To determine whether this apparent morphological switch corresponds to Fra-1 expression, I have checked the expression and subcellular localization of Fra-1 by immunofluorescence. Immunofluorescence analysis revealed strong and exclusively nuclear signal in all Fra-1 expressing clones (**Figure 13A-B;** lower panel). This indicated that the exogenous protein is efficiently transported into the nucleus where it is transcriptionally active (**Figure 13A-B;** lower panel). Additionally, these results also suggested that the observed morphological switch

from epithelial to fibroblastoid morphology could be directly correlated to ectopic Fra-1 expression.

To further investigate the effect of Fra-1 expression on the epithelial cell phenotype, I analysed the cells for actin cytoskeleton organization. Immunofluorescent analyses revealed extensive cytoskeletal rearrangements in all Fra-1 expressing cells (**Figure 14 A-B**).

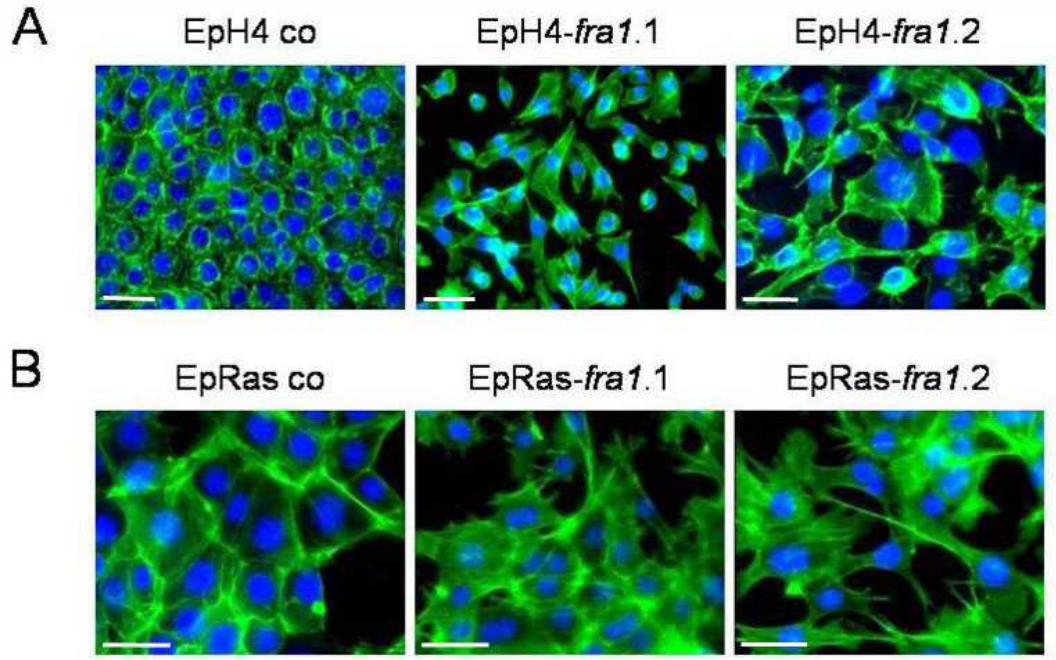

Figure 14. Cytoskeletal rearrangements in Fra-1overexpressing cells. EpH4cells grown on porous support were stained with Alexa488-coupled phalloidin to visualize F-actin. Nuclei were counterstained with DAPI (blue). Magnification is 20X. Scale bar, 20μM.

Both EpH4 and EpRas control cells showed strictly cortical actin distribution characteristic for polarized epithelial cells. However, all Fra-1 expressing clones formed extensive lamellipodia. In addition, the cells displayed strong accumulation of actin-rich structures forming membrane ruffles mainly located at the leading edge of numerous cellular protrusions. Such cytoskelatal organization is characteristic of highly motile fibroblastoid cells. These results clearly showed that Fra-1 expression was sufficient to induce an epithelial to fibroblastoid conversion of EpH4 and EpRas cells.

3.4 Fra-1 expressing cells show increased motility and invasiveness *in vitro*

As fibroblastoid morphology is characteristic of highly motile and migratory cells, I have next examined the migration potential of EpH4-*fra1* and EpRas-*fra1* cells using two independent assays. An *in vitro* wound-healing assay clearly indicated that ectopic Fra-1 expression results in a significant increase in random motility of the cells. However, this effect was more pronounced in EpH4-*fra1* cells (**Figure 15A**). The cells no longer migrated in a form of a sheet but rather invaded the wound area as single cells. Furthermore, the overall migration capacity of both EpH4-*fra1* and EpRas-*fra1* cells was markedly increased as shown by accelerated wound closure (**Figure 15 A-B**).

To further confirm these findings and quantify the migration capacity of the cells, I performed direct transwell migration assays (**Figure 15C**). This assay again revealed a significant increase in migration capacity of both EpH4-*fra1* and EpRas-*fra1* cells. The overall migration of EpH4-*fra-1* and EpRas-*fra1* cells was increased roughly 5-fold and 2-3-fold, respectively. An additional feature of cells undergoing EMT is increased invasiveness that is in part linked to enhanced motility. To determine the invasive potential of Fra-1 expressing cells, I have performed Matrigel invasion assay. Both EpH4-*fra1* and EpRas-*fra1* cells exhibited a significant increase in invasive capacity as shown by increased ability to migrate through Matrigel layers when compared to control cells (**Figure 15D**).

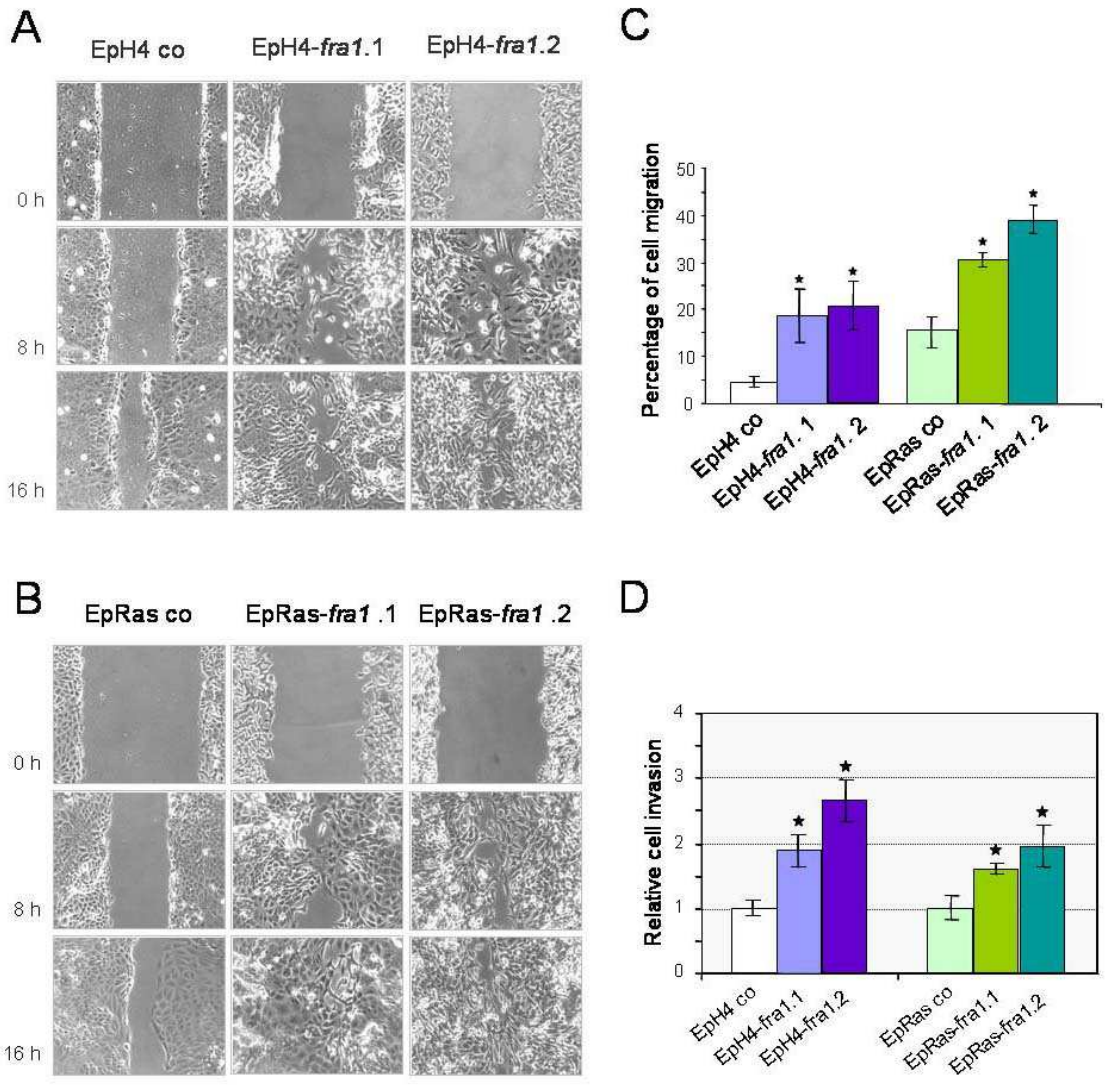

Figure 15. Fra-1 expression enhances cell motility and invasiveness. An i*n vitro* wound healing assay performed with EpH4-*fra1* **(A)** and EpRas-*fra1* **(B)** cells revealed an increase in cell motility and migration capacity. Significantly increased migration capacity was confirmed in Transwell migration assay **(C)**. Both EpH4-*fra1* and EpRas-*fra1* cells display increased *in vitro* invasiveness as determined by Matrigel invasion assay **(D)**. The results are presented as mean values, error bars representing standard deviation are shown. P values <0.05 were considered significant (*).

These results clearly show that Fra-1 ectopic expression is sufficient to induce highly motile and invasive behaviour of EpH4 and EpRas cells. Furthermore, the effect of Fra-1 on cell migration and invasion appeared to be dosage-dependent since in both cases higher expressing clones showed a more pronounced phenotype. The obtained results are in accordance with previous investigations that have reported increased cell migration and invasiveness upon ectopic Fra-1 expression in several murine and human cell lines (Kustikova et al., 1998; Tkach et al., 2003; Milde-Langosch et al., 2004; Andersen et al., 2005; Belguise et al., 2005; Debinski and Gibo, 2005).

3.5 Fra-1 triggers EMT in EpH4 and EpRas cells

In addition to conversion from epithelial to fibroblastoid morphology, cells that undergo a full EMT are characterized at the molecular level by downregulation/loss of epithelial markers and upregulation/*de novo* expression of mesenchymal markers. To determine whether Fra-1 induces a full EMT in EpH4 and EpRas cells, I have analysed the expression of epithelial and mesenchymal marker proteins by Western blotting. Interestingly, I observed a striking downregulation of the major epithelial marker protein E-cadherin (**Figure 16A**). Furthermore, the levels of adherens junction proteins α-, β-, γ-, and p120-catenin were also downregulated in all Fra-1 expressing cells (**Figure 16A-C**).

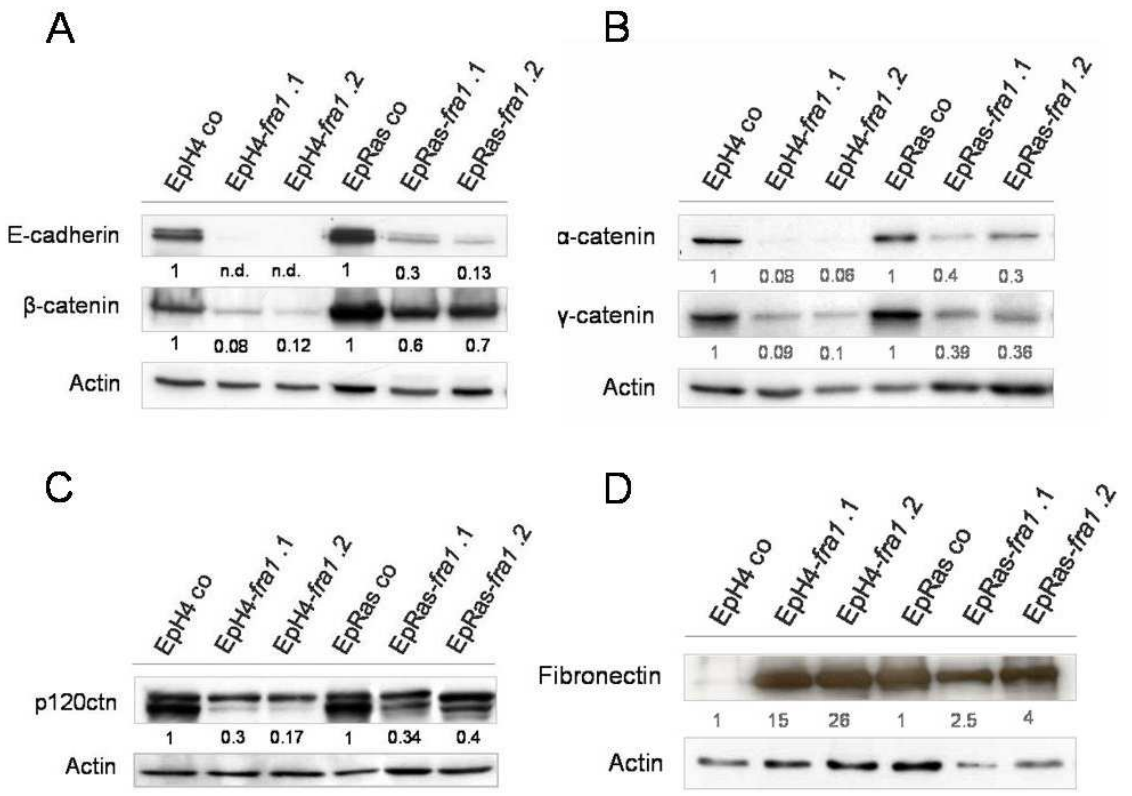

Figure 16. Ectopic Fra-1 expression downregulates epithelial markers and upregulates the mesenchymal marker fibronectin. Total cell lysates were analysed by Western blot for the expression of epithelial markers **(A-C)** and the mesenchymal marker fibronectin **(D)**. Actin was used as a loading control. Quantification of protein bands after normalisation for loading is shown as fold change when compared to the respective control cells.

In EpH4-*fra1* cells E-cadherin protein levels were too low to be detectable by Western blot. The levels of α-catenin were only barely detectable and the levels of β-catenin and γ-catenin were strongly decreased (**Figure 16A-B**). However, in EpRas-*fra1* cells, even though I could still detect E-cadherin, its level was strongly downregulated (**Figure 16A**). Similarly, the levels of α-catenin and γ-catenin were also significantly decreased (**Figure 16B**). In contrast to EpH4-*fra1* cells that showed strong downregulation of β-catenin, only a moderate decrease was detected in EpRas-*fra1* cells. Interestingly, besides apparent decrease, I have observed a dramatic change in the expression pattern of p120 catenin (p120ctn) in all Fra-1 expressing cells (**Figure 16C**). In epithelial EpH4 and EpRas control cells, p120ctn was detected as a double band of approximate sizes of 120 kDa and 100 kDa, the lower molecular weight band being more prominent than the higher molecular weight band. The sizes of the detected bands corresponded to published splicing isoforms 1 and 3 of p120ctn (Mo and Reynolds, 1996; Keirsebilck et al., 1998). It has previously been published that motile cells, such as fibroblasts and macrophages preferentially express p120ctn isoform 1, while epithelial cells preferentially express isoform 3 (Mo and Reynolds, 1996; Keirsebilck et al., 1998). Interestingly, all Fra-1 expressing cells almost completely lost the 100kDA isoform 3 of p120ctn, but retained significant levels of the p120ctn 120kDa isoform 1. This observation is in agreement with published studies that have reported p120ctn isoform 1 as the predominant protein form expressed in cells after EMT (Eger et al., 2000; Ohkubo and Ozawa, 2004). Importantly, I also detected a marked increase in expression levels of the mesenchymal marker protein fibronectin in both EpH4-*fra1* and EpRas-*fra1* cells (**Figure 16D**). However, the expression of other mesenchymal marker proteins such as N-cadherin and vimentin were not detectable by Western blot (data not shown), suggesting that Fra-1-induced EMT differs from TGFβ-induced EMT in our model.

To further confirm the observed marker switch indicative of an EMT phenotype, I have checked the expression and subcellular localisation of adherens junction proteins and mesenchymal markers by immunofluorescence (**Figure 17 and 18**). In both EpH4 and EpRas control cells all adherens junction proteins exhibited strong membranous staining localised at cell-cell contacts indicating a polarized cellular phenotype. As expected, immuofluorescent analyses of EpH4-*fra1* cells revealed a

complete absence of E-cadherin and α-catenin (**Figure 17**). Furthermore, only a faint cytoplasmic staining for β-catenin and γ-catenin was detected. Similarly, the staining for p120ctn revealed an overall downregulation and relocalisation of the protein from cell-cell contact sites to the cytoplasm (**Figure 17**). Additionally, no apparent relocalisation of β-catenin or p120ctn to the nucleus was observed. Furthermore, I could detect a strong staining showing the accumulation of fibronectin in the cytoplasm of EpH4-*fra1* cells that was completely absent in the EpH4 control cells.

Immunofluoresecent analyses for adherens junction proteins in EpRas-*fra1* cells revealed no complete loss of E-cadherin, but a significant decrease in E-cadherin levels and partial relocalisation to the cytoplasm (**Figure 18**). Similarly, the expression and localisation of γ-catenin and p120ctn was also altered. I could detect a strong downregulation and relocalisation of both proteins to the cytoplasm of Fra-1 expressing cells, even though a proportion of p120ctn could still be detected at cell-cell contacts. Furthermore, I could not detect any signal for α-catenin. In line with the results obtained by Western blot, β-catenin staining was not significantly decreased in EpRas-*fra1* cells and showed mainly membranous staining (**Figure 18**). Although EpRas control cells express a certain level of fibronectin, I could still detect a significant increase in its expression in the cytoplasm of EpRas-*fra1* cells.

Taken together, these results clearly show that Fra-1 expression is sufficient to induce epithelial dedifferentiation and hallmarks of EMT in both EpH4 and EpRas cells. Most strikingly, the effect of Fra-1 expression was more pronounced in EpH4- than in EpRas cells, suggesting that Fra-1 can induce EMT without the contribution of TGFβ.

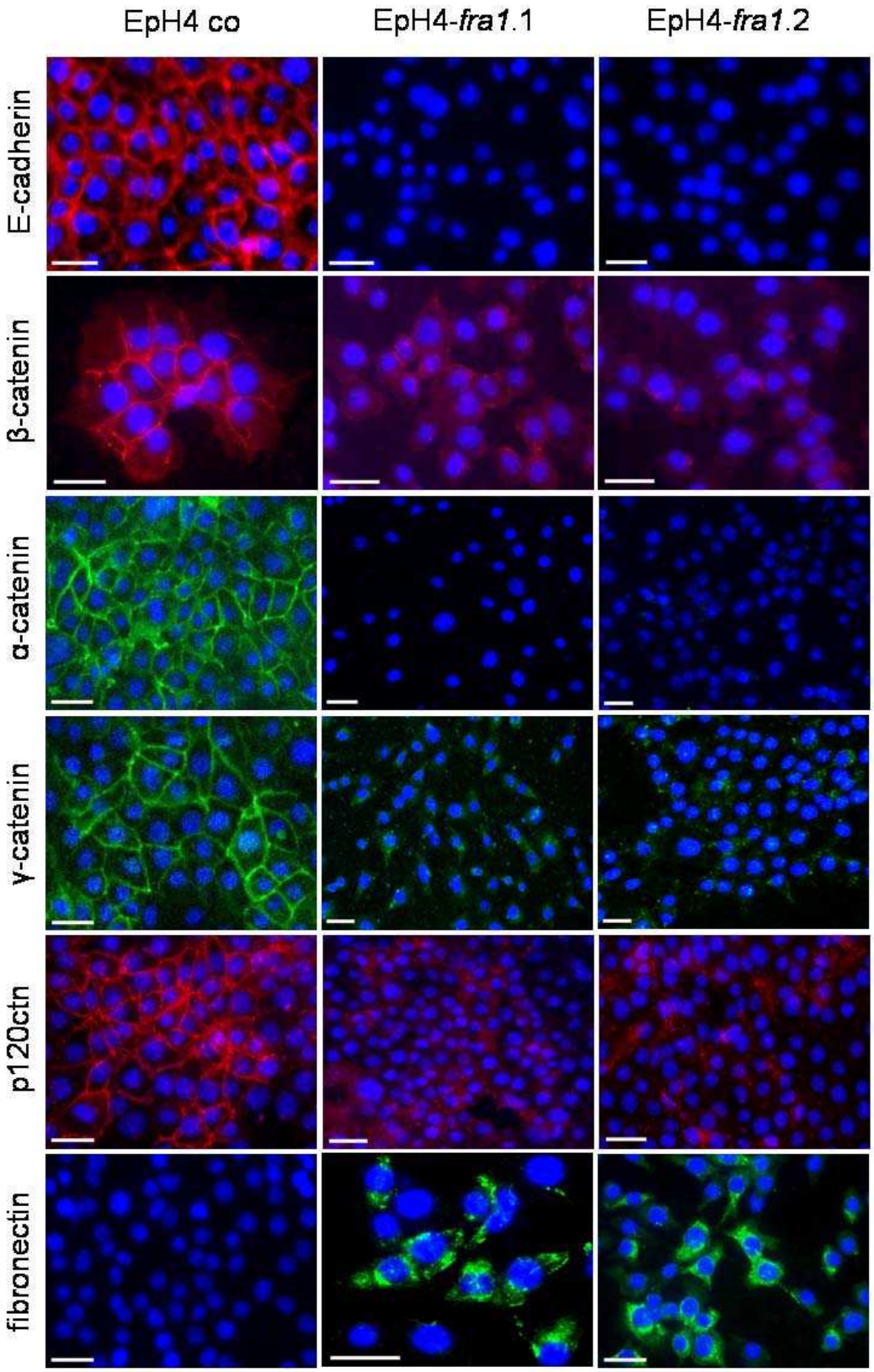

Figure 17. Fra-1 induces EMT in EpH4 cells. Immunofluorescence analyses for the expression and subcellular localization of epithelial markers and mesenchymal marker fibronectin in EpH4 control cells and Fra-1 expressing clones. Nuclei were counterstained with DAPI (blue). Scale bar, 20μM.

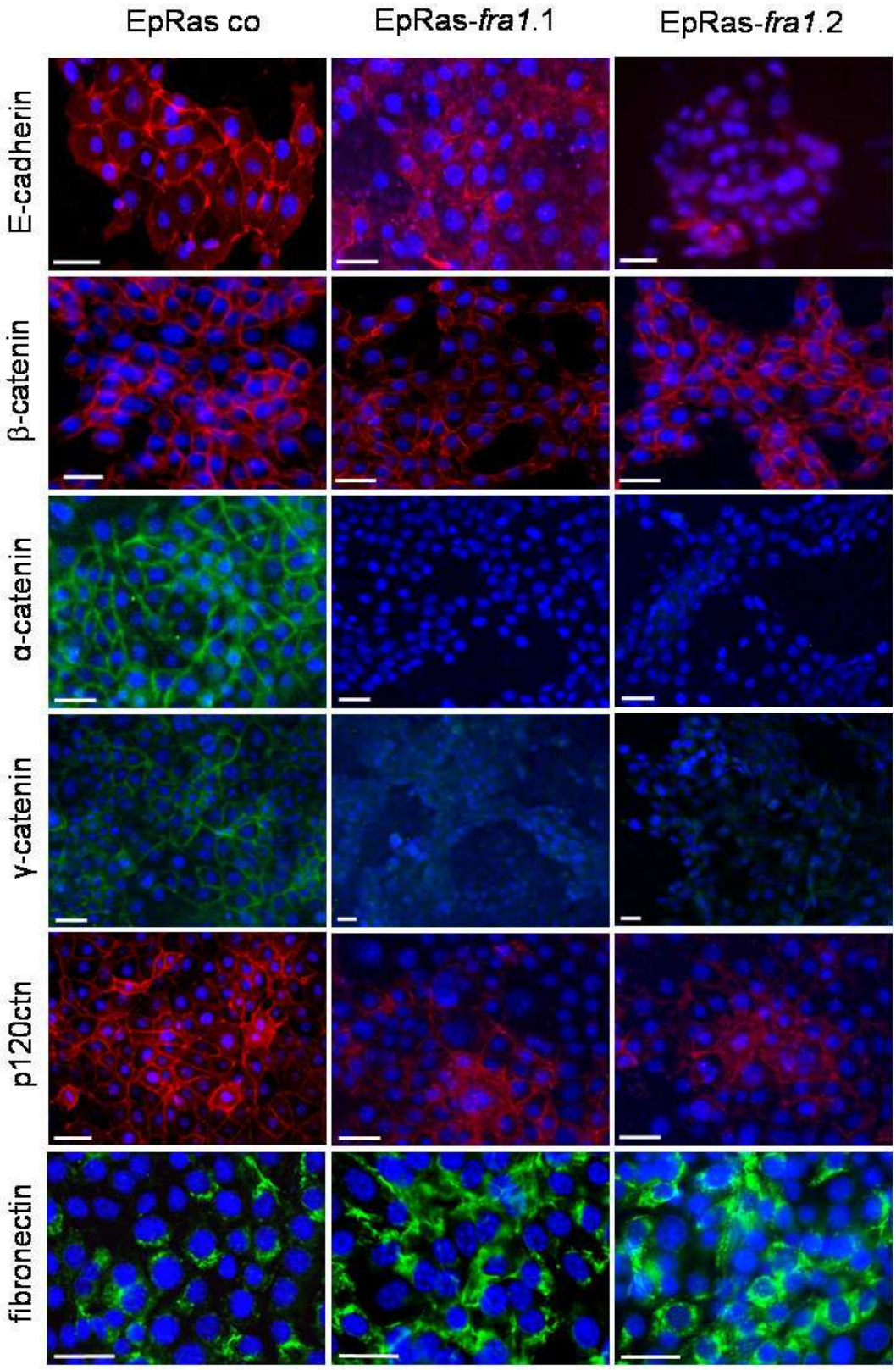

Figure 18. Fra-1 induces EMT in EpRas cells. Immunofluorescence analyses for the expression and subcellular localization of epithelial markers and mesenchymal marker fibronectin in EpRas control cells and Fra-1 expressing clones. Nuclei were counterstained with DAPI (blue). Scale bar, 20μM.

3.6 Induction and maintenance of EMT by Fra-1 in EpH4/EpRas system is independent of TGF-β1

Previous studies using EpH4/EpRas cell system have shown that EMT requires a cooperation of active Ras signalling and cytokine TGF-β1 (Oft et al., 1996). Furthermore, it was shown that the cells that have undergone EMT (EpRasXT cells) sustain the mesenchymal phenotype by an autoregulatory TGF-β1 loop (Oft et al., 1996; Oft et al., 1998). To determine whether this might be the mechanism by which Fra-1 elicits EMT, I have assayed the cells for TGF-β1 production (**Figure 19**).

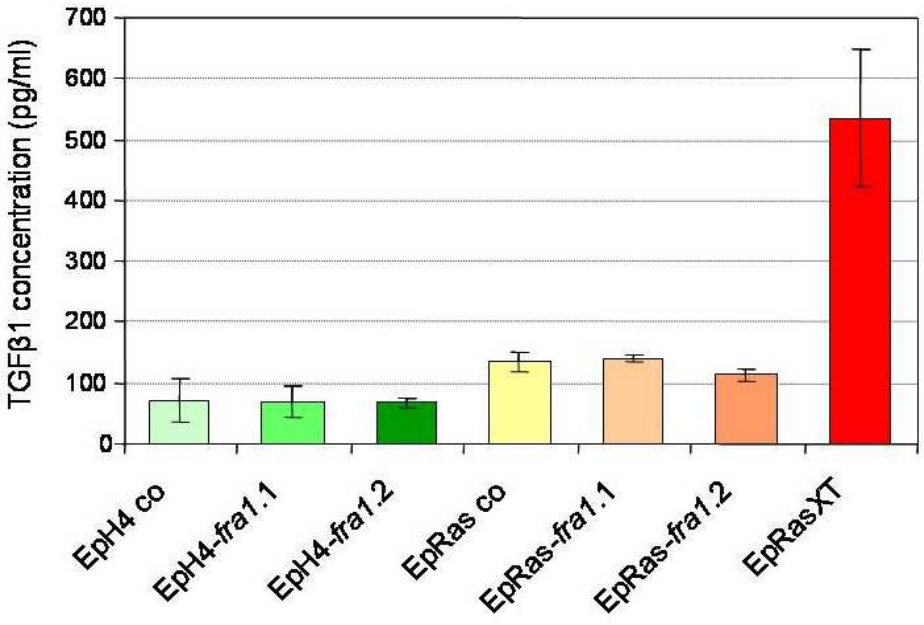

Figure 19. Fra-1 expression does not induce TGF-β1 production. Cells were grown in serum-free medium for 24h before assaying for TGF-β1 levels. Conditioned media was collected and concentrated prior to performing an ELISA assay. EpRasXT cells that produce and secrete high levels of TGF-β1 were used as a positive control. The results are shown as mean and error bars represent standard deviation.

For this, cells were exposed to serum-free media for 24-48h prior to analysis. Conditioned media was collected, concentrated and assayed by ELISA using conditioned medium from EpRasXT cells-known to produce high levels of TGF-β1- as positive control. However, no increase in active TGF-β1 levels could be detected in any of the conditioned supernatants of Fra-1 expressing cells (**Figure 19**). These results indicated that Fra-1 does not require cooperation with TGF-β1 for induction of EMT and maintenance of the mesenchymal phenotype.

3.7 Fra-1 renders EpH4 cells tumorigenic and metastatic and increases the metastatic potential of EpRas cells

To further address the relevance of the results obtained by the above *in vitro* assays, I have analysed the behaviour of these cell lines *in vivo*. It was previously shown that EpH4 cells are non-tumorigenic and non-metastatic *in vivo,* (i.e. EpH4 cells at most forming small, regressing skin nodules (Reichman et al., 1989; Oft et al., 1996; Oft et al., 1998; Janda et al., 2002). Interestingly, I observed that orthotopic injection of EpH4-*fra1* cells into mammary gland fat pads of immunocompromised mice resulted in formation of fast growing tumors, while the injected control cells only formed the previously reported small, regressing nodules (Oft et al., 1996; **Figure 20A-B**).

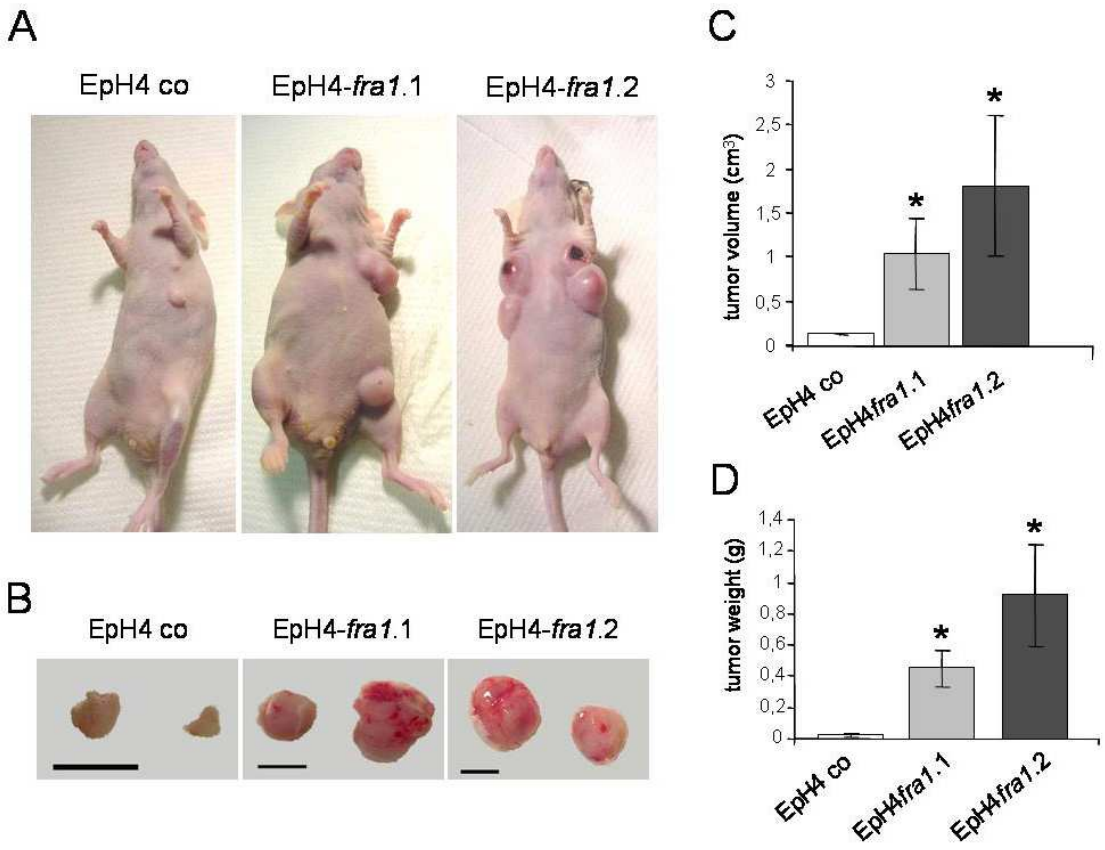

Figure 20. EpH4-*fra1* cells are tumorigenic *in vivo*. (A) Photographs of representative mice injected with EpH4 control and EpH-*fra1* cells. EpH4-*fra1* cells formed tumors at all injection sites (n=3 mice per cell type after 14 days. **(B)** Photographs of isolated representative tumors prior to fixation. Tumors formed by EpH4-*fra1* cells have significantly increased volume **(C)** and weight **(D)** when compared to tumors formed by control cells. Data are presented as mean (n=3) and error bars represent st. dev. *P*-values ≤0.05 were considered significant (*). Scale bar, 1cm.

Each mouse was injected with $1.5x10^5$ cells into 2-4 mammary gland fat pads and monitored for tumor formation on a daily basis. Injection of EpH4-*fra1* cells resulted in efficient tumor formation at all injection sites after 14 days, while the EpH4 control cells formed only small tumor nodules at 50% frequency (**Figure 20A-B**). I have also checked several organs for metastasis formation, but could not detect any signs of metastasis formation in the lungs, kidney or liver in these mice (data not shown). In addition to significantly increased tumor weight and volume (**Figure 20C-D**), macroscopic inspection of isolated tumors revealed increased vascularisation of tumours formed by EpH4-*fra1* cells (**Figure 20B**). H&E staining of tumor sections confirmed this observation (**Figure 21**). In addition, the EpH4 nodules had a sharp boundary and were surrounded by stroma, while the inner mass of the EpH4-fra1 tumors appeared necrotic, most likely due to extremely fast tumor growth.

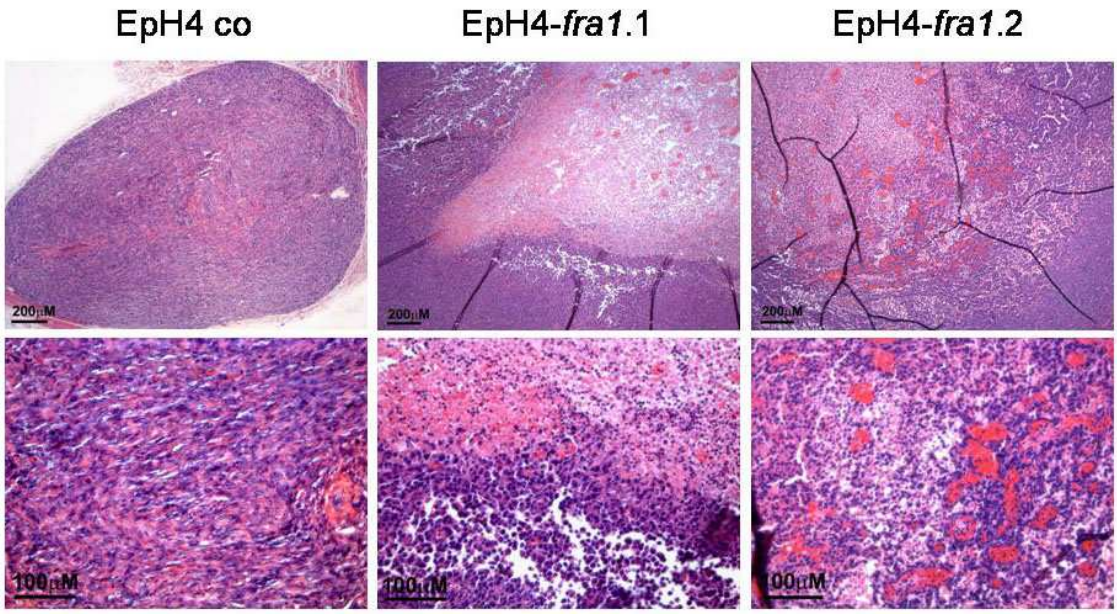

Figure 21. Histological analyses of tumors formed by EpH4-*fra1* cells. H&E staining revealed increased vascularisation of tumors formed by EpH4-*fra1* cells. Magnification is 5X and 20X, respectively. Scale bars are indicated. (n=3).

Ki67 staining revealed a significantly increased number of positive cells in the tumors formed by EpH4-*fra1* cells that were mainly located at the outer regions of the tumors, while the EpH4 control tumors showed only low numbers of proliferating, Ki67 positive cells (**Figure 22A-B**).

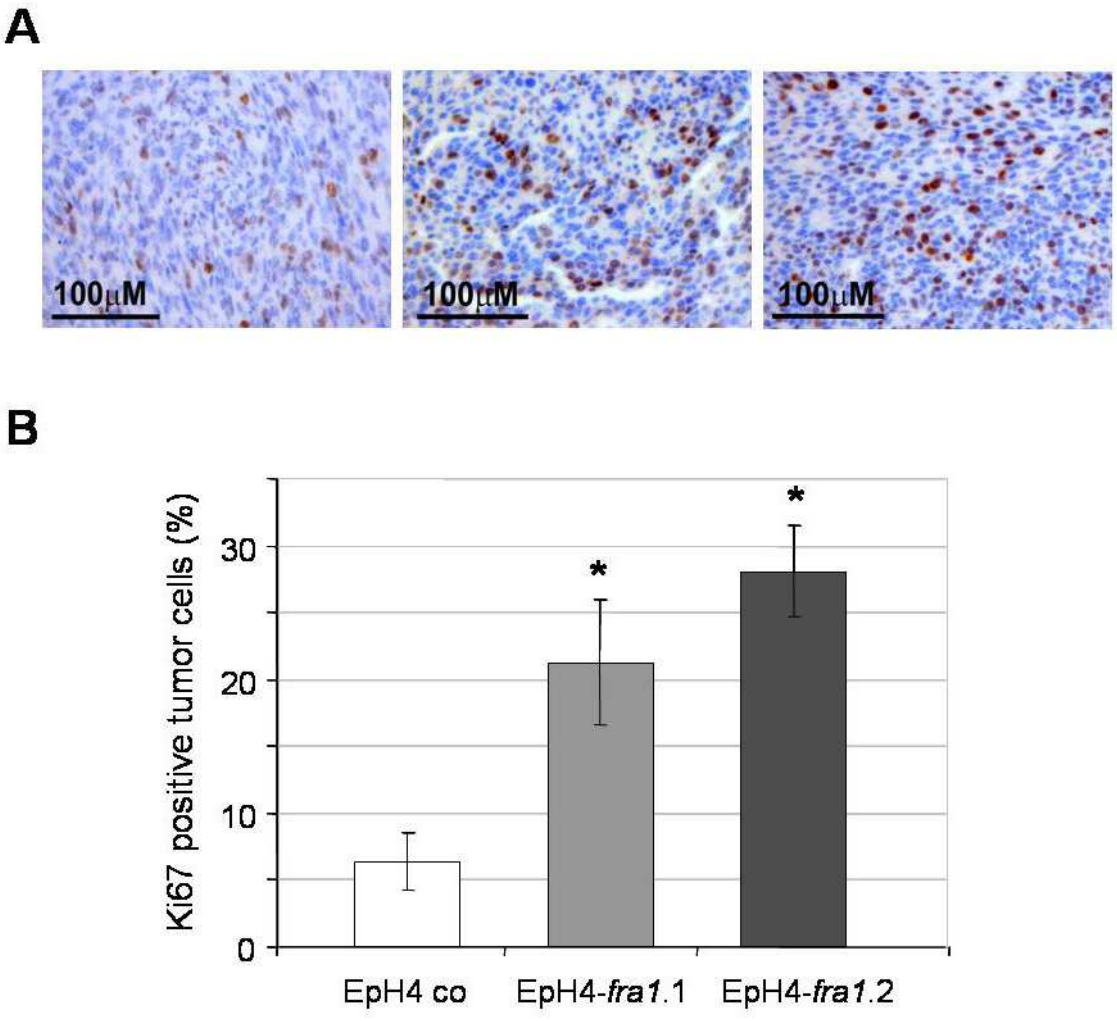

Figure 22. Tumors formed by EpH4-fra1 cells are highly proliferative. (A) Tumor cell proliferation was assessed by immunohistochemical detection of the proliferation marker Ki67. Magnification is 20X and scale bars are indicated. **(B)** Bar graph shows quantification of Ki67 positive cells performed by counting stained cells in 5 different fields using a 20X objective. Data are presented as mean (n=3) and error bars representing standard deviation are shown. P values ≤0.05 were considered significant (*).

Due to the known limitations of the EpH4/EpRas model that fails to metastasize from orthotopic tumors (Janda et al., 2002), and the overall high proliferative capacity of tumors formed by EpH4-*fra1* cells, I was not able to determine whether these cells acquired the ability to metastasize from orthotopic sites. To determine

the metastatic potential of the cells, I have performed lung colonisation assay by injecting $1.5x10^5$ EpH4 cells or $1x10^5$ EpRas cells and their respective Fra-1 expressing clones into the tail vein of immunocompromised mice. The mice were observed on a daily basis and sacrificed when becoming moribund. Most strikingly, both EpH4-*fra1* and EpRas-*fra1* cells formed numerous metastases in the lungs of all experimental mice (n=4) 4 weeks after injection (**Figure 23A and B**).

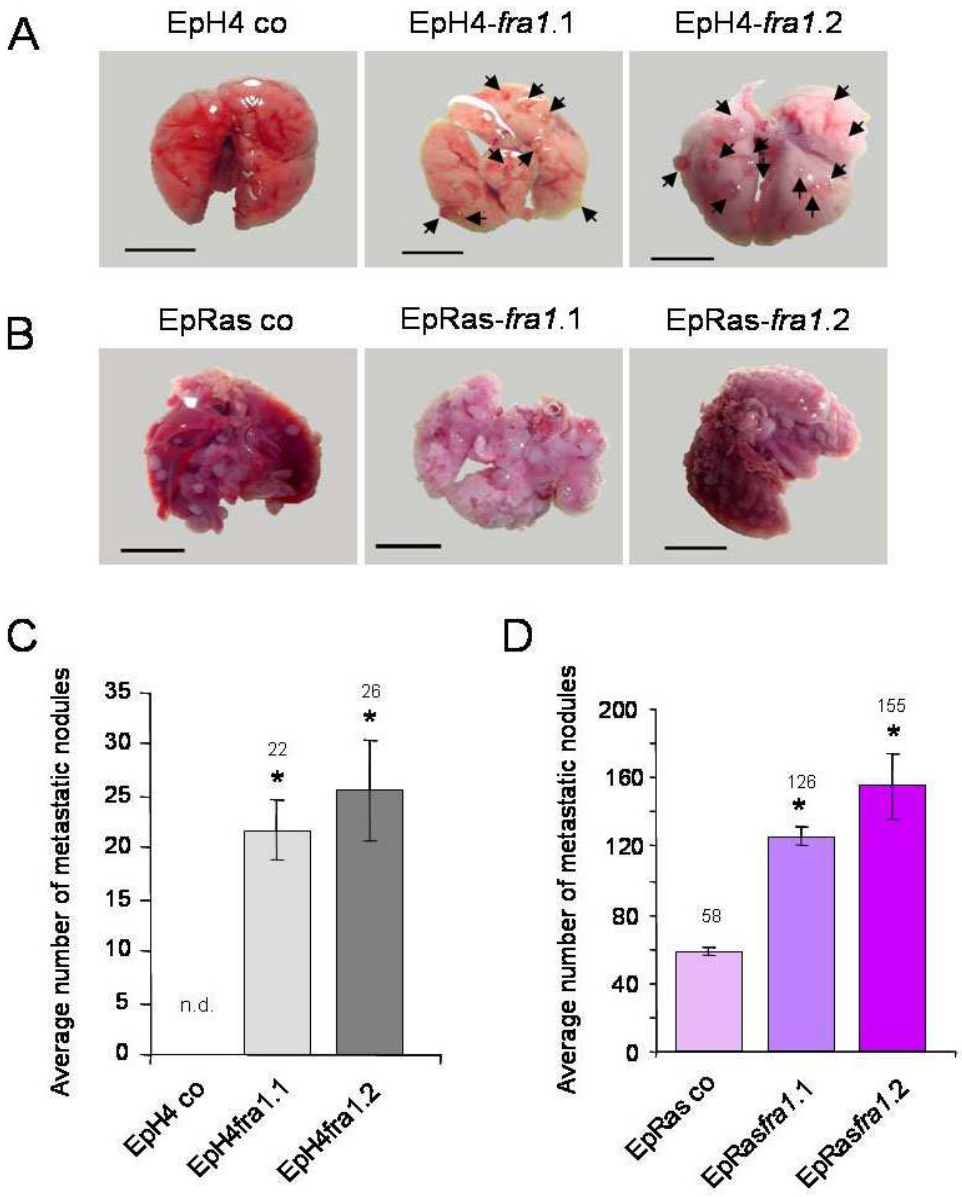

Figure 23. Fra-1 expression renders EpH4 cells metastatic and increases metastatic potential of EpRas cells. (A) Photographs of representative lungs isolated from mice (n=4) injected with EpH4-*fra1* or EpRas-*fra1* cells **(B)** and their respective control cells. Arrows point to macroscopically visible metastatic nodules formed by EpH4-*fra1* cells. Scale bar, 1cm. Quantification of metastatic nodules formed by EpH4-*fra1* **(C)** and EpRas-*fra1* **(D)** cells was performed by counting visible nodules on the surface of isolated lungs. Note that EpH4 control cells did not form metastasis in the lung.

Importantly, there were no macroscopically detectable metastatic nodules seen on the surface of lungs injected with EpH4 control cells (**Figure 23A**). EpRas cells were previously shown to form metastases upon tail vein injection into immunocompromised mice (Oft et al., 1996; Janda et al., 2002). Nevertheless, expression of Fra-1 significantly increased the number of macroscopically visible metastatic nodules (**Figure 23B and D**). These observations were further confirmed by histological analysis of the lungs. H&E staining revealed numerous metastatic lesions in the lungs of mice injected with EpH4-*fra1* cells that were absent in the lungs injected with control cells (**Figure 24A**), as well as an increased number of metastatic nodules in lungs of mice injected with EpRas-*fra1* cells (**Figure 24B**).

Immunostaining for the proliferation marker Ki67 revealed strong proliferation of cells within the nodules formed by EpH4-*fra1* cells (**Figure 25A**). However, as expected, there was no significant difference in the number of positive cells within the nodules formed by EpRas control and EpRas-*fra1* cells, since nodule size was similar in the absence or presence of Fra-1 (**Figure 25B**). Further immunohistochemical analysis revealed strong correlation in cell dedifferentiation and Fra-1 expression in metastatic lesions formed by both EpH4-*fra1* and EpRas-*fra1* cells (**Figure 26 and 27**). In both cases, I could detect strong and mainly nuclear staining for Fra-1 only within the metastatic nodules (**Figure26A and 27A**). Most importantly, the same regions were E-cadherin negative. I could only detect a weak cytoplasmic signal in a few random cells (**Figure 26B and 27B**). Furthermore, I detected strong cytoplasmic staining for fibronectin within the metastatic lesions that was completely absent from normal lung tissue in mice injected with EpH4 control cells (**Figure 26C**). Similarly, even though fibronectin was present in metastatic nodules formed by EpRas control cells, the staining was much stronger in the nodules formed by EpRas-*fra1* cells (**Figure 27C**). In both cases, the staining appeared to be more pronounced at the outer edges of proliferating nodules.

These observations confirmed the results obtained by *in vitro* assays and clearly demonstrated that Fra-1 expression is sufficient to induce EMT of mammary epithelial cells. Moreover, the observed lack of E-cadherin expression and significant upregulation of fibronectin, correlated with Fra-1 expression in metastatic nodules further demonstrated the ability of Fra-1 expressing cells to undergo EMT *in vivo*.

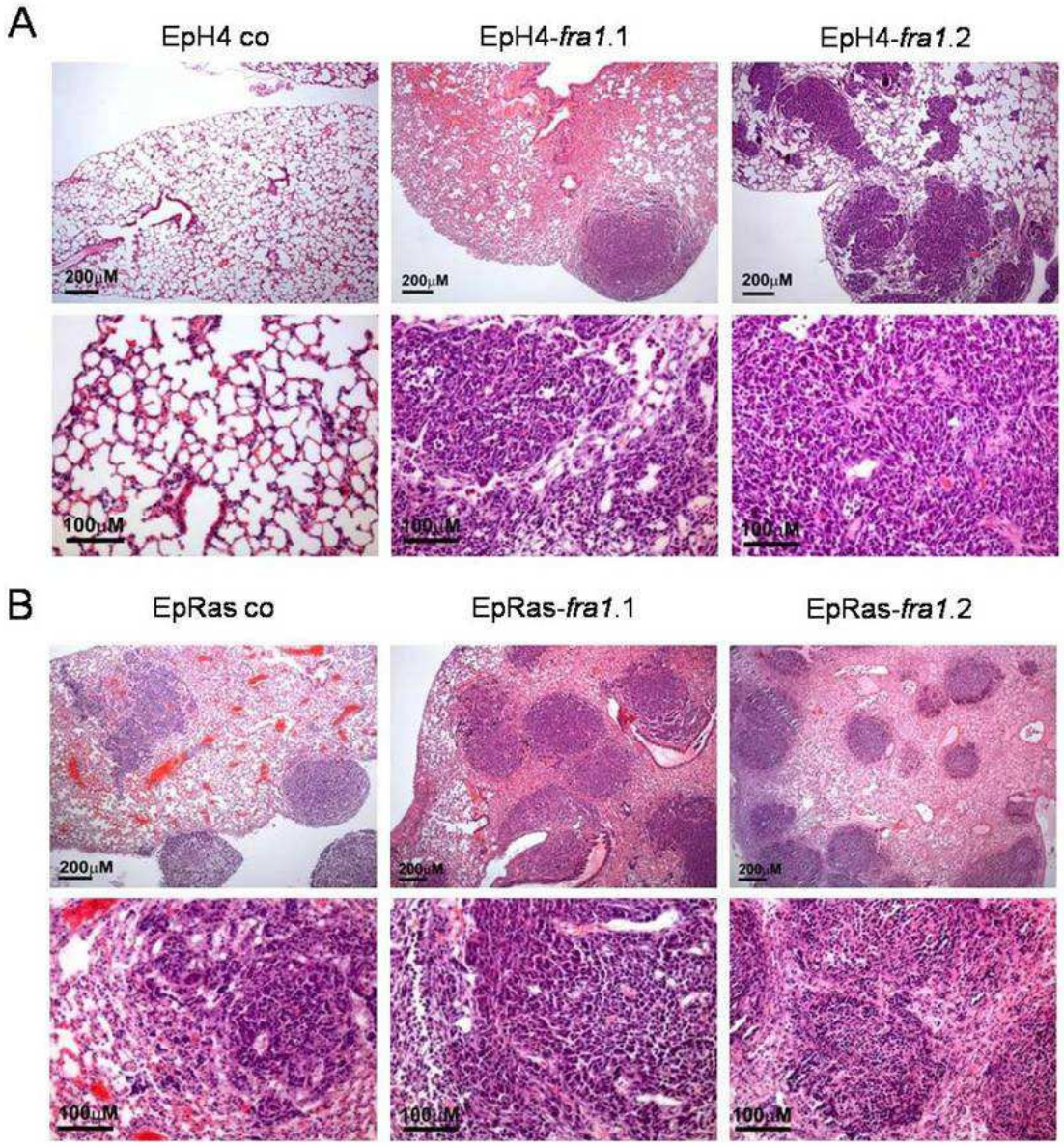

Figure 24. Pathological changes in lungs of mice injected with Fra-1 expressing EpH4 and EpRas cells. H&E staining reveals formation of metastatic nodules in the lungs after tail vein injection of EpH4-*fra1* cells not present in the lungs of mice injected with EpH4 control cells (n=4) **(A)**. Increased number of metatatic nodules in mice injected with EpRas-*fra1* cells **(B)**. Magnification is 5X (upper panels) and 20X (lower panels). Scale bars are shown.

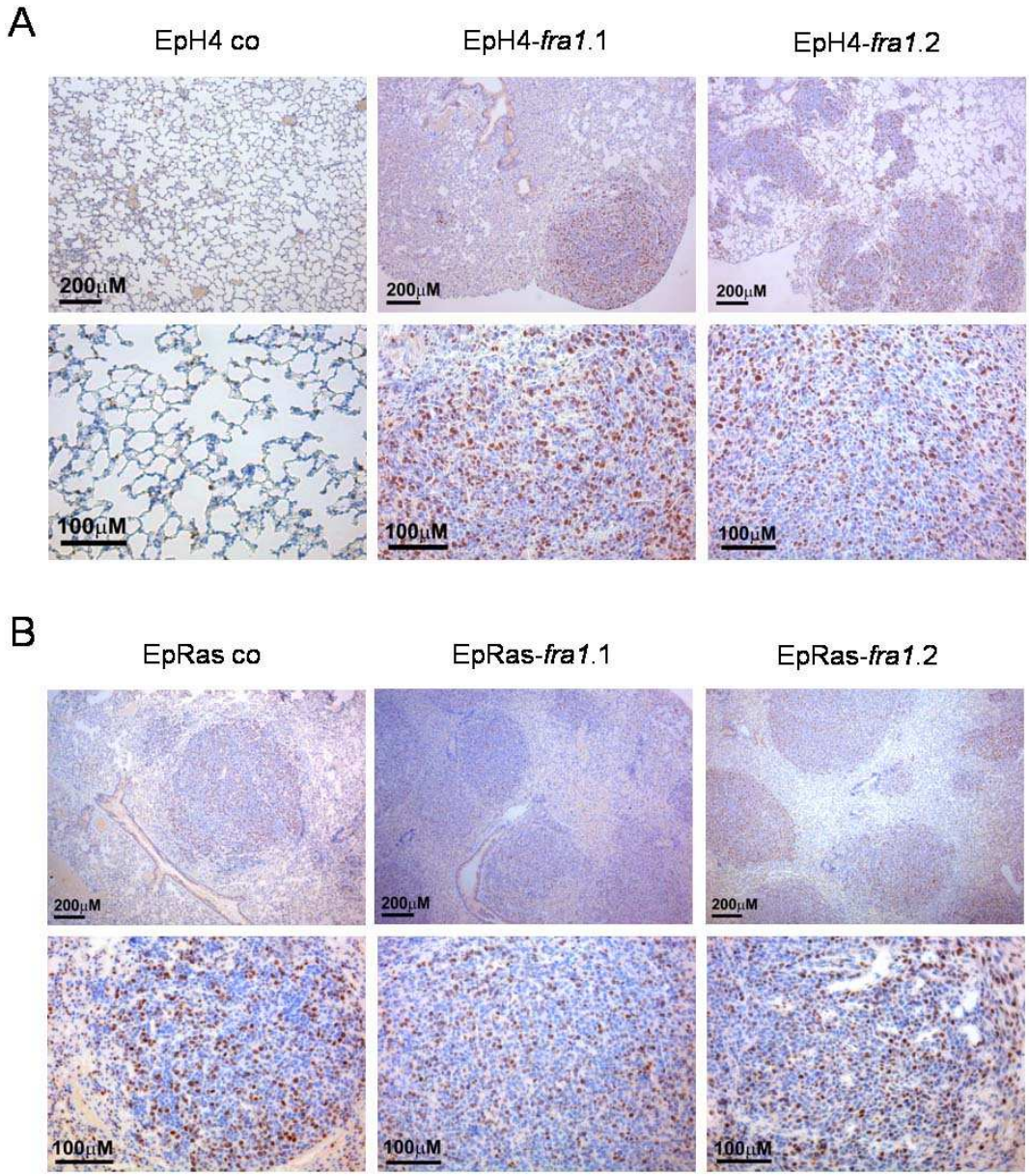

Figure 25. Immunohistochemical analysis of cell proliferation in metastatic nodules. (A) Immunohistochemical staining for the proliferation marker Ki67 shows strong cell proliferation in nodules formed by EpH4-*fra1* cells. **(B)** Ki67 staining shows no major difference in cell proliferation within the metastatic nodules formed by EpRas control and EpRas-*fra1* cells (n=4). Magnification is 5X (upper panels) and 20X (lower panels). Scale bars are indicated.

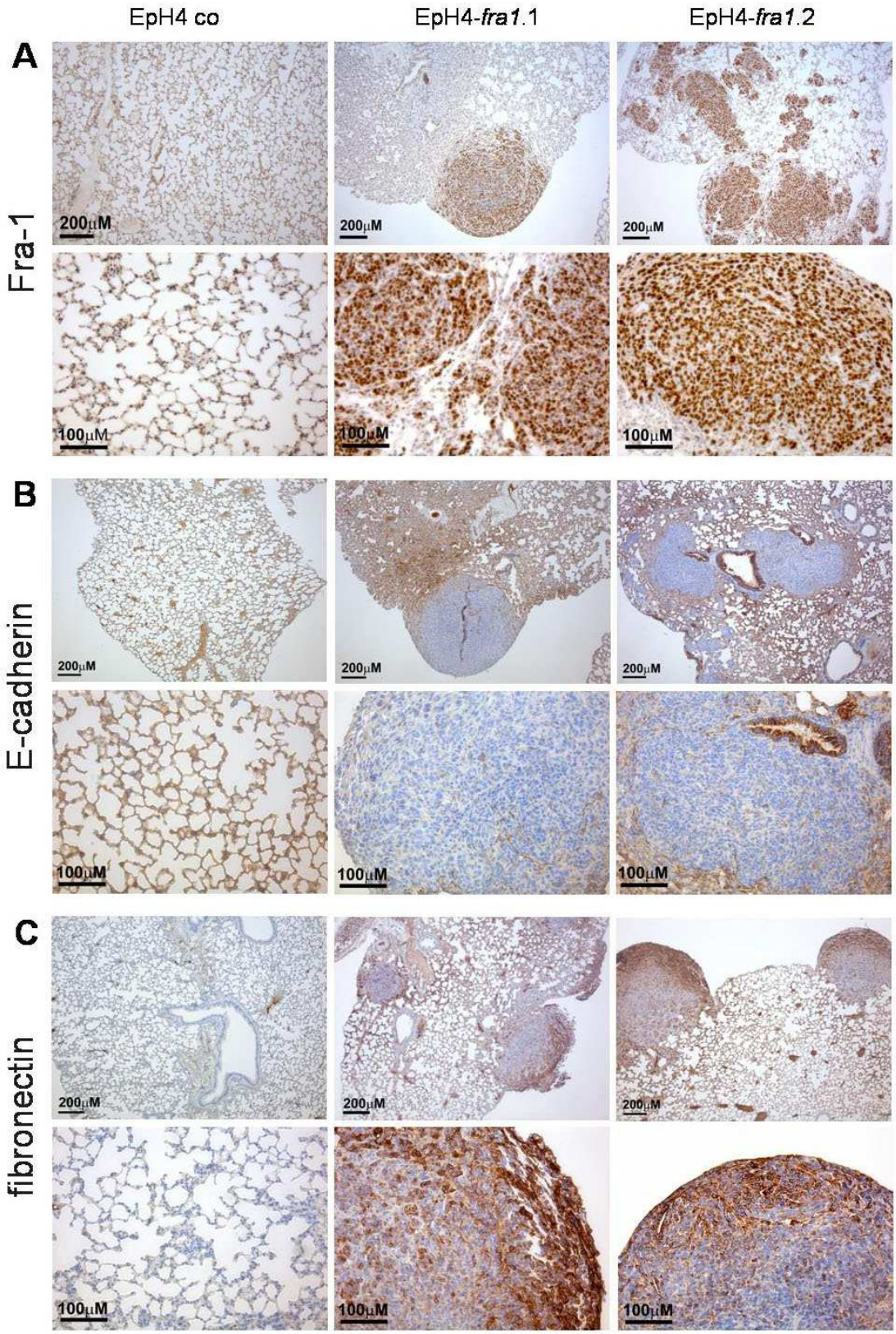

Figure 26. Cell dedifferentiation within metastatic nodules formed by EpH4-*fra1* cells correlates with Fra-1 expression. Immunohistochemical staining for Fra-1 **(A)**, the epithelial marker protein E-cadherin **(B)** and the mesenchymal marker protein fibronectin **(C)** revealed a positive correlation in Fra-1 expression and cell dedifferentiation *in vivo* (n=4). Magnification is 5X (upper panels) and 20X (lower panels). Scale bars are indicated.

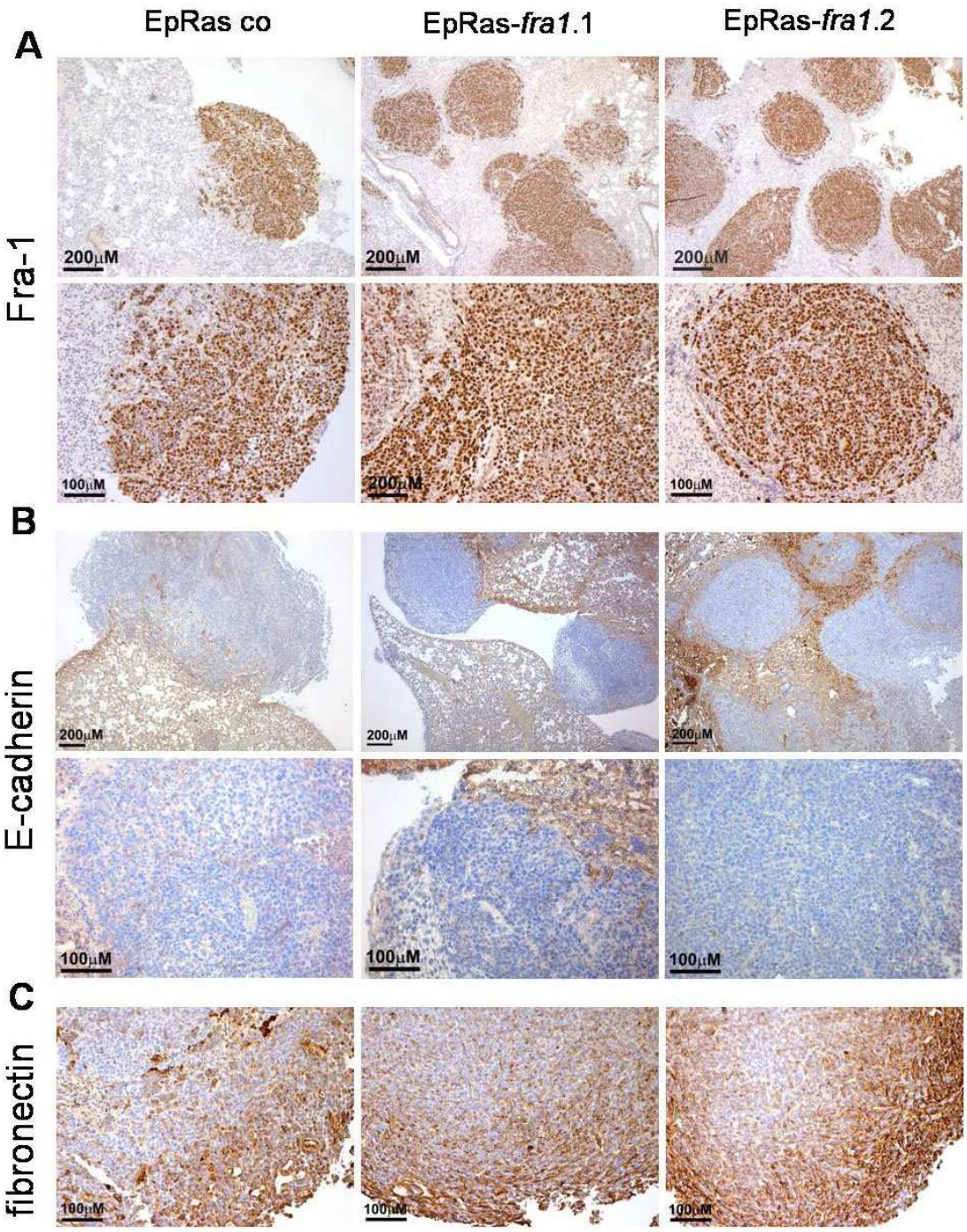

Figure 27. Cell dedifferentiation within metastatic nodules formed by EpRas-*fra1* cells correlate with Fra-1 expression. Immunohistochemical staining for Fra-1 **(A)**, the epithelial marker protein E-cadherin **(B)** and the mesenchymal marker protein fibronectin **(C)** revealed a positive correlation in Fra-1 expression and cell dedifferentiation *in vivo* (n=4). Magnification is 5X (upper panels) and 20X (lower panels). Scale bars are indicated.

3.8 Summary and conclusions

In the first part of this study, I have employed a gain-of-function approach to determine the role of Fra-1 in induction and maintenance of EMT using the *in vitro* EpH4/EpRas cellular model. I was able to show that ectopic expression of Fra-1 in epithelial EpH4 and EpRas cells results in epithelial to fibroblastoid conversion accompanied by profound cytoskeletal rearrangements. Furthermore, Fra-1 expressing cells showed an increased proliferation rate, migratory and invasive potential *in vitro*. Molecular analyses revealed downregulation of epithelial marker proteins (E-cadherin, α-, β-, γ-catenin and p120 catenin) and upregulation of mesenchymal marker fibronectin. Based on these results I conclude that Fra-1 expression is sufficient to induce all hallmarks of EMT. Additionally, the effect of Fra-1 appeared to be dosage-dependent and did not require cooperation with TGF-β1 signalling.

Further *in vivo* characterization revealed that Fra-1 expression is sufficient for tumorigenic transformation of EpH4 cells, as shown by formation of fast growing tumors upon orthotopic injections into mammary gland fat pads of immunocompromised mice. Most strikingly, Fra-1 expression in EpH4 cells was sufficient to render these cells metastatic. Similarly, Fra-1 expression in EpRas cells further increased their metastatic potential. Immunohistochemical analyses revealed positive correlation between Fra-1 expression, increased cell proliferation and expression of mesenchymal marker protein fibronectin. In contrast, the expression of Fra-1 and the major epithelial marker protein E-cadherin showed strong inverse correlation. Taken together, these results are consistent with the idea that Fra-1/AP-1 plays a major role in induction of EMT both *in vitro* and *in vivo*.

PART II

Mechanism of Fra-1 induced EMT: identification of Fra-1/AP-1 targets

3.9 Fra-1 induces transcriptional downregulation of E-cadherin

The finding, that Fra-1 is able to induce EMT, promped me to address in more detail the molecular mechanism of Fra-1 action. E-cadherin downregulation is frequently observed in carcinomas and it is thought to be one of the most important events during carcinoma progression (Birchmeier and Behrens, 1994). Furthermore, downregulation/loss of E-cadherin is considered as a major step in induction of EMT (Thiery, 2002; Yang and Weinberg, 2008). Therefore, I focused my efforts on identifying the mechanism of Fra-1-dependent E-cadherin downregulation. To determine whether E-cadherin levels are transcriptionally regulated, I first determined E-cadherin mRNA levels. Quantitative real-time RT-PCR (qPCR) analysis revealed that the observed E-cadherin downregulation occurs at the transcriptional level (**Figure 28**).

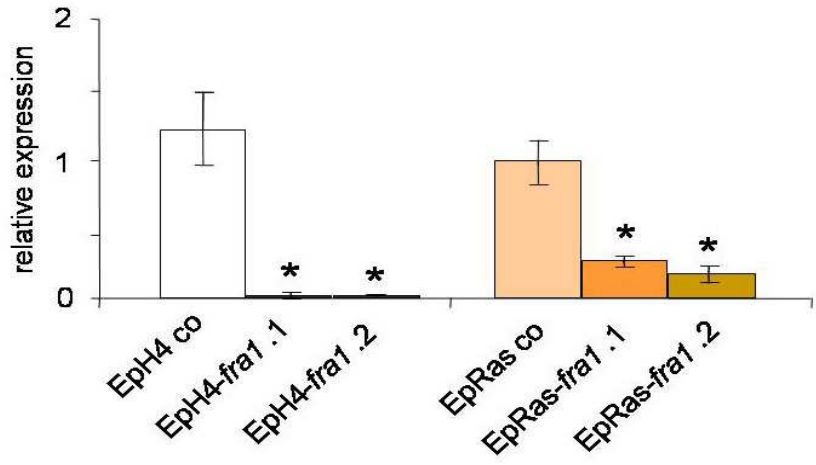

Figure 28. Transcriptional downregulation of E-cadherin in EpH4-*fra1* and EpRas-*fra1* cells. Shown are quantitative real-time PCR (qPCR) analysis data, i.e. mean values and error bars. *P* -values <0.05 were considered significant (*)

E-cadherin mRNA was almost completely undetectable by qPCR in EpH4-*fra1* cells. However, even though the level of E-cadherin transcript was strongly downregulated (roughly 3- fold and 4-fold, respectively), I could still detect it in EpRas-*fra1* cells. These observations are in accordance with the results previously obtained by Western blot and immunofluorescence analysis and suggested that Fra-1 induces EMT by regulating E-cadherin transcription. To check whether this might be due to direct transcriptional repression by Fra-1, I analysed the E-cadherin promoter including a 4000 bp upstream region for potential AP-1 binding sites. Bioinformatics analysis identified two potential AP-1 sites located at -3493 and -1278 upstream from the transcription start site. However, after performing chromatin immunoprecipitation (ChIP) experiment with Fra-1 specific antibody, I was not able to amplify those fragments by qPCR (data not shown). This result suggested that Fra-1 most likely does not repress E-cadherin transcription by direct binding to these sites in the E-cadhrin promoter.

3.9.1 Transcriptional downregulation of E-cadherin in EpH4-*fra1* cells does not involve promoter hypermethylation or histone acetylation

Transcriptional downregulation of E-cadherin can occur as a consequence of anomalous promoter hypermethylation (Graff et al., 1995; Strathdee, 2002), histone H3 and H4 deacetylation (Koizume et al., 2002), or alternatively, can be due to direct transcriptional repression by the members of the Snail (Batlle et al., 2000; Cano et al., 2000), E47/E12- (Perez-Moreno et al., 2001) and ZEB- (Grooteclaes and Frisch, 2000; Comijn et al., 2001; Eger et al., 2005) families of transcription factors. It was recently shown that transcriptional repression of the E-cadherin gene by c-Fos involves hypermethylation of the E-cadherin promoter (Mejlvang et al., 2007). Another study reported upregulation of DNA methytransferase-1(Dnmt1) upon v-Fos^{FBR} transformation (Bakin and Curran, 1999). Interestingly, treatment of cells with Dnmt inhibitor, 5-azadeoxycytidine (5-Aza-CdR), or histone acethylase inhibitor, trichostatin A (TSA), blocked v-Fos-mediated transformation (Bakin and Curran, 1999; McGarry et al., 2004). Likewise, it was recently published that Fra-1 can repress the expression of the IL-8 gene through direct interaction with histone

deacetylase-1 (HDAC1) (Hoffman et al., 2005). It was suggested by the authors that Fra-1-mediated recruitment of HDAC1 to the IL-8 promoter might affect acetylation of individual lysines of histones H3 or H4, thereby leading to alteration of chromatin structure from open to closed conformation, resulting in transcriptional repression (Hoffman et al., 2005). To determine whether the observed strong E-cadherin downregulation in EpH4-*fra1* cells might be due to promoter hypermethylation, I have treated the cells with two different histone methyltransferase inhibitors, 5-Aza-2-deoxycytidine (5-Aza-CdR) and Zebularine, for up to 4 days. E-cadherin expression was analysed by qPCR (**Figure 30**) and immunofluorescence (**Figure 29**).

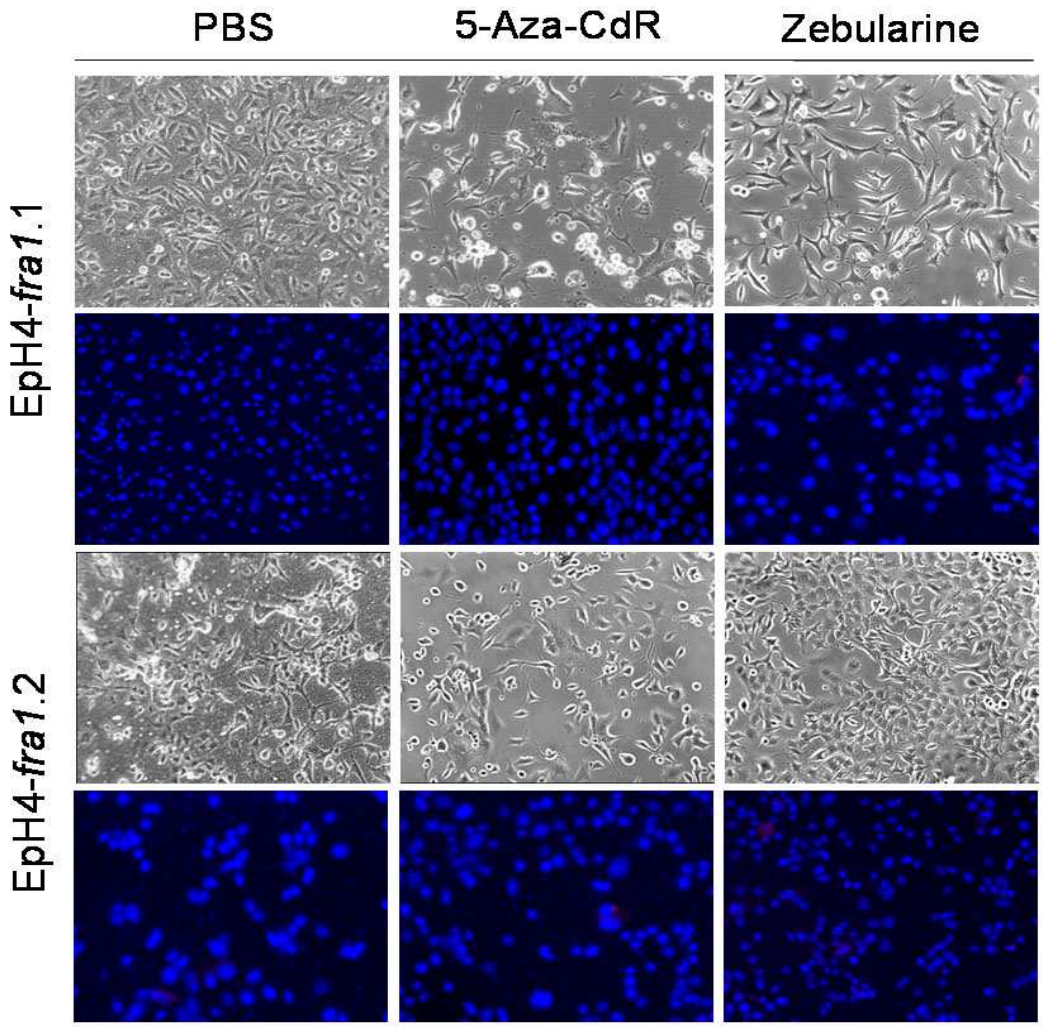

Figure 29. Inhibition of DNA methyltransferase in EpH4-*fra1* cells does not restore E-cadherin expression. Phase-contrast images of EpH4-fra1 cells treated with 5-aza-2-deoxycytiine (5-Aza-CdR) or Zebularine for 72h show no change in cell morphology (upper panels) or E-cadherin expression following treatment as shown by immunofluorescent staining for E-cadherin (lower panels). Nuclei were counterstained with DAPI (blue).

Interestingly, inhibitor treatments had no effect on cell morphology suggesting that that the cells did not restore E-cadherin expression (**Figure 29**). However, I could observe reduced cell proliferation and increased number of dying cells during the treatment. This effect was more pronounced in cells treated with 5-Aza-CdR most probably due to the known growth inhibitory and toxic effect of the compound. Following treatment, the cells were further analysed by qPCR and immunofluorescence for reexpression of E-cadherin. However, I was not able to detected neither E-cadherin mRNA (amplification only in reaction cycle 33), nor protein expression (**Figure 29 and Figure 30**). Since histone methytransferase inhibitors alone had no effect on E-cadherin expression, I combined them with histone deacetylase inhibitor TSA. Likewise, combined treatment of the cells did not result in E-cadherin reexpression (data not shown).

As a positive control of the assay, I have analysed the expression of p16i^{nk4a} tumor suppressor gene by qPCR (**Figure 30**). Expression of p16i^{nk4a} in carcinomas is often silenced by promoter methylation (Herman et al., 1995; Merlo et al., 1995) and it was previously shown that it can be re-expressed following treatment with either 5-Aza-CdR, or Zebularine (Bender et al., 1998; Cheng et al., 2004). Importantly, while could not detect a significant increase in E-cadherin expression, inhibitor treatments restored the expression of p16i^{nk4a} indicating that the assay worked technically (**Figure 30**).

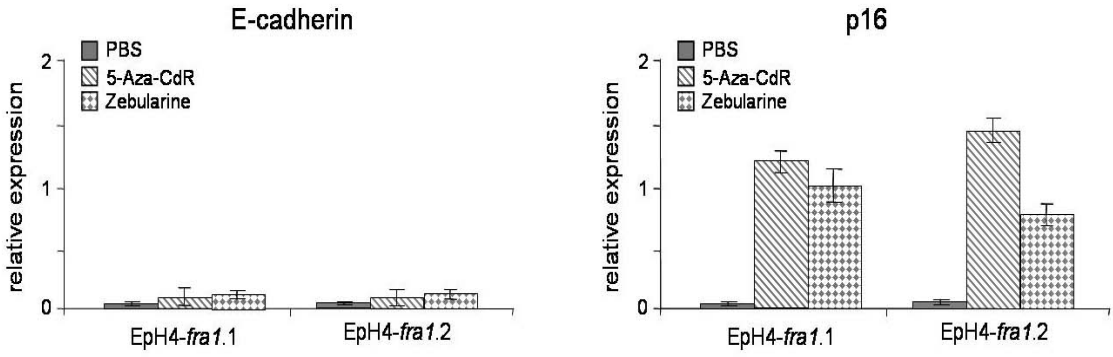

Figure 30. Expression of E-cadherin and p16i^{nk4a} tumor suppressor gene. Bar graphs show no significant increase in E-cadherin expression, while the expression of p16 gene was strongly induced following DNA methyl transferase inhibitor treatments. The data is presented as mean and error bars are designated.

Thus, these results strongly indicated that methylation of E-cadherin promoter, or chromatin remodelling due to histone deacetylase activity, is not involved in mechanism of Fra-1-mediated transcriptional downregulation of E-cadherin in EpH4-*fra1* cells.

3.10 Gene expression profiling in EpH4-*fra1* and EpRas-*fra1* cells: Fra-1 modulates RNA expression of genes implicated in EMT

To gain a more general overview of the genes affected by Fra-1 expression, and to further explore the molecular basis underlying Fra-1-mediated E-cadherin downregulation and subsequent induction of EMT, I performed genome-wide gene expression profiling. Total RNA isolated from EpH4-*fra1* and EpRas-*fra1* cells was hybridized to oligonucliotide microarray slides provided by the IMP microarray facility. Only annotated genes showing significant (*p*-value <0.05), at least 2-fold changes in expression and similarly regulated in both clones, were included in further analyses (**Figure 31**). Ectopic Fra-1 expression in EpH4 cells affected the expression of 660 genes, while 471 genes were affected in EpRas cells. Out of 660 genes, 402 genes were upregulated and 239 genes downregulated in EpH4-*fra1* cells. In EpRas-*fra1* cells, 258 genes were upregulated and 232 downregulated. Interestingly, among differentially regulated genes, I identified several known AP-1 target genes, such as matrix matalloproteases (MMPs) that had previously been implicated in cancer progression and EMT. Furthermore, a number of known EMT related genes were also found to be regulated by Fra-1 expression (**Table 1 and Table 2**). Differentially expressed genes were clustered according to their functional annotation (**Figure 32 and Figure 33**). Interestingly, the majority of genes downregulated following Fra-1 expression, could functionally be assigned to epithelial and adhesion/junction clusters, followed by proteases, tumor suppression and chemokine/cytokine clusters (**Figure 32**). As expected, the majority of upregulated genes could be grouped in the mesenchymal/matrix/bone, growth factor, proteases, transcription factors and tumor/invasion/metastasis clusters (**Figure 33**).

Some interesting examples of upregulated genes in EpH4-*fra1* cells include several proteases, such as MMP-2, -3, -13, -14 and Plat (member of the uPAR system) that are widely implicated in cancer progression and EMT (Egeblad and Werb, 2002; Sidenius and Blasi, 2003; Lagamba et al., 2005), and known EMT-inducers, such as chemokine Cxcl12/SDF-1α (Muller et al., 2001; Onoue et al., 2006), cytokine TGF-β2 (Nawshad et al., 2004; Timmerman et al., 2004), extracellular matrix protein SPARC/osteonectin (Framson and Sage, 2004; Robert et al., 2006; Sarrio et al., 2008) and a direct Fra-1 target gene, the matrix Gla protein (MGP) (Chen et al., 1990; Eferl et al., 2004; Yoshimura et al., 2009). Finally, transcription factors associated with cancer progression such as Stat1 and Stat3 (Yu and Jove, 2004; Jechlinger et al., 2003), hypoxia-induced HIF-1α (Bando et al., 2003; Pouyssegur et al., 2006; Yang et al., 2008; Sahlgren et al., 2008), as well as E-cadherin transcriptional repressors, transcription factors ZEB1 and ZEB2 (Comijn et al., 2001; Vandewalle et al., 2005; Eger et al., 2005; Peinado et al., 2007; Vandewalle et al., 2009) were found to be significantly upregulated (**Table 1**).

Similarly, Fra-1 overexpression in EpRas cells resulted in upregulation of several invasion related proteases, such as ADAM8 and ADAM10, MMP-1, and MMP12 (Egeblad and Werb, 2002; Maretzky et al., 2005;), adhesion molecules implicated in invasion/metastasis, such as N-cadherin (CDH2) and L1 CAM (Derycke and Bracke, 2004; Christofori, 2006; Shtutman et al., 2006; Raveh et al., 2009; Wheelock et al., 2008), as well as direct Fra-1 target genes, the hyaluronan receptor CD44 (Hoffman et al., 1993; Lamb et al., 1997; Zajchowski et al., 2001; Andersen et al., 2002; Ramos-Nino et al., 2003) and matrix Gla protein. Further examples include EMT-inducing zinc finger transcription factors KLF8 (Wang, et al., 2007), Snai2/Slug (Hajra et al., 2002b; Bolos et al., 2003) and ZEB2 (**Table 2**). Consistently, genes typical of epithelial cells were strongly downregulated in both EpH4-*fra1* and Ep-Ras-*fra1* cells. Examples include components of desmosomes, such as desmoglein 2, tight junctions components, such as occludin and several claudins, as well as epithelial intermediate filaments, cytokeratins 8/18, all of which are regarded as markers of epithelial phenotype and are downregulated during EMT (Miyoshi and Takai, 2005; Lagamba et al., 2005; Thiery and Sleeman, 2006; De Wever et al., 2008). Most importantly, and in agreement with previous findings,

the array screen revealed a significant transcriptional downregulation of E-cadherin in both cell types (**Table 1 and Table 2**).

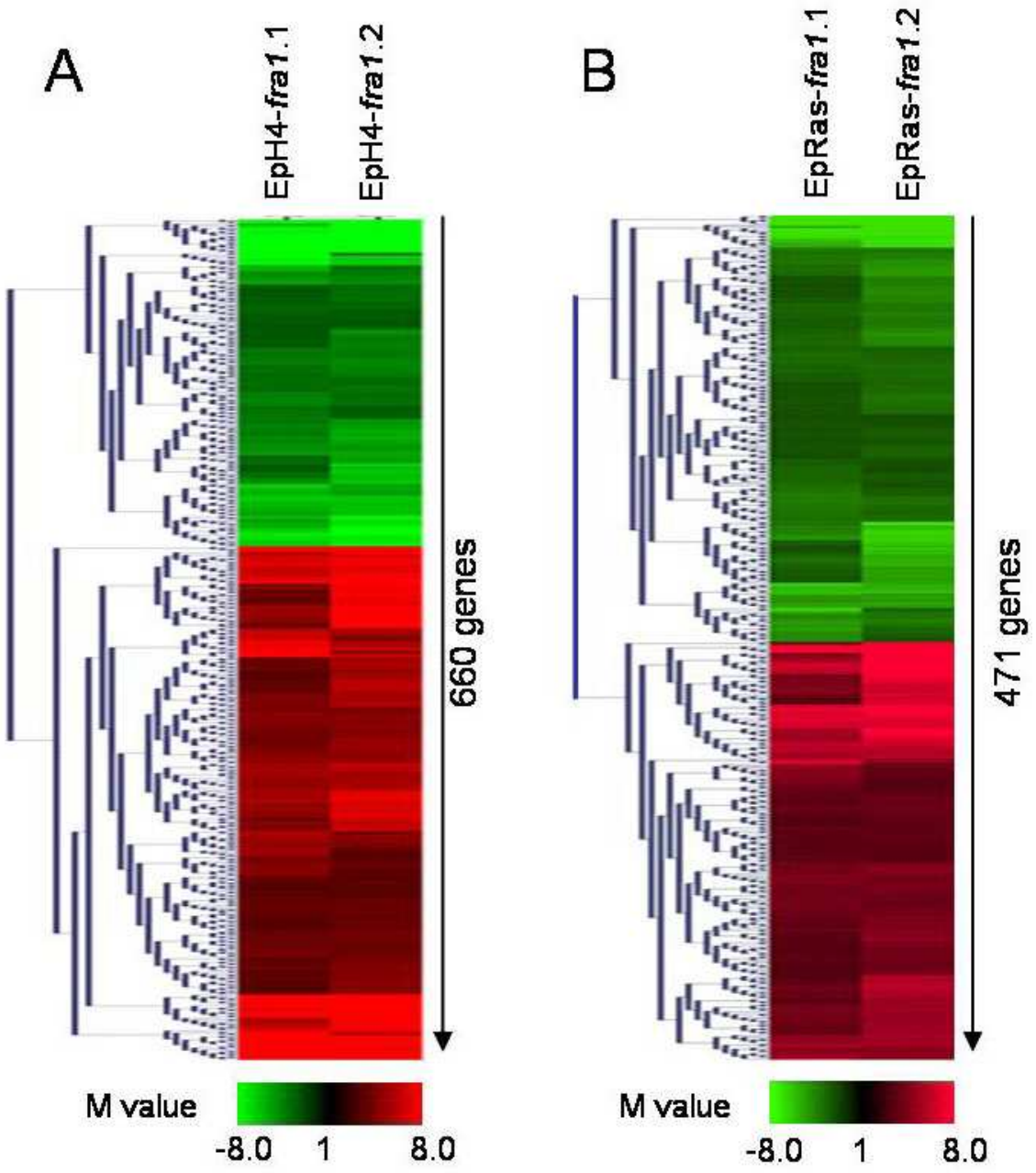

Figure 31. Heat-map for differentially expressed genes following ectopic Fra-1 expression. Only annotated genes with at least 2-fold change in expression and *p*-value<0.05 were considered as significant. **(A)** In EpH4-*fra1* cells, the expression of 660 genes was affected, while the expression of 471 genes was affected in EpRas-*fra1* cells **(B)**. M value represents the log2 ratio of gene expression between the individual sample and average of all samples.

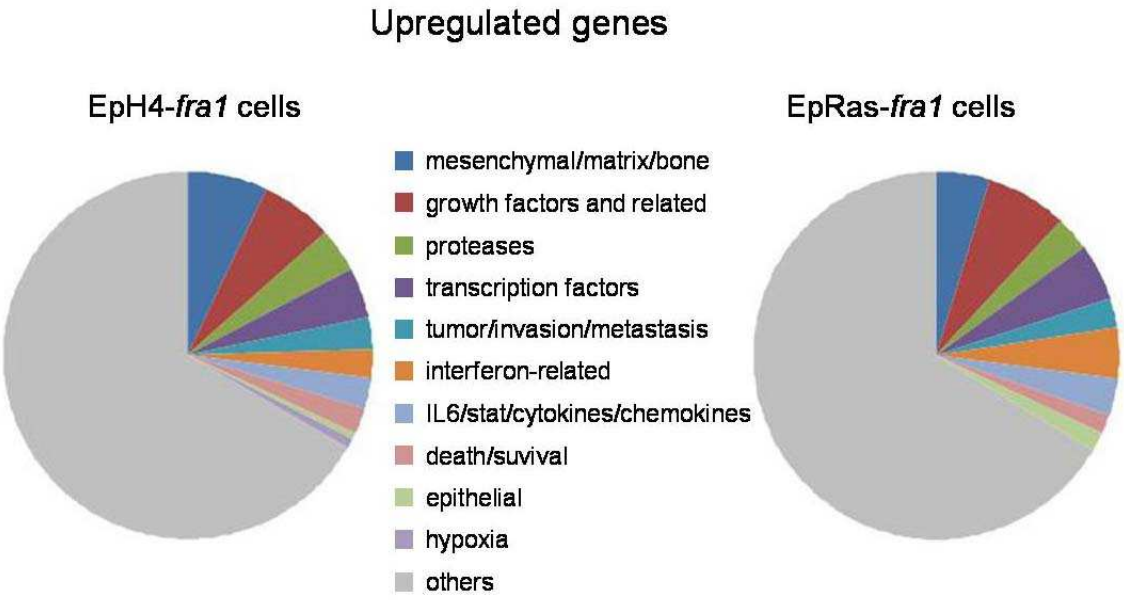

Figure 32. Gene cluster analysis of upregulated genes. Schematic representation showing the major upregulated gene clusters in EpH4-*fra1* and EpRas-*fra1* cells. The genes were organised in clusters according to their functional annotation.

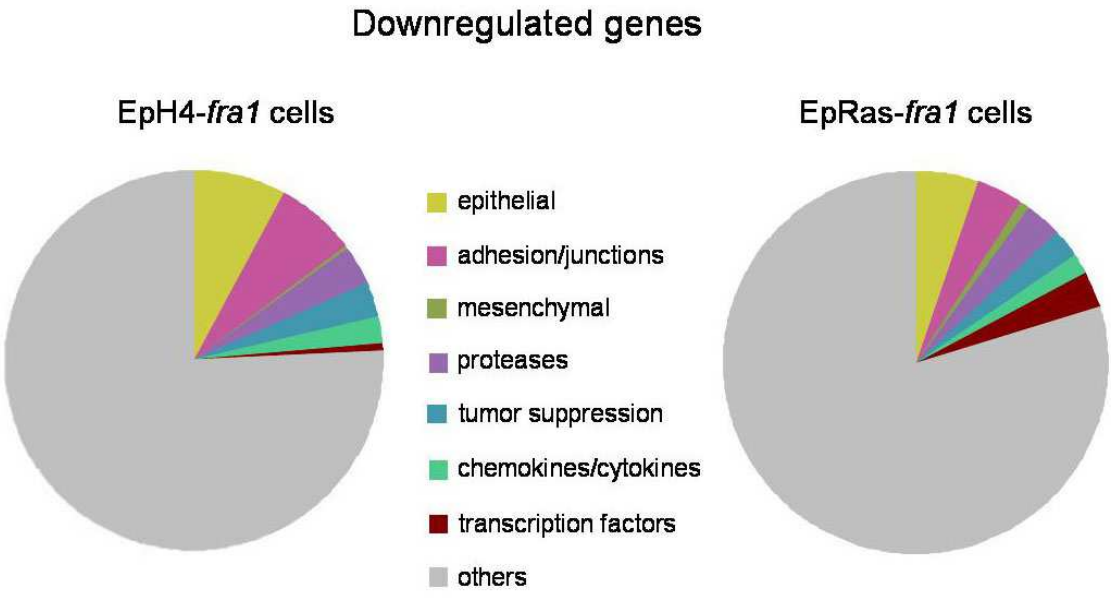

Figure 33. Gene cluster analysis of downregulated genes. Schematic representation showing the major upregulated gene clusters in EpH4-*fra1* and EpRas-*fra1* cells. The genes were organised in clusters according to their functional annotation.

Table 1. Selection of genes deregulated in EpH4-*fra1* cells previously implicated in cancer progression and EMT

Gene ID	Gene name	Fold change		Functional assignment
		EpH4*fra1*.1	**EpH4*fra1*.2**	
Mmp3	matrix metallopeptidase 3	80.1	33.2	Protease/Invasion
Ecm1	extracellular matrix protein 1	20.3	14.0	Matrix/Invasion
Zeb1	zinc finger E-box binding homeobox 1	12.6	11.2	Transcription factor
Mmp13	matrix metallopeptidase 13	12.2	12.0	Protease/Invasion
Mmp2	matrix metallopeptidase 2	9.4	44.5	Protease/Invasion
Plat	plasminogen activator, tissue	7.5	4.9	Protease/invasion
Cxcl12	chemokine (C-X-C motif) ligand 12	7.0	4.9	Chemokine/Invasion
Itga5	integrin alpha 5 (fibronectin receptor alpha)	5.0	5.2	Matrix/Invasion
Sparc	secreted acidic cysteine rich glycoprotein	4.7	5.9	Matrix/invasion
Tgfb2	transforming growth factor, beta 2	4.4	13.1	Cytokine/invasion
Mmp11	matrix metallopeptidase 11	3.9	3.8	Protease/Invasion
Stat3	signal transducer and activator of transcription 3	3.9	3.8	Transcription factor
Zeb2	zinc finger E-box binding homeobox 2	3.8	5.0	Transcription factor
Mapk3	mitogen activated protein kinase 3	3.5	2.5	Signal transduction/Invasion
Fgfr1	fibroblast growth factor receptor 1	3.4	4.1	Growth factor receptor
Mmp14	matrix metallopeptidase 14 (membrane-inserted)	3.3	3.5	Protease/Invasion
Fn1	fibronectin 1	2.9	5.4	Matrix/Invasion
Rhob	ras homolog gene family, member B	2.4	7.9	Cytoskeleton/Invasion
Stat1	signal transducer and activator of transcription 1	2.3	13.3	Transcription factor
Hif1a	hypoxia inducible factor 1, alpha subunit	2.2	2.1	Hypoxia/Invasion
Ctsb	cathepsin B	2.1	3.2	Protease/Invasion
Dsg2	desmoglein 2	-2.1	-3.3	Epithelial/Adhesion
Wnt7a	wingless-related MMTV integration site 7A	-18.3	-18.6	Growth factor
Tacstd1	tumor-associated calcium signal transducer 1	-11.3	-86.8	Epithelial/Adhesion
Lama3	laminin, alpha 3	-8.9	-24.0	Epithelial/Adhesion
St14	suppression of tumorigenicity 14	-7.6	-13.5	Tumor suppressor/Invasion
Krt18	keratin 18	-7.2	-5.2	Epithelial
Cldn3	claudin 3	-6.5	-8.2	Epithelial/Adhesion
Cldn1	claudin 1	-5.5	-6.0	Epithelial/Adhesion
Cst6	cystatin E/M	-5.2	-4.0	Protease/Invasion
Cdh1	cadherin 1	-4.3	-7.5	Epithelial/Adhesion
Cldn7	claudin 7	-3.9	-3.3	Epithelial/Adhesion
Tspan1	tetraspanin 1	-2.8	-2.8	Epithelial/Adhesion
Krt8	keratin 8	-2.5	-2.1	Epithelial

*Upregulated genes are represented by positive fold change values and downregulated genes by negative values. Only annotated genes were analysed and are listed alphabetically.

Table 2. Selection of genes deregulated in EpRas-*fra1* cells previously implicated in cancer progression and EMT

Gene ID	Gene name	Fold change		Functional assignment
		EpRas*fra1*.1	EpRas*fra1*.2	
L1cam	L1 cell adhesion molecule	5.4	5.1	Mesenchymal/Adhesion
Mgp	matrix Gla protein	3.9	13.8	Matrix
Fgfr1	fibroblast growth factor receptor 1	3.2	2.8	Growth factor receptor
Fn1	fibronectin 1	3.2	5.1	Matrix/Invasion
Ctsb	cathepsin B	3.1	5.5	Protease/invasion
Adam10	a disintegrin and metallopeptidase domain 10	2.9	3.1	Protease/invasion
Stat1	signal transducer and activator of transcription 1	2.7	3.8	Transcription factor
Mmp1a	matrix metallopeptidase 1a (interstitial collagenase)	2.4	4.8	Protease/invasion
Cdh2	cadherin 2	2.3	2.5	Mesenchymal/Invasion
Klf8	Kruppel-like factor 8	2.3	4.1	Transcription factor
Snai2	snail homolog 2 (Drosophila)	2.3	4.3	Transcription factor
Mmp12	matrix metallopeptidase 12	2.2	4.2	Protease/invasion
Adam8	a disintegrin and metallopeptidase domain 8	2.1	3.1	Protease/invasion
Cd44	CD44 antigen	2.1	5.0	Signaling/Invasion
Ctnnb1	catenin (cadherin associated protein). beta 1	2.1	4.2	Transcription factor
Mmp19	matrix metallopeptidase 19	2.1	2.7	Protease/invasion
Wnt7a	wingless-related MMTV integration site 7A	-5.3	-11.6	Growth factor
St14	suppression of tumorigenicity 14	-4.0	-6.4	Tumor suppressor/Invasion
Zeb2	zinc finger E-box binding homeobox 2	-3.8	-5.0	Transcription factor
Cldn6	claudin 6	-3.8	-8.0	Epithelial/Adhesion
Ocln	occludin	-3.6	-5.9	Epithelial/Adhesion
Cdh1	cadherin 1	-2.9	-6.5	Epithelial/Adhesion
Cldn7	claudin 7	-2.5	-2.6	Epithelial/Adhesion
Krt18	keratin 18	-2.5	-2.6	Epithelial/Adhesion
Des	desmin	-2.1	-2.2	Epithelial/Adhesion

*Upregulated genes are represented by positive fold change values and downregulated genes by negative values. Only annotated genes were analysed and are listed alphabetically.

As exemplified above, Fra-1 overexpression in epithelial EpH4 and EpRas cells resulted in substantial upregulation of a number of genes that have previously been implicated either in induction of EMT or maintenance of the invasive phenotype. Accordingly, genes typical of epithelial cells, mainly involved in cell adhesion, as well as those involved in tumor suppression were found to be downregulated. However, not all of these genes showed common regulation in both cell types. Therefore, to reduce the number of candidate genes for further analysis, I divided the genes into two main groups. All genes that were commonly regulated in EpH4-*fra1* and EpRas-*fra1* cells were assigned to one group. In the second group, I organized the genes that were directly related to commonly regulated genes, such as members of the same family, but were not differentially regulated in both cell types (**Figure 34**). The remaining genes with no relation to commonly regulated

genes were excluded from further analysis. I found 51 commonly upregulated and 60 commonly downregulated genes (**Table 3**). Additionally, I found 50 upregulated and 34 downregulated "related-common genes" in EpH4-*fra1* cells, and 45 upregulated and 26 downregulated "related-common" genes in EpRas-*fra1* cells, respectively.

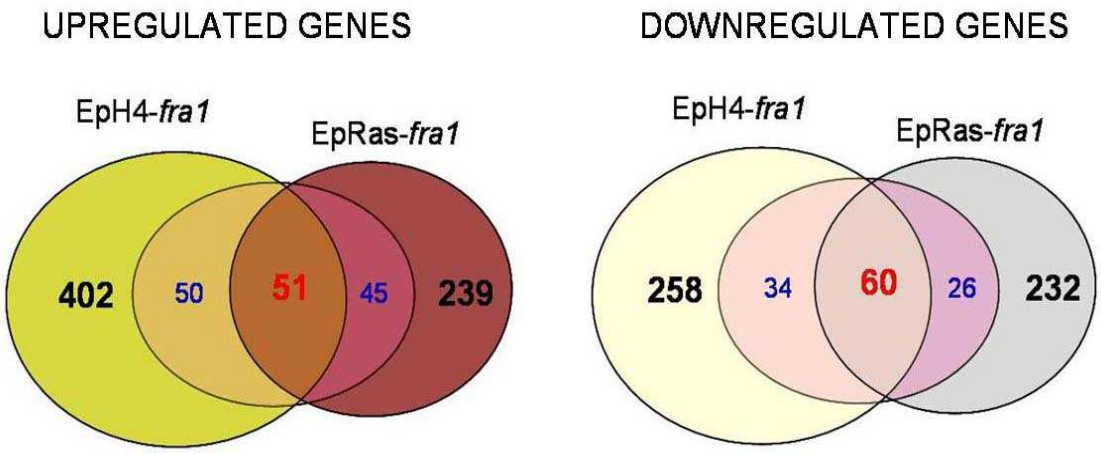

Figure 34. Schematic representation of differentially regulated genes common in EpH4-*fra1* and EpRas-*fra1* cells. Numbers in black represent total number of differentially regulated genes; numbers of strictly common regulated genes are depicted in red and the numbers of related-common genes in blue.

Table 3. List of commonly regulated genes in EpH4-*fra1* and EpRas-*fra1* cells

GENE ID	GENE NAME	FOLD CHANGE			
		EpH4*fra1*.1	EpH4*fra1*.1	EpRas*fra1*.1	EpRas*fra1*.2
Mmp12	matrix metallopeptidase 12	37.5	13.1	2.2	4.2
Msr1	macrophage scavenger receptor 1	21.9	16.9	2.6	2.2
Pde2a	phosphodiesterase 2A. cGMP-stimulated	17.2	26.6	7.9	10.3
Cp	ceruloplasmin	15.6	14.1	2.7	2.7
Ppap2b	phosphatidic acid phosphatase type 2B	14.5	24.7	2.7	2.2
Lbp	lipopolysaccharide binding protein	9.6	19.8	3.7	4.2
Ncf4	neutrophil cytosolic factor 4	7.9	28.4	3.5	2.2
Txnip	thioredoxin interacting protein	6.6	21.7	4.3	2.9
Mgp	matrix Gla protein	6.5	25.7	3.9	13.8
Cdh13	cadherin 13	6.1	5.0	2.0	3.4
Slc41a2	solute carrier family 41. member 2	5.8	7.5	2.2	3.4
Fkbp14	FK506 binding protein 14	5.6	6.3	3.2	7.2
Sh3kbp1	SH3-domain kinase binding protein 1	5.3	3.6	2.5	5.0
Tsc22d1	TSC22 domain family. member 1	5.1	6.9	2.5	2.6
Sorbs1	sorbin and SH3 domain containing 1	4.3	4.6	2.6	2.5
Sulf2	sulfatase 2	4.2	21.8	3.7	6.2

Pik3ip1	phosphoinositide-3-kinase interacting protein 1	3.8	12.1	2.6	2.4
Zeb2	zinc finger E-box binding homeobox 2	3.8	5.0	3.0	3.7
Iigp1	interferon inducible GTPase 1	3.7	33.5	3.6	2.2
Casp12	caspase 12	3.5	6.2	5.6	10.5
Fgfr1	fibroblast growth factor receptor 1	3.4	4.1	3.2	2.8
Gja1	gap junction protein. alpha 1	3.4	3.1	2.1	6.0
Krt39	keratin 39	3.4	3.9	2.1	2.1
Pnrc1	proline-rich nuclear receptor coactivator 1	3.4	2.8	2.9	2.5
Adcy9	adenylate cyclase 9	3.3	4.9	2.1	2.2
Casp1	caspase 1	3.3	6.6	24.2	36.9
Sgk	serum/glucocorticoid regulated kinase	3.1	2.5	2.5	2.9
Evi2a	ecotropic viral integration site 2a	3.0	3.5	4.0	6.5
Scara5	scavenger receptor class A. member 5 (putative)	2.9	2.9	3.6	6.7
Fn1	fibronectin 1	2.9	5.4	3.2	5.1
Cd47	CD47 antigen	2.8	4.2	2.1	2.0
Lhfpl2	lipoma HMGIC fusion partner-like 2	2.8	5.0	2.1	3.1
Ptprs	protein tyrosine phosphatase. receptor type. S	2.8	3.7	2.5	3.0
Col4a5	collagen type IV. alpha 5	2.7	3.1	2.8	4.0
Fosl1	fos-like antigen 1	2.7	3.8	2.5	3.1
Ypel2	yippee-like 2 (Drosophila)	2.7	4.9	2.2	3.3
Col4a5	collagen type IV. alpha 5	2.7	3.1	2.8	4.0
Mfge8	milk fat globule-EGF factor 8 protein	2.6	3.6	2.5	2.2
Ifi202b	interferon activated gene 202B	2.4	6.4	2.3	2.6
Pink1	PTEN induced putative kinase 1	2.4	4.0	2.5	2.7
Sepn1	selenoprotein N. 1	2.4	2.1	2.9	2.6
Vim	vimentin	2.4	3.8	-6.0	-6.2
Grn	granulin	2.3	6.5	2.3	2.9
Il6st	interleukin 6 signal transducer	2.3	3.3	2.2	3.5
Mmp19	matrix metallopeptidase 19	2.3	2.4	2.1	2.7
Rcn1	reticulocalbin 1	2.3	2.9	8.1	12.6
Stat1	signal transducer and activator of transcription 1	2.3	13.3	2.7	3.8
Ypel1	yippee-like 1 (Drosophila)	2.3	2.4	3.2	3.2
Maged1	melanoma antigen. family D. 1	2.2	2.8	2.4	3.9
Timp2	tissue inhibitor of metalloproteinase 2	2.2	3.1	2.2	2.3
Ctsb	cathepsin B	2.1	3.2	3.1	5.5
Ifi203	interferon activated gene 203	2.1	7.3	4.1	3.3
Sox4	SRY-box containing gene 4	2.1	2.9	2.1	2.2
Wnt7a	wingless-related MMTV integration site 7A	-18.3	-18.7	-5.3	-11.6
Mal	myelin and lymphocyte protein. T-cell differentiation protein	-18.0	-38.2	-3.4	-12.2
Tmem54	transmembrane protein 54	-17.1	-31.4	-3.7	-13.5
Psg30	pregnancy-specific glycoprotein 30	-16.7	-33.3	-4.6	-16.3
Fgfbp1	fibroblast growth factor binding protein 1	-16.1	-43.1	-4.4	-16.7
Krt7	keratin 7	-14.7	-26.5	-4.8	-12.7
Rab25	RAB25. member RAS oncogene family	-14.6	-52.2	-3.3	-46.6
Mcpt8	mast cell protease 8	-13.2	-14.1	-5.9	-7.7
Kcnk1	potassium channel. subfamily K. member 1	-12.8	-28.0	-2.8	-14.2
Itm2a	integral membrane protein 2A	-12.0	-2.1	-2.1	-4.2
Tacstd1	tumor-associated calcium signal transducer	-11.3	-86.8	-2.5	-57.4
Gpr87	G protein-coupled receptor 87	-10.0	-18.9	-4.8	-5.6
Lama3	laminin. alpha 3	-8.9	-8.9	-24.0	-24.0
Ppbp	pro-platelet basic protein	-8.9	-49.6	-2.0	-2.6
Ripk4	receptor-interacting serine-threonine kinase 4	-8.7	-25.1	-2.7	-18.5

Rbm35a	RNA binding motif protein 35A	-8.6	-12.5	-2.5	-8.8
Wnt10a	wingless related MMTV integration site 10a	-8.3	-9.7	-3.1	-2.4
St14	suppression of tumorigenicity 14 (colon carcinoma)	-7.6	-13.5	-4.0	-6.4
Tmem16j	transmembrane protein 16J	-7.6	-7.0	-2.5	-3.4
Car7	carbonic anhydrase 7	-7.5	-9.9	-3.9	-9.4
Grb7	growth factor receptor bound protein 7	-7.4	-14.0	-4.0	-8.1
Krt18	keratin 18	-7.2	-5.2	-2.5	-2.6
Cldn3	claudin 3	-6.5	-8.2	-2.9	-3.1
Mpzl2	myelin protein zero-like 2	-6.5	-4.7	-2.8	-5.6
Mal2	mal. T-cell differentiation protein 2	-5.3	-10.8	-2.7	-5.2
Entpd3	ectonucleoside triphosphate diphosphohydrolase 3	-5.2	-3.9	-2.1	-2.7
Epb4.1l5	erythrocyte protein band 4.1-like 5	-5.2	-6.9	-2.4	-4.2
Ddah1	dimethylarginine dimethylaminohydrolase 1	-5.1	-13.1	-5.9	-6.0
Nrarp	Notch-regulated ankyrin repeat protein	-5.1	-6.9	-4.1	-3.9
Ankrd22	ankyrin repeat domain 22	-4.9	-9.0	-2.4	-3.6
Nrg1	neuregulin 1	-4.5	-2.8	-2.2	-2.3
Atp8b1	ATPase. class I. type 8B. member 1	-4.3	-5.9	-2.0	-3.6
Cdh1	cadherin 1	-4.3	-7.5	-2.9	-6.5
Lsr	lipolysis stimulated lipoprotein receptor	-4.2	-6.1	-2.3	-11.8
Krt5	keratin 5	-4.1	-4.8	-2.1	-2.4
Ovol2	ovo-like 2 (Drosophila)	-4.1	-6.5	-2.4	-4.1
Cldn6	claudin 6	-3.9	-3.7	-3.8	-8.0
Cldn7	claudin 7	-3.9	-3.3	-2.5	-2.6
Sigirr	single immunoglobulin and toll-interleukin 1 receptor (TIR) domain	-3.9	-3.7	-2.8	-3.8
Rras2	related RAS viral (r-ras) oncogene homolog 2	-3.7	-3.9	-2.5	-2.5
Odc1	ornithine decarboxylase. structural 1	-3.6	-4.6	-2.4	-2.1
Ocln	occludin	-3.5	-6.5	-3.6	-5.9
Csf3	colony stimulating factor 3 (granulocyte)	-3.3	-7.8	-2.2	-5.5
Prss16	protease. serine. 16 (thymus)	-3.3	-2.7	-2.4	-3.9
Krt76	keratin 76	-3.2	-3.4	-2.2	-2.2
Tnc	tenascin C	-3.2	-5.3	-3.1	-5.6
Aurka	aurora kinase A	-3.1	-4.4	-2.5	-2.4
Dos	downstream of Stk11	-3.1	-4.7	-2.0	-2.3
Tspan1	tetraspanin 1	-2.8	-2.8	-2.8	-2.6
Ctsw	cathepsin W	-2.7	-2.8	-3.9	-4.5
Hs3st1	heparan sulfate (glucosamine) 3-O-sulfotransferase 1	-2.7	-2.9	-2.6	-2.7
Adamts5	a disintegrin-like and metallopeptidase (reprolysin type) with thrombospondin type 1 motif. 5	-2.6	-2.3	-2.7	-8.5
Mbnl3	muscleblind-like 3 (Drosophila)	-2.5	-4.6	-2.8	-2.2
Krt75	keratin 75	-2.3	-2.5	-2.1	-2.3
Shmt1	serine hydroxymethyltransferase 1 (soluble)	-2.1	-5.1	-2.7	-2.1
Ccdc33	coiled-coil domain containing 33	-2.0	-2.5	-2.4	-2.1
Ncaph	non-SMC condensin I complex. subunit H	-2.0	-5.0	-3.4	-2.6
Pawr	PRKC. apoptosis. WT1. regulator	-2.0	-2.8	-2.1	-2.5
Serpinb5	serine (or cysteine) peptidase inhibitor. clade B. member 5	-2.0	-4.5	-7.6	-10.7

*Upregulated genes are represented by positive fold change values and downregulated genes by negative values. Only annotated genes were analysed and are listed alphabetically.

Next, I have clustered commonly regulated genes according to their functional annotation and predominant expression pattern in epithelial vs mesenchymal cells (**Figure 35**).

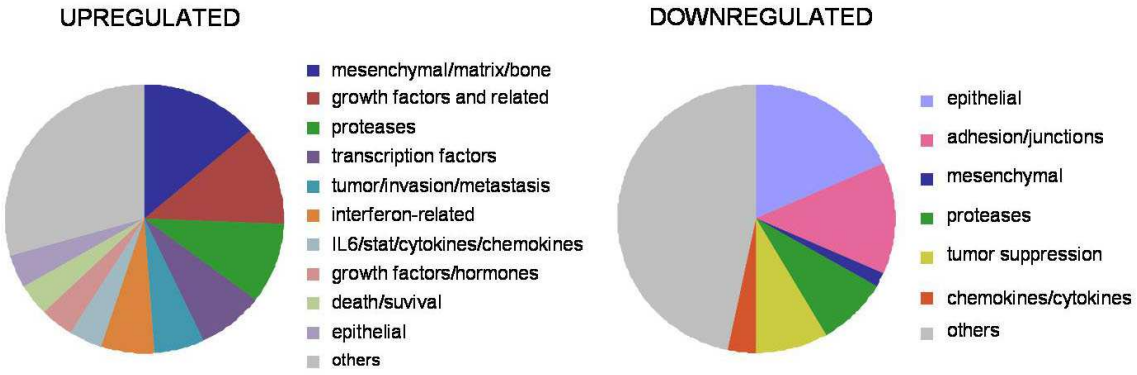

Figure 35. Gene cluster analysis of commonly regulated genes in EpH4-*fra1* and EpRas-*fra1* cells. Genes were grouped in clusters according to their functional annotation.

As expected, the majority of commonly upregulated genes were those encoding proteins typically found expressed in, and/or produced by mesenchymal cells. The second most abundant functional gene cluster was comprised of several growth factors, growth factor receptors and their interactors, followed by clusters of proteases, transcription factors and genes implicated in tumor invasion and metastasis. On the other hand, majority of downregulated genes were typical of epithelial cells and mainly involved in cell adhesion and tumor suppression. Thus, the overall gene expression signature of Fra-1 expressing cells was clearly shifted towards invasive, mesenchymal profile (**Figure 35**). Furthermore, there were a number of genes previously identified as expressed in metastatic derivatives of EpH4 cells modified with different oncogenes, which showed similar expression pattern in Fra-1 expressing cells (Jechlinger et al., 2002; Jechlinger et al., 2006).

Among those genes, zinc-finger transcription factor and direct E-cadherin repressor ZEB1 (ZFXH1a, TCF8, δEF1) and closely related ZEB2 (ZFXH1b, SIP1) that were significantly upregulated following Fra-1 overexpression, seemed like promising candidates for further analysis. In addition to E-cadherin repression, ZEB1 and ZEB2 are known to negatively regulate the expression of other EMT-related genes. Examples of EMT-related ZEB1 and ZEB2 target genes that were found to be downregulated in Fra-1 expressing cells include: laminin-alpha3 (Lama3), occludin (Ocln), claudin 7(Cldn7), connexin 26 (Gjb2), Crumbs homologue 3 (*Drosophila*) (Crb3), shroom (shrm), tetraspanin 1 (Tspan1), tumor-associated calcium signal transducer 1 and 2 (Tacstd1, Tacstd2) , Mal, T-cell differentiation protein 2 (Mal2) and cyclin D1 (Ccnd1) (Aigner et al., 2007; Vandewalle et al., 2005; Vandewalle et al., 2009). Additionally, genes that were previously found to be upregulated following ZEB1 or ZEB2 expression, such as cyclin G2 (Ccng2) and MMP-1, -2, and MT1-MMP (MMP-14) were also upregulated in Fra-1 expressing cells (Miyoshi et al., 2004; Chen et al., 2006). Taken together, these results strongly suggested that upregulation of ZEB1 and ZEB2 following Fra-1 overexpression might be an important downstream effect in induction of EMT.

To further confirm these results, I have analysed the expression of several of these genes as well as several other interesting genes relevant for EMT by qPCR (**Table 4**). The results obtained by the array and qPCR analysis for selected genes were in good overall correlation. However, while ZEB2 was consistently upregulated in both EpH4-*fra1* and EpRas-*fra1* cells, ZEB1 expression was found upregulated by the array only in EpH4-*fra1* cells. Interestingly, ZEB1 target genes were, however, deregulated also in EpRas-*fra1* cells. In addition, qPCR analysis revealed significant, roughly 2-fold and 3-fold induction of ZEB1 mRNA in EpRas-*fra1* cells (**Figure 36A**).

Table 4. QPCR verification of array results for selected genes.

GENE ID	GENE NAME	FOLD CHANGE (ARRAY / qPCR)			
		EpH4*fra1*.1	EpH4*fra1*.1	EpRas*fra1*.1	EpRas*fra1*.2
Tnc	tenascin C	-3.2 / -1.3	-5.3 / -1.3	-3.1 / -1.1	-5.6 / -1.4
Cd44	CD44 antigen	n.s.	n.s.	2.1 / 3.2	5.0 / 8.4
Cldn3	claudin 3	-6.5 / -4.2	-8.2 / -3.5	-2.9 / -2.0	-3.1 / -2.0
Cldn6	claudin 6	-3.9 / -3.3	-3.7 / -3.5	-3.8 / -3.0	-8.0 / -3.5
Cldn7	claudin 7	-3.9 / -2.8	-3.3 / -2.8	-2.5 / -2.2	-2.6 / -2.0
Ctsb	cathepsin B	2.1/ 2.5	3.2 / 2.6	3.1 / 2.8	5.5 / 3.4
Krt18	keratin 18	-7.2 / -5.7	-5.2 / -6.0	-2.5 / -2.0	-2.6 / -2.0
Lama3	laminin alpha 3	-8.9 / -4.4	-24 / -9.7	n.s./ -1.2	n.s./ -1.1
Snai2	snail homolog 2 (Drosophila)	n.s.	n.s.	2.3 / 1.6	4.3 / 2.2
Fgfr1	fibroblast growth factor receptor 1	3.4 / 2.9	4.1 / 2.7	3.2 / 2.9	2.8 / 2.3
Sparc	secreted acidic cysteine rich glycoprotein	4.7/ 1.4	5.9/ 2.3	n.s.	n.s.
Vim	vimentin	2.4 / 2.0	3.8 / 4.0	-6.0 / -20.0	-6.2 / -19.4
Wnt7a	wingless-related MMTV integration site 7A	-18.3 / -4.2	-18.7 / -4.0	-5.3 / -2.4	-11.6 / -3.7
Zeb1	zinc finger E-box binding homeobox 1	12.6 / 7.2	11.2 / 9.1	n.s. / 2.2	n.s. / 3.1
Zeb2	zinc finger E-box binding homeobox 2	3.2 / 5.2	4.9 / 7.1	3.0 / 4.1	3.7 / 8.3
Tspan1	tetraspanin 1	-2.8 / -1.9	-2.8 / -1.7	-2.8 / -1.1	-2.6 / -1.0
Stat1	signal transducer and activator of transcription 1	2.3 / 3.1	13.3 / 3.4	2.7 / 2.0	3.8 / 2.2
Ocln	occludin	-3.5 / -3.2	-6.5 / -3.9	-3.6 / -3.1	-5.9 / -3.3

* n.s., not significant. Fold downregulation (negative values) and fold upregulation (positive values) is shown.

The elevated levels of ZEB1 protein were further confirmed both in EpH4-*fra1* and EpRas-*fra1* cells by Western blotting (**Figure 36B**). Most likely, the reason for the obvious discrepancy in the expression pattern of ZEB1 in EpRas-*fra1* cells detected by the microarray, qPCR and Western blot, is the fact that in the process of the array data analysis I decided to use very stringent filtering parameters. That way, any gene with less than two-fold change in expression was designated as not significantly deregulated. In addition, another possible explanation lies in the known technical limitations of the microarray as a genome-wide screening method. It happens quite often that due to insufficient probe labelling and/or weak hybridization, false-negative results for gene expression are obtained, further highlighting the necessity for additional verification of the obtained results by other methods such as qPCR or Northern blot.

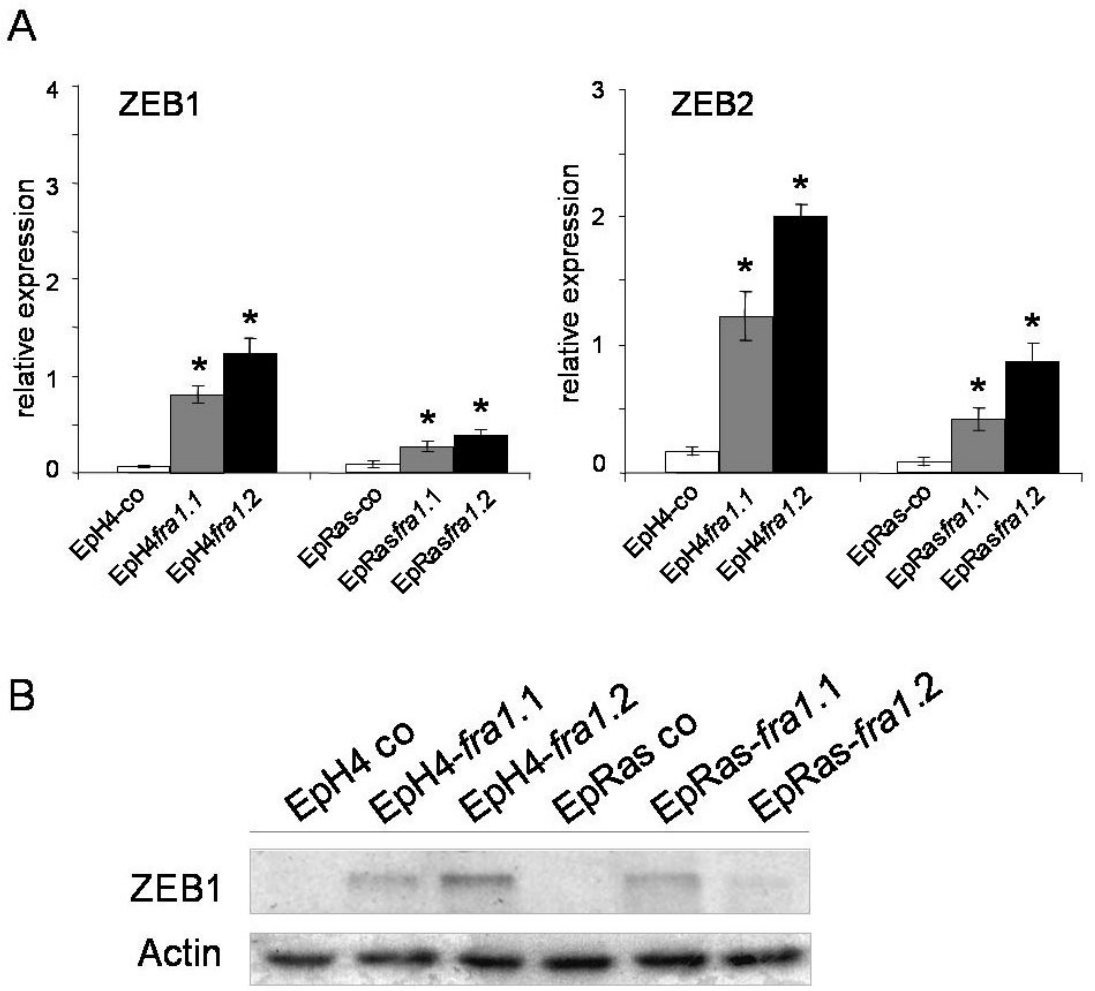

Figure 36. Induction of ZEB1 and ZEB2 expression by Fra-1. (A) Increased ZEB1 and ZEB2 expression levels detected in the array were confirmed by qPCR analysis. Error bars are indicated and p-values< 0.05 were considered significant (*). **(B)** ZEB1 protein level was additionally determined by Western blot.

In line with the epithelial phenotype of both EpH4 and EpRas cells, these cells normally express comparable (EpRas cells show 0.2-fold higher ZEB1 expression) and only barely detectable levels of ZEB1 and ZEB2 mRNAs. Consistent with these results, in both EpH4 and EpRas cells, ZEB1 protein levels were not detectable by Western blot (**Figure 36B**, lanes 1 and 4). Unfortunately, however, after several attempts and using two different antibodies, I did not succeed in detecting ZEB2 protein levels by Western blot or immunofluorescence. Since significantly increased levels of ZEB2 mRNA were detected by the microarray and subsequently verified by qPCR analysis, I could only conclude that the inability to detect the corresponding increase in protein levels was due to technical reasons, because of

the low quality of commercially available ZEB2 antibodies. However, even though it is well known that the anti-ZEB2 antibodies often fail to detect the ZEB2 protein (A. Eger, pers. comm.), I can not completely exclude the possibility that the ZEB2 protein is not expressed in these cells even though high amounts of ZEB2 mRNA are present. Another possible explanation is that due to known high turn-over rate of the protein, the protein itself is expressed, but at very low levels that are beneath the detection threshold of the antibody.

3.10.1 Transient silencing of ZEB1 and/or ZEB2 in EpH4-*fra1* and EpRas-*fra1* cells relieves transcriptional repression of E-cadherin

To further test whether E-cadherin transcriptional repression is mediated by Fra-1-induced upregulation of ZEB1 and ZEB2, I used siRNA oligonucleotides to transiently knock-down ZEB1 and ZEB2 in EpH4-*fra1* and EpRas-*fra1* cells (**Figure 37**). The cells were transfected with a pooled set of four different siRNA oligonucleotides complementary to the mRNAs of ZEB1, ZEB2, or both combined. As a negative control I used non-targeting siRNA. To ensure a maximal silencing effect, the cells were transfected with siRNAs, cultured for 96h, then re-plated and transfected again. Knock-down efficiency was examined by qPCR 96h after the second transfection. Transfection of cells with both ZEB1 and ZEB2 siRNAs resulted in significantly reduced (by 80-90%) corresponding mRNA levels (**Figure 37A**).

In addition, silencing ZEB1 had only minor (0.1-fold) and non significant effect on the expression of ZEB2, while ZEB2 silencing had no effect on the expression of ZEB1 mRNA (data not shown). Furthermore, silencing either ZEB1 or ZEB2 alone resulted in transcriptional upregulation of E-cadherin (**Figure 37B**). However, ZEB1 knock-down seemed to have a slightly stronger effect on E-cadherin reexpression in EpH4-*fra1* cells, while ZEB2 knock-down had slightly stronger effect in EpRas cells. In both cell types, however, silencing both ZEB1 and ZEB2 had a cumulative effect and resulted in slightly higher re-expression of E-cadherin than seen by silencing either gene alone.

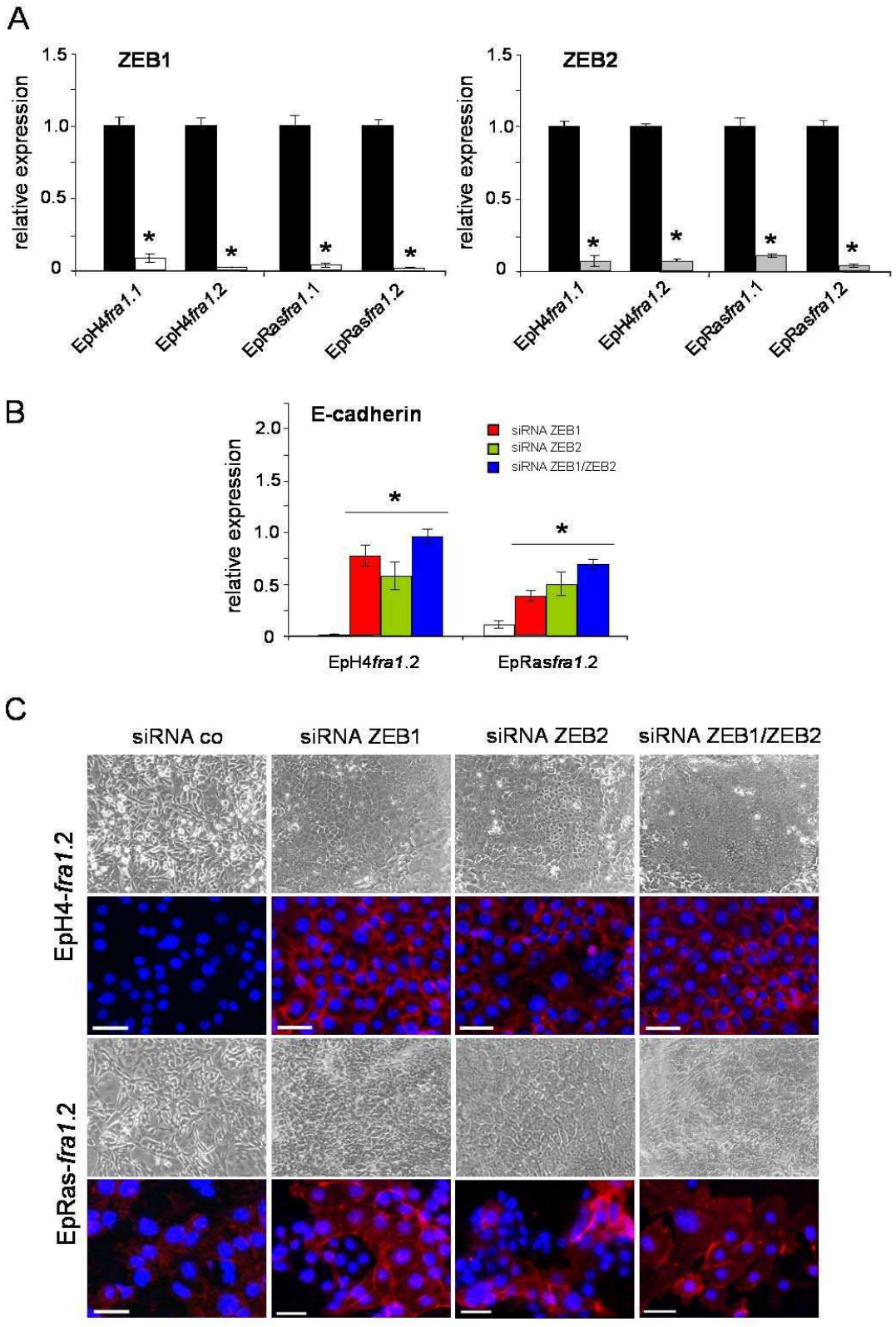

Figure 37. ZEB1 and ZEB2 knock-down relieves E-cadherin repression. (A) ZEB1 and ZEB2 expression was determined by qPCR analysis. **(B)** QPCR analysis showed reexpression of E-cadherin mRNA following transient knock-down of ZEB1 and/or ZEB2. Results are presented as mean and error bars are indicated. *P*-values <0.05 were considered significant (*). **(C)** Phase-contrast images (upper panels) and immunofluorescent staining for E-cadherin (lower panels) of one representative EpH4-*fra1* and EpRas-*fra1* clone shows reversal of epithelial morphology and corresponding reexpression of E-cadherin. Nuclei were counterstained with DAPI (blue). Scale bar, 20μM.

Consistent with E-cadherin reexpression, the cells regained epithelial morphology, even though the effect was more pronounced in EpH4 cells (**Figure 37C**). Immunofluorescent staining confirmed reexpression and predominantly membranous localisation of E-cadherin in EpH4-*fra1* cells. However, immunofluorescent staining revealed that even though EpRas-*fra1* cells upregulated E-cadherin, it was still mainly localised to the cytoplasm and not strongly expressed in all cells. It was only by combined silencing of ZEB1 and ZEB2 that the cells restored E-cadherin expression comparable to that of EpRas cells. These results suggested that both ZEB1 and ZEB2 are necessary for both transcriptional downregulation of E-cadherin and induction of an EMT-like phenotype in Fra-1 expressing cells.

3.10.2 Fra-1 binds to the ZEB1 promoter *in vivo*

After confirming that ZEB1 and ZEB2 are responsible for transcriptional downregulation of E-cadherin in EpH4-*fra1* and EpRas-*fra1* cells, I further explored the possible link with Fra-1/AP-1. It has been only recently reported that in the human breast cancer cell line MDA-MB-231, bone morphogenic protein-6 (BMP6) negatively regulates ZEB1 transcription in an AP-1 dependent manner resulting in re-expression of E-cadherin. In that study, the authors have shown that BMP-6 treatment repressed ZEB1 transcription by downregulating c-Fos and c-Jun protein levels resulting in significantly decreased binding of c-Fos/c-Jun to the endogenous ZEB1 promoter. In addition, mutation of the TRE element (TGAGGAA) located at position -254/-248 of the human ZEB1 promoter abolished the repressive effect of ZEB1 transcription by BMP-6 (Yang et al., 2009). However, the authors did not further explore the potential involvement of other AP-1 members in that context.

To determine if ZEB1 is a direct transcriptional target of Fra-1/AP-1, I first searched for potential AP-1 binding sites within the mouse ZEB1 promoter region. . Promoter analysis revealed four TRE elements located within 2000 bp upstream of transcription initiation site (**Figure 38A**).

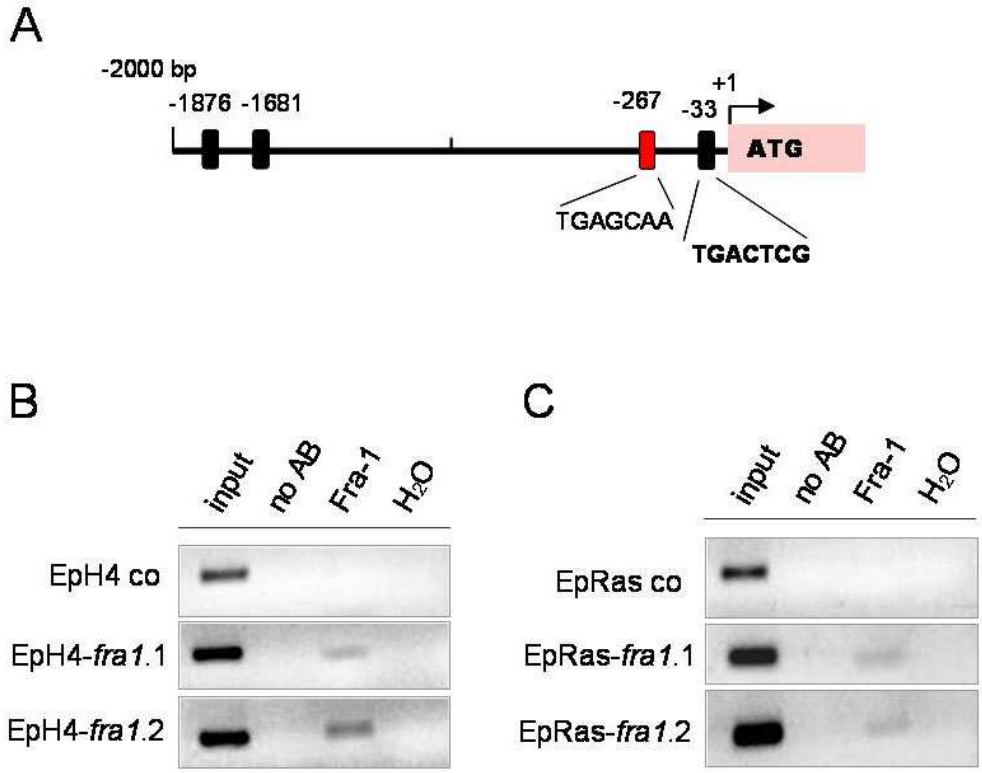

Figure 38. Fra-1/AP-1 directly binds to ZEB1 promoter. (A) Schematic representation of mouse ZEB1 promoter including 2000bp region upstream from transcription start site. Relative positions of TRE elements (potential AP-1 binding sites) are depicted by black boxes. Red box represents partially conserved previously published functional AP-1 site in human breast cancer cell line MDA-MB-231. **(B)** End-point products of QPCR reactions performed on immunoprecipitated chromatin bound by Fra-1 with ZEB1 promoter specific primers shows direct binding of Fra-1 to the proximal TRE element.

Interestingly, the previously published TRE element appeared to be partially conserved in the mouse ZEB1 promoter and located at position -267/-260 upstream from the transcription start site. Furthermore, I detected an additional TRE element (TGACTCG) located at position -33/-26 of the mouse ZEB1 promoter. To test if Fra-1 directly binds to the ZEB1 promoter *in vivo*, I have performed ChIP experiments. Quantitative RT-PCR analysis with primers spanning the two proximal TRE elements revealed that immunoprecipitation of cross-linked chromatin from both EpH4-*fra1* and EpRas-*fra1* cells with Fra-1 specific antibody efficiently pulled down ZEB1 proximal promoter fragment (**Figure 38B-C**). These results clearly suggest that Fra-1/AP-1 is able to directly bind to the ZEB1 promoter in EpH4 and EpRas cells. To further substantiate these findings, I am currently performing additional gene reporter assays using the proximal promoter region of ZEB1 harbouring wild-

type and mutated TRE elements to determine whether and to what extent, binding of Fra-1 results in transcriptional activation of the ZEB1 promoter.

3.10.3 ZEB2 as potential Fra-1/AP-1 target gene

Since ZEB2 expression was also significantly upregulated in both EpH4-*fra1* and EpRas-*fra1* cells and its transient silencing resulted in E-cadherin reexpression, I suspected that in addition to ZEB1, Fra-1 might also directly regulate ZEB2 expression. Besides its high structural similarity to the ZEB1 gene, recently published characterization of the mouse ZEB2 gene revealed that the gene is being alternatively transcribed from three TATA-less promoters; the most distal-P1, middle-P2 showing the highest *in vitro* activity, and the most proximal-P3 (Nelles et al., 2003). Interestingly, the authors have shown that the predominant activity of a given promoter is tissue/cell-type specific and that the most proximal P3 promoter seems to be predominantly active in mouse mammary epithelial NMuMG cells. Analysis of P3 promoter region mapped immediately upstream from exon 1 at -551/-8 from transcriptional start site, revealed 3 TRE elements located within a stretch of roughly 140bp (**Figure 39**).

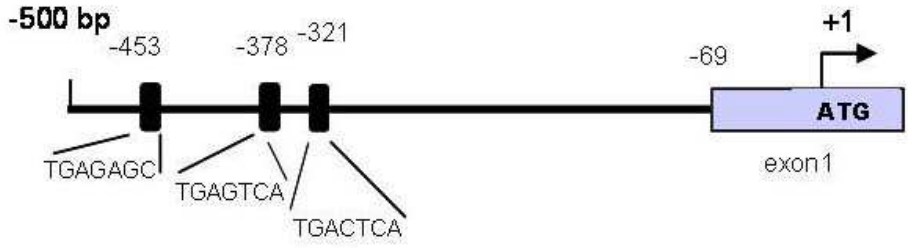

Figure 39. Schematic representation of ZEB2 most proximal P3 promoter region. Positions of the identified TRE elements relative to transcription start site are depicted in black boxes.

This finding strongly suggested that the Fra-1-containing AP-1 complexes could potentially bind to the ZEB2 promoter and directly regulate its expression *in vivo*. Chromatin-immunoprecipitation experiments combined with gene reporter assays are currently being performed to test this hypothesis.

3.11 Summary and conclusions

In the second part of my thesis, I focused my efforts on identifying potential EMT-related Fra-1 target genes and on understanding the molecular mechanism of Fra-1-mediated E-cadherin downregulation. I was able to show that E-cadherin is downregulated at the transcriptional level expression following ectopic Fra-1 expression and that the downregulation is apparently not due to promoter hypermethylation. To gain insight into changes in signalling pathways relevant for EMT downstream of Fra-1/AP-1, I performed genome-wide gene expression profiling using EpH4-*fra1* and EpRas-*fra1* cells. Fra-1 overexpression in EpH4 cells resulted in upregulation of 402 genes and downregulation of 239 genes. In EpRas cells, 258 genes were found to be upregulated and 232 genes downregulated. Subsequent analysis and functional clustering of differentially regulated genes revealed overall downregulation of genes specific of epithelial cells and upregulation of genes specific of invasive, mesenchymal cells as well as several known AP-1 target genes, such as MMPs and MGP, implicated in EMT and cancer progression. In addition, gene expression profiling confirmed the observed E-cadherin transcriptional downregulation and identified ZEB1 and ZEB2 as potential candidate genes downstream of Fra-1 that might directly be involved in E-cadherin transcriptional regulation.

Using siRNAs directed against ZEB1 and/or ZEB2 I was able to show that Fra-1-mediated upregulation of ZEB1 and ZEB2 is responsible for downregulation of E-cadherin, since transient knock-down of ZEB1 and/or ZEB2 resulted in re-expression of E-cadherin and reversal of the epithelial phenotype in Fra-1 expressing cells. Furthermore, promoter analysis revealed several potential AP-1 binding sites located within the ZEB1 promoter region suggesting a potential direct regulation by Fra-1. By performing ChIP experiments I was able to show that Fra-1 directly binds to the ZEB1 promoter *in vivo* thereby identifying ZEB-1 as a novel, direct transcriptional target of Fra-1/AP-1. Whether Fra-1 binding to the ZEB-1 promoter is sufficient for its transcriptional activation remains to be determined. To answer that question, gene reporter assays using the ZEB1 proximal promoter region harbouring original or mutated AP-1 sites are currently being performed.

In addition, analysis of the ZEB2 most proximal P3 promoter region that has been reported as predominantly active in mouse mammary epithelial NMuMG cells, revealed several potential AP-1 binding sites suggesting that in addition to ZEB1, ZEB2 might also be a direct Fra-1/AP-1 target gene. However, potential binding of Fra-1 to the ZEB2 promoter remains to be determined.

PART III

Fra-1 expression is both necessary and sufficient for EMT: Fra-1 knock-down by RNAi in EpRas and EpRasXT cells

3.12 Effect of Fra-1 silencing on TGF-β1-induced EMT

As the second approach to study the role of Fra-1 in EMT, I have attempted to stably knock-down the endogenous Fra-1 in EpRas and EpRasXT cells by RNA interference (RNAi). Since exogenous overexpression of Fra-1 resulted in induction of EMT in both EpH4 and EpRas cells, RNAi-mediated knock-down of endogenous Fra-1 in EpRas cells was expected to prevent TGFβ-induced EMT provided Fra-1 is indeed a major player in induction and maintenance of EMT. More importantly, Fra-1 knock-down in EpRasXT cells should, at least partially, result in reversal of the EMT phenotype.To test that hypothesis, I took advantage of commercially available lentiviruses expressing siRNA knock-down constructs for the entire mouse genome. I employed a set of lentiviruses containing five different, validated constructs targeting Fra-1 mRNA and a non-targeting hairpin as a negative control. Following infection with these lentiviruses, the cells were selected for 14 days in the presence of puromycin and pools of infected cells were assayed for Fra-1 expression levels by qPCR (data not shown). The control shRNA construct had no effect on Fra-1 transcript levels. However, only two out of five shRNA constructs resulted in significant knock-down of endogenous Fra-1 and were further used to derive single cell clones. Knock-down efficiency in several selected clones was examined by qPCR and Western blot analysis (**Figure 40B-C**). All selected clones showed 80-90% reduction in Fra-1 mRNA and protein levels. Interestingly, silencing of ectopic Fra-1 in EpRas cells resulted in formation of monolayers with improved epithelial polarity, resembling those formed by EpH4 cells, suggesting that the effects of Ras on epithelial cell behaviour were due to Fra-1. I therefore selected two clones that showed the most prominent morphological change for further functional characterization (**Figure 40A**). At the same time, there was no

significant change in mRNA expression of other Fos family members ruling out any off-targeting effect of the selected siRNA (**Figure 40D**).

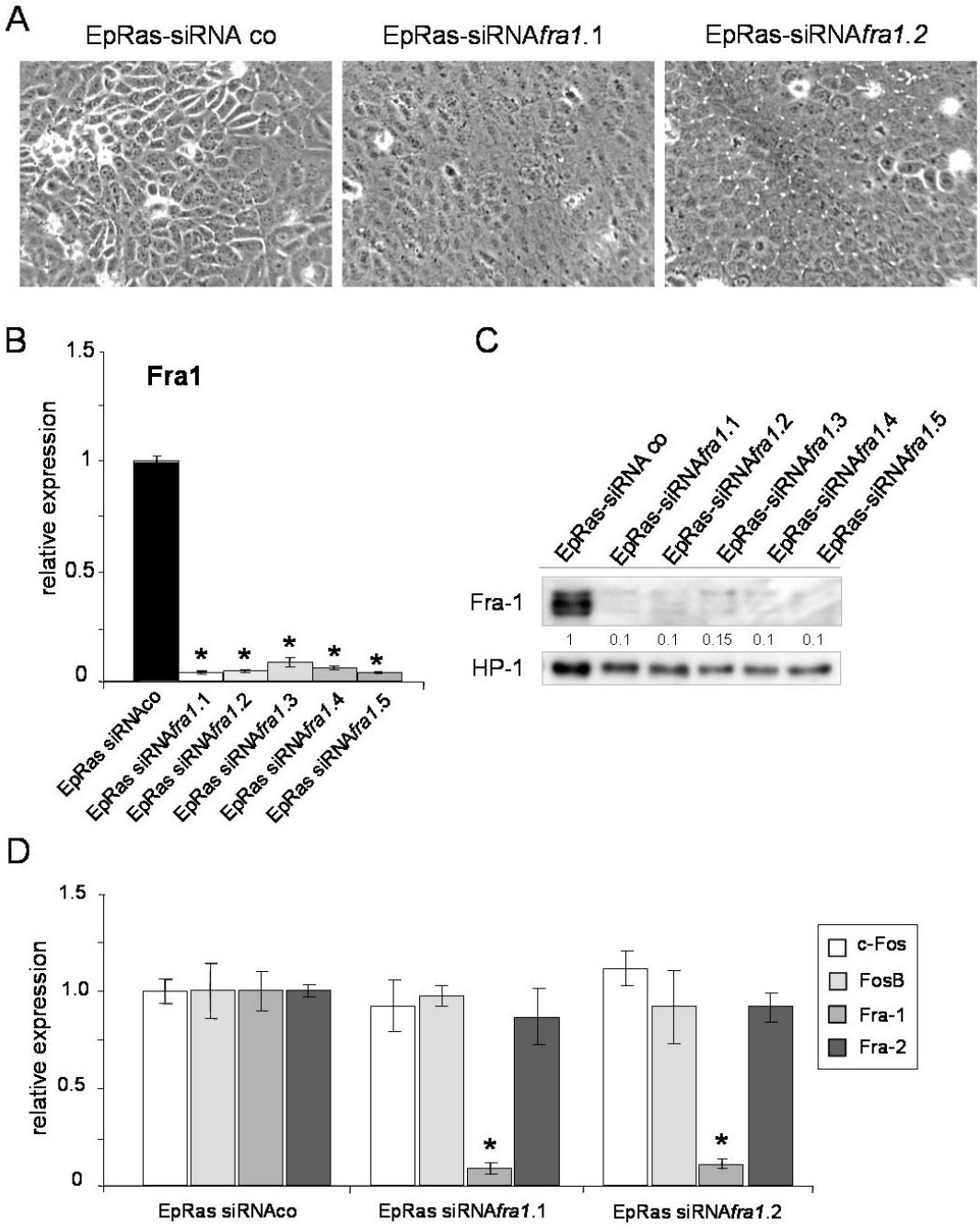

Figure 40. Endogenous Fra-1 silencing in EpRas cells affects cell morphology. (A) Phase-contrast images of two representative EpRas clones showing change in cell morphology following Fra-1 knock-down. Efficient Fra-1 knock-down was confirmed in several clones by qPCR **(B)** and Western blot analysis **(C)**. The shRNA construct targeting Fra-1 shows high specificity since no significant change in mRNA levels of other Fos members could be detected by qPCR (D). The results in bar graph are presented as mean and error bars are designated. *P*-values<0.05 were considered significant (*).Quantification of protein bands after normalisation for loading (HP-1) is shown as fold change when compared to the respective control cells.

As expected, when compared to EpRas control cells, these clones did not show any apparent differences in expression of E-cadherin, other adherens junction proteins (data not shown). Furthermore, silencing of endogenous Fra-1 levels had no significant effect on cell proliferation rate (**Figure 41A**). Since EpRas cells do not proliferate much faster than EpH4 cells, this was again expected. Migration potential of EpRas-siRNA*fra1* cells was evaluated independently by *in vitro* wound healing and direct transwell migration assays (**Figure 41B-C**). As seen for proliferation, Fra-1 silencing did not further reduce the low, basal migratory and invasive ability of the epithelioid EpRas cells (**Figure 41C-D**). Even though it was previously published that Fra-1 silencing negatively affects cell migration and invasion potential of human breast cancer cell lines (Belguise et al., 2005), the cells used in afore mentioned study were not of mouse origin and were not as epithelial as EpRas cells. Thus, these results suggested that the effect of Fra-1 on cell migration and invasiveness might be cell-type specific.

Previously published results indicated that EpRas cells undergo EMT accompanied by downregulation of E-cadherin and induction of vimentin expression when treated with TGF-β1, (Janda et al., 2002). To determine whether endogenous Fra-1 expression is necessary for TGF-β1-induced EMT of EpRas cells, I treated the cells with 5ng/ml TGF-β1 for 7 days. Surprisingly, TGF-β1 treatment induced not only the expected change from epithelial to fibroblastoid morphology in EpRas control cells, but also caused partial loss of epithelial morphology in Fra-1 knock-down cells (**Figure 42A**). Although Fra-1 knock-down cells also acquired a somewhat fibroblastoid appearance, they did not efficiently scatter but remained in rather tight cell islands and formed long protrusions only at the island borders (**Figure 42A**, upper panel). To determine whether silencing of endogenous Fra-1 could inhibit the TGFβ-induced loss of E-cadherin and gain of vimentin, I analysed TGF-β1 treated cells by immunofluorescence (**Figure 42B**). Interestingly, while TGF-β1 induced complete loss of Ecadherin and high vimentin expression in EpRas control cells, Fra-1 knock-down cells retained low, cytoplasmic E-cadherin expression (**Figure 42B**, upper panels) and showed weaker vimentin expression in only part of the cells (**Figure 42B**, lower panels). These results suggested that Fra-1 knock-down only partially interfered with TGF-β1-mediated induction of EMT.

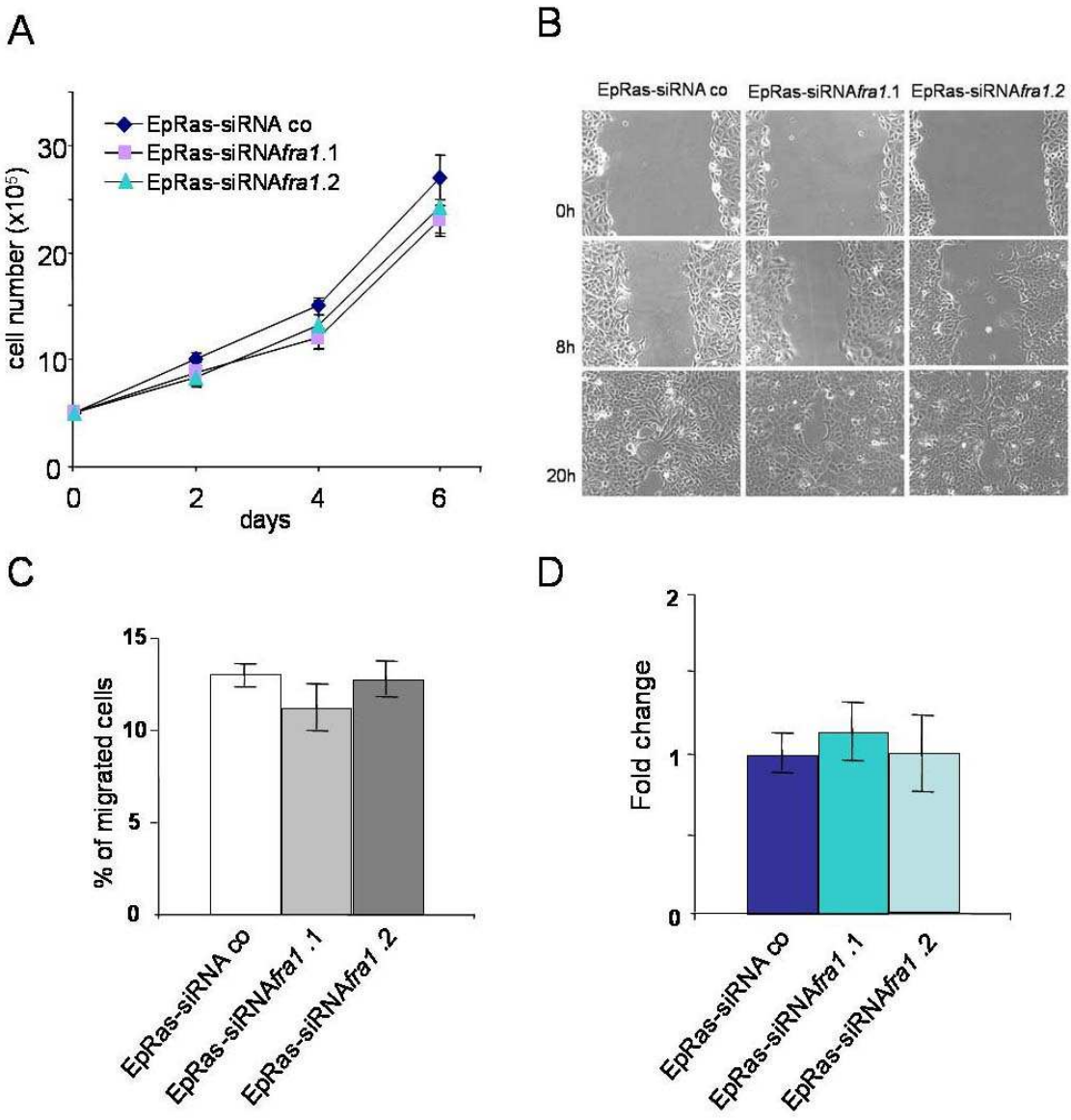

Figure 41. Endogenous Fra-1 knock-down does not affect proliferation, migration or invasive capacity of the epithelial EpRas cells. (A) Growth curve of EpRas-siRNA*fra1* cells shows no significant effect of Fra-1 knock-down on cell proliferation. The cells were grown in standard growth medium and counted in 48h intervals. The mean cell number values of triplicate cultures are shown plotted against time. **(B)** *In vitro* wound healing assay and direct transwell migration assay **(C)** showed no significant difference in cell motility or migration capacity following Fra-1 knock-down. **(D)** Matrigel invasion assay showed that Fra-1 knock-down in EpRas cells has no effect on cell invasion capability. The results are presented as mean and error bars are designated.

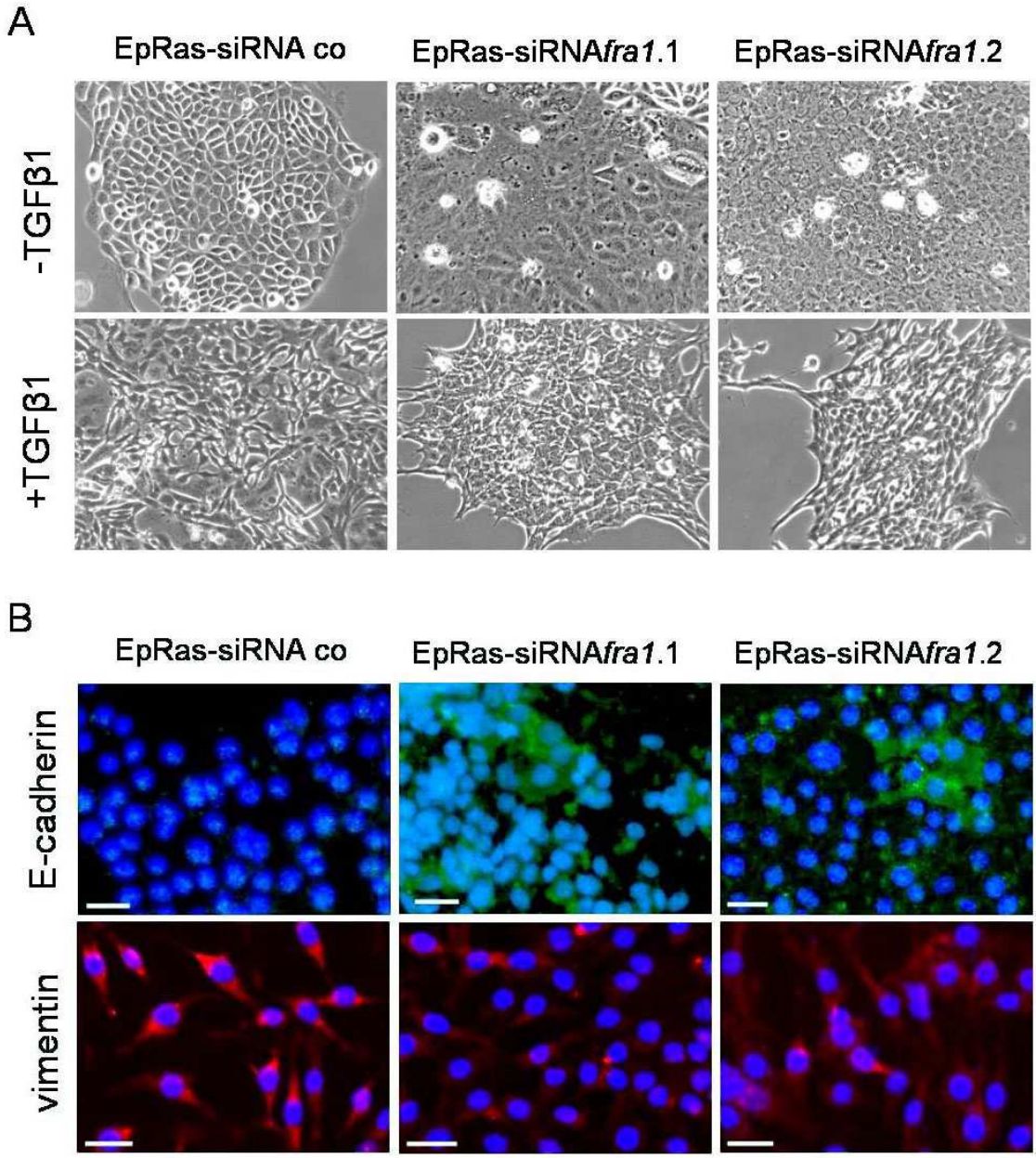

Figure 42. Endogenous silencing of Fra-1 in EpRas cells only partially affects the response to TGF-β1 induced EMT. (A) Phase-contrast images of EpRas-siRNA*fra1* cells treated and untreated with TGF-β1 for 7 days. **(B)** immunofluorescence analysis of TGF-β1 treated cells for epithelial marker protein E-cadherin and mesenchymal marker protein vimentin. Nuclei were counterstained with DAPI (blue). Scale bar, 20μM.

Since the effect of Fra-1 knock-down in EpRas cells was not as severe as I expected, I performed the same set of experiments with two additional clones that previously showed similar level of Fra-1 knock-down. However, the results did not differ significantly (data not shown). Therefore, I checked Fra-1 knock-down efficiency in several other clones by qPCR using previously characterized clones as

a positive control. Strikingly, qPCR analysis revealed that all previously characterized clones, that showed significant (80-90%) silencing of endogenous Fra-1 (**Figure 40**), again upregulated Fra-1 expression. Furthermore, Western blot analysis revealed significant reexpression of Fra-1 protein in these cells indicating that Fra-1 knock-down is unstable (**Figure 43A-B**).

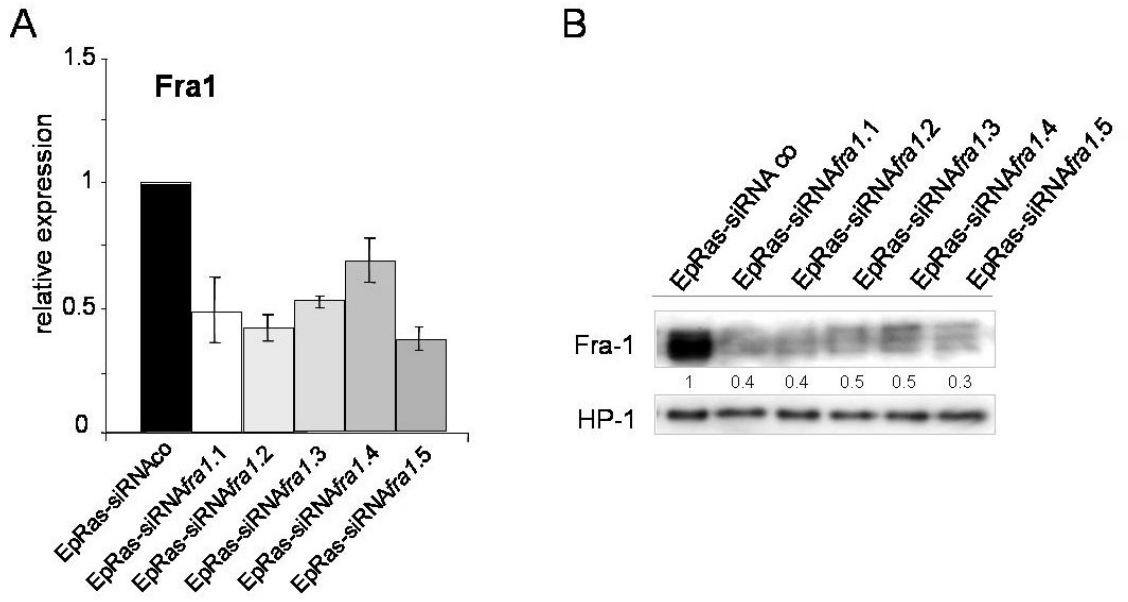

Figure 43. Endougenous Fra-1 knock-down is not stable in EpRas cells. (A) qPCR analysis revealed significant upregulation of Fra-1 transcript. Upregulation of Fra-1 in EpRas-siRNA*fra1* cells was further confirmed by Western blot **(B)**. Results in bar graph are presented as mean and error bars are indicated. Quantification of protein bands after normalisation for loading (HP-1) is shown as fold change when compared to the respective control cells.

Since this reexpression occurred in the presence of puromycin, it could not be due to loss of the shRNA construct from the genome. However, after prolonged culturing, due to unknown compensatory mechanism the cells managed to overcome the inhibitory effect of shRNA. One possible explanation might be that a strong selective pressure existed for overcoming the siRNA-mediated expression block upon serial cultivation during expansion of the Fra-1 knock-down clones. A similar loss of an epithelial phenotype initially induced by RNAi-knock-down of EMT-inducing genes was observed for three other EMT-specific genes, which became reexpressed upon expansion of respective knock-down clones (S. Maschler and H. Beug, unpublished). Since it has previously been shown that Fra-1 knock-down can negatively influence cell proliferation (Belguise et al., 2005),

reversal of Fra-1 knock-down could be simply due to negative selection of slow growing cells with low Fra-1 expression upon prolonged cultivation. Unfortunately, this unstable phenotype prevented us from further analysing the tumorigenic potential or metastatic abilities of these cells by *in vivo* xenograft transplantation assays.

3.12.1 Silencing Fra-1 reverses morphological changes and restores the expression of epithelial marker proteins in EpH4-*fra1* cells

To further analyse the effect of effective, siRNA-mediated Fra-1 knock-down on Fra-1-induced EMT, I attempted to revert the phenotype of EpH4-*fra1* cells by silencing Fra-1 (**Figure 44**), since these cells essentially lack endogenous Fra-1 (**Figure 6B**). Interestingly, I could observe morphological changes in pools of infected cells as early as 48h post-infection. The cells started to regain an epithelial phenotype, finally showing a typical, cobblestone epithelial cell morphology (**Figure 44A**). Western blot analysis revealed an 80-90%-complete downregulation of exogenous Fra-1 protein levels, suggesting effective silencing (**Figure 44B**). Most importantly, reversal of the epithelial phenotype after Fra-1 silencing resulted in significant downregulation of ZEB1 and ZEB2 mRNA levels and corresponding upregulation of E-cadherin mRNA and protein levels (**Figure 44C**). This result further supports previously obtained results suggesting that Fra-1 downregulates E-cadherin expression and elicits EMT by positively regulating the expression of ZEB1 and ZEB2 genes.

Even though Fra-1 silencing had no effect on β-catenin protein levels (**Figure 44D**), other two members of adherens junctions, α- and γ-catenin, that were strongly downregulated following Fra-1 overexpression, were also upregulated (**Figure 44E**). These results suggest that exogenous Fra-1 expression is not only sufficient, but also essential for epithelial-fibroblastoid conversion of EpH4 cells in the Fra-1 overexpressing clones. Since these EpH4-*fra1*siRNA*fra1* cells appear to be more stable than the above EpRas-siRNA*fra1* cells, I plan to further analyse them for their *in vivo* tumorigenic and metastatic potential.

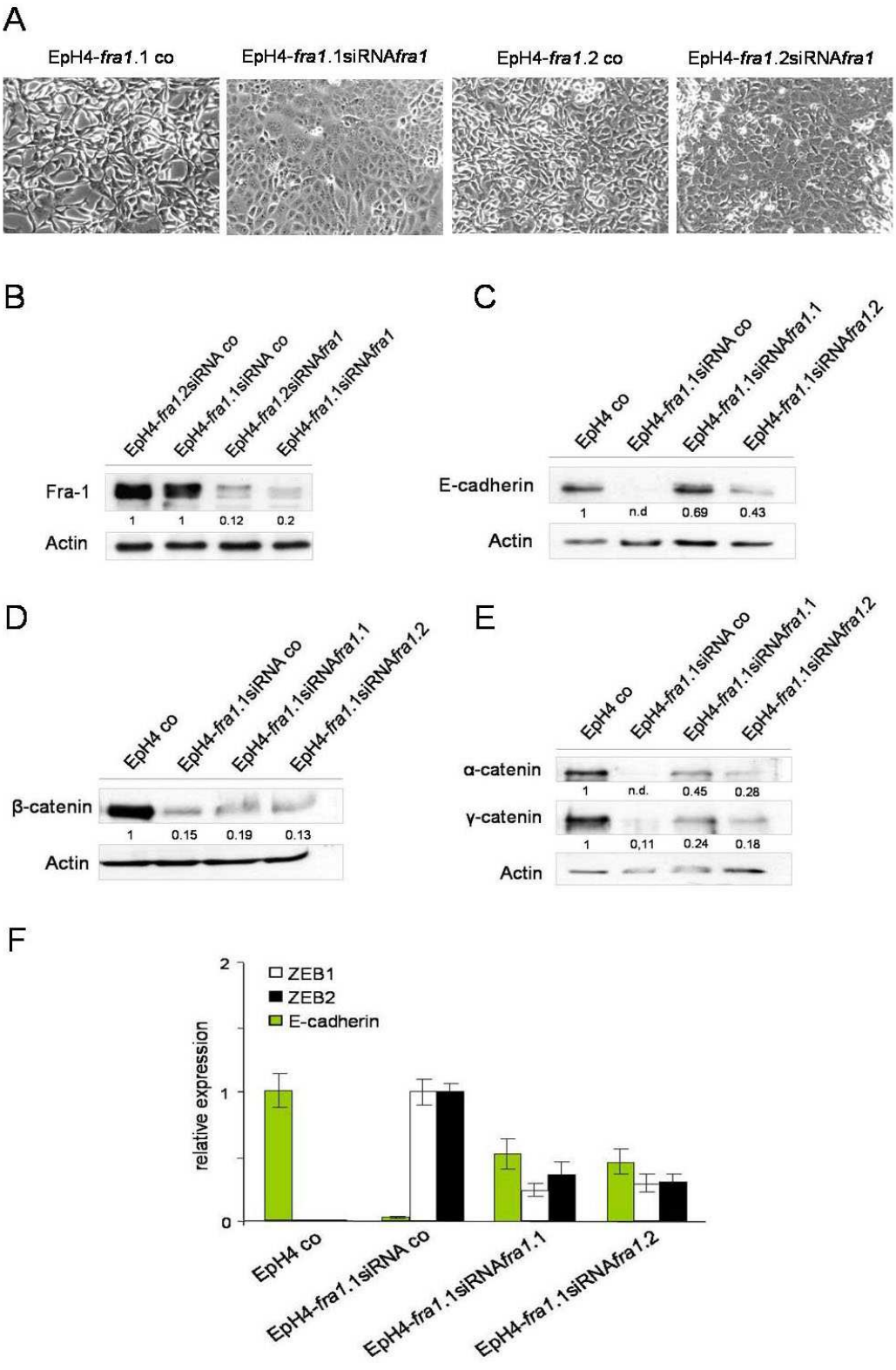

Figure 44. Silencing Fra-1 in EpH4-*fra1* cells restores epithelial morphology and expression of adherens junction proteins. (A) Phase-contrast images showing reversal of the phenotype after exogenous Fra-1 knock-down. Fra-1 protein levels were decresed 80-90% by shRNA **(B)** resulting in reexpression of E-cadherin **(C)**. **(D)** Levels of β-catenin were not affected by Fra-1 knock-down while α-catenin and γ-catenin protein levels were increased. Fra-1 silencing resulted in ZEB1 and ZEB2 mRNA downregulation and E-cadherin mRNA reexpression **(F)**. Quantification of protein bands after normalization for loading is shown as fold change when compared to the respective control cells. The data presented in the bar graph are shown as mean and error bars are designated.

3.12.2 Fra-1 expression is needed for effective proliferation of EpRasXT cells

After confirming that Fra-1-shRNA constructs can efficiently silence exogenous Fra-1 in EpH4-*fra1* cells, I next attempted to silence the highly elevated, endogenous Fra-1 in EpRasXT cells. These cells have already performed complete EMT and maintain this phenotype by an autocrine TGFβ-loop. EMT in these cells can be completely reversed by a Ras-farnesylation inhibitor, while a TGFβRI-kinase inhibitor induced E-cadherin reexpression and loss of vimentin, but failed to alter the fibroblastoid morphology of EpRas-XT cells. To determine, to what extent knock-down of endogenous Fra-1 would alter the EMT phenotype of these cells, they were infected with the previously tested viruses and subjected to puromycin selection 48h after infection. Interestingly, I observed marked morphological changes in pools of cells infected with two out of five shRNA constructs (**Figure 45**). While the cells infected with shRNA control construct (**a**) and the cells infected with shRNA*fra-1* constructs 84 (**c**), 85 (**d**) and 87(**f**) remained spindle shaped showing no morphological change, cells infected with constructs 83 (**b**) and 86 (**e**) drastically changed their appearance. These cells acquired a more epithelial-like morphology and formed clusters. Interestingly, the same cells showed strongly reduced proliferation phenotype that was not observed either in control cells or in the cells with unaltered morphology. Even when cultured in medium containing 15% FCS, they proliferated extremely slowly. This prevented me from further characterizing the behaviour of these cells in *in vitro/in vivo* assays.

QPCR analysis of Fra-1 expression revealed that the altered morphology and reduced proliferation correlated with Fra-1 knock-down. In the cells that were proliferating normally and showed unaltered morphology, Fra-1 knock-down was not significant. However, low-proliferating, epithelial-like pools of cells showed roughly 70-80% reduction in Fra-1 mRNA. In addition, I observed increased numbers of dying cells in pools of cells infected with shRNA construct 85. Even though the overall silencing of Fra-1 in this pool of cells was only around 20%, one could speculate that the dying cells might have silenced Fra-1 to a higher extended causing them to undergo apoptosis. Thus, these preliminary results suggest that

Fra-1 might also be involved in the regulation of cell proliferation and/or survival of fully transformed EpRasXT cells.

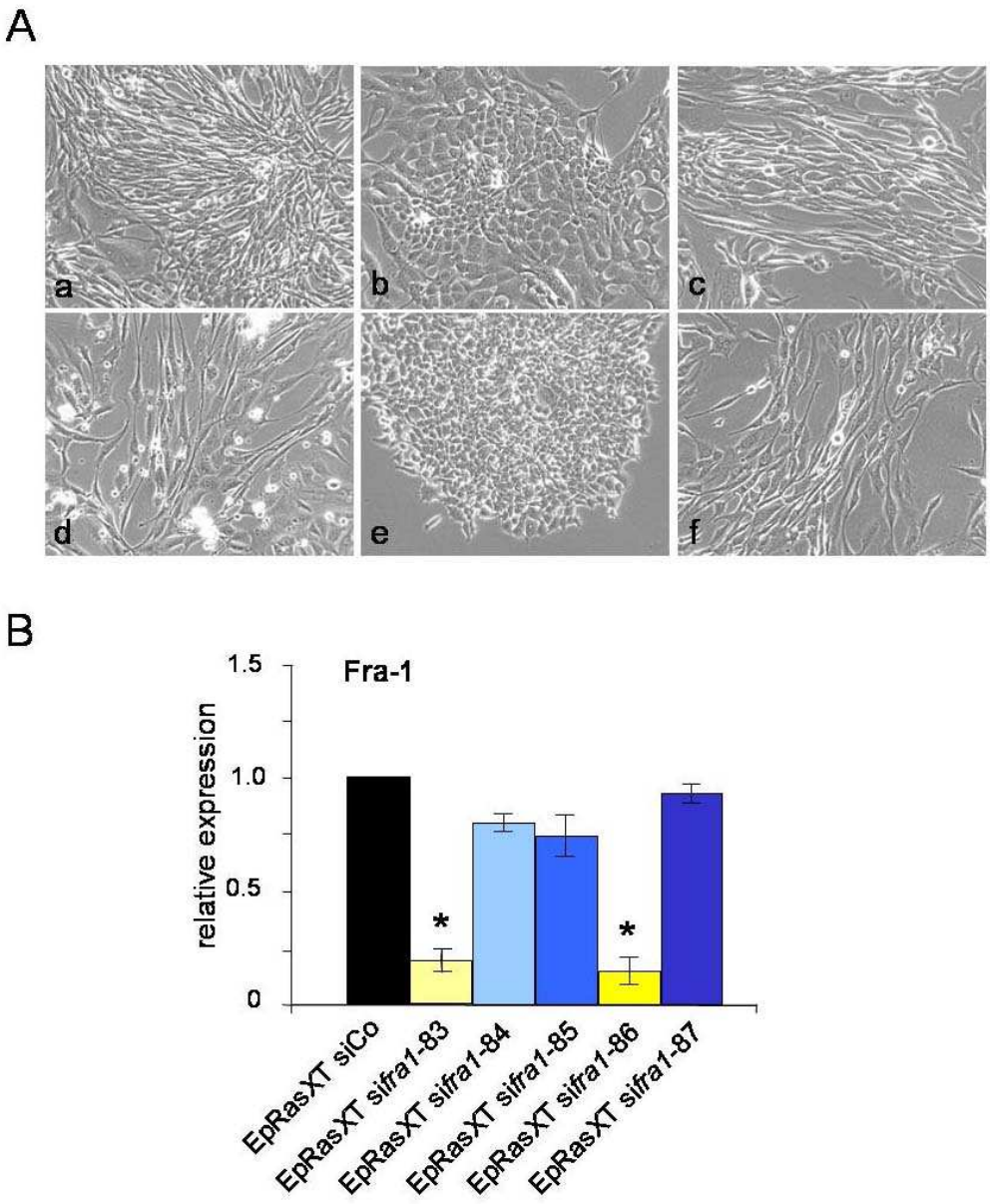

Figure 45. Endogenous Fra-1 knock-down in EpRasXT cells. (A) Phase-contrast images showing pools of EpRasXT cells transfected with control shRNA construct **(a)**, and five different shRNA constructs targeting Fra-1**(b-f)**. **(B)** qPCR analysis revealed significant silencing of endogenous Fra-1 by two out of five shRNA constructs. Data are presented as mean and error bars are designated. *P*-values <0.05 were considered significant (∗).

A recent investigation that reported Fra-1 to promote growth and survival in Ras-transformed thyroid cells by controlling cyclin A transcription is in favour of this hypothesis (Casalino et al., 2007).

3.13 Summary and conclusions

In the third and last part of my study, I employed a loss-of-function approach to determine whether Fra-1 expression is necessary for maintenance of the EMT phenotype. To test whether Fra-1 is a major downstream effector of TGF-β1signalling in EMT, I attempted to stably knock-down the expression of endogenous Fra-1 in EpRas and EpRasXT cells by RNAi. Even though the initial analysis in EpRas cells transfected with shRNA targeting Fra-1 revealed significant decrease in endogenous Fra-1 mRNA and protein levels, this had no strong effects on cell proliferation, migration and invasive potential of the cells *in vitro*, causing however, a normalisation of the EpRas epithelial phenotype to that of oncogene-free EpH4 cells. In addition, silencing Fra-1 in EpRas only partially inhibited EMT induction of the EpRas-siRNAfra1 cells upon exposure to TGF-β1. This was likely due to reexpression of Fra-1 in the knock-down cells after some time in culture, possibly due to selection against probably slower growing cells showing a complete resistance to EMT induction. Taking this into account, it remained unclear, to what extent the elevated levels of Fra-1 in EpRas cells are necessary for EMT induction. On the other hand, I was able to successfully knock-down Fra-1 in the EpH4-*fra1* cells. This resulted in strong downregulation of ZEB1 and ZEB2 gene expression and an almost complete reversal of the Fra-1-induced EMT to an epithelial phenotype.

Thus, based on these experiments I conclude that the shRNA constructs are efficient in silencing Fra-1 in EpH4 cells and that Fra-1 is necessary and sufficient for EMT-induction in oncogene-free EpH4 cells. Silencing endogenous Fra-1 in EpRasXT cells further supports this idea, since the reversal of the mesenchymal phenotype in these cells could be correlated with Fra-1 knock-down. My preliminary observations also suggest that Fra-1 might be indispensable for effective proliferation of these cells. However, further experiments are needed to confirm this data. In addition, the overall impact of Fra-1 knock-down on the expression of molecular markers and functional behaviour of these cells *in vitro* and *in vivo* remains to be analysed.

4. Discussion

Epithelial-mesenchymal transition (EMT) is a fundamental multi-step process involved in normal embryonic development. However, in recent years it is becoming evident that deregulated EMT plays an important role in cancer progression. An important step in cancer progression is metastasis, the acquired ability of primary tumor cells to disseminate to distant organs. In fact, most cancer fatalities are actually due to carcinoma cell invasion and metastasis, rather than to the primary tumors (Sporn, 1996; Tse and Kalluri, 2007). It is believed that during this process, cancer cells transiently acquire mesenchymal properties by undergoing EMT. Therefore, understanding the molecular mechanisms that govern EMT and the particular roles of individual genes involved in that process might unravel new prognostic markers and potential therapeutic targets.

In this study, I have defined the role of Fra-1/AP-1 in EMT using the EpH4/EpRas cellular models of EMT (Reichman et al., 1989; Oft et al., 1996; Janda et al., 2002) combined with xenograft transplantation experiments. Previous studies have shown that an inducible form of c-Fos (FosER) is able to induce EMT, when ectopically expressed in non-transformed EpH4 mammary epithelial cells (Reichman et al., 1992). In addition, inducible expression of another AP-1 member, c-Jun (JunER), in the same cells caused loss of cellular polarity and cell scattering, but failed to induce EMT (Fialka et al., 1996). However, specific roles of other AP-1 members in this context were not studied. Preliminary analysis of the expression pattern of all Fos and Jun family members revealed a strong correlation of increased Fra-1 expression and an EMT phenotype implying that Fra-1 might be a major player in the induction and maintenance of EMT. By employing a gain-of-function approach, I was able to show that stable Fra-1 expression positively regulates cell proliferation and results in epithelial to fibroblastoid transition (EMT) of EpH4 and EpRas cells. This morphological switch was accompanied by profound cytoskeletal rearrangements characteristic of highly motile fibroblastic cells. Furthermore, cell motility as well as migration and invasion capacity of epithelial EpH4 and EpRas cells were significantly increased following ectopic Fra-1 expression *in vitro*. Another interesting observation was that Fra-1 seemed to affect the behaviour of

the cells in a dose-dependent manner, since the severity of the phenotypes detected correlated with Fra-1 levels.

Molecular characterisation revealed that the cells have undergone EMT as characterized by downregulation of epithelial marker proteins (E-cadherin, p120 catenin (p120ctn), α-, β- and γ-catenin) and upregulation of the mesenchymal marker protein fibronectin. However, the overall phenotype was more pronounced in EpH4 cells that completely lost the expression of major epithelial marker protein E-cadherin, as opposed to its strong downregulation and cytoplasmic relocalisation in EpRas cells. Similarly, the overall downregulation of β-catenin was more striking in EpH4 cells, even though no apparent relocalisation of β-catenin to the nucleus was observed in either cell type. In line with these results, an apparent switch in expression pattern of p120ctn isoforms was observed following Fra-1 overexpression. It has previously been shown that epithelial cells predominantly express the 100kDa-p120ctn isoform 3, whereas mesenchymal cells express predominantly 120kDa-p120ctn isoform 1(Mo and Reynolds, 1996; Keirsebilick et al., 1998). Beside its downregulation, and unlike the control cells, which express the 100kDA-p120ctn isoform 3, both EpH4-*fra1* and EpRas-*fra1* cells predominantly expressed the mesenchyme-specific, p120ctn isoform 1. Several recent studies have implicated the expression of this isoform in EMT and tumor cell invasion (Eger et al., 2000; Ohkubo and Ozawa, 2004; Yanagisawa et al., 2008), further supporting the idea that Fra-1 expression is sufficient to induce EMT in these cells.

Previous studies have shown that in the majority of epithelial cell types, requirements for EMT include cooperation of TGFβ-signalling with oncogenic Ras, receptor-tyrosine kinases (RTKs) or their downstream effectors (Huber et al., 2005; Zavadil and Bottinger, 2005; Xu et al., 2009). However, this was not the case in Fra-1-mediated induction of EMT, as no increase in TGF-β1 production could be detected. Additionally, the fact that Fra-1 ectopic expression had stronger effect in non-transformed EpH4 cells suggested that Fra-1/AP-1 is able to elicit EMT by a novel, Ras and TGFβ-independent mechanism. Interestingly, a number of novel EMT-specific genes, which cause EMT by gain (ILEI, CREG) or loss of function (Annexin A1, m-Scribble) strictly require oncogenic Ras for EMT induction, but like Fra-1 act in a TGFβ-independent fashion (S. Maschler, A. Csiszar, M. Alacakaptan

and H. Beug, unpublished). The observation that Fra-1 requires neither oncogenic Ras nor TGFβ suggests that Fra-1 is unique among the rapidly increasing number of known, EMT-inducing proteins (Tanos and Rodriguez-Boulan, 2008).

EMT *in vitro* is considered to be a faithful correlate of late stage tumor progression and metastasis (Oft et al., 1998; Lehmann et al., 2000; Janda et al., 2002). Therefore, the behaviour of these cells was further examined by xenograft transplantation assays. Interestingly, injection of EpH4-*fra1* cells into mammary gland fat pads resulted in formation of fast growing, strongly vascularised tumors, while the control cells formed only tiny, encapsulated nodules at 50% frequency. This finding strongly argues that Fra-1 expression in epithelial non-transformed and oncogene-free EpH4 cells is sufficient for cellular transformation and *in vivo* tumor formation. Furthermore, this result is particularly interesting, since Fra-1 was originally proposed to have only limited transformation ability, when compared to c-Fos (Widsom and Verma, 1993; Bergers et al., 1995). Intriguingly, it has been reported that FosER cells, even though being able to undergo EMT *in vitro*, remain non-tumorigenic *in vivo* (Reichmann et al., 1992; Eger et al., 2000). This strongly suggests that Fra-1, rather than c-Fos itself, might have a pivotal role in tumor progression. In line with this idea, several recent investigations have reported elevated levels of Fra-1 in numerous mouse and human cancer cell lines as well as clinical tumor samples (Kustikova et al., 1998; Chiappetta et al., 2000; Zoumpourlis et al., 2000; Zajchowski et al., 2001; Ramos-Nino et al., 2003; Belguise et al., 2005; Debinski and Gibo, 2005; Mangone et al., 2005; Milde-Langosch, 2005; Young and Colburn, 2006; Chiappetta et al., 2007).

On the other hand, unlike the c-Fos transgenic mice that develop osteosarcomas (Grigoriadis et al., 1993), Fra-1 transgenic mice do not show a cancer phenotype (Jochum et al., 2002). In addition, even though increased expression of Fra-1 was observed in human colitis-associated cancer (CAC), *fra-1* mRNA was hardly detectable and Fra-1 expression seemed to be dispensable for colitis-associated tumorigenesis in a mouse model of chemically-induced CAC, since tumor numbers and size were not altered in mice lacking *fra-1* (*fra-1*$^{\Delta/\Delta}$ mice) (Hasselblatt et al., 2008). However, the same was true for single inactivation of all other Fos and Jun members. Therefore, it was suggested by the authors that not only the inhibition of

Fra-1, but the inhibition of a single AP-1 protein is not a limiting factor in CAC in mice. However, unlike in the case of CAC, Fra-1 expression was found elevated both in human and mouse breast cancer cell lines, as well as in clinical tumor samples, suggesting a more general role for Fra-1 in the course of progression of both human and mouse breast cancer (Milde-Langosch, 2005; Chiappetta et al., 2007). Supporting that view and even more striking was the finding that upon tail vein injections, EpH4-*fra1* cells successfully induced lung metastasis, while mice injected with EpH4 control cells developed no detectable pathological changes in their lungs. This result demonstrated that Fra-1 expression is sufficient to render non-transformed, non-tumorigenic EpH4 cells tumorigenic and metastatic. Similarly, Fra-1 expression significantly increased metastatic potential of tumorigenic and metastatic EpRas cells, as judged by increased overall numbers of macroscopically visible metastatic nodules present on the lung surface. Most importantly, immunohistochemical (IHC) analyses revealed a correlation between Fra-1 expression and strong increase of cell proliferation, as determined by IHC-staining for the proliferation marker Ki67, and an induction of EMT *in vivo*, as indicated by loss of E-cadherin and strong fibronectin expression detected by IHC staining of the metastatic nodules. These findings strongly argue that Fra-1 expressing cells undergo EMT both *in vitro* and *in vivo*.

One major hallmark of EMT is strong downregulation or even loss of the adhesion protein E-cadherin. Loss or downregulation of its expression has also been shown to inversely correlate with tumor grade and patient survival (Perl et al., 1998; Hirohashi, 1998; Van Aken et al., 2001). In recent years, several molecular mechanisms underlying E-cadherin downregulation have been discovered or suggested. In most carcinomas, direct transcriptional repression and aberrant promoter hypermethylation emerged as the main mechanisms of E-cadherin downregulation (Graff et al., 1995; Graff et al., 2000; Di Croce and Pellici, 2003). Interestingly, a recent study reported that ectopic expression of c-Fos causes methylation-dependent E-cadherin downregulation and EMT in mouse mammary adenocarcinoma cell lines (Mejlvang et al., 2007). However, the transcriptional downregulation of E-cadherin that was observed in Fra-1 expressing cells was not dependent on promoter methylation or histone acetylation, since treatment of the cells with two different DNA-methylase inhibitors and histone-acetylase inhibitor

failed to restore E-cadherin expression. In a further attempt to identify molecular mechanisms that may explain transcriptional repression of E-cadherin by Fra-1, and to identify new EMT-relevant target genes downstream of Fra-1/AP-1, I performed genome-wide gene expression profiling. Gene array analysis confirmed E-cadherin transcriptional downregulation in both cell types and revealed that the overall gene expression signature of Fra-1 expressing cells has shifted towards a mesenchymal profile. A number of genes upregulated by Fra-1 overexpression has been previously implicated in cancer progression and EMT.

In addition to several proteases normally expressed by migratory and invasive mesenchymal cells, two two-handed zinc finger transcription factors and direct E-cadherin repressors ZEB1 (ZFHX1A, δEF1, TCF8) and ZEB2 (ZFHX1B, SIP1) were found to be consistently upregulated following Fra-1 overexpression. Interestingly, ZEB1 was recently identified as a strictly EMT-specific gene in a polysome-bound mRNA screen employing multiple EpH4-based cell clones modified by different oncogenes and undergoing scattering or EMT (Jechlinger et al., 2002; Jechlinger et al., 2006). ZEB1 and ZEB2 are two closely related transcription factors that are essential during normal embryonic development and whose expression has been recently linked to the induction of EMT and cancer progression (Vandewalle et al., 2009). In addition to direct transcriptional repression of the E-cadherin gene, they can negatively regulate the expression of several other epithelial specific genes such as claudin, plakophilin, occludin as well as activate the expression of mesenchymal genes such as N-cadherin and several MMPs (Eger et al., 2005; Vandewalle et al., 2005; Aigner et al., 2007; Vandewalle et al., 2009). A number of these genes were also found to be deregulated in EpH4-*fra1* and EpRas-*fra1* cells, further supporting the idea that ZEB1 and ZEB2 might be responsible for loss of the epithelial phenotype. By performing transient knock-down experiments, I was able to demonstrate that this was indeed the case and that Fra-1-mediated induction of ZEB1 and ZEB2 was responsible for transcriptional downregulation of E-cadherin in EpH4 and EpRas cells. Even though ZEB genes have been intensively studied in the recent years, precise mechanisms of their transcriptional regulation are still largely obscure. Thus, they were perfect candidates for further characterisation with respect to their possible direct transcriptional regulation by Fra-1/AP-1.

Promoter analysis revealed several potential AP-1 binding sites located within the mouse ZEB1 promoter region. Subsequent chromatin-immunoprecipitation experiments revealed that Fra-1 directly binds to ZEB1 promoter *in vivo*, thereby for the first time identifying ZEB1 as a direct Fra-1/AP-1 target gene. In addition, three potential AP-1 binding sites were also identified within the most proximal, P3 promoter of the mouse ZEB2 gene. This promoter was reported as being the predominantly active one in mouse breast cancer cell line NMuMG, strongly suggesting that as ZEB1, ZEB2 might also be a direct target of Fra-1/AP-1 in mammary epithelial cells (Nelles et al., 2003). However, further chromatin-immunoprecipitation experiments along with reporter assays are currently being performed to test that hypothesis and to determine what effect Fra-1 binding has on transcriptional regulation of these two genes.

Interestingly, several attempts to ectopically express ZEB1 in oncogene-free EpH4 cells resulted in cellular senescence and cell death (A. Eger pers. comm.). The effect was probably due to direct, ZEB1-mediated transcriptional repression of cell-cycle progression genes such as cyclin D1. Even though Fra-1 expressing EpH4 cells significantly upregulated the expression of both ZEB1 and ZEB2 genes (known to repress the expression of cell-cycle progression related cyclins D1 and D2, and activate the expression of cell-cycle arrest related cyclin G2), these cells did not show a proliferation defect. On the contrary, the cells have significantly increased their proliferation rate, when compared to EpH4 control cells. These results suggest that in the context of epithelial cell transformation and EMT, Fra-1 plays an important role not only in the regulation of genes involved in cellular dedifferentiation and invasiveness, but also in regulating the expression of pro-survival and cell cycle progression genes.

In an effort to further define the extent of Fra-1 involvement in the maintenance of EMT, I employed a loss-of-function approach in EpRas, EpH4-*fra1* and mesenchymal EpRasXT cells. The endogenous Fra-1 knock-down in EpRas cells improved the epithelial polarity of the cells, suggesting that the effects of Ras on epithelial cell behaviour were due to Fra-1. On the other hand, endogenous Fra-1 knock-down did not have an apparent effect on proliferative, migratory and invasive capacity of the cells. Even though it was previously published that Fra-1 silencing

negatively affects cell migration and invasion potential of human breast cancer cell lines (Belguise et al., 2005), these results were not completely unexpected, since the cell lines used in the above mentioned study were of human origin and not as epithelial as EpRas cells. Unexpectedly, however, the treatment of EpRas-*fra1* knock-down cells with TGF-β1 caused only partial loss of epithelial morphology while it induced the expected change from epithelial to fibroblastoid morphology in EpRas control cells. Although Fra-1 knock-down cells acquired a somewhat fibroblastoid appearance, they did not efficiently scatter, but remained in rather tight cell islands and formed long protrusions only at the island borders. In addition, Fra-1 knock-down only partially interfered with TGF-β1-mediated loss of E-cadherin and gain of vimentin expression. In a search of the possible explanation for this unexpected ability of RNAi-mediated Fra-1 knock-down to block TGF-β1-mediated EMT in EpRas cells, I discovered that the knock-down phenotype was unstable after prolonged cell cultivation. One possible explanation for the observed compensatory reexpression of Fra-1 mRNA and protein is that a strong selective pressure existed for overcoming the siRNA-mediated expression block upon serial cultivation during expansion of the Fra-1 knock-down clones. Since this reexpression occurred in the presence of puromycin, it could not be due to loss of the shRNA construct from the genome. Interestingly, a similar loss of an epithelial phenotype initially induced by RNAi-knock-down of EMT-inducing genes was observed for three other EMT-specific genes, which became reexpressed upon expansion of respective knock-down clones (S. Maschler and H. Beug, unpublished). Since it has previously been shown that Fra-1 knock-down can negatively influence cell proliferation (Belguise et al., 2005), reversal of Fra-1 knock-down could be simply due to negative selection of slow growing cells with low Fra-1 expression upon prolonged cultivation. Unfortunately, this unstable phenotype prevented me from further analysing the tumorigenic potential or metastatic abilities of these cells by *in vivo* xenograft transplantation assays.

On the other hand, my attempts to stably knock-down Fra-1 in EpH4-*fra1* cells were successful, further ruling out any possible technical problems that might have been the cause of Fra-1 reexpression in EpRas-siRNA*fra1* cells. More importantly, this experiment further proved that Fra-1 expression is indeed responsible for the observed EMT in these cells, since its knock-down resulted in transcriptional

downregulation of ZEB1 and ZEB2 genes, reexpression of E-cadherin, and reversal of the EMT-phenotype to an epithelial one. In addition, these results clearly showed that Fra-1 expression is not only sufficient, but also essential for epithelial-fibroblastoid conversion of EpH4 cells. Since these EpH4-*fra1*.1siRNA*fra1* cells appear to be more stable than the above EpRas-siRNA*fra1* cells, it would be interesting to analyse these cells for their *in vivo* tumorigenic and metastatic potential. In addition, since Fra-1 knock-down resulted in correspondingly decreased transcriptional expression of ZEB1 and ZEB2 genes and reexpression of the E-cadherin gene, further analysis is needed to determine whether a corresponding correlation in the expression pattern of the above genes could be detected in human invasive breast cancer clinical samples. Interestingly, a recent study has reported elevated expression of ZEB1 in human invasive lobular breast carcinoma specimens (Aigner et al., 2007), while another study reported elevated Fra-1 expression in the same type of human breast cancer (Chiappetta et al., 2007), suggesting that the results obtained in this study might have clinical relevance.

Similarly to EpRas cells, an attempt to stably knock-down endogenous Fra-1 in mesenchymal EpRasXT cells caused strong reversal to an epithelial morphology, but also induced a strong proliferation defect, implying that Fra-1 expression is required for cell proliferation of these highla transformed cell lines. This observation is in accordance with a recently published study proposing Fra-1 to be essential for growth and survival of Ras-transformed thyroid cells (Casalino et al., 2007), and might point to a more general role of Fra-1 in regulating cell proliferation and survival in the context of a Ras-transformed background. However, this hypothesis remains to be tested and further molecular analyses are needed to address this question. Nevertheless, if this proves to be the case, targeting Fra-1 expression could provide a very promising therapeutic avenue for invasive cancers.

4.1 Summary and future perspectives

In this study, I could demonstrate that Fra-1/AP-1 has a pivotal role in initiating and maintaining EMT. By employing an *in vitro* gain-of-function approach combined with *in vivo* xenograft transplantation experiments and genome-wide gene expression profiling, I was able to demonstrate that Fra-1 expression is sufficient to elicit EMT in non-transformed, mammary epithelial EpH4 cells and their Ras-transformed derivatives by a novel, TGF-β1-independent mechanism involving transcriptional upregulation of ZEB1 and ZEB2 genes (**Figure 46**). Chromatin immunoprecipitation experiments demonstrated that Fra-1 binds to the ZEB1 proximal promoter *in vivo*, thereby identifying ZEB1 as a new, direct Fra-1/AP-1 target gene. Furthermore, analysis of the mouse ZEB2 promoter revealed several potential AP-1 binding sites, suggesting a possible direct binding and regulation by Fra-1/AP-1.

On the other hand, the loss-of-function experiments in epithelial EpRas cells resulted in improved epithelial polarity of the cells, suggesting that the effects of Ras-expression on epithelial cell behaviour are Fra-1-dependent. Furthermore, silencing Fra-1 in EpH4-*fra1* cells resulted in corresponding transcriptional downregulation of ZEB1 and ZEB2 genes, transcriptional upregulation of E-cadherin and reversal of the epithelial phenotype demonstrating that Fra-1 expression is not only sufficient, but essential for the observed EMT phenotype. Similarly, knock-down of endogenous Fra-1 in mesenchymal EpRasXT cells resulted in reversal of the epithelial phenotype and suggested that besides its role in regulation of epithelial phenotype, Fra-1 plays an important role in cell proliferation and survival.

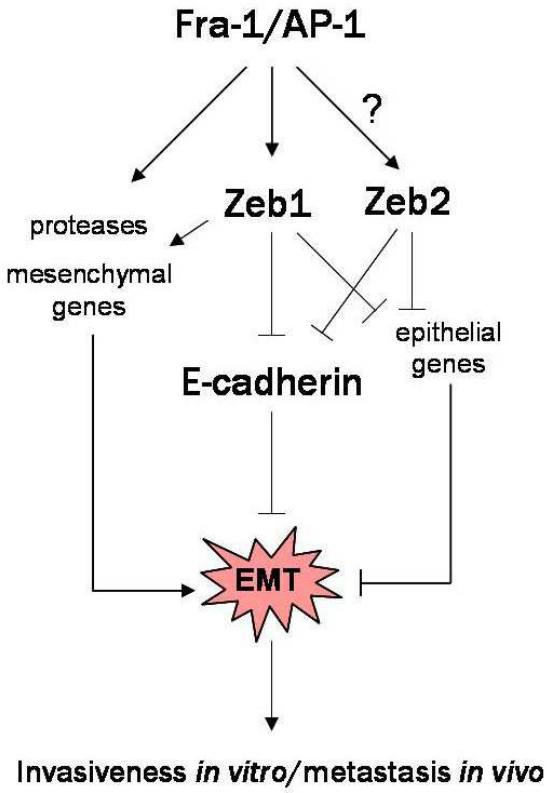

Figure 46. Proposed model of Fra-1-mediated induction of EMT. In mouse mammary epithelial EpH4 and EpRas cell lines, Fra-1 induces EMT by directly upregulating the expression of ZEB1 and ZEB2 genes, that are responsible for transcriptional downregulation of E-cadherin and other epithelial specific genes, such as claudins and occludin, resulting in loss of the epithelial phenotype. At the same time, Fra-1 and ZEB1-mediated upregulation of several proteases, such as MMPs and members of the uPAR system, along with several other mesenchymal-specific genes such as fibronectin, thrombospondin-1, and matrix Gla protein, increases *in vitro* the migratory and invasive potential of the cells and enables them to metastasise *in vivo*.

Even though this study provided evidence for a new, yet unreported mechanism of EMT induction by Fra-1/AP-1, involving upregulation of ZEB genes, there are still several interesting questions that remain unanswered. For example, it would be interesting to identify the major Fra-1 dimerizing partner and its possible interactions with other transcription factors in activation/repression of EMT-related genes. For that purpose co-immunoprecipitation experiments combined with mass-spectrometry analysis could be employed. Additionally, to identify the composition of Fra-1-containing dimers regulating the expression of specific genes, one could overexpress forced dimers of Fra-1 with each of the Jun proteins or several other bZIP proteins previously shown to interact with Fra-1, in EpH4 and/or EpRas cells

(Bakiri et al., 2002; Bakiri et al., 2007). Interestingly, a recent study reported that Fra-1 and Stat3 synergistically regulate the expression of the human MMP9 gene (Song et al., 2008). In that study, by employing co-immunoprecipitation experiments, the authors have shown that Stat3 can associate with Fra-1 and c-Jun *in vivo*. In line with the finding that two Stat family members, Stat1 and Stat3, were found upregulated in Fra-1 expressing cells, it would be interesting to investigate whether Jun/Fra-1/Stat1 or Jun/Fra-1/Stat3 complexes are present in Fra-1-overexpressing cells and, if this is the case, to identify the genes whose expression is regulated by these complexes.

To identify additional direct Fra-1/AP-1 target genes in the context of EMT and cancer cell metastasis, the obtained gene expression profiling results could be compared with additional chromatin immunoprecipitation experiments coupled to "deep sequencing" analysis. Several genes that were deregulated following Fra-1 overexpression in EpH4 and EpRas cells are promising candidates for further characterization as they have previously been associated with tumor cell invasion and proposed as direct Fra-1 target genes. These include proteins of the ECM; such as matrix Gla protein and thrombospondin-1, as well as the cell surface receptor CD44, matrix-degrading proteases, such as MMPs and several members of the uPAR system (Andersen et al., 2002; Ramos-Nino et al., 2003; Eferl et al., 2004). In addition, to address the contribution of a particular Fra-1 target gene or the combinatorial effect of several genes in the process of EMT and metastasis, siRNA-mediated silencing of candidate genes coupled to *in vitro* functional assays and *in vivo* xenograft experiments could be employed. Since elevated Fra-1 expression was reported in a variety of human epithelial tumors and cancer cell lines, it would be interesting to correlate the expression of Fra-1 and its target genes with the invasive potential of these cell lines and human tumors on a wider scale. One possible approach would include transcriptomic profiling of clinical tumor samples at different stages of cancer progression, combined with tissue arrays using tumor samples of patients with known disease history. This approach might result in identification of new molecular markers with clinical prognostic value and/or potential therapeutic targets.

The generation of an inducible Fra-1 construct would enable us to study in more detail the kinetics of Fra-1-mediated induction of EMT, its role in cell growth and survival, as well as the contribution of Fra-1 in specific aspects of cancer cell metastasis. The process of metastasis comprises of several distinct steps. This invasion-metastasis cascade involves the initial acquisition of the migratory and invasive behaviour necessary for basement membrane degradation and intravasation into the circulatory system. However, once the cancer cells enter the blood or lymphatic stream, their survival is further dependent on the expression of additional pro-survival genes that enables these cells to overcome anoikis, as well as to successfully adhere to endothelial cells and subsequently extravasate to colonize targeted secondary organs. In this study I was able to demonstrate *in vitro*, that Fra-1 plays a major role in the initial step of breast cancer metastasis by eliciting an EMT program. However, due to the limitations of the cell system used (that fails to metastasise from orthotopic sites), direct *in vivo* role of Fra-1 in specific steps of invasion-metastasis cascade, namely intravasation, evasion of anoikis, extravasation and organ-specific metastasis remain unexplored. Nevertheless, the fact that Fra-1 expression rendered non-tumorigenic EpH4 cells metastatic and significantly increased the number of metastatic nodules formed by metastatic EpRas cells following tail vein injection, suggests that Fra-1 expression can provide anoikis resistance and positively influence the extravasation efficiency of these cells. To further explore this possibility, these cells can be tested *in vitro* for anoikis-resistance and transendothelial migration. In addition, the use of other mouse and/or human breast cancer cell lines with the capability to metastasize from orthotopic sites could be employed. For example, the well characterized human MDA-MB 231 breast cancer cell line that expresses high levels of Fra-1 (Belguise et al., 2005) could be used for these studies. However, in this case the generation of cell clones expressing an inducible shRNA construct targeting Fra-1 would be required. Given the availability of several MDA-MB 231-derived cell clones showing organ-specific metastatic potential (bone vs lung) (Minn et al., 2005), the *in vivo* role of Fra-1 in regulation of tissue tropism could be addressed by employing xenograft mouse models.

Finally, to analyse the direct *in vivo* role of Fra-1 in breast cancer progression and EMT, transgenic mouse models could be employed. Up to date, a number of different transgenic mouse models of breast cancer metastasis have been generated (reviewed by Fantozzi and Christofori, 2006). The most widely used single-transgenic mouse models of breast cancer metastasis are MMTV-PyMT and MMTV-Neu transgenic mice with mammary gland-specific expression of PyMT (polyoma middle T antigen) or ErB2 (EGF receptor family member) under the control of the MMTV (mouse mammary tumor virus) promoter/enhancer. These mice develop mammary tumors with high incidence of lung metastasis. Therefore, it would be interesting to cross these mice with the conditional *fra-1* knock-out mice (*fra-1*$^{\Delta/\Delta}$ mice; Eferl et al., 2004) to determine whether the ablation of the *fra-1* gene might delay or block tumor progression and metastasis. Another approach would be to generate double-transgenic mice by intercrossing *fra-1* transgenic mice (Jochum et al., 2000) with MMTV-PyMT or MMTV-Neu transgenic mice to determine, whether these double-transgenic mice would show accelerated tumor progression. Alternatively, the generation of an inducible *fra-1*-transgenic mouse would allow tightly controlled overexpression of *fra-1* in a tumor stage-specific and/or cell-/tissue-specific manner. This gain-of-function approach could then be complemented with the loss-of function approach by conditional ablation of *fra-1* by intercrossing an inducible, mammary gland-specific Cre mouse line with mice carrying a conditional floxed allele of *fra*-1(fra-*1*$^{f/f}$, Eferl et al., 2004).

Taking advantage of these existing mice that ubiquitously overexpress *fra-1* as well as conditional *fra-1* knock-out mice (*fra-1*$^{\Delta/\Delta}$ mice), a direct *in vivo* role of Fra-1 in EMT could be studied using for example the well established mouse skin two-step chemical carcinogenesis model. This model involves initial treatment of the skin with the carcinogen 7,12-dimethylbenzanthracebe (DMBA), which acts as a tumor initiator and causes an activating mutation in H-ras oncogene. Continuous treatment of the mice with a tumor promoter, 12-O-tetradecanoylphorbol-13-acetate (TPA) causes the development of benign papillomas, which after some time convert to malignant and locally invasive squamous cell carcinoma. Finally, the tumor cells undergo EMT characterized by loss of differentiation and change to a metastatic spindle cell carcinoma. Interestingly, elevated levels of Fra-1 and phosphorylated Fra-1 have previously been reported in the squamous carcinoma

cell lines and especially in the metastatic spindle cell carcinoma cell lines obtained from tumors initiated *in vivo* by DMBA, suggesting that Fra-1 might play an important role in the progression of mouse skin tumors (Zoumpourlis et al., 2000). The use of the above described mouse skin carcinogenesis model would allow us to study the *in vivo* cooperation of activated *H-ras* and *fra-1* during multistage skin carcinogenesis and EMT. However, due to the chemically induced origin of the papillomas and their chemically-driven progression to spindle cell carcinoma, this model has its limitations. In addition, unlike the *K-ras* mutational activation, activating mutations of *H-ras* oncogene are a relatively rare event in human cancers (rate of activating mutation being 22% and 3.7% for *K-ras* and *H-ras*, respectively). Therefore, to address the role of Fra-1 in cancer development in a situation that more accurately simulates the pathology of human disease, other transgenic mouse models could be employed.

For example, the well characterized conditional *K-ras*^{LSLG12D} or the *K-ras*^{V12} transgenic mouse, widely used for modelling of lung cancer (Jackson et al., 2001; Guerra, et al., 2003) could be employed. The advantage of this transgenic mouse model is that the development and the progression of lung cancer closely mimic the situation in humans. The *K-ras*^{LSLG12D} transgenic mouse strain harbours an activating mutation (G12D) encoded in exon 1 of *K-ras* oncogene that occurs in 25-50% of human lung adenocarcinomas. This *K-ras* allele is functionally inactive due to the presence of a stop-cassette flanked by loxP sites (LSL) inserted in front of the exon 1. The expression of the mutated allele in the lung epithelia is activated following intranasal infection with adenovirus containing the Cre-recombinase (AdCre) or alternatively, by crossing these mice with the cell type-specific Cre mouse line. The AdCre-mediated removal of the stop-cassette enables the expression of the mutated allele at physiological levels, resulting in the development of lung tumors. This model was recently used to generate the compound conditional *K-ras*^{LSLG12D}*; p53* transgenic mouse, that revealed cooperation between loos of *p53* function and activation of *K-ras* during lung cancer progression (Jackson et al., 2005). Given that in the lung epithelial cells, Fra-1 expression was shown to be strongly induced by carcinogens such as asbestos and tobacco smoke (Ramos-Nino et al., 2003; Zhang et al., 2005), that it is highly expressed in lung cancer cell lines (Risse-Hackl et al., 1998), and that its ectopic

expression induces lung epithelial cell invasion (Adiseshaiah et al.,2007), the above model would be particularly useful to study the role of Fra-1 in the development and progression of lung cancer. One approach would include crossing the *K-ras*^{LSLG12D} mice with *fra-1*$^{f/f}$ mice that carry a conditional floxed allele of *fra-1*. The Cre-mediated recombination induced by intranasal infection with AdCre, or alternatively, by crossing these compound *K-ras*^{LSLG12D}; *fra-1*$^{f/f}$ mice with lung epithelial cell-specific Cre mouse line, would result in simultaneous *K-ras* activation and *fra-1* ablation that would answer the question whether Fra-1 is an essential downstream target of activated *K-ras* signalling in lung cancer development.

In conclusion, this study has provided new evidence for the essential role of Fra-1/AP-1 in the regulation of epithelial cell plasticity. The finding that Fra-1 expression is both necessary and sufficient for the induction of EMT and metastasis has opened new unexplored areas in the field of EMT and cancer research. However, further studies are required to more specifically define the exact steps of the invasion process that are dependent on Fra-1 expression, and to address the possibility that this is a general mechanism in the progression of different epithelial cancers in both mouse models and humans. Therefore, the afore mentioned experiments aimed to elucidate the molecular mechanisms by which Fra-1 contributes to tumor cell metastasis, as well as the identification of Fra-1 target genes with prognostic relevance have important implications for future prevention and treatment of invasive cancers.

5. Materials and Methods

5.1 Abbreviations

5-Aza-CdR	-	5-aza-2'-deoxycytidine
bp	-	base pairs
BPE	-	bovine pituitary extract
BSA	-	bovine serum albumin
℃	-	degree Celsius
ChIP	-	chromatin immunoprecipitation
conc	-	concentration
DAPI	-	4, 6-diamidino-2-phenylindole
DEPC	-	diethyl pyrocarbonate
Dexa	-	dexamethason
DMBA	-	7,12-dimethylbenz(a)anthracene
DMEM	-	Dulbecco's Modified Eagle's Minimal Essential Medium
DMSO	-	dimethylsulfoxide
DNA	-	deoxyribonucleic acid
dNTP	-	deoxyribonucleoside triphosphate
dsDNA	-	double-stranded DNA
DTT	-	dithiothreitol
ECM	-	extracellular matrix
E. coli	-	*Escherichia coli*
EDTA	-	ethylene-diamine-tetra-acetic acid
EGTA	-	ethylene-glycol-bis(2-aminoethyl ether)-N.N.N'N'-tetra-acetic acid
EMT	-	epithelial-mesenchymal transition
et al	-	et altera
EtOH	-	ethanol
FCS	-	fetal calf serum
g	-	gravity
GAPDH	-	glyceraldehydes-3-phosphate dehydrogenase
GF	-	growth factor
h	-	hour
HCl	-	hydrochloric acid

HEPES	-	4-(2-hydroxyethyl) piperazin-1-ethansulfonic acid
HPRT	-	hypoxanthine-guanine phosphoribosyltransferase
HRP	-	horseradish peroxidase
HXM	-	hypoxantine-xantine-mycophenolic acid
IgG	-	immunoglobulins
IP	-	Isopropteriol
kb	-	kilobase pairs
kDa	-	kilodalton
L	-	liter
M	-	molar
mA	-	miliamper
max	-	maximum
mg	-	miligram
$MgCl_2$	-	magnesium chloride
min	-	minute
mM	-	milimolar
NaCl	-	sodium chloride
NaF	-	sodium fluoride
NaN_3	-	sodium azide
NaOH	-	sodium hydroxide
Na3VO4	-	sodium orthovanadate
ng	-	nanogram
nm	-	nanometer
nM	-	nanomolar
NP-40	-	Nonidet P-40
OD	-	optical density
PBS	-	phosphate-buffered saline
PBS-T	-	PBS-0.1% Tween
PCR	-	polymerase chain reaction
PFA	-	paraformaldehyde
pH	-	potentia hydrogenii
PMSF	-	phenylmethylsulfonylfluoride
RNA	-	ribonucleic acid
rpm	-	rotations per minute
RT	-	room temperature
s.d.	-	standard deviation
SDS	-	sodium dodecyl sulfate
SDS-PAGE	-	SDS-polyacrylamide gel electrophoresis

sec	-	second
ssRNA	-	single-stranded RNA
TAE	-	Tris-acetate-EDTA buffer
TBS	-	Tris-buffered saline
TBS-T	-	TBS-0.1% Twen
TE	-	Tris-EDTA buffer
TGFα	-	transforming growth factor alpha
TGFβ	-	transforming growth factor beta
TPA	-	12-*O*-tetradecanoylphorbol-13-acetate
TSA	-	Trichostatin A
TRE	-	12-*O*-tetradecanoylphorbol-13-acetate-response element
Tris-HCl	-	Tris hydrochloride
TSA	-	trichostatin A
UV	-	ultraviolet light
V	-	voltage
vs	-	*versus*
Vol	-	volume
w/v	-	weight to volume
µg	-	microgram
µl	-	microliter
µM	-	micromolar

5.2 Materials

5.2.1 Chemicals and reagents

All chemicals, reagents, antibodies, oligonucleotides and kits used for this study were purchased from the following companies: Abcam, Amersham Biosciences, BD Biosciences, BioRad, Cell Signaling, Epicentre Biotechnologies, Eppendorf International, Fermentas, Gibco, Invitrogen, MWG Biotech, Novocastra, Promega, Roche, Sigma-Aldrich, Santa Cruz, BD Transduction Laboratories, Upstate, Vectastain and Qiagen.

5.2.2 Media

LB medium:

In 500 ml H_2O dissolve 5 g Bacto tryptone, 2.5 g Bacto yeast extract and 2.5 g NaCl, autoclave and store on room temperature.

HXM medium:

To 450 ml of Dulbecco's Modified Eagle Media (DME) add 50 ml newborn calf serum, 5 ml antibiotic (Pen-Strep), 0.75 ml of 10 mg/ml Hypoxantine (Sigma Aldrich; final conc. 15 µg/ml), 12.5 ml of 10 mg/ml Xanthine (Sigma Aldrich; final conc. 250 µg/ml), 1.25 ml 10mg/ml Mycophenolic acid (Sigma Aldrich; final conc. 25 µg/ml) and 120 µl of concentrated HCl. Hypoxantine, Xanthine and Mycophenolic acid stock solutions were made in 0.1 N NaOH.

Serum free cell culture medium:

DMEM medium supplemented with 1% L-Glutamine, 1% Pen-Strep, 2% 1M HEPES pH 7.3 and 0.2% BSA.

5.2.3 Antibodies used for Western Blotting and Immunohistochemistry

Primary:

Antigen	**Host**	**Dilution**	**Supplier**
Actin	rabbit	1:5000	Sigma
α-catenin	mouse	1:1000	Transduction Labs
β-catenin	mouse	1:1000	Transduction Labs
c- Fos	rabbit	1:1000	Santa Cruz
c-Jun	mouse	1:1000	Transduction Labs
E-cadherin	mouse	1:1000	Transduction Labs
Fibronectin	rabbit	1:750	Sigma
FosB	mouse	1:1000	Santa Cruz
Fra-1	rabbit	1:1000	Santa Cruz
Fra-2	rabbit	1:1000	Santa Cruz
γ-catenin	mouse	1:1000	Transduction Labs

HP-1α	mouse	1:500	Euromedex
JunB	rabbit	1:1000	Santa Cruz
JunD	rabbit	1:1000	Santa Cruz
panERK	mouse	1:1000	Transduction Labs
p-ERK1/2	mouse	1:300	Transduction Labs
p120-catenin	mouse	1:1000	Transduction Labs
Stat1	rabbit	1:750	Cell Signaling
Stat3	mouse	1:1000	Cell Signaling
Vimentin	mouse	1:1000	Sigma
Zeb-1	goat	1:500	Santa Cruz

Secondary:

α-goat IgG HRP-linked (Jackson ImmunoResearch Laboratories); 1:5000
α-rabbit IgG HRP-linked (GE Healthcare. Amersham Biosciences); 1:5000
α-mouse IgG HRP-linked (GE Healthcare. Amersham Biosciences); 1:5000

All antibody solutions used for Western blotting were supplemented with 0.02% NaN_3 after first incubation and kept at 4℃ for reuse.

5.2.4 Antibodies used for Immunofluorescence

Primary:

For protein visualization and localization, the same primary E-cadherin, Fra-1, α-catenin, β-catenin, γ-catenin, p120-catenin, fibronectin and vimentin antibodies were used as for Western blotting only at 1:200 dilutions. Additionally, for F-actin visualization, Alexa 488-Phalloidin coupled antibody (Invitrogen. A12379) was used at 1:250 dilution.

Secondary:

Alexa 488 - conjugated goat anti-mouse IgG (Jackson ImmunoResearch Laboratories)
Alexa 488 - conjugated goat anti-rabbit IgG (Jackson ImmunoResearch Laboratories)
Alexa 488 - conjugated donkey anti-goat IgG (Jackson ImmunoResearch Laboratories)

DyLight™ 549 - conjugated goat anti-mouse IgG (Pierce)
DyLight™ 549 - conjugated goat anti-rabbit IgG (Pierce)

All secondary antibodies were used at 1:250 dilutions.

5.2.5 Antibodies used for Chromatin Immunoprecipitation (ChIP)

Antigen	**Host**	**Supplier**	**Catalogue number**
Fra-1	rabbit	Santa Cruz	sc-183 (clone N-17)

Each ChIP sample was immunoprecipitated with 5g of antibody.

5.2.6 MISSION™ shRNA Library

MISSION™ shRNA are sequence-verified shRNA lentiviral plasmids for gene silencing in mammalian cells. Parental vector pLKO.1-puro allows stable selection via Puromycin resistance. Two of the following target gene sets were used:

MISSION™ TRC shRNA Target Set **Fosl1 (Fra-1)** NM_010235 (Sigma Aldrich)
Insert sequences:
TRCN0000042683
CCGGCGACAAATTGGAGGATGAGAACTCGAGTTCTCATCCTCCAATTTGTCGTTTTTG
TRCN0000042684
CCGGGCTCTCCTACACTCCTGGCTTCTCGAGAAGCCAGGAGTGTAGGAGAGCTTTTTG
TRCN0000042685
CCGGCCAGGAGTCATACGAGCCCTACTCGAGTAGGGCTCGTATGACTCCTGGTTTTTG
TRCN0000042686
CCGGCCTCCGCTCACCGAAAGAGTACTCGAGTACTCTTTCGGTGAGCGGAGGTTTTTG
TRCN0000042687
CCGGCCAGTGCCTTGCATCTCCCTTCTCGAGAAGGGAGATGCAAGGCACTGGTTTTTG

MISSION® shRNA Non-Target shRNA **Control Vector** (Sigma Aldrich. SHC002)
This non-targeting shRNA vector is a useful negative control that activates RISC and the RNAi pathway but does not target any human or mouse gene. The short-

hairpin sequence contains 5 base pair mismatches to any known human or mouse gene and allows the examination of the effects of shRNA transfection on gene expression.

Insert sequence:
CCGG**CAACAAGATGAAGAGCACCAA**CTCGAG**TTGGTGCTCTTCATCTTGTTG**TTTTT

5.2.7 siRNA oligonucleotides

For transient gene silencing experiments Dharmacon ON-TARGETplus SMARTpool siRNA double-stranded oligonucletides were used (Thermo Scientific-Dharmacon, Inc.) according to the manufacturer's protocols and recommendations. The following ON-TARGETplus SMARTpools were used:

ON-TARGETplus SMARTpool L-051513-01-0005. **Mouse ZFHX1A**. NM_011546

ON-TARGETplus SMARTpool siRNA J-051513-09. ZFHX1A
Target sequence: UGUAGAUGGUAACGUAAUA
ON-TARGETplus SMARTpool J-051513-10. ZFHX1A
Target sequence: GAAAGAGCACUUACGGAUU
ON-TARGETplus SMARTpool J-051513-11. ZFHX1A
Target sequence: GCGCAAUAACGUUACAAAU
ON-TARGETplus SMARTpool J-051513-12. ZFHX1A
Target sequence: CGGCAUGGCUAGCAGUAUU

ON-TARGETplus SMARTpool Non-targeting Pool D-001810-10-05

ON-TARGETplus SMARTpool siRNA J-051513-09. ZFHX1A
Target sequence: UGUAGAUGGUAACGUAAUA
ON-TARGETplus SMARTpool J-051513-10. ZFHX1A
Target sequence: GAAAGAGCACUUACGGAUU
ON-TARGETplus SMARTpool J-051513-11. ZFHX1A
Target sequence: GCGCAAUAACGUUACAAAU
ON-TARGETplus SMARTpool J-051513-12. ZFHX1A
Target sequence: CGGCAUGGCUAGCAGUAUU

siGENOME SMARTpool M-059671-01-0005. **Mouse Zeb2**. NM_015753

siGENOME SMARTpool siRNA D-059671-01,ZFHX1B
Target sequence: GUAAAUGGCCGAAUGAGAA
siGENOME SMARTpool siRNA D-059671-02,ZFHX1B
Target sequence: GCGACACGGCCAUUAUUUA
siGENOME SMARTpool siRNA D-059671-03,ZFHX1B
Target sequence: GCAGGUAACCGCAAGUUCA
siGENOME SMARTpool siRNA D-059671-04,ZFHX1B
Target sequence: UAGAUUUGGUCACUGAUGA

For transfection reactions Dharmacon transfection reagents 1 and 2 were used according to manufacturer's instructions.

5.3 Methods

5.3.1 Transformation of *E. coli* with plasmid DNA

Prior to transformation with plasmid DNA an aliquot of competent *E. coli* (DH5alpha) cells was thawn on ice. 100 µl of bacterial suspension was transferred to 1.5 ml eppendorf tube, mixed with 10 ng of target plasmid DNA and incubated on ice for 15 min. Bacterial suspension was heat-shocked in a waterbath at 37℃ for 1 min followed by 1 min incubation on ice. Next, 1 ml of fresh LB media without antibiotics was added and suspension further incubated for 1 h on a heating block at 37℃ with shaking. After incubation, 100 µl of bacterial suspension was plated onto LB plate containing Ampicilin (100 µg/ml) and incubated overnight at 37℃ in an incubator.

5.3.2 Plasmid DNA preparation

Plasmid DNA was isolated using QIAGEN Plasmid Maxi Kit according to the manufacturer's instructions. For pLKO.1 lentiviral vectors plasmid DNA was

isolated using Promega PureYield™ Plasmid Midiprep System with endotoxine removal step according to the protocol provided with the kit.

5.3.3 RNA isolation

Total RNA was isolated from cells using TRIzol® Reagent (Invitrogen™) according to manufacturer's instructions. Briefly, cells were washed once with PBS, trypsinized and pelleted. Pellet was resuspended in 1ml of TRIzol® Reagent, incubated on room temperature for 5 min and centrifuged at 12.000 x g for 10 min (4℃). Supernatant was transferred to a new tube and 0.2 ml of chloroform was added, homogenate vortexed, incubated at room temperature for 2-3 min and centrifuged for 15 min at 12.000 x g (4℃). The upper aqueous phase was transferred to a new tube and RNA precipitated by adding 0.5 ml isopropanol for 10 min at room temperature followed by centrifugation for 10 min at 12000 x g (4℃). Supernatant was removed and RNA pellet washed twice by adding 1 ml of 75% EtOH followed by centrifugation at 7.500 x g for 5 min (4℃). RNA pellet was air-dried for 5-10 min, dissolved in DEPC-treated H_2O and incubated for 10 min at 55-60℃. Concentration was determined by UV spectrophotometry (OD_{260}=1.0 equals 40 µg/ml of ssRNA). RNA was stored at -80℃ until further use.

5.3.4 RNase Protection Assay (RPA)

For each RPA reaction, 10 µg total RNA isolated from cells was used. RPA was performed using BD RiboQuant Multi-Probe RNase Protection Assay System (BD PharMingen) according to manufacturer's instructions. Two following multi-probe template sets were used: mFos/Jun and mMMP-2.

5.3.5 cDNA synthesis

cDNA was synthesized from 2 µg of total RNA using "Ready-To-Go You-Prime First-Strand Beads" kit (Amersham Biosciences) and random primer

oligonucleotides (Invitrogen) according to the manufacturer's instructions. Synthesized cDNA was stored at -20℃.

5.3.6 Quantitative Real-time RT-PCR

Quantitative real-time RT-PCR (qPCR) was performed to verify the results obtained by the cDNA microarray analysis, examine and quantify transcript levels of candidate genes.

Primers were designed using Primer3 software or retrieved from the online PrimerBank database (http://pga.mgh.harvard.edu/primerbank/index.html). 1 µl of cDNA was used per reaction and reactions were performed using SYBR Green (Molecular Probes) on an Opticon2 Monitor Fluorescence Thermocycler (MJ Research) in a 25 µl reaction volume for 40 cycles using the following protocol:

Temperature	Time	Number of cycles
94℃	50 sec	1
94℃	15 sec	40
57℃	35 sec	
72℃	45 sec	
Melting curve 64℃-94℃	Read every 0.4℃	1

Comparative Ct (cycle threshold) method was used to quantify the amplified fragments and RNA expression levels were normalized to at least one housekeeping gene (actin, HPRT, GAPDH).

Primers sequences are listed in the table bellow:

Gene	Primer sequence	Gene	Primer sequence
GAPDH forward	ACCCAGAAGACTGTGGATGG	vimentin forward	GTGCGCCAGCAGTATGAAAG
GAPDH reverse	CACATTGGGGGTAGGAACAC	vimentin reverse	GCATCGTTGTTCCGGTTGG
Cldn3 forward	ACCAACTGCGTACAAGACGAG	Wnt7a forward	CCTTGTTGCGCTTGTTCTCC
Cldn3 reverse	CAGAGCCGCCAACAGGAAA	Wnt7a reverse	GGCGGGGCAATCCACATAG
E.cadherin forward	CAGCCTTCTTTTCGGAAGACT	occludin forward	TTGAAAGTCCACCTCCTTACAGA
Ecadherin reverse	GGTAGACAGCTCCCTATGACTG	occludin reverse	CCGGATAAAAAGAGTACGCTGG
Fra-1 forward	CAGCCTCATTTCCTGGGACC	FosB forward	TTTTCCCGGAGACTACGATC
Fra-1 reverse	CCTTTCTTCGGTTTCTGCACT	FosB reverse	GTGATTGCGGTGACCGTTG
HPRT forward	CTGGTGAAAAGGACCTCTCG	MMP14 forward	CAGTATGGCTACCTACCTCCAG
HPRT reverse	CACAGGACTAGAACACCTGC	MMP14 reverse	GCCTTGCCTGTCACTTGTAAA
IL6 forward	TAGTCCTTCCTACCCCAATTTCC	SPARC forward	GTGGAAATGGGAGAATTTGAGGA
IL6 reverse	TTGGTCCTTAGCCACTCCTTC	SPARC reverse	CTCACACACCTTGCCATGTTT
KLF8 f orward	GCAGCCATTCCTACTGTTCTC	c-Jun forward	CCTTCTACGACGATGCCCTC
KLF8 reverse	CATAGGCAAAGACTGGACCAC	c-Jun reverse	GGTTCAAGGTCATGCTCTGTTT
Krt 18 forward	GTCAGAGACTGGGGCCACTA	CathepsinB forward	TCCTTGATCCTTCTTTCTTGCC
Krt18 reverse	CTCTAAAGTCATCGGCGGCAA	CathepsinB reverse	ACAGTGCCACACAGCTTCTTC
Krt8 fforward	TGTCTACTCGGTCGGACTTCT	c-Fos forward	CGGGTTTCAACGCCGACTA
Krt8 reverse	GCTGCTACCTAGCTGACATGC	c-Fos reverse	TTGGCACTAGAGACGGACAGA
Lama3 forward	GTAAGGGTGAGATTGTCTGTGAG	JunB forward	TCACGACGACTCTTACGCAG
Lama3 reverse	ATATGGCTTCCGTTCCAGGAC	JunB reverse	CCTTGAGACCCCGATAGGGA
MMP1 forward	CTTCTTCTTGTTGAGCTGGACTC	Fra-2 forward	CCAGCAGAAGTTCCGGGTAG
MMP1 reverse	CTGTGGAGGTCACTGTAGACT	fra-2 reverse	GTAGGGATGTGAGCGTGGATA
MMP12 forward	GAGTCCAGCCACCAACATTAC	JunD forward	GAAACGCCCTTCTATGGCGA
MMP12 reverse	GCGAAGTGGGTCAAAGACAG	Jund reverse	CAGCGCGTCTTTCTTCAGC
MMP2 forward	GACCTTGACCAGAACACCATC	CD44 forward	CACCATTGCCTCAACTGTGC
MMP2 reverse	CATCCACGGTTTCAGGGTCC	CD44 reverse	TTGTGGGCTCCTGAGTCTGA
Snai1 forward	CACACGCTGCCTTGTGTCT	Tnc forward	GCATCCGTACCAAAACCATCA
Snai1 reverse	GGTCAGCAAAAGCACGGTT	Tnc reverse	AACCCGTAGGGATTAGTGTCG
Snai2 forward	CCTTGGGGCGTGTAAGTCC	ZO1 forward	CCGGCCAGCCACATATTTGTA
Snai2 reverse	TTCTCAGCTTCGATGGCATGG	ZO1 reverse	CGCTCATCTCTTTGCACTACCA
ZEB1 forward	GCTGGCAAGACAACGTGAAAG	Stat1 forward	CGGAGTCGGAGGCCCTAAT
ZEB1 reverse	GCCTCAGGATAAATGACGGC	Stat1 reverse	ACAGCAGGTGCTTCTTAATGAG
ZEB2 forward	CATGGCAGTATCCAGGCAGG	Fgfr1 forward	GGGAGTATGTGTGTAAGGTTTCC
ZEB2 reverse	AGTCTTCCACTAGCAGCCTTT	Fgfr1 reverse	CTTGGTGCCGCTCTTCATCTT
p16 forward	AACTCTTTCGGTCGTACCCC	Tspan1 forward	CTGTGGGAATCTGGGTGTCC
p16 reverse	GCGTGCTTGAGCTGAAGCTA	Tspan1 reverse	CACACTTGTTCTCAGAGTGAGC
Cldn6 forward	ATGGCCTCTACTGGTCTGCAA	Cldn7 forward	GGCCTGATAGCGAGCACTG
Cldn6 reverse	GCCAACAGTGAGTCATACACCTT	Cldn7 reverse	GTGACGCACTCCATCCAGA

5.3.7 RNA preparation and microarray analysis

For wide-range gene expression analysis an in-house printed oligonucleotide slides containing over 22500 oligonucliotide sequences were used. Total RNA was extracted from cells cultured to 70-80% confluence, using TRIzol® Reagent (Invitrogen™) according to manufacturer's instructions. Approximately 3µg of total RNA was synthesized into a double-stranded cDNA followed by an *in vitro* transcription reaction and labelling with reactive fluorescent dyes (Alexa 555 and

Alexa 647) and hybridized onto slides in triplicates. Hybridized slides were scanned on a fluorescent scanner Axon 4000B and the results were obtained as red and green images. These images were further analysed for spot and local background identification by GenePix Pro 6.0 software. The data generated by the image software analysis were further analysed using R (statistical programming language) and several packages from Bioconductor, mainly *Limma*, by subtracting the background from the foreground signal (background correction) and normalised (method: NormalizeWithinArray and NormalizeBetweenArray) to adjust the differences in labelling and detection deviations as well as differences in the amount of the input RNA. The obtained results included (log) fold changes, standard errors, t-statistics and *p*-values ($p<0.05$ was classified as significant). The basic statistic used for significance analysis was the moderated t-statistic, which was computed for each probe and for each contrast. The M-value (M) is the value of the contrast that represents a log2-fold change between two or more experimental conditions (control vs target sample).

5.3.8 Chromatin Immunoprecipitation (ChIP)

Sample preparation:

Cells were cultured in 15 cm dishes to 80% confluence and approximately $6x10^7$ cells (two dishes) were used for each immunoprecipitation reaction. Proteins and DNA were cross-linked by addition of 1% formaldehyde strait to the cell culture media and incubated on a rocking platform with gentle agitation for 10 min at room temperature. The reaction was quenched by adding 125mM glycine for 5 min at room temperature, the cells were washed two times with PBS, scraped from the plates and lysed in 2 ml of freshly prepared Lysis buffer (1% SDS; 10mM EDTA; 50mM Tris-HCl pH 8.1 and 1 complete Mini EDTA-free protease inhibitor tablet (Roche diagnostics) per 10 ml of buffer) for 30 min at 4℃. To shear chromatin, the samples were sonicated in de-ionized water bath using Covaris S2 machine to yield 200-500 bp fragments. Number of pulses and length of sonication was determined for each sample by checking shearing efficiency. Briefly, 100 µl aliquots were taken after different sonication cycles and mixed with H_2O to a volume of 500µl, 5 µl of RNase A (10 µg/µl) was added and the samples were incubated in a thermo block

for 30-60 min at 37℃. 5 µl Proteinase K (20 µg/µl) was added and the samples were incubated in a thermo block for 30-60 min at 55℃ with shaking (750 rpm) followed by reverse cross-linking at 65℃ overnight (or min 6h). DNA was isolated by phenol:chloroform:isoamyl-alcohol (25:24:1) extraction. Briefly, 1/1 volume of the organic solvent was added, the sample was vortexed, centrifuged for 10 min at 13000 rpm and the water phase containing DNA was collected in a new tube. DNA was precipitated by adding 2-2.5 volumes of 100% ethanol, 1/10 volume 3M NaAc, 2 µl glycogen (GycoBlue. 1.5µg/µl. Ambion) to better visualize the pellet, and incubated at -20℃ for 2 h. The samples were centri fuged for 20 min at 13000 rpm (4℃), the supernatant was discarded and DNA-contai ning pellet washed with 1 ml of 70% EtOH, air dried and dissolved in 50 µl of TE buffer. Sheared DNA was subjected to electrophoresis in 2% TAE-agarose gels pre-mixed with ethidium bromide (0.5µg/ml) and visualised under UV light. Once the fragments of proper size were obtained, DNA concentration was determined by UV spectrophotometry (OD_{260} = 1.0 equals 50 µg/ml of dsDNA). If not used immediately, the lysates were stored at 4℃.

Immunoprecipitation:

For each immunoprecipitation reaction 200-400 µg of chromatin was used. 1/100 volume of the sample was taken and used for input while the rest of the sample was 10 fold diluted with Dilution buffer (0.01% SDS; 1.1% Triton X-100; 1.2 mM EDTA; 16.7 mM Tris-HCl pH 8.1; 167 mM NaCl). Chromatin solution was pre-cleared by adding 50 µl Protein A/G coated beads pre-incubated with 1%BSA for 2h, and rotating the sample for 2 h (4℃), followed by centrifugation at 2000 rpm for 5 min (4℃). The supernatant was collected and divi ded into two equal samples. One sample was used for immunoprecipitation with antibody of interest and the other one used as a negative control (no antibody addition). The samples were further treated in the same way. Immunoprecipitiation was done using 5 µg of Fra-1 antibody and rotating the samples overnight at 4°C. The imune complexes were harvested by adding 50 µl of protein A/G coated beads, rotating the sample for 2h (4℃) and centrifuging at 2000 rpm for 5 min. The s upernatant was carefully discarded and the beads were washed by adding 1 ml of buffer, centrifuging at 2000 rpm for 5 min and discarding the supernatant. The buffers were used in the following order: 1x Low Salt buffer (0.1% SDS; 1% Triton X-100; 1.2mM EDTA;

20mM Tris-HCl pH 8.1; 150mM NaCl). 1x High Salt buffer (0.1% SDS; 1% Triton X-100; 1.2mM EDTA; 20mM Tris-HCl pH 8.1; 500mM NaCl). 1x LiCl buffer (0.25M LiCl; 1% NP-40; 1% deoxycholate; 1mM EDTA; 10mM Tris-HCl pH 8.1; 150mM NaCl) and 2x TE buffer. To elute the immune complexes, 250 µl of freshly prepared Elution buffer (1% SDS; 100mM $NaHCO_3$) was added to the beads; the samples were briefly vortexed and incubated for 15 min at room temperature with shaking. Following centrifugation at 2000rpm for 2 min, the supernatant was collected in a new tube, elution step repeated and the eluates combined. 500µl of the Elution buffer was added to the input sample that was further on treated like an IP sample. 16µl of 5M NaCl and 12.5 µl of 10µg/µl RNase A was added to every sample followed by 1h incubation at 37℃ and overnight rev erse cross-linking at 65℃. Next, 16µl 1M Tris pH 6.5, 8 µl 0.5M EDTA and 12.5 µl of 20 µg/µl Proteinase K was added to each sample followed by 1-2h incubation at 45℃. DNA was recovered by performing 1xphenol:chloroform:isoamyl-alcohol (25:24:1) extraction and 1x chloroform extraction. Briefly, 1/1 volume of organic solvent was added, the samples were vortexed, centrifuged at 13000rpm for 10 min, and the water phase was collected. DNA was precipitated by adding 2-2.5 volumes of 100% EtOH, 1/10 volume 3M Na-Acetate, 1µl of 20 µg/µl glycogen for better visualisation of the pellet, and incubated at -20℃ for 4h or overnight. The samples were centrifuged at 13000rpm for 10 min, the supernatant was discarded, DNA pellet washed by adding 1ml of 70% EtOH and centrifuged again for 10 min at 13000rpm. Supernatant was discarded, pellet dried for 10 min at 37℃ and dissolved in 50 µl of 1xTE buffer. Chromatin was quantified using PicoGreen Assay and 1 µl of each sample was used for quantitative real-time PCR analysis.

For detection of AP-1 sites within the ZEB1 promoter, the following two primer sets were used with standard qPCR protocol:

ChIP1 forward: GCCGCTAGGTGTTAGGAAGG
ChIP1 reverse: CGCTTGTGTCTAAATGCTCG

ChIP2 forward CAAAGTGCGCAACTCGTCT
ChIP2 reverse: GGACGCTGCAGAGTTTGAAT

5.3.9 Nuclear extract preparation

Cells were washed once with PBS, trypsinized, pelleted and lysed in 400 µl of ice cold Buffer A (10mM HEPES pH 7.9; 10mM KCl; 0.1mM EDTA; 0.1mM EGTA; 1mM DTT; 0.5mM PMSF and 1 complete Mini EDTA-free protease inhibitor tablet (Roche diagnostics) per 10 ml of buffer) on ice for 15 min. Next, 40 µl of 10% NP40 was added and the lysate was votexed. Homogenate was centrifuged at 2600 rpm / 5 min and the supernatant containing the cytoplasmic fraction was discarded. Pellet containing the nuclei was than lysed by addition of 60 µl of ice cold Buffer B (20mM HEPES pH 7.9; 1mM EDTA; 1mM EGTA; 1mM DTT; 1mM PMSF and 1 complete Mini EDTA-free protease inhibitor tablet (Roche diagnostics) and incubated in a shaker for 10-15 min (4℃). Lysates were centrifuged at max speed for 5 min (4℃). Pellet was discarded and the super natant transferred to a new tube. Protein concentration was measured by spectrophotometry (absorption at 595 nm) in Bradford protein assay using BioRad Protein Assay Dye Reagent according to manufacturer's instructions. BSA aliquots of known concentrations were used as standards and the lysates were stored at -80℃.

5.3.10 Total cell lysate preparation

For total cell lysate, the cells were washed once with PBS, trypsinized, pelleted and lysed in 1 ml of ice cold modified RIPA (RadioImmunoPrecipitation Assay) buffer (50mM Tris-HCl pH 7.4; 150mM NaCl; 1mM EDTA; 1% NP-40; 1% Sodium-deoxycholate; 1mM Na_3VO_4; 25mM NaF; 1mM PMSF; 1% 1M DTT; 1% β-glycerol phosphate; 10 µg/µl Aprotinin and 1 complete Mini EDTA-free protease inhibitor tablet (Roche diagnostics) per 10 ml of buffer) for 20 min on ice with repeated vortexing. Homogenate was centrifuged at max speed for 10 min (4℃). The pellet was discarded and the supernatant was transferred to a new tube. Protein concentration was measured by spectrophotometry (absorption at 595 nm) in Bradford protein assay using BioRad Protein Assay Dye Reagent according to manufacturer's instructions. BSA aliquots of known concentrations were used as standards and the lysates were stored at -80℃.

5.3.11 Western blotting

SDS-PAGE electrophoresis of proteins and Western blotting were performed using Mini-PROTEAN II and Mini Trans-Blot electrophoretic system (BioRad) according to manufacturer's instructions. Briefly, 10 µg (nuclear extracts for AP-1 proteins) or 30 µg (total cell lysates) of proteins were mixed with 2x Laemmli Loading Buffer (50mM Tris-HCl pH 6.8; 2% SDS; 0.1% Bromophenol Blue; 10% glycerol; 100mM DTT) in a 15 - 25 µl volume and denatured for 3-5 min at 95℃. Proteins were separated on 8%-15% SDS-polyacrylamide gel at 80-120 V for 1-2 h in electrophoresis buffer (0.25M Tris-HCl pH 8.3; 1.92M glycine; 5 g/L SDS) and electrophoretically transferred to Polyvinylidene difluoride (PVDF) membranes (Immobilion-P; Millipore Corp, Bedford, MA) pre-activated in methanol for 1 min, by semi-dry transfer at 95mA (1.2 mA/cm^2) for 1 h 30 min in semi-dry transfer buffer (48mM Tris base; 39mM glycine; 0.037% SDS; 20% methanol). For detection of higher molecular weight proteins, the wet-transfer method onto a nitrocellulose membrane (BioRad) in Mini Trans-Blot electrophoretic system (BioRad) at 100 V (4℃) for 2h.

5.3.12 Immunodetection of proteins

To prevent non-specific binding of the antibodies, PVDF membranes were incubated for 1 h in blocking solution (5% non-fat dry milk/PBS-T) followed by washing 3x5 min in PBS-T and incubation with the primary antibody solution (antibody diluted in 1% BSA/PBS-T) overnight at 4℃. The membranes were washed 3x10 min in PBS-T and incubated with the secondary HRP-linked antibody solution (antibody diluted in blocking solution) for 1 h at room temperature followed by 3x10 min wash in PBS-T. All washing and incubation steps were performed with gentle agitation on a rocking platform. Immunoreactive bands were visualized using chemiluminiscent ECL reagent (Amersham Biosciences) according to manufacturer's instructions, and exposed to Hyperfilm™ ECL (Amersham Biosciences) for various time. For re-probing, the membranes were washed for 5 min in PBS-T, stripped for 10-15 min in striping buffer (2% SDS; 62.5mM Tris-HCl pH 6.7 and 0.8 ml β-mercaptoethanol per 100 ml of buffer) at 50℃ in a waterbath

with gentle agitation, and extensively washed in PBS-T prior to blocking and re-probing with different antibody.

5.3.13 Immunofluorescence

Cells grown on filters (# 353090, 0.4 µm pore size; Falcon, Becton Dickinson, Franklin Lakes, New Jersey, USA) were fixed in 4% PFA/PBS for 15 min at room temperature, washed once with PBS and incubated in 100nM Glycine/PBS for 20 min at room temperature. Cells were washed once with PBS followed by a second fixation in Methanol at -20℃ for 6 min and permeab ilization with 0.1% Triton X-100 for 2 min at room temperature. After blocking in 1% BSA/PBS for 30 min at room temperature, the filters were cut into pieces. Each piece was incubated with primary antibody (dilution 1:200) diluted in 0.5% BSA/PBS for 1h 30 min in a humid chamber. After washing three times with PBS, the cells were incubated with the secondary fluorescent antibody (dilution 1:250) diluted in 0.5% BSA/PBS for 45 - 60 min. For actin cytoskeleton staining, Alexa Fluor 488-Phalloidin (Invitrogen) diluted in 0.5% BSA/PBS (dilution 1:250) for 45 - 60 min was used. Cells were washed three times with PBS and costained for DNA using DAPI (1mg/ml stock diluted 1:10000 in PBS) in a final washing step. Negative control staining was done in parallel using only the secondary fluorescent antibodies. Filter pieces were additionally washed two times with distilled H_2O, mounted onto microscope glass slides (SuperFost®Plus; Menzel-Gläser) using Vectashield (Vector Laboratories Inc., Burlingame, CA), covered with coverslips and sealed at the edges with transparent nail polish. The slides were subjected to fluorescence microscopy on a Zeiss Axioplan 2 imaging microscope (Carl Zeiss. Oberkochen. Germany) equipped with Metamorph software. Images were captured using CoolSnap HQ camera (Photometrics).

5.3.14 Cells and cell culture

The origin of EpH4 mouse mammary epithelial cell and their Ha-RasV12 transformed derivative EpRas has been described earlier (Reichmann et al., 1989;

Oft et al., 1996). Fra-1 overexpressing EpH4 and EpRas cells were generated by retroviral gene transfer. Fra-1-knock-down EpRas and EprasXT cells were generated using lentiviral shRNA.

5.3.14.1 Culturing of cells

EpH4 cells, EpRas cells, and their respective Fra-1 overexpressing and knock-down clones were maintained in DMEM (Dulbecco's Modified Eagle's Minimal Essential Medium) containing 5% fetal calf serum (FCS; Sigma). 1% Pen-Strep, 1% L-Glutamine and 2% 1M HEPES pH 7.3; EpRasXT cells were maintained in 2:1 ratio of DMEM media supplemented with 10x more nonessential amino acids, 15% FCS, 1% Pen-Strep, 1% L-Glutamine, and 2% 1M HEPES pH 7.3; and filtered conditioned media from the same cells. NIH 3T3 fibroblasts and HEK-293T cells were maintained in DMEM containing 10% FCS, 1% Pen-Strep, 1% L-Glutamine, and 2% 1M HEPES pH 7.3. GP+E 86 retroviral packaging cells (Markowitz et al. 1988) were grown in HXM media to ensure optimal packaging of viral particles. All cells were grown in a tissue culture incubator at 37℃ and 5% CO_2.

5.3.14.2 Retroviral production

Retroviral vectors pBabe-Puro and pBabe-puro-Fra1 have been described previously (Matsuo et al., 2000). GP+E 86 retroviral packaging cells were maintained in HXM media for a few days prior to transfection with plasmid DNA. One day before transfection, cells were splited, transferred to a 6-well Falcon cell culture plate ($3x10^5$ cells per well) and cultured overnight in DMEM supplemented with 10% FCS. Prior to transfection, cells were washed once with PBS and 800 µl of serum free media was added per well. The cells were transfected with plasmid DNA using PolyFect Transfection Reagent (QIAGEN Gmbh) according to manufacturer's instructions. Briefly, for every well, 150 µl of serum free media was mixed with 1.5 µg target plasmid DNA, vortexed and left on room temperature for 1 min. Next, 10 µl of PolyFect reagent was added, mixture was vortexed for 5 s and incubated on room temperature for 15 min prior to addition to the cells. The cells

were incubated with the mixture for 4 h, then 1ml of standard serum containing culture media was added and cells were left overnight in an incubator at 37℃ and 5% CO_2. The next day, medium was changed and the supernatants containing viral particles were harvested in 48 h intervals. Aliquots were stored at -80℃ until further use.

5.3.14.3 Lentiviral production

For lentiviral production, HEK-293T packaging cells were used. 2.5 x10^6 cells were plated in 10 cm cell culture dishes one day prior to transfection with plasmid DNA. The cells were co-transfected with target pLKO.1 constructs, psPAX2 packaging plasmid and pMD2.G envelope plasmid using Lipofectamine Plus reagent (Invitrogen) with the following protocol. In one eppendorf tube, 750 µl of DMEM medium containing 1% L-Glutamine (no antibiotics or FCS) was mixed with 3.33 µg of the target plasmid DNA, 2.5 µg of psPAX2 DNA, 1µg of pMD2.G DNA, and 20 µl of Plus reagent (Invitrogen). In a second tube, same volume of DMEM medium containing 1% L-Glutamine was mixed with 30µL of Lipofectamine (Invitrogen). Tubes were incubated for 15 min at room temperature in a cell culture hood. After the incubation, the suspensions were mixed and incubated for additional 15 min. HEK-293T packaging cells were washed with PBS and 5ml of DMEM containing 1% L-Glutamine was added. Plasmid suspension was evenly distributed over the dish and subsequently incubated for 3-4 h at 37℃ and 5% CO_2 in a tissue culture incubator. Following incubation, the cells were washed with PBS and 10 ml of fresh DMEM media supplemented with 10% FCS, 1% L-Glutamine, 1% Pen-Strep and 2% HEPES pH 7.3 was added. The supernatants containing viral particles were harvested in 48 h intervals, centrifuged for 5 min at 1500 rpm, aliquoted and stored at - 80℃ until use.

5.3.14.4 Retroviral and Lentiviral infection

Cells were seeded in 6-well cell culture plates (3x10^5 cells per well) one day before infection. Cells were washed once with PBS and 2 ml of the viral supernatant

supplemented with 8mg/ml Polybrene was added per well, and cultured for the next 24h. The cells were washed two times with PBS and the standard culture media containing 2.5 µg/ml Puromycin was added for selection of infected cells.

5.3.14.5 Cell doubling time

To determine cell doubling time, $5x10^5$ cells were plated in 10 cm cell culture dish in triplicate and cultured in standard culture media for 48 - 96 h in a tissue culture incubator at 37℃ and 5% CO_2. Cells were trypsinized, stained with trypan blue to exclude dead cells and counted using hemocytometer. Cell doubling time was calculated using following formulas:

number of cells plated x 2^n = number of cells after 48 or 96 h; where n = number of divisions
cell doubling time = incubation time (h) / number of divisions

5.3.14.6 Cell proliferation assay

For the cell proliferation assays, $5x10^4$ cells were plated in 10 cm cell culture dish in triplicates and cultured in the standard culture media. Every second day for the period of 6 consecutive days, the cells were trypsinized, stained with trypan blue dye for dead cell exclusion, counted using hemocytometer and replated. Triplicates were counted for each cell line and every time point. Proliferation curve was plotted as cell number vs. time.

5.3.14.7 Cell migration assays

Transwell (Boyden Chamber) migration assay

Cell migration was determined using 24-well cell culture plate with 0.8 µm pore size filter inserts (Falcon BD, # 353097). Cells were serum-starved overnight; trypsinized, counted, and $5x10^4$ cells were resuspended in 500 µl of the starvation media and added to the interior of the insert. Conditioned medium from NIH 3T3

fibroblasts was added to the lower chamber as chemoattractant and cells were incubated for 24 h at 37℃ and 5% CO_2 in a tissue culture incubator. For comparison, the same number of control inserts with 0.4 µm pore size (Falcon BD. # 353095) was filled in the same way for proliferation control. After incubation, the cells in the upper chamber were removed with a cotton swab and the cells that had traversed the membrane and attached to the lower surface of the filter were fixed in 4% PFA/PBS and stained with crystal violet (0.5% in 20% methanol). Inserts were washed in distilled H_2O and left to air-dry. Filters were carefully excised from the inserts and mounted onto microscope glass slides. Cell migration was evaluated by counting cells under a phase-contrast microscope (Carl Zeiss, Oberkochen, Germany) at 20X magnification in five random fields per filter. The experiment was carried out in triplicates and repeated three times.

Wound healing assay

Cells were plated in 10 cm Falcon cell culture dishes and allowed to reach confluence. A scratch was introduced to the monolayer using p200 pipette tip, wound region was marked at the bottom of the plate using waterproof marker and the cells were washed two times with PBS to remove all debris and unattached cells. Starvation media was added, images of the wound region were captured immediately under a phase-contrast microscope at 4X magnification at various time points till wound closure. The experiment was carried out in triplicates and repeated two times.

5.3.14.8 Cell Invasion assay

The invasive potential of the cells was evaluated using CHEMICON Cell Invasion Assay Kit (24 well tissue culture plate with 12 cell culture inserts; Chemicon International, Inc.) according to the manufacturer's instructions. Briefly, the cells were trypsinized, counted and resuspended in a serum free media. Equal number of cells ($1.5x10^5$) in 300 µl of serum free media was added to the interior of previously rehydrated inserts of the invasion assay and 500 µl of NIH 3T3 fibroblasts conditioned media was added to the lower chamber as chemoattractant.

For comparison, the same number of control inserts without ECM gel (Falcon BD. # 353095) was filled in the same way for proliferation control. All tests were done in parallel. The cells were incubated for 48 h at 37℃ and 5% CO_2 in a tissue culture incubator. After incubation, non-invading cells and ECM gel was removed from the interior of the inserts with a cotton swab and invasive cells on the lower surface of the membrane were stained by dipping inserts in the staining solution supplied in the kit for 20 min. Inserts were washed in a beaker of water and left to air dry. Quantification was done by dissolving stained cells in 10% acetic acid (200µl/well) followed by colorimetric reading of OD at 560 nm using ELISA plate reader.

5.3.14.9 Inhibitor treatments

For methylase and acetylase inhibitor treatments, $1x10^5$ cells were plated in 6-well cell culture plates and cell culture inserts filters (#353090, 0.4 µm pore size; Falcon, Becton Dickinson, Franklin Lakes, New Jersey, USA) treated in parallel with different concentrations of 5-Aza-CdR and zebularine alone or in combination with trichostatin A (TSA) dissolved in 1xPBS for up to 96h. Following treatment, the cells grown on filters were fixed with 4%PFA/PBS and subjected to immunofluorescentce staining for E-cadherin and the cells grown in cell culture plates were used for RNA preparation.

5.3.14.10 TGF-β1 ELISA

To measure TGF-β1 levels, the cells were grown in 10 cm cell culture dishes to 60-70% confluence, washed three times with PBS and incubated with 5 ml of serum free media for 24-48 h. Conditioned media was collected, centrifuged for 5 min at 1500 rpm to remove cell debris, concentrated and assayed using Quantikine Mouse/Rat/Porcine TGF-β1 Immunoassay Kit (# MB100, BD Bioscineces) according to manufacturer's instructions. Conditioned media from EpRasXT cells - known to produce high levels of TGF-β1-was used as a positive control.

5.3.15 Animal experiments and histological analysis

5.3.15.1 *In vivo* Tumorigenicity Assay

Tumorigenic capacity of EpH4-*fra1* cells was determined by orthotropic injections of the cells into mammary gland fat pads of 6-8 weeks old female NMRI nu/nu atymic mice. Briefly, the cells were washed with PBS, trypsinized, counted and resuspended in PBS. For each injection, $1x10^5$ EpH4-*fra1* cells or their respective control cells was resuspended in 25µl of PBS. The mice were weighted and anesthetised with mixture of Ketamine (5 mg/ml) and Xylazine (0.8 mg/ml) using 0.2 ml/10g body weight administered by intraperitoneal injection. Cell suspension was injected at 2-4 injection sites per mouse by shallow injection into the nipple area and the mice were left on a heating block (37°C) to recover. At least 3 experimental mice per each cell clone were used. Tumor formation was monitored every second day and after 14 days mice were killed by cervical dislocation, tumors were carefully excised without skin, photographed, tumor dimensions and tumor mass was measured and tumors were further processed for histologicaly analysis. Tumor volume was calculated using the formula: $lenght x width^2/2$.

5.3.15.2 Metastasis induction

To evaluate the metastatic potential of the cells, $1.5x10^5$ cells (EpH4 cells and their clones) or $1x10^5$ cells (EpRas and their clones) was injected into the tail vein of 6-8 weeks old female NMRI nu/nu athymic mice (n=4 mice/cell type). The mice were warmed under a light bulb for 15-20 min to cause vasodilatation, immobilized in a restraining device and the cells were injected in a 100 µl volume into the lateral tail vein. Mice were sacrificed 4 weeks post-injection; lungs were dissected, checked macroscopically for metastasis formation, photographed and further processed for histological analysis.

5.3.15.3 Preparation of tissue samples for histological analysis

Tumors and lungs isolated from mice were fixed overnight in 4% PFA/PBS solution followed by dehydration in Tissue-Tek® VIP™ machine (Sakura, SANOVA) and embedded in hot paraffin for histological analysis. Solid paraffin blocks were cut on a microtome (MICROM) and 3-5μM thick serial tissue sections were mounted onto microscopic slides and incubated overnight or for min of 6h in an incubator at 50℃.

5.3.15.4 Immunohistochemical staining procedures

Hematoxylin and eosin staining (H&E):

H&E stainig was performed on paraffin tissue sections under standard conditions, using fully automatic Veristain Gemini System (Histo Com). Slides were mounted with standard coverslips (Menzel-Gläser) using fully automatic Tissue-Tek®GLCTM (Sakura, SANOVA).

Ki67, Fra-1, E-cadherin and Fibronectin staining:

Ki67, Fra-1, E-cadherin and Fibronectin IHC were performed under standard conditions using fully automatic VENTANA Discovery System (Arizona, USA) according to the manufacturer's instructions. The following antibodies were used: Ki67 (rabbit) from Novocastra (dilution 1:1000), Fra-1 (rabbit) from Santaa Cruz (dilution 1:100), E-cadherin (mouse) from Transduction Labs (dilution 1: 1000) and Fibronectin (rabbit) from Sigma (dilution 1:2000). Sections were counterstained for 5 min with hematoxylin. Stained slides were automatically mounted with standard coverslips (Menzel-Gläser) (Tissue-Tek® GLCTM; Sakura, SANOVA).

Statistical analysis:

Data are presented as the mean± s.d. The significance of differences between means was evaluated by the Student's *t*-test. *P*-values ≤0.05 were considered significant. All calculations were done using Microsoft Office Excel program (Microsoft Corp.. Redmond WA. USA).

Quantification of Western blots:

Intensity of bands was calculated using ImageJ program. Intensity of every band was normalised to respective background intensity and loading.

References

Abate, C., Luk, D., Gentz, R., Rauscher III, F. J., and Curran, T. **1990**. Expression and purification of the leucine zipper and DANN-binding domains of Fos and Jun: Both Fos and Jun contact DNA directly. *Proc. Natl. Acad. Sci.* 87: 1032-1036.

Adiseshaiah, P., Lindner, D. J., Kalvakolanu, D. V. and Reddy, S. P. **2007**. FRA-1 proto-oncogene induces lung epithelial cell invasion and anchorage-independent growth *in vitro*, but is insufficient to promote tumor growth *in vivo*. *Cancer Res* 67: 6204-6211.

Aigner, K., Dampier, B., Descovich, L., Mikula, M., Sultan, A., Schreiber, M., Mikulits, W., Brabletz, T., Strand, D., Obrist, P., Sommergruber, W., Schweifer, N., Wernitznig, A., Beug, H., Foisner, R. and Eger, A. **2007**. The transcription factor ZEB1 (δEF1) promotes tumour cell dedifferentiation by repressing master regulators of epithelial polarity. *Oncogene* 26: 6979-6988.

Andersen H., Mahmood, S., Tkach, V., Cohn, M., Kustikova, O., Grigorian, M., Berezin, V., Bock, E., Lukanidin, E. and Tulchinsky E. **2002**. The ability of Fos family members to produce phenotypic changes in epitheloid cells is not directly linked to their transactivation potentials. *Oncogene* 21: 4843-4848.

Angel, P., Imagawa, M., Chiu, R., Stein, B., Imbra, R. J., Rahmsdorf, H. J., Jonat, C., Herrlich, P., and Karin, M. **1987**. Phorbol ester-inducible genes contain a common cis element recognized by a TPA-modulated trans-acting factor. *Cell* 49: 729-739.

Angel, P. and Karin, M. 1991. The role of Jun, Fos and the AP-1 complex in cell proliferation and transformation. *Biochim Biophys Acta* 1072: 129-157.

Artinian, V. and Kvale, P. A. 2004. Cancer and interstitial lung disease. *Curr Opin Pulm Med* 10: 425-434.

Bakin, A. V., Tomlinson, A. K., Bhowmick, N. A., Moses, H. L. and Arteaga, C. L. **2000**. Phosphatidylinositol-3 kinase function is required for TGFbeta-mediated epithelial to mesenchymal transition and cell migration. *J Biol Chem* 275: 36803-36810.

Bakin, A. V. and Curran, T. 1999. Role of DNA 5-methylcytosine transferase in cell transformation by fos. *Science* 283: 387-390.

Bakiri, L., Lallemand, D., Bossy-Wetzel, E. and Yaniv, M. **2000**. Cell cycle dependent variations in c-Jun and JunB phosphorylation: a role in the control of cyclin D1 expression. *EMBO J* 19: 2056-2068.

Bakiri, L., Matsuo, K., Wisniewska, M. B., Wagner, E. F. and Yaniv, M. **2002**. Promoter specificity and biological activity of tethered AP-1 dimers. *Moll Cell Biol* 22: 4952-4964.

Bakiri, L., Takada, Y., Rdolf, M., Eferl, R., Yaniv, M., Wagner, E. F. and Matsuo, K. **2007**. Role of heterodimerization of c-Fos and Fra-1 proteins in osteoclast differentiation. *Bone* 40:867-875.

Bamberger, A-M., Methner, C., Lisboa, B. W., Städtler, C., Schulte, H. M., Löning, T. and Milde-Langosch, K. **1999** Expression pattern of the AP-1 family in breast cancer: association of fosB expression with a well-differentiated, receptor-positive phenotype. *Int J Cancer* 84: 553-558.

Bando, H., Toi, M., Kitada, K. and Koike, M. **2003**. Genes commonly upregulated by hypoxia in human breast cancer cells MCF-7 and MDA-MB-231. *Biomed Pharmacother* 57: 333-340.

Bar-Sagi, D. and Hall, A. 2000. Ras and Rho GTPases: a family reunion. *Cell*. 103: 227-238.

Basbous, J., Chalbos, D., Hipskind, R., Jariel-Encontre, I. and Piechaczyk, M. **2007**. Ubiquitin-independent proteasomal degradation of fra-1 is antagonized by erk1/2 pathway-mediated phosphorylation of a unique C-terminal destabilizer. *Mol Cell Biol* 27: 3936-3950.

Bataller, R. and Brenner, D. A. 2005. Liver fibrosis. *J Clin Invest* 115: 209-218.

Battista, S., de Nigris, F., Fedele, M., Chiappetta, G., S. Scala, S., Vallone D., Pierantoni, G. M., Megar, T., Santoro, M., Viglietto, G., Verde, P. and Fusco, A. **1998**. Increase in AP-1 activity is a general event in thyroid cell transformation in vitro and in vivo, *Oncogene* 17: 377-385.

Batlle. E., Sancho, E., Franci, C., Dominguez, D., Monfar, M., Baulida, J. and Garcia De Herreros, A. **2000**. The transcription factor snail is a repressor of E-cadherin gene expression in epithelial tumour cells. *Nat Cell Biol* 2: 84-89.

Baum, B., Settleman, J., and Quinlan, M. P. **2008**. Transitions between epithelial and mesenchymal states in development and disease. *Seminars in Cell & Developmental Biology* 19: 294-308.

Beavon, I. R. G. 2000. The E-cadherin-catenin complex in tumour metastasis: structure, function and regulation. *Eur J Cancer* 36: 1607-1620.

Behrens, J., Mareel, M. M., Van Roy, F. M. and Birchmeier, W. **1989**. Dissecting tumor cell invasion: epithelial cells acquire invasive properties after the loss of uvomorulin-mediated cell-cell adhesion. *J Cell Biol* 108: 2435-2447.

Behrens, A., Sibilia, M., and Wagner, E.F. **1999**. Amino-terminal phosphorylation of c-Jun regulates stress-induced apoptosis and cellular proliferation. *Nat Genet* 21: 326-329.

Behrens, A., Jochum, W., Sibilia, M. and Wagner, E. F. **2000**. Oncogenic transformation by ras and fos is mediated by c-Jun N-terminal phosphorylation. *Oncogene* 19: 2657-2663.

Behrens, A., Sibilia, M., David, J.P., Mohle-Steinlein, U., Tronche, F., Schutz, G., and Wagner, E.F. **2002**. Impaired postnatal hepatocyte proliferation and liver regeneration in mice lacking c-jun in the liver. *Embo J* 21: 1782-1790.

Behrens, A., Haigh, J., Mechta-Grigoriou, F., Nagy, A., Yaniv, M. and Wagner E. F. **2003**. Impaired intervertebral disc formation in the absence of Jun. *Development* 130: 103-109.

Belguise, K., Kersual, N., Galtier, F. and Chalbos, D. **2005**. FRA-1 expression level regulates proliferation and invasiveness of breast cancer cells. *Oncogene* 24: 1434-1444.

Bender, C. M., Pao, M. M. and Jones, P. A. **1998**. Inhibition of DNA methylation by 5-aza-2'-deoxycytidine suppresses the growth of human tumor cell lines. *Cancer Res* 58: 5-101.

Bergers, G., Graninger, P., Braselmann, S., Wrighton, C. and Busslinger, M. **1995**. Transcriptional activation of the *fra-1* gene by AP-1 is mediated by regulatory sequences in the first intron. *Mol Cell Biol* 15: 3748-3758.

Berx, G., Nollet, F. and van Roy, F. **1998**. Dysregulation of the E-cadherin/catenin complex by irreversible mutations in human carcinomas. *Cell Adhes Commun* 6: 171-184.

Berx, G. and Van Roy, F. 2001. The E-cadherin/catenin complex: an important gatekeeper in breast cancer tumorigenesis and malignant progression. *Breast Cancer Res* 3: 289-293.

Berx, G., Raspe, E., Christofori, G., Thiery, J. P. and Sleeman, J. P. **2007**. Pre-EMTing metastasis? Recapitulation of morphogenetic processes in cancer. *Clin Exp Metastasis* 24: 587-597.

Bhowmick, N.A , Ghiassi, M., Bakin, A., Aakre, M., Lundquist, C. A., Engel, M. E., Arteaga, C. L. and Moses, H. L. **2001**. Transforming growth factor-beta1 mediates epithelial to mesenchymal transdifferentiation through a RhoA-dependent mechanism. *Mol Biol Cell* 12: 27-36.

Birchmeier, W. and Behrens, J. 1994. Cadherin expression in carcinomas: role in the formation of cell junctions and the prevention of invasiveness. *Biochim Biophys Acta* 1198: 11-26.

Bissell, D. M. 2001. Chronic liver injury, TGF-beta, and cancer. *Exp Mol Med* 33: 179-190.

Bolos, V., Peinado, H., Perez-moreno, M. A., Fraga, M. F., Esteller, M. and Cano, A. **2002**. The transcription factor Slug represses E-cadherin expression and induces epithelial to mesenchymal transitions: a comparison with Snail and E47repressors. *J Cell Sci* 116: 499-511.

Boyd, N. F., Dite, G. S., Stone, J., Gunasekara, A., English, D. R., McCredie, M. R., Giles, G. G., Tritchler, D., Chiarelli, A., Yaffe MJ, Hopper JL. **2002**. Heritability of mammographic density, a risk factor for breast cancer. *N Engl J Med* 347: 886-894.

Boyd, N. F., Rommens, J. M., Vogt, K., Lee, V., Hopper, J. L., Yaffe, M. J. and Paterson, A. D. **2005**. Mammographic breast density as an intermediate phenotype for breast cancer. *Lancet Oncol* 6: 798-808.

Bozec, A., Bakiri, L., Hoebertz, A., Eferl, R., Schilling, A. F., Komnenovic, V., Scheuch, H., Priemel, M., Stewart, C. L., Amling, M. and Wagner, E. F. **2008**. Osteoclast size is controlled by Fra-2 through LIF/LIF-receptor signalling and hypoxia. *Nature* 454: 221-226.

Brown, P. H., Alani, R., Pries, L. H., Szabo, E. and Birrer, M. J. **1993**. Suppression of oncogene-induced transformation by a deletion mutant of c-jun. *Oncogene* 8: 877-886.

Brown, J. R., Ye, H., Bronson, R. T., Dikkes, P. and Greenberg, M. E. **1996**. A defect in nurturing in mice lacking the immediate early gene fosB. *Cell* 86:297-309.

Brown, J. R., Nigh, E., Lee, R. J., Ye, H., Thompson, M. A., Saudou, F., Pestell, R. G. and Greenberg, M. E. **1998**. Fos family members induce cell cycle entry by activating cyclin D1. *Mol. Cell. Biol* 18: 5609-5619.

Brüsselbach, S., Möhle-Steinlein, U., Wang, Z-Q., Schreiber, M., Lucibello, F. C., Müller, R. and Wagner, E. F. **1995**. Cell proliferation and cell cycle progression are not impaired in fibroblasts and ES cells lacking c-Fos. *Oncogene* 10: 79-86.

Cano, A., Perez-Moreno, M. A., Rodrigo, I., Locascio, A., Blanco, M. J., del Barrio, M. G., Portillo, F. and Nieto, M. A. **2000**. The transcription factor snail controls epithelial-mesenchymal transitions by repressing E-cadherin expression. *Nat Cell Biol* 2: 76-83.

Carrozza, M.L., Jacobs, H., Acton, D., Verma, I. and Berns, A. **1997**. Overexpression of the FosB2 gene in thymocytes causes abberant development of T cells and thymic epithelial cells. *Oncogene* 14: 1083-1091.

Casalino, L., De Cesare, D. and Verde, P. **2003**. Accumulation of Fra-1 in ras-transformed cells depends on both transcriptional autoregulation and MEK.dependent posttranslational stabilization. *Mol Cell Biol* 12: 4401-4415.

Casalino, L., Bakiri, L., Talotta, F., Weitzman, J. B., Fusco, A., Yaniv, M. And Verde P. **2007**. Fra-1 promotes growth and survival in RAS-transformed thyroid cells by controlling cyclin A transcription. *EMBO J* 26: 1878-1890.

Cavalieri, F., Ruscio, T., Tinoco, R., Benedict, S., Davis, C., and Vogt, P.K. **1985**. Isolation of three new avian sarcoma viruses: ASV 9, ASV 17, and ASV 25. *Virology* 143: 680-683.

Cavallaro, U. and Christofori, G. 2004. Cell adhesion and signalling by cadherins and Ig-CAMs in cancer. *Nature Rev Cancer* 4: 118-132.

Chalmers, C.J., Gilley, R., March, H. N., Balmanno, K. and Cook, S. J. **2007**. The duration of ERK1/2 activity determines the activation of c-Fos and Fra-1 and the composition and quantitative transcriptional output of AP-1. *Cell Signal* 19: 695-704.

Chen, L., O'Bryan, J. P., Smith, H. S. and Liu, E. **1990**. Overexpression of matrix Gla protein mRNA in malignant human breast cells: isolation by differential c-DNA hybridization. *Oncogene* 5: 1391-1395.

Cheng, J. C., Yoo, C. B., Weisenberger, D. J., Chuang, J., Wozniak, C., Liaang, G., Marquez, V. E., Greer, S., Orntoft, T. F., Thykjaer, T. and Jones, P. A. **2004**. Preferential response of cancer cells to zebularine. *Cancer Cell* 6: 151-158.

Chiappetta, G., Tallini, G., De Biasio, M. C., Pentimalli, F., de Nigris, F., Losito, S., Fedele, M., Battista, S., Verde, P., Santoro, M. and Fusco, A. **2000**. FRA-1 expression in hyperplastic and neoplastic thyroid disease. *Clin Cancer Res* 6: 4300-4307.

Chiappetta, G., Ferraro, A., Botti, G., Monaco, M., Pasquinelli, R., Vuttariello, E., Arnaldi, L., Di Bonito, M., D'Aiuto, G., Pierantoni, G. M. and Fusco, A. **2007**. FRA-1 protein overexpression is a feature of hyperplastic and neoplastic breast disorders. *BMC Cancer* 7: 1-11.

Chinenov, Y. and Kerppola, T.K. 2001. Close encounters of many kinds: Fos-Jun interactions that mediate transcription regulatory specificity. *Oncogene* 20: 2438-2452.

Christiansen, J. J. and Rajasekaran, A. K. 2006. Reassessing epithelial to mesenchymal transition as a prerequisite for carcinoma invasion and metastasis. *Cancer Res* 66: 8319- 8326.

Christofori, G. 2006. New signals from invasive front. *Nature* 441: 444-450.

Cohen, D.R. and Curran, T. 1988. fra-1: a serum-inducible, cellular immediate early gene that encodes a fos-related antigen. *Mol Cell Biol* 8: 2063-2069.

Cohen, D. R., Ferreira, P. C., Gentz, R., Franza Jr., B. R. and Curran, T. **1989**. The product of a fos-related gene, fra-1, binds cooperatively to the AP-1 site with Jun: transcription factor AP-1 is comprised of multiple protein complexes. *Genes Dev* 3: 173-184.

Comb, M., Birnberg, N.C., Seasholtz, A., Herbert, E., and Goodman, H.M. **1986**. A cyclic AMP- and phorbol ester-inducible DNA element. *Nature* 323: 353-356.

Comijn, J., Berx, G., Vermassen, P., Verschueren, K., Van Grunsven, L., Bruyneel, E., Mareel, M., Huylebroeck, D. and Van Roy, F. **2001**. The two-handed E box binding zinc-finger protein Sip1 downregulates E-cadherin and induces invasion. *Moll Cell* 7: 1267-1278.

Condeelis, J. and Seegal, J. E. 2003. Intravital imaging of cell movement in tumors. *Nat Rev Cancer* 3: 921-930.

Connaci-Sorrell, M., Zhurinsky, J. and Ben-Ze'ev, A. **2002**. The cadherin-catenin adhesion system in signalling and cancer. *J Clin Investig* 109: 987-991.

Curran, T. and Teich, N.M. 1982b. Identification of a 39,000-dalton protein in cells transformed by the FBJ murine osteosarcoma virus. *Virology* 116: 221-235.

Curran, T., Peters, G., Van Beveren, C., Teich, N.M., and Verma, I.M. **1982**. FBJ murine osteosarcoma virus: identification and molecular cloning of biologically active proviral DNA. *J Virol* 44: 674-682.

Daniels, C. E. and Jett, J. R. 2005. Does interstitial lung disease predispose to lung cancer? *Curr Opin Pulm Med* 11:431-437.

Debinski, W. and Gibo, D. M. 2005. Fos-related antigen 1 modulates malignant features of glioma cells. *Mol Cancer Res* 3: 237-249.

De Cesare, D., Vallone, D., Caracciolo, A., Sassone-Corsi, P., Nerlov, C. and Verde, P. **1995**. Heterodimerization of c-Jun with ATF-2 and C-Fos is required for positive and negative regulation of the human urokinase enhancer. *Oncogene* 11: 365-376.

Derycke, L. D. M. and Bracke, M. E. 2004. N-cadherin in the spotlight of cell-cell adhesion, differentiation, embryogenesis, invasion and signalling. *Int J Dev Biol* 48: 463-476.

Derynck, R., Zhang, Y. and Feng, X. H. **1998**. Smads: transcriptional activators of TGF-beta responses. *Cell* 95: 737-740.

De Wever, O., Pauwels, P., De Craene, B., Sabbah, M., Emami, S., Redeuilh, G., Gespach, C., Bracke, M. and Berx, G. **2008**. Molecular and pathological signatures of Epithelial-mesenchymal transitions at the cancer invasion front. *Histochem Cell Biol* 130: 481-494.

Di Croce, L. and Pelicci, P. 2003. Tumour-associated hypermethylation: silencing E-cadherin expression enhances invasion and metastasis. *Eur J Cancer* 39: 413-414.

Doehn, U., Hauge, C., Frank, S. R., Jensen, C. J., Duda, K., Nielsen, J. V., Cohen, M. S., Johansen, J. V., Winther, B. R., Lund, L. R., Winther, O., Taunton, J., Hansen, S. H. and Frödin, M. **2009**. RSK is a principal effector of the RAS-ERK Pathway for

eliciting a coordinate promotile/invasive gene program and phenotype in epithelial cells. *Mol Cell* 35: 511-522.

Duband, J.L., Monier, F., Delannet, M., and Newgreen, D. **1995**. Epithelium-mesenchyme transition during neural crest development. *Acta Anat*. (Basel) 154: 63-78.

Durchdewald, M., Guinea-Viniegra, J., Haag, D., Riehl, A., Lichter, P., Hahn, M., Wagner, E. F., Angel, P. and Hess, J. **2008**. Podoplanin is a novel Fos target gene in skin carcinogenesis. *Cancer Res* 68: 6877-6883.

Eferl, R., Sibilia, M., Hilberg, F., Fuchsbichler, A., Kufferath, I., Guertl, B., Zenz, R., Wagner, E.F., and Zatloukal, K. **1999**. Functions of c-Jun in liver and heart development. *J Cell Biol* 145: 1049-1061.

Eferl, R. and Wagner, E.F. 2003. AP-1: a double-edged sword in tumorigenesis. *Nat Rev Cancer* 3: 859-868.

Eferl, R., Hoebertz, A., Schilling, A.F., Rath, M., Karreth, F., Kenner, L., Amling, M., and Wagner, E.F. **2004.** The Fos-related antigen Fra-1 is an activator of bone matrix formation. *Embo J* 23: 2789-2799.

Eferl, R., Zenz, R., Theussl, H.C. and Wagner, E. F. **2007**. Simultaneous generation of fra-2 conditional and fra-2 knock-out mice. *Genesis* 45:447-451.

Eferl, R., Hasselblatt, P., Rath, M., Popper, H., Zenz, R., Komnenovic, V., Idarraga, M-H., Kenner, L. and Wagner, E. F. **2008**. Development of pulmonary fibrosis through a pathway involving the transcription factor Fra-2/AP-1. *PNAS* 105: 10525-10530.

Egeblad, M. and Werb, Z. 2002. New functions for the matrix metalloproteinases in cancer progression. *Nature Rev Cancer* 2: 161-174.

Eger, A., Stockinger, A., Schaffhauser, B., Beug, H., and Foisner, R. **2000**. Epithelial mesenchymal transition by c-Fos estrogen receptor activation involves nuclear translocation of beta-catenin and upregulation of beta-catenin/lymphoid enhancer binding factor-1 transcriptional activity. *J Cell Biol* 148: 173-188.

Eger, A., Aigner, K., Sonderegger, S., Dampier, B., Oehler, S., Schreiber, M., Berx, G., Cano, A., Beug, H., and Foisner, R. **2005**. DeltaEF1 is a transcriptional repressor of E-cadherin and regulates epithelial plasticity in breast cancer cells. *Oncogene* 24: 2375-2385.

Etienne-Manneville, S. and Hall, A. 2002. Rho GTPases in cell biology. *Nature*. 420: 629-635.

Fantozzi, and Christofori, G. 2006. Mouse models of breast cancer metastasis. *Breast Cancer Res* 8(4):212

Fialka, I., Schwarz, H., Reichmann, E., Oft, M., Busslinger, M. and Beug, H. **1996**. The Estrogen-dependent c-JunER protein causes a reversible loss of mammary epithelial cell polarity involving a destabilization of adherens junctions. *J Cell Biol* 132: 1115-1132.

Fleischmann, A. 2000. ***Dissertation***: Genetic analysis of Fos proteins in mice and the role of EGFR signalling during skin tumor development. *Research Institute of Molecular Pathology and Universität Wien*.

Fleischmann, A., Hafezi, F., Elliott, C., Reme, C.E., Ruther, U., and Wagner, E.F. **2000**. Fra-1 replaces c-Fos-dependent functions in mice. *Genes Dev* 14: 2695-2700.

Fleischmann, A., Hvalby, O., Jensen, V., Strekalova, T., Zacher, C., Layer, L. E., Kvello, A., Reschke, M., Spanagel, R., Sprengel, R., Wagner, E. F. and Gass, P. **2003a**. Impaired long-term memory and NR2A-type NMDA receptor-dependent synaptic plasticity in mice lacking c-Fos in the CNS. *J Neurosci* 23: 9116-9122.

Fleischmann, A., Jochum, W., Eferl, R., Witowsky, J., and Wagner, E.F. **2003b**. Rhabdomyosarcoma development in mice lacking Trp53 and Fos: tumor suppression by the Fos protooncogene. *Cancer Cell* 4: 477-482.

Florin, L., Knebel, J., Zigrino, P., Vonderstrass, B., Mauch, C., Schorpp-Kistner, M., Szabowski, A. and Angel, P. **2006**. Delayed wound healing and epidermal hyperproliferation in mice lacking JunB in the skin. *J Invest Dermatol* 126: 902-911.

Foletta, V.C., Sonobe, M.H., Suzuki, T., Endo, T., Iba, H., and Cohen, D.R. **1994**. Cloning and characterisation of the mouse fra-2 gene. *Oncogene* 9: 3305-3311.

Framson, P.E. and Sage, E. H. 2004. SPARC and tumor growth: where the seed meets the soil? *J Cell Biochem* 92: 679-90.

Funk, M., Poensgen, B., Graulich, W., Jerome, V., and Muller, R. **1997**. A novel, transformation-relevant activation domain in Fos proteins. *Mol Cell Biol* 17: 537-544.

Gass, P., Fleischmann, A., Hvalby, O., Jensen, V., Zacher, C., Strekalova, T., Kvello, A., Wagner, E. F. and Sprengel, R. **2004**. Mice with a fra-1 knock-in into the c-fos locus show impaired spatial but regular contextual learning and normal LTP. *Mol Brain Res* 130: 16-22.

Gerdes, M. J., Myakishev, M., Frost, N. A., Rishi, V., Moitra, J., Acharya, A., Levy, M. R., Park, S-W., Glick, A., Yuspa, S. H. and Vinson, C. **2006**. Activator protein-1 activity regulates epithelial tumor cell identity.*Cancer Res* 66: 7578-7588.

Getsios, S., Huen, A. C. and Green, K. J. **2004**. Working out the strength and flexibility of desmosomes. *Nat Rev Mol Cell Biol* 5: 271-281.

Giancotti, V. 2006. Breast cancer markers. *Cancer Letters* 243:145-159.

Glover, J.N. and Harrison, S.C. 1995. Crystal structure of the heterodimeric bZIP transcription factor c-Fos-c-Jun bound to DNA. *Nature* 373: 257-261.

Graff, J. R., Herman, J. G., Lapidus, R. G., Chopra, H., Xu, R., Jarrad, D. F., Isaacs, W. B., Pitha, P. M., Davidson, N. E. and Baylin, S. B. **1995**. E-cadherin expression is silenced by DNA hypermethylation in human breast and prostate carcinomas. *Cancer Res* 55: 5195-5199.

Graff, J. R., Gabrielson, E., Fujii, H., Baylin, S. B. and Herman, J. G. **2000**. Methylation patterns of the E-cadherin 5'CpG island are unstable and reflect the dynamic, heterogeneous loss of E-cadherin expression during metastatic progression. *J Biol Chem* 275: 2727-2732.

Grigoriadis, A. E., Schellander, K., Wang, Z. Q. and Wagner, E. F. **1993**. Osteoblasts are target cells for transformation in c-fos transgenic mice. *J Cell Biol* 122: 685-701.

Grigoriadis, A. E., Wang, Z. Q., Cecchini, M. G., Hofstetter, W., Felix, R., Fleisch, H. A. and Wagner, E. F. **1994**. c-Fos: a key regulator of osteoclast-macrophage lineage determination and bone remodeling. *Science* 266: 443-448.

Grooteclaes, M. L. and Frisch, S. M. 2000. Evidence for a function of CtBP in epithelial gene regulation and anoikis. *Oncogene* 19: 3823-3828.

Gruda, M. C., Kovary, K., Metz, R. and Bravo, R. **1994**. Regulation of Fra-1 and Fra-2 phosphorylation differs during the cell cycle of fibroblasts and phosphorylation in vitro by MAP kinase affects DNA binding activity. *Oncogene* 9: 2537-2547.

Gruda, M.C., van Amsterdam, J., Rizzo, C.A., Durham, S.K., Lira, S., and Bravo, R. **1996**. Expression of FosB during mouse development: normal development of FosB knockout mice. *Oncogene* 12: 2177-2185.

Grunert, S., Jechlinger, M., and Beug, H. **2003**. Diverse cellular and molecular mechanisms contribute to epithelial plasticity and metastasis. *Nat Rev Mol Cell Biol* 4: 657-665.

Guarino, M. 2007. Epithelial-masenchymal transition and tumour invasion. *Int J Biochem Cell Biol* 39: 2153-2160.

Guerra, C., Mijimolle, N., Dhawahir, A., Dubus, P., Barradas, M., Serrano, M., Campuzano, V. and Barbacid, M. **2003**. Tumor induction by an endogenous K-ras oncogene is highly dependent on cellular context. *Cacer Cell* 4: 111-120.

Hai, T. and Curran, T. 1991. Cross-family dimerization of transcription factors Fos/Jun and ATF/CREB alters DNA binding specificity. *Proc Natl Acad Sci U S A* 88: 3720-3724.

Hajra, K. M. and Fearon, E. R. 2002a. Cadherin and catenin alternations in human cancer. *Genes Chromosomes Cancer* 34: 255-268.

Hajra, K. M., Chen, D. Y-S. and Fearon, E. R. **2002b**. The SLUG tinc-finger protein represses E-cadherin in breast cancer. *Cancer Res* 62: 1613-1618.

Hall, A. 1998. Rho GTPases and the actin cytoskeleton. *Science*. 279: 509-514.

Hasselblatt, P., Gresh, L., Kudo, H., Guinea-Viniehra, J. and Wagner, E. F. **2008**. The role of the transcription factor AP-1 in colitis-associated and β-catenin-dependent intestinal tumorigenesis in mice. *Oncogene* 27: 6102-6109.

Hay ED. 2005. The mesenchymal cell, its role in the embryo, and the remarkable signaling mechanisms that create it*. Dev Dyn* 233: 706-720.

Herman, J. G., Merlo, A., Mao, L., Lapidus, R. G., Issa, J. P. J., Davidson, N. E., Sidransky, D. and Baylin, S. B. **1995**. Inactivation of the CDKN2/p16/mts-1 gene is frequently associated with aberrant DNA methylation in all common human cancers. *Cancer Res* 55: 4525-4530.

Hess, J., Angel, P. and Schorpp-Kistner, M. **2004.** AP-1 subunits: quarrel and harmony among siblings. *J Cell Sci* 117: 5965-5973.

Hilberg, F., Aguzzi, A., Howells, N., and Wagner, E.F. **1993**. c-jun is essential for normal mouse development and hepatogenesis. *Nature* 365: 179-181.

Hill, C. S. and Treisman, R. 1995. Transcriptional regulation by extracellular signals: mechanisms and specificity. *Cell* 80: 199-211.

Hirai, S.I., Ryseck, R.P., Mechta, F., Bravo, R., and Yaniv, M. **1989**. Characterization of junD: a new member of the jun proto-oncogene family. *Embo J 8*: 1433-1439.

Hirohashi, S. 1998. Inactivation of the E-cadherin-mediated cell adhesion system in human cancers. *Am J Pathol* 153: 333-339.

Hoffman, E., Thiefes, A., Buhrow, D., Dittrich-Breiholz, O., Schneider, H., Resch, K. and Krach, M. **2005**. MEK1-dependent delayed expression of Fos-related antigen-1 counteracts c-Fos and p65 NF-κB-mediated Interleukin-8 transcription in response to cytokines or growth factors. *J Biol Chem* 280: 9706-9718.

Hofmann, M., Rudy, W., Gunthert, U., Zimmer, S., Zawadzki, V., Zoller, M., Lichtner, R., Herrlich, P. and Ponta, H. **1993**. A link between ras and metastatic behaviour of tumor cells: ras induces CD44 promoter activity and leads to low-level expression of metastasis-specific variants of CD44 in CREF cells. *Cancer Res* 53: 1516-1521.

Huber, M. A., Kraut, N., and Beug, H. **2005**. Molecular Requirements for Epithelial-Mesenchymal Transition During Tumor Progression. *Curr Opin Cell Biol* 17: 548-558.

Hugo, H., Ackland, M. L., Blick, T., Lawrence, M. G., Clements, J. A., Williams, E. D. and Thompson, E. W. **2007**. Epithelial-mesenchymal and mesenchymal-epithelial transitions in carcinoma progression. *J Cell Physiol* 213: 374-383.

Hulboy, D. L., Matrisian, L. M. and Crawford, H. C. **2001**. Loss of JunB activity enhances stromelysin 1 expression in a model of the epithelial-to-mesenchymal transition of mouse skin tumors. *Mol Cell Biol* 21: 5478-5487.

Hurd, T. W., Culbert, A. A., Webster, K. J. and Tavare, J. M. **2002**. Dual role for mitogen-activated protein kinase (Erk) in insulin-dependent regulation of Fra-1 (fos-related antigen-1) transcription and phosphorylation. *Biochem J* 368: 573-580.

Iwano, M., D. Plieth, T.M. Danoff, C. Xue, H. Okada, and E.G. Neilson. **2002**. Evidence that fibroblasts derive from epithelium during tissue fibrosis. *J Clin Invest* 110: 341-350.

Jackson, E. L., Willis, N., Mercer, K., Bronson, R. T., Crowely, D., Montoya, R., Jacks, T. and Tuveson, D. A. **2001**. Analysis of lung tumor initiation and progression using conditional expression of oncogenic K-ras. *Genes Dev* 15: 3243-3248.

Jackson, E. L., Olive, K. P., Tuveson, D. A., Bronson, R. T., Crowely, D., Brown, M. and Jacks, T. **2005**. The differential effects of mutant p53 alleles on advanced murine lung cancer. *Cancer Res* 65: 10280-10288.

Janda, E., Lehmann, K., Killisch, I., Jechlinger, M., Herzig, M., Downward, J., Beug, H., and Grunert, S. **2002**. Ras and TGF[beta] cooperatively regulate epithelial cell plasticity and metastasis: dissection of Ras signaling pathways. *J Cell Biol 156*: 299-313.

Jechlinger, M., Grunert, S., and Beug, H. **2002**. Mechanisms in epithelial plasticity and metastasis: insights from 3D cultures and expression profiling. *J Mammary Gland Biol Neoplasia* 7: 415-432.

Jechlinger, M., Grunert, S., Tamir, I. H., Janda, E., Ludemann, S., Waerner, T., Seither, P., Weith, A., Beug, H. and Kraut, N. **2003**. Expression profiling of epithelial plasticity in tumor progression. *Oncogene* 22: 7155-7169.

Jechlinger, M., Sommer, A., Moriggl, R., Seither, P., Kraut, N., Capodiecci, P., Donovan, M., Cordon-Cardo, C., Beug, H., and Grunert, S. **2006**. Autocrine PDGFR signaling promotes mammary cancer metastasis. *J Clin Invest* 116: 1561-1570.

Jenuwein, T. and Muller, R. 1987. Structure-function analysis of fos protein: a single amino acid change activates the immortalizing potential of v-fos. *Cell* 48: 647-657.

Jochum, W., David, J.P., Elliott, C., Wutz, A., Plenk, H., Jr., Matsuo, K., and Wagner, E.F. **2000**. Increased bone formation and osteosclerosis in mice overexpressing the transcription factor Fra-1. *Nat Med* 6: 980-984.

Jochum, W., Passegue, E., and Wagner, E.F. **2001**. AP-1 in mouse development and tumorigenesis. *Oncogene* 20: 2401-2412.

Johnson, R.S., Spiegelman, B.M., and Papaioannou, V. **1992**. Pleiotropic effects of a null mutation in the c-fos proto-oncogene. *Cell* 71: 577-586.

Johnson, R., Spiegelman, B., Hanahan, D., and Wisdom, R. **1996**. Cellular transformation and malignancy induced by ras require c-jun. *Mol Cell Biol* 16: 4504-4511.

Jooss, K.U., Funk, M., and Muller, R. **1994**. An autonomous N-terminal transactivation domain in Fos protein plays a crucial role in transformation. *Embo J* 13: 1467-1475.

Kalluri, R., and E.G. Neilson. 2003. Epithelial-mesenchymal transition and its implications for fibrosis. *J Clin Invest* 112: 1776-1784.

Karin, M. 1995. The regulation of AP-1 activity by mitogen-activated protein kinases. *J Biol Chem* 270: 16483-16486.

Karreth, F., Hoebertz, A., Scheuch, H., Eferl, R., and Wagner, E.F. **2004**. The AP1 transcription factor Fra2 is required for efficient cartilage development. *Development* 131: 5717-5725.

Keirseblick, A., Bonne, S., Staes, K., van Hengel, J., Nollet, F., Reynolds, A., and van Roy, F. **1998**. Molecular cloning of the human p120ctn catenin gene (CTNND1): expression of multiple alternatively spliced isoforms. *Genomics* 50: 129-146.

Kenner, L., Hoebertz, A., Beil, T., Keon, N., Karreth, F., Eferl, R., Scheuch, H., Szremska, A., Amling, M., Schorpp-Kistner, M., Angel, P., and Wagner, E.F. **2004**. Mice lacking JunB are osteopenic due to cell-autonomous osteoblast and osteoclast defects. *J Cell Biol* 164: 613-623.

Kerppola, T. K. and Curran, T. 1991. Transcription factor interactions: basics on zippers. *Curr Opin Struct Biol* 1: 71-79.

Kerppola, T. K. and Curran, T. 1994. A conserved region adjacent to the basic domain is required for recognition of an extended DNA binding site by Maf/Nrl family proteins. Oncogene 9: 3149-3158.

Kim, K.K., Kugler, M.C., Wolters, P.J., Robillard, L., Galvez, M.G., Brumwell, A. N., Sheppard, D. and Chapman, H. A. **2006**. Alveolar epithelial cell mesenchymal transition develops in vivo during pulmonary fibrosis and is regulated by the extracellular matrix. *Proc Natl Acad Sci USA* 103:13180-13185.

Kisseleva, T. and Brenner, D. A. 2008. Mechanisms of Fibrogenesis. *Exp Biol Med* 233: 109-122.

Kockel, L., Homsy, J.G., and Bohmann, D. **2001**. Drosophila AP-1: lessons from an invertebrate. *Oncogene* 20: 2347-2364.

Koizume, S., Tachibana, K., Sekiya, T., Hirohashi, S. and Shiraishi, M. **2002**. Heterogeneity in the modification and involvement of chromatin components of the CpG island of the silenced human *CDH1* gene in cancer cells. *Nucleic Acid Research* 30: 4770-4780.

Kuphal, F. and Behrens, J. 2006. E-cadherin modulates Wnt-dependent transcription in colorectal cancer cells but does not alter Wnt-independent gene expression in fibroblasts. *Experimental Cell Research* 312: 457-467.

Kustikova, O., Kramerrov, D., Grigorian, M., Berezin, V., Bock, E., Lukanidin, E. and Tulchinsky, E. **1998**. Fra-1 induces morphological transformation and increases in vitro invasiveness and motility of epithelioid adenocarcinoma cells. *Mol Cell Biol* 18: 7095-7105.

Lagamba, D., Nawshad, A. and Hay, E. D. **2005**. Microarray analysis of gene expression during epithelial-mesenchymal transformation. *Dev Dyn* 234: 132-42.

Lamb, R., Hennigan, R., Turnbull, K., Katsanakis, K., MacKenzie, E., Birnie, G., and Ozanne, B. **1997**. AP-1 mediated invasion requires increased expression of the hyaluronan receptor CD44. *Mol Cell Biol 17:* 963-976.

Landschulz, W.H., Johnson, P.F. and McKnight, S.L. **1988**. The leucine zipper: a hypothetical structure common to a new class of DNA binding proteins. *Science* 240: 1759-1764.

Lee, J. M., Dedhar, S., Kalluri, R., and Thompson E. W. **2006**. The epithelial-mesenchymal transition: new insights in signaling, development, and disease. *J Cell Biol* 172: 973-981.

Lee H. Y., Chaudhary, J., Walsh, G., Hong, W. and Kurie, J. **1998**. Supression of c-Fos gene transcription with malignant transformation of human bronchial epithelial cells. *Oncogene*, 16: 3039-3048.

Lee, W., Haslinger, A., Karin, M., and Tjian, R. **1987a**. Activation of transcription by two factors that bind promoter and enhancer sequences of the human metallothionein gene and SV40. *Nature* 325: 368-372.

Lee, W., Mitchell, P., and Tjian, R. **1987b**. Purified transcription factor AP-1 interacts with TPA-inducible enhancer elements. *Cell* 49: 741-752.

Lehmann, K., Janda, E., Pierreux, C. E., Rytomaa, M., Schulze, A., McMahon, M., Hill, C. S., Beug, H. and Downward, J. **2000**. Raf induces TGFβ production while blocking its apoptotic but not invasive responses: a mechanism leading to increased malignancy in epithelial cells. *Genes Dev* 14: 2610-2622.

Levayer, R. and Lecuit, T. 2008. Breaking down EMT. *Nature Cell Biol* 10: 757-759.

Lewis, T. S., Shapiro, P. S. and Ahn, N. G. **1998**. Signal transduction through MAP kinase cascades. *Adv Cancer Res* 74: 49- 139.

Luo, Y., Zhou, H., Mizutani, M., Mizutani, N., Reisfeld, R. A. and Xiang, R. **2003**. Transcription factor Fos-related antigen 1 is an effective target for breast cancer vaccine. *Proc Natl Acad Sci U S A* 100: 8850-8855.

Luo, Y., Zhou, H., Mizutani, M., Mizutani, N., Liu, C., Xiang, R. and Reisfeld, R. A. **2005**. A DNA vaccine targeting Fos-related antigen 1 enhanced by IL-18 induces long-lived T-cell memory against tumor recurrence. *Cancer Res* 65: 3419-3427.

Maki, Y., Bos, T.J., Davis, C., Starbuck, M., and Vogt, P.K. **1987**. Avian sarcoma virus 17 carries the jun oncogene. *Proc Natl Acad Sci U S A* 84: 2848-2852.

Mangone, F.R., Brentani, M.M., Nonogaki, S., Begnami, M.D., Campos, A.H., Walder, F., Carvalho, M.B., Soares, F.A., Torloni, H., Kowalski, L.P., Federico, M.H.,

2005. Overexpression of Fos-related antigen-1 in head and neck squamous cell carcinoma. Int J Exp Pathol 86: 205-212.

Maretzky, T., Reiss, K., Ludwig, A., Bucholz, J., Scholz, F., Proksch, E., de Strooper, B., Hartmann, D. and Saftig, P. **2005**. ADAM10 mediates E-cadherin shedding and regulates epithelial cell-cell adhesion, migration and β-catenin translocation. *PNAS* 26: 9182-9187.

Matsuo, K., Owens, J.M., Tonko, M., Elliott, C., Chambers, T.J., and Wagner, E.F. **2000**. Fosl1 is a transcriptional target of c-Fos during osteoclast differentiation. *Nat Genet* 24: 184-187.

McCawley, L. J. and Matrisian,L. M. 2001. Matrix metalloproteinases: they're not just for matrix anymore! *Curr Opin Cell Biol* 15: 534-540.

Mechta, F., Lallemand, D., Pfarr, C. M. and Yaniv, M. 1997. Transformation by ras modifies AP1 composition and activity. *Oncogene* 14: 837-847.

Mechta-Grigoriou, F., Gerald, D., and Yaniv, M. **2001**. The mammalian Jun proteins: redundancy and specificity. *Oncogene* 20: 2378-2389.

Meixner, A., Zenz, R., Schonthaler, H. B., Kenner, L., Scheuch, H., Penninger, J. M. and Wagner, E. F. **2008**. Epidermal JunB represses G-CSF transcription and affects haematopoieis and bone formation. *Nat Cell Biol* 8: 1003-1011.

Mejlvang, J., Kriajevska, M., Berditchevski, F., Bronstein, I., Lukanidin, E. M., Pringle, J. H., Mellon, J. K. and Tulchinsky, E. M. **2007**. Characterization of E-cadherin-dependent and –independent events in a new model of c-Fos-mediated epithelial-mesenchymal transition. *Exp Cell Res* 313: 380-393.

Merlo, A., Herman, J. G., Mao, L., Lee, D. J., Gabrielson, E., Burger, P. C., Baylin, S. B. and Sidransky, D. **1995**. 5'-CpG-island methylation is associated with transcriptional silencing of the tumor suppressor p16/CDKN2/MTS1 in human cancers. *Nat Med* 1:682-692.

Miettinen PJ, Ebner R, Lopez AR and Derynck R. **1994**. TGF-beta induced transdifferentiation of mammary epithelial cells to mesenchymal cells: involvement of type I receptors. *J Cell Biol* 127: 2021-2036.

Milde-Langosch, K., Röder, H., Andritzky, B., Aslan, B., Hemminger, G., Brinkmann, A., Bamberger, C. M., Löning, T. and Bamberger A-M. **2004**. The role of the AP-1 transcription factors c-Fos, FosB, Fra-1 and Fra-2 in the invasion process of mammary carcinomas. *Breast Cancer Res Treat* 86: 139-152.

Milde-Langosch K. 2005. The Fos family of transcription factors and their role in tumourigenesis. *E J Cancer* 41: 2449-2461.

Milde-Langosch, K., Janke, S., Wagner, I., Schröder, C., Streichert, T., Bamberger, A-M., Jänicke, F. and Löning, T. **2008**. Role of Fra-2 in breast cancer: influence on tumor cell invasion and motility. *Breast Cancer Res Treat* 107: 337-347.

Miller, A. D., Curran, T. and Verma, I. M. **1984**. c-fos protein can induce cellular transformation: a novel mechanism of activation of a cellular oncogene. *Cell* 36: 51-60.

Miyoshi, J. and Takai, Y. 2005. Molecular perspective on tight-junction assembly and epithelial polarity. *Adv Drug Deliv Rev* 57: 815-855.

Mo, Y.-Y. and Reynolds, A. B. 1996. Identification of murine p120cas isoforms and heterogeneous expression of p120cas isoform in human tumor cell lines. *Cancer Res* 56: 2633-2640.

Moreno-Bueno, G., Portillo, F. and Cano, A. **2008**. Transcriptional regulation of cell polarity in EMT and cancer. *Oncogene* 27: 6958-6969.

Moustakas, A. and Heldin, C-H. 2007. Signaling networks guiding epithelial-mesenchymal transitions during embryogenesis and cancer progression. *Cancer Sci* 98: 1513-1520.

Muller, A., Homey, B., Soto, H., Ge, N., Catron, D., Buchanan, M. E., McClanahan, T., Murphy, E., Yuan, W., Wagner, S. N., Barrera, J. L., Mohar. A., Verastegui, E. and Zlotnik, A. **2001**. Involvement of chemokine receptors in breast cancer metastasis. *Nature* 410: 50-56.

Mumberg, D., Lucibello, F. C., Schuermann, M. and Muller, R. **1991**. Alternative splicing of fosB transcripts results in differentially expressed mRNAs encoding functionally antagonistic proteins. *Genes Dev* 5: 1212-1223.

Murakami, M., Sonobe, M., Ul, M., Kabuyama, Y., Watanabe, H., Wada, T., Handa, H. and Iba, H. **1997**. Phosphorylation and high level expression of Fra-2 in *v-src* transformed cells: a pathway of activation of endogenous AP-1. *Oncogene* 14: 2435-2444.

Nakabeppu, Y. and Nathans, D. 1991. A naturally ocuring truncated form of FosB that inhibits Fos/Jun transcriptional activity. *Cell* 64: 751-759.

Nawshad, A., LaGamba, D. and Hay, E. D. **2004**. Transforming growth factor β (TGFβ) signalling in palatal growth, apoptosis and epithelial mesenchymal transformation (EMT). *Arch Oral Biol* 49: 675–89.

Nelles, L., Van de Putte, T., van Grunsven, L., Huylebroeck, D. and Verschueren, K. **2003**. Organization of the mouse *Zfhx1b* gene encoding the two-handed zinc finger Smad-interacting protein-1. *Genomics* 82: 460-469.

Nieto, M.A. 2002. The snail superfamily of zinc-finger transcription factors. *Nat Rev Mol Cell Biol* 3: 155-166.

Nieto, M. A. 2008. Epithelial-mesenchymal transitions in development and disease: old views and new perspectives. *Int J Dev Biol* 52: 1-7.

Nishina, H., Sato, H., Suzuki, T., Sato, M. and Iba, H. **1990**. Isolation and characterization of fra-2, an additional member of the fos gene familiy. *Proc Natl Acad Sci USA* 87: 369-3623.

Oft, M., Peli, J., Rudaz, C., Schwarz, H., Beug, H., and Reichmann, E. **1996**. TGF-beta1 and Ha-Ras collaborate in modulating the phenotypic plasticity and invasiveness of epithelial tumor cells. *Genes Dev* 10: 2462-2477.

Oft, M., Heider, K. H. and Beug, H. **1998**. TGFbeta signaling is necessary for carcinoma cell invasiveness and metastasis. *Curr Biol* 19: 1243-1252.

Ohkubo, T. and Ozawa, M. 2004. The transcription factor Snail downregulates the tight junction components independently of E-cadherin downregulation. *J Cell Sci* 117: 1675-1685.

Okada, H., Danoff, T.M., Kalluri, R. and Neilson, E.G. **1997**. The early role of FSP1 in epithelial-mesenchymal transformation. *Am J Physiol* 273: 563-574.

Onoue, T., Uchida, D., Begum, N. M., Tomizuka, Y., Yoshida, H. and Sazo, M. **2006**. Epithelial-mesenchymal transition induced by stromal cell-derived fractor-1/CXCR4 system in oral squamous cell carcinoma cells. *Int J Oncol* 29: 1133-1138.

Ozanne, B. W., Spence, H. J., McGarry, L. C. and Hennigan, R. F. **2007**. Transcription factors control invasion: AP-1 the first among equals. *Oncogene* 26: 1-10.

Ozdamar, B., Bose, R., Barrios-Rodiles, M., Wang, H. R., Zhang, Y. and Wrana, J. L. **2005**. Regulation of the polarity protein Par6 by TGFβ receptors controls epithelial cell plasticity. *Science* 307: 1603-1609.

Passegue, E. and Wagner, E. F. 2000. JunB suppresses cell proliferation by transcriptional activation of p16(INK4a) expression. *EMBO J* 19: 2969-2979.

Passegue, E., Jochum, W., Schorpp-Kistner, M., Mohle-Steinlein, U., and Wagner, E.F. **2001**. Chronic myeloid leukemia with increased granulocyte progenitors in mice lacking junB expression in the myeloid lineage. *Cell* 104: 21-32.

Passegue, E., Jochum, W., Behrens, A., Ricci, R., and Wagner, E.F. **2002**. JunB can substitute for Jun in mouse development and cell proliferation. *Nat Genet* 30: 158-166.

Peinado,H., Portillo, F. and Cano, A. **2004**. Transcriptional regulation of cadherins during development and carcinogenesis. *Int J Dev Biol* 48: 365-375.

Peinado,H., Portillo, F. and Cano, A. **2007**. Snail, Zeb and bHLH factors in tumor progression: an alliance against the epithelial phenotype? *Nat Rev Cancer* 7: 415-428.

Perez-Moreno, M.A., Locascio, A., Rodrigo, I., Dhondt, G., Portillo, F., Nieto, M. A. and Cano, A. **2001**. A new role for E12/E47 in the repression of E-cadherin expression and epithelial-mesenchymal transitions. *J Biol Chem* 276:27424-2743.

Perl, A. K., Wilgenbus, P.., Dahl, U., Semb, H. and Christofori, G. **1998**. A causal role for E-cadherin in the transition from adenoma to carcinoma. *Nature* 392: 190-193.

Petersen, O. W., Nielsen, H. L., Gudjonsson, T., Villadsen, R., Rank, F., Niebuhr, E., Bissell, M. J. and Ronnov-Jessen, L: **2003**. Epithelial-tomesenchymal transition in human breast cancer can provide a nonmalignant stroma. *Am J Pathol* 162: 391-402.

Pfarr, C.M., Mechta, F., Spyrou, G., Lallemand, D., Carillo, S. and Yaniv, M. **1994**. Mouse JunD negatively regulates fibroblast growth and antagonizes transformation by ras. *Cell* 76: 747-760.

Piek E, Moustakas A, Kurisaki A, Heldin CH and ten Dijke P. **1999**. TGF-(beta) type I receptor/ALK-5 and Smad proteins mediate epithelial to mesenchymal transdifferentiation in NMuMG breast epithelial cells. *J Cell Sci* 112: 4557-4568.

Pognonec, P., Boulukos, K. E., Aperlo, C., Fujimoto, M., Ariga, H., Nomoto, A. and Kato, H. **1997**. Cross-family interaction between bHLHZip USF and bZip Fra1 proteins results in downregulation of AP1 activty. *Oncogene* 14: 2091-2098.

Pouyssegur, J., Dayan, F. and Mazure, N. M. **2006**. Hypoxia signalling in cancer and approaches to enforce tumour regression. *Nature* 441: 437-443.

Prindull, G. 2005. Hypothesis: Cell plasticity, linking embryonal stem cells to adult stem cell reservoirs and metastatic cancer cells? *Experimental Hematology* 33: 738-746.

Radisky, D. C., Kenny, P. A. and Bissell, M. J. **2007**. Fibrosis and Cancer: do myofibroblasts come also from epithelial cell via EMT?. *J Cell Biochem* 101: 830-839.

Ramos-Nino, M. E., Scapoli, L., Martinelli, M., Land, S. and Mossman, B. T. **2003**. Microarray analysis and RNA silencing link *fra-1* to *cd44* and c-met expression in mesothelioma. *Cancer Res* 63: 3539-3545.

Ransone, L. J. and Verma, I. M. 1990. Nuclear proto-oncogenes *fos* and *jun*. *Annu Rev Cell Biol* 6: 539-557.

Rauscher, F.J., 3rd, Sambucetti, L.C., Curran, T., Distel, R.J., and Spiegelman, B.M. **1988a**. Common DNA binding site for Fos protein complexes and transcription factor AP-1. *Cell 52*: 471-480.

Rauscher, F.J., 3rd, Cohen, D.R., Curran, T., Bos, T.J., Vogt, P.K., Bohmann, D., Tjian, R., and Franza, B.R., Jr. **1988b**. Fos-associated protein p39 is the product of the jun proto-oncogene. *Science* 240: 1010-1016.

Rauscher, F.J., 3rd, Voulalas, P.J., Franza, B.R., Jr., and Curran, T. **1988c**. Fos and Jun bind cooperatively to the AP-1 site: reconstitution in vitro. *Genes Dev* 2: 1687-1699.

Reichmann, E., Ball, R., Groner, B., and Friis, R. R. **1989**. New mammary epithelial and Fibroblastic cell clones in coculture form structures competent to differentiate functionally. *J Cell Biol* 108: 1127-1138.

Reichmann, E., Schwarz, H., Deiner, E. M., Leitner, I., Eilers, M., Berger, J., Busslinger, M., and Beug, H. **1992**. Activation of an inducible c-FosER fusion protein causes loss of epithelial polarity and triggers epithelial-fibroblastoid cell conversion. *Cell* 71: 1103-1116.

Rinehart-Kim, L., Johnson, M., Birrer, M. and Bos, T. **2000**. Alternations in the gene expression profile of MCF-7 breast tumor cells in response to c-Jun. *Int J Cancer* 88: 180-190.

Risse, G., Jooss, K., Neuberg, M., Brüller, J. and Müller, R. **1989**. Asymetrical recognition of the palindromic AP-1 binding site (TRE) by Fos protein complexes. *EMBO J* 8: 3825-3832.

Risse-Hackl, G., Adamkiewicz, J., Wimmel, A. and Schuermann, M. **1998**. Transition from SCLC to NSCLC phenotype is accompanied by an increased TRE-binding activity and recruitment of specific AP-1 proteins*. Oncogene* 16: 3057-3068.

Ryder, K., Lau, L.F., and Nathans, D. **1988**. A gene activated by growth factors is related to the oncogene v-jun. *Proc Natl Acad Sci U S A* 85: 1487-1491.

Ryseck, R. P. and Bravo, R. 1991. c-Jun, JunB and JunD differ in their binding affinities to AP-1 and CRE consensus sequences; effect of Fos proteins. *Oncogene* 6: 533-542.

Sabatakos, G., Sims, N. A., Chen, J., Aoki, K., Kelz, M. B., Amling, M., Bouali, Y., Mukhopadhyay, K., Ford, K., Nestler, E. J. and Baron, R. **2000**. Overexpression of ΔFosB transcription factor(s) increases bone formation and inhibits adipogenesis. *Nat Med* 6: 985-990.

Saez, E., Rutberg, S. E., Mueller, E., Oppenheim, H., Smoluk, J., Yuspa, S. H. and Spiegelman, B. M. **1995**. c-fos is required for malignant progression of skin tumors. *Cell* 82: 721-732.

Sarrio, D., Rodriguez-Pinilla, S.M., Hardisson, D., Cano, A., Moreno-Bueno, G. and Palacios, J. **2008**. Epithelial-mesenchymal transition in breast cancer relates to the basal-like phenotype. *Cancer Res* 68: 989-997.

Schmitz, A. A., Govek, E. E., Bottner, B. and Van Aelst, L. 2000. Rho GTPases: signaling, migration, and invasion. *Exp Cell Res* 261: 1-12.

Schonthal, A., Buscher, M., Angel, P., Rahmsdorf, H.J., Ponta, H., Hattori, K., Chiu, R., Karin, M., and Herrlich, P. **1989**. The Fos and Jun/AP-1 proteins are involved in the downregulation of Fos transcription. *Oncogene* 4: 629-636.

Schorpp-Kistner, M., Wang, Z.Q., Angel, P., and Wagner, E.F. **1999**. JunB is essential for mammalian placentation. *Embo J* 18: 934-948.

Schreiber, M., Baumann, B., Cotten, M., Angel, P., and Wagner, E.F. **1995**. Fos is an essential component of the mammalian UV response. *Embo J* 14: 5338-5349.

Schreiber, M., Kolbus, A., Piu, F., Szabowski, A., Mohle-Steinlein, U., Tian, J., Karin, M., Angel, P., and Wagner, E.F. **1999**. Control of cell cycle progression by c-Jun is p53 dependent. *Genes Dev* 13: 607-619.

Schreiber, M., Poirier, C., Franchi, A., Kurzbauer, R., Guenet, J-L., Carle, G. and Wagner, E. F. **1997**. Structure and chromosomal assignment of the mouse *fra-1* gene, and its exclusion as a candidate gene for oc (osteosclerosis). *Oncogene* 15: 11-71-1178.

Schreiber, M., Wang, Z.Q., Jochum, W., Fetka, I., Elliott, C., and Wagner, E.F. **2000**. Placental vascularisation requires the AP-1 component fra1. *Development* 127: 4937-4948.

Schutte, J., Minna, J.D., and Birrer, M.J. **1989**. Deregulated expression of human c-jun transforms primary rat embryo cells in cooperation with an activated c- Ha-ras gene and transforms rat-1a cells as a single gene. *Proc Natl Acad Sci U S A* 86: 2257-2261.

Shaulian, E. and Karin, M. 2001. AP-1 in cell proliferation and survival. *Oncogene* 20: 2390-2400.

Shaulian, E. and Karin, M. 2002. AP-1 as a regulator of cell life and death. *Nat Cell Biol* 4: 131-136.

Shtutman, M., Levina, E., Ohouo, P., Baig, M. and Roninson, I. B. **2006**. Cell adhesion molecule L1 disrupts E-cadherin-containing adherens junctions and increases scattering and motility of MCF7 breast carcinoma cells. *Cancer Res* 66: 11370-11380.

Shook, D. and Keller, R. 2003. Mechanisms, mechanics and function of epithelial-mesenchymal transitions in early development*. Mech Dev* 120*:* 1351-1383.

Sidenius, N. and Blasi, F. 2003. The urokinase plasminogen activator system in cancer: Recent advances and implications for prognosis and therapy. *Cancer Metastasis Reviews* 22: 205-222.

Smeyne, R.J., Schilling, K., Oberdick, J., Robertson, L., Luk, D., Curran, T., and Morgan, J.I. **1993a**. A fos-lac Z transgenic mouse that can be used for neuroanatomic mapping. *Adv Neurol* 59: 285-291.

Smeyne, R.J., Vendrell, M., Hayward, M., Baker, S.J., Miao, G.G., Schilling, K., Robertson, L.M., Curran, T., and Morgan, J.I. **1993b**. Continuous c-fos expression precedes programmed cell death in vivo. *Nature* 363: 166-169.

Song, Y., Qian, L., Song, S., Chen, L., Zhang, Y., Yuan, G., Zhang, H., Xia, Q., Hu, M., Shi, M., Jiang, Z. and Guo, N. 2008. Fra-1 and Stat3 synergistically regulate activation of human MMP-9 gene. Mol Immunol 45 :137-143.

Stepniak, E., Ricci, R., Eferl, R., Sumara, G., Sumara, I., Rath, M., Hui, L., and Wagner, E.F. **2006**. c-Jun/AP-1 controls liver regeneration by repressing p53/p21 and p38 MAPK activity. *Genes Dev* 20: 2306-2314.

Sternlicht, M. D., and Werb, Z. 2001. How matrix metalloproteinases regulate cell behavior. *Annu Rev Cell Dev Biol* 17: 463-516.

Strathdee, G. 2002. Epigenetic versus genetic alternations in the inactivation of E-cadherin. *Semin Cancer Biol* 12: 373-379.

Suzuki, T., Okuno, H., Yoshida, T., Endo, T., Nishina, H. and Iba H. **1991**. Difference in transcriptional regulatory function between c-Fos and Fra-2. *Nucleic Acid Res* 19: 5537-5542.

Suzuki, T., Murakami, M., Onai, N., Fukuda, E., Hashimoto, Y., Sonobe, M. H., Kameda, T., Ichinose, M., Miki, K. and Iba, H. **1994**. Analysis of AP-1 function in cellular transformation pathways. *J. Virol.* 68: 3527-3535.

Tanos, B. and Rodriguez-Boulan, E. 2008. The epithelial polarity program: machineries involved and their hijacking by cancer. *Oncogene* 27: 6939-6957.

Terasawa, K., Okazaki, K. and Nishida, E. 2003. Regulation of *c-Fos* and *Fra-1* by the MEK5-ERK5 pathway. *Genes Cells* 8: 263-273.

Tester, A. M., Ruangpanit, N., Anderson, R. L. and Thompson, E. W. **2001**. MMP-9 secretion and MMP-2 activation distinguish invasive and metastatic sublines of a mouse mammary carcinoma system showing epithelial-mesenchymal transition traits. *Clin Exp Metastasis* 18: 553-560.

Thannickal, V. J., Toews, G. B., White, E. S., Lynch, J. P. 3rd, Martinez , F. J. **2004**. Mechanisms of pulmonary fibrosis. *Annu Rev Med* 55: 395-417.

Thepot, D., Weitzman, J.B., Barra, J., Segretain, D., Stinnakre, M.G., Babinet, C., and Yaniv, M. **2000**. Targeted disruption of the murine junD gene results in multiple defects in male reproductive function. *Development* 127: 143-153.

Thiery, J. P. and Chopin, D. 1999. Epithelial cell plasticity in development and tumor progression. *Cancer and Metastasis Reviews* 18: 31-42.

Thiery, J. P. 2002. Epithelial-mesenchymal transitions in tumour progression. *Nature Rev Cancer* 2: 443-454.

Thiery, J. P. 2003. Epithelial–mesenchymal transitions in development and pathologies. *Cur. Opin Cell Biol* 15: 740-746.

Thiery, J. P and Sleeman, J. P. 2006. Complex networks orchestrate epithelial-mesenchymal transitions. *Nature Rev Mol Cell Biol* 7: 132-142.

Timmerman, L. A., Grego-Bessa, J., Raya, A., Bertran, E., Perez-Pomares, J. M., Diez, J., Aranda, S., Palomo, S., McCormick, F., Izpisua-Belmonte, J. C. and de la Pompa, J. L. **2004**. Notch promotes epithelialmesenchymal transition during cardiac development and oncogenic transformation. *Genes Dev* 18: 99-115.

Tkach, V., Tulchinsky, E., Lukanidin, E., Vinson, C., Bock, E. and Berezin, V. **2003**. Role of the Fos familiy members, c-Fos, Fra-1 and Fra-2, in the regulation of cell motility. *Oncogene* 22: 5045-5054.

Tse, J. C. and Kalluri, R. 2007. Mechanisms of metastasis: Epithelial-to-mesenchymal transition and contribution of tumor microenvironment. *J Cell Biochem* 101: 816-829.

Tulchinsky, E. 2000. Fos family members: regulation, structure and role in oncogenic transformation. *Histol Histopathol* 15: 921-928.

Van Aken. E., De Wever, O., Correia da Rocha, A. S. and Mareel, M. **2001**. Defective E-cadherin/catenin complexes in human cancer. *Virchows Arch* 439: 725-751.

Vallone, D., Battista, S., Pierantoni, G. M., Fedele, M., Casalino, L., Santoro, M., Viglietto, G., Fusco, A. and Verde, P. **1997**. Neoplastic transformation of rat thyroid cells requires the junB and fra-1 gene induction which is dependent on the HMGI-C gene product. *EMBO J* 16: 5310-5321.

Vandewalle, C., Comijn, J., De Craene, B., Vermassen, P., Bruyneel, E., Andersen, H., Tulchinsky, E., Van Roy, E. and Berx, G. **2005**. SIP1/ZEB2 induces EMT by repressing genes of different epithelial cell-cell junctions. *Nucl Acid Res* 33: 6566-6578.

Vandewalle, C., Van Roy, F. and Berx, G. **2009**. The role of the ZEB family of transcription factors in development and disease. *Cell Mol Life Sci* 66: 773-787.

Verde, P., Casalino, L., Talotta, F., Yaniv, M. and Weitzman, J. B. **2007**. Deciphering the role of AP-1 in tumorigenesis, Fra-ternizing on target promoters. *Cell Cycle* 21: 2632-2639.

Vial, E. and Marshall, C. J. 2003. Elevated ERK-MAP kinase activity protects the FOS family member FRA-1 against proteosomal degradation in colon carcinoma cells. *J Cell Sci* 116: 4957-4963.

Vial, E., Sahai, E. and Marshall, C. **2003**. ERK-MAPK signalling co-ordinately regulates activity of Rac1 and RhoA for tumour cell motility. *Cancer Cell* 4: 67-79.

Vogt, P.K. and Bos, T.J. 1990. jun: oncogene and transcription factor. *Adv Cancer Res* 55: 1-35.

Vogt, P.K. 2001. Jun, the oncoprotein. *Oncogene* 20: 2365-2377.

Vogt, P.K. 2002. Fortuitous convergences: the beginnings of JUN. *Nat Rev Cancer* 2: 465-469.

Vinson, C. R., Sigler, P. B. and McKnight, S. L. **1989**. Scissors-grip model for DNA recognition by a family of leucine zipper proteins. *Science* 246: 911-916.

Wagner, E. F. and Eferl, R. 2005. Fos/AP-1 proteins in bone and the immune system. *Immunol Rev* 208: 126-140.

Wang, Z.Q., Grigoriadis, A.E., Mohle-Steinlein, U., and Wagner, E.F. **1991**. A novel target cell for c-fos-induced oncogenesis: development of chondrogenic tumours in embryonic stem cell chimeras. *Embo J* 10: 2437-2450.

Wang, Z.Q., Ovitt, C., Grigoriadis, A.E., Mohle-Steinlein, U., Ruther, U., and Wagner, E.F. **1992**. Bone and haematopoietic defects in mice lacking c-fos. *Nature* 360: 741-745.

Wang, Z.Q., Liang, J., Schellander, K., Wagner, E.F., and Grigoriadis, A.E. **1995**. c-fos-induced osteosarcoma formation in transgenic mice: cooperativity with cjun and the role of endogenous c-fos. *Cancer Res* 55: 6244-6251.

Weitzman, J. B., Fiette, L., Matsuo, K. and Yaniv, M. **2000**. JunD protects cells from p53-dependent senescence and apoptosis. *Mol Cell* 6 :1109-1119.

Wheelock, M. J., Shintani Y, Maeda M, Fukumoto, Y. and Johnson, K. R. **2008**. Cadherin switching. *J Cell Sci* 121:727-735.

Wisdom, R. and Verma, I.M. 1993. Transformation by Fos proteins requires a C terminal transactivation domain. *Mol Cell Biol* 13: 7429-7438.

Wisdom, R., Johnson, R. S. and Moore, C. **1999**. c-Jun regulates cell cycle progression and apoptosis by distinct mechanisms. *EMBO J* 18: 188-197.

Willert, K. and Nusse, R.. 1998. β-Catenin: a key mediator of Wnt signaling. *Curr. Opin. Genet. Dev.* 8: 95-102.

Xu, J., Lamouille, S. and Derynck, R. **2009**. TGF-β-induced epithelial to mesenchymal transition. *Cell Research* 19: 156-172.

Xue, C., Plieth, D., Venkov, C., Xu, C. and Neilson, E. G. **2003**. The gatekeeper effect of epithelial-mesenchymal transition regulates the frequency of breast cancer metastasis. *Cancer Res* 63: 3386-3394.

Yanagisawa, M., Huveld, D., Kreinest, P., Lohse, C. M., Cheville, J. C., Parker, A. S., Copland, J. A. and Anastasiadis, P. Z. **2008**. A p120 catenin isoform switch affects Rho activity, induces tumor cell invasion, and predicts metastatic disease. *J Biol Chem* 26: 18344-18354.

Yang, J. and Weinberg, R. A. 2008. Epithelial-mesenchymal transition at the crossroads of development and tumor metastasis. *Developmental Cell* 14: 818-829.

Yang, J., Mani, S.A., Donaher, J. L., Ramaswamy, S., Itzykson, R. A:, Come, C., Savanger, P., Gitelman, I., Richardson, A. and Weinberg, R. A. **2004**. Twist, a master regulator of morphogenesis, plays an essential role in tumor metastasis. *Cell* 117: 927-939.

Yang, M-H., Wu, M-Z., Chiou, S-H., Chen, P-M., Chang, S-Y., Liu, C-J., Teng, S-C. and Wu, K-J. **2008**. Direct regulation of TWIST by HIF-1α promotes metastasis. *Nat Cell Biol* 10: 295-305.

Yang, S.-H., Sharrocks, D. and Whitmarsh, A. J. **2003**. Transcriptional regulation by MAP kinase signalling cascades. *Gene* 320: 3-21.

Yang, S., Du, J., Wang, Z., Yan, J., Yuan, W., Zhang, J. and Zhu, T. **2009**. Dual mechanism of δEF-1 expression regulated by bone morphogenic protein-6 in breast cancer. I*nt J Biochem Cell Biol* 41: 853-861.

Yoshimura, K., Takeuchi, K., Nagasaki, K., Ogishima, S., Tanaka, H., Iwase, T., Akiy Ama, Y., Kuroda, Y. and Miki, Y. **2009**. Prognostic value of matrix Gla protein in breast cancer. *Mol Med Reports* 2: 549-553.

Yoshioka, K., Deng, T., Cavigelli, M. and Karin, M. **1995**. Antitumor promotion by phenolic antioxidants: inhibition of AP-1 activity through induction of Fra expression. *Proc Natl Acad Sci USA* 92: 4972-4976.

Young, M. R., Li, J. J., Rincon, M., Flawell, R. A., Sathyanarayana, B. K., Hunziker, R. and Colburn, N. H. **1999.** Transgenic mice demonstrate AP-1 (activator protein-1) transactivation is required for tumor promotion. *Proc Natl Acad Sci. USA* 96: 9827-9832.

Young, M. R., Farerell, L., Lambert, P., Awasthi, P. and Colburn, N. H. **2002a**. Protection against human papillomavirus type 16-E7 oncogene-induced tumorigenesis by in vivo expression of dominant-negtive c-jun*. Mol Carcinog* 34: 72-77.

Young, M. R., Nair, R., Bucheimer, N., Tulsian, P., Brown, N., Chapp, C., Hsu, T. C. and Colburn, N. H. **2002b**. Transactivation of Fra-1 and consequent activation of AP-1 occur extracellular signal-regulated kinase dependently. *Mol Cell Biol* 22: 587-598.

Young, M. R. and Colburn, N. H. 2006. Fra-1 a target for cancer prevention or intervention. *Gene* 379: 1-11.

Yu, H. and Jove, R. The STATS of cancer-new molecular targets come of age. **2004**. *Nat Rev Cancer* 4: 7-105.

Zajchowski, D. A., Bartholdi, M. F., Gong, Y., Webster, L., Liu, H. L., Munishkin, A., Beauheim, C., Harvey, S., Ethier, S. P. and Johnson, P. H., **2001**. Identification of gene expression profiles that predict the aggressive behavior of breast cancer cells. *Cancer Res* 61: 5168-5178.

Zavadil, J., Bitzer, M., Liang, D., Yang, Y. C., Massimi, A., Kneitz, S., Piek, E. and Bottinger, E. P. **2001**. Genetic programs of epithelial cell plasticity directed by transforming growth factor-beta. *Proc Natl Acad Sci USA* 98: 6686-6691.

Zavadil, J., and Böttinger, E. P. 2005. TGF-β and epithelial-to-mesenchymal transitions. *Oncogene* 24: 5764-5774.

Zenz, R., Scheuch, H., Martin, P., Frank, C., Eferl, R., Kenner, L., Sibilia, M., and Wagner, E.F. **2003**. c-Jun regulates eyelid closure and skin tumor development through EGFR signaling. *Dev Cell* 4: 879-889.

Zenz, R., Eferl, R., Kenner, L., Florin, L., Hummerich, L., Mehic, D., Scheuch, H., Angel, P., Tschachler, E., and Wagner, E.F. **2005**. Psoriasis-like skin disease and arthritis caused by inducible epidermal deletion of Jun proteins. *Nature* 437: 369-375.

Zenz, R., Eferl, R., Scheinecker, C.,Redlich, K., Smolen, J., Schonthaler, H. B., Kenner, L., Tschachler, E. and Wagner, E. F. **2008**. Activator protein 1 (Fos/Jun) functions in inflammatory bone and skin disease. *Arthritis Res Ther* 10: 1-10.

Zerial, M., Toschi, L., Ryseck, R.P., Schuermann, M., Muller, R., and Bravo, R. **1989**. The product of a novel growth factor activated gene, fos B, interacts with JUN proteins enhancing their DNA binding activity. *Embo J* 8: 805-813.

Zhang, K., Chaillet, J. R., Perkins, L. A., Halazonetis, T. D. and Perrimon, N. **1990**. Drosophila homolog of the mammalian jun oncogene is expressed during embryonic

development and activates transcription in mammalian cells. *Proc Natl Acad Sci USA* 87: 6281-6285.

Zhang, Q., Adiseshaiah, P. and Reddy, S. P. **2005**. Matrix metalloproteinase/epidermal growth factor receptor/mitogen-activated protein kinase signaling regulate fra-1 induction by cigarette smoke in lung epithelial cells. *Am J Resp Cell Mol Biol* 32: 72-81.

Zoumpourlis, V., Papassava, P., Linardopoulos, S., Gillespie, D., Balmain, A. and Pintzas, A. **2000**. High levels of phosphorylated c-Jun, Fra-1, Fra-2 and ATF-2 proteins correlate with malignant phenotypes in the multistage mouse skin carcinogenesis model. *Oncogene* 19: 4011-4021.

Zuber, J., Tchernitsa, O. I., Hinzmann, B., Schmitz, A. C., Grips, M., Hellriegel, M., Sers, C., Rosenthal, A. and Schafer, R. **2000**. A genome-wide survey of RAS transformation targets. *Nat Genet* 24: 144-152.

CURRICULUM VITAE

Personal Information:

Full Name	Ivana Ćustić
Date of birth	18.01.1980
Place of birth	Zagreb, Croatia
Nationality	Croatian

Work address:

Research Institute of Molecular Pathology (IMP)
Beug lab
Dr. Bohr-gasse 7
1030 Vienna, Austria
E-mail: custic@imp.ac.at

Education:

2005 – 2009	PhD studies in Molecular Biology Vienna Biocenter International PhD Programme, University of Vienna, Vienna, Austria
1998 – 2005	Diploma studies in General Biology (Teaching Degree) and Molecular Biology University of Zagreb, Faculty of Natural Sciences and Mathematics, Biology Department, Zagreb, Croatia
1994 – 1998	Secondary school, VII Gymnasium, Zagreb, Croatia

Research experience:

2005 – 2009	PhD Project at the Institute of Molecular Pathology (IMP), Vienna, Austria, supervised by Drs. Hartmut Beug and Erwin Wagner. Thesis title: *"The role of the AP-1 member Fra-1 in Epithelial-Mesenchymal Transition and Carcinogenesis"*

2004 – 2005 Diploma Thesis research project at the Clinical Hospital Center Zagreb, Urology Clinic, Referral Center for Tissue Typing and Transplantation, Zagreb, Croatia, supervised by Prof. Dr. sc. Vesna Kerhin- Brkljacic. Thesis title: *"The role of HLA class II antibodies in patients on the waiting list for kidney transplantation"*

2003 Research project at the Division of Molecular Medicine, Laboratory of Molecular Oncology, Rudjer Boskovic Institute, Zagreb, Croatia, supervised by Dr. sc. Sanja Kapitanovic. Project title: *"Genetic analysis and screening for Single Nucleotide Polymorphisms in E-cadherin gene locus in human colon carcinoma"*

2002 – 2003 Research project at the Division of Molecular Biology, Laboratory for Microbial Genetics, Rudjer Boskovic Institute, Zagreb, Croatia, supervised by Prof. Dr. sc. Krunoslav Brcic-Kostic and Prof. Dr. sc. Erika Salaj-Smic. Project title: *"The role of recombination in DNA repair and genome stability"*

Career-related activities:

2003 – 2005 Teaching Assistant for the undergraduate practical course in Biochemistry, University of Zagreb, Faculty of Natural Sciences and Mathematics, Department of Biochemistry, Zagreb, Croatia

Posters:

Ivana Custic, Latifa Bakiri, Hartmut Beug and Erwin F. Wagner "The role of Fra/AP-1 proteins in EMT." *IMP Recess* 2007

Ivana Custic, Latifa Bakiri, Hartmut Beug and Erwin F. Wagner "The role of Fra/AP-1 proteins in EMT." *IMP Recess* 2008

Publications:

Ivana Custic, Latifa Bakiri, Memetcan Alacakaptan, Hartmut Beug and Erwin F Wagner " The transcription factor Fra-1 regulates epithelial plasticity." *manuscript in preparation*